ELECTROCOAGULATION AND ADVANCED OXIDATION AS INTERMEDIATE EFFLUENT TREATMENT STEPS FOR WATER REUSE IN A TEXTILE DYEING PLANT

by

Gilbert İzzet Alaton

B.S., Chemical Engineering, İstanbul Technical University, 1995

M.S., Environmental Technology, Boğaziçi University, 1998

Submitted to the Institute of Environmental Sciences
in partial fulfillment of the requirements for the degree of
Doctor of Philosophy

Graduate Program in Environmental Technology
Boğaziçi University
2005

ACKNOWLEDGEMENTS

I would like to express my sincere gratitude towards my supervisor Prof. Dr. Nilsun İnce for her valuable guidance, supportive comments, encouragement and patience throughout the study as it progressed.

I am also very thankful to Mr. Mehmet Ali İnce for his motivation and support during my experimental work and beyond.

I deeply acknowledge my jury members Prof. Dr. Ferhan Çeçen, Prof. Dr. Orhan Yenigün, Prof. Dr. Ömer Saygın and Prof. Dr. Ahmet Mete Saatçi for their valuable criticism.

I would like to thank my wife Assoc. Prof. Dr. İdil Arslan Alaton for her immense assistance, help and interest during my thesis, and for living with me through these times of extra hard work.

Many many thanks also to my mother Esther Apikyan and my brother Robert Apikyan for their ever endless love, patience and support throughout my whole life. I know that they are always with me.

ABSTRACT

Dyehouse effluents are highly colored and contain significant amounts of dissolved and suspended solids so that in most cases the use of membrane separation technologies as a final treatment stage becomes inevitable to achieve high quality process water for reuse purposes. The inherent disadvantage associated with most chemical treatment processes is that they increase the salinity of the final, treated effluent and hence chemical intense methods are generally considered as impractical or impossible to prepare water for reuse. A successful reuse plant for textile dyehouse effluent should ideally involve a system, which will compensate for all sudden changes in the biotreated effluent in order to ensure safe and stable operation of the membrane units. Consequently, the treatment unit that is going to be implemented has to be flexible enough to comply with the existing treatment units.

The present experimental work aimed at proposing advanced chemical treatment schemes (electrolysis and ozonation) for the effective and economical remediation of biologically pre-treated textile industry wastewater (average COD_o = 370 mg/L; BOD_5 < 20 mg/L; Suspended Solids (SS) = 130 mg/L; Dissolved Solids (DS) = 10,000 mg/L; Color as absorbance at 436 nm = 0.280 1/cm; pH = 7.5; SO_4^{2-} = 1250 mg/L) instead of the more commonly applied “phase – transfer” – limited multi-stage filtration processes. In addition, a more recently developed advanced oxidation process (sonochemical treatment) was employed for the degradation of the most problematic effluent stream of the textile dyeing and finishing sector, namely the dyebath effluent. Spent dyebaths were simulated to explore the effect of ultrasound on decoloration and degradation of dyes in auxiliaries present in spent dyebaths under varying reaction conditions.

Electrolysis of biotreated dyehouse effluent appeared to be effective in terms of COD, color and SS once optimized for operating conditions (pH, current, contact time) and electrode materials (iron, aluminum, iron/aluminum). It was also shown that different color removal mechanisms existed for different electrode materials. Indirect redox reactions were found to be responsible for color abatement during electrolysis using iron electrodes, whereas color removal with aluminum electrodes occurred via physical adsorption.

A continuous electrochemical system was also developed to simulate real electrochemical treatment conditions and estimate operating costs. The system enabled satisfactory floc formation, coagulation, flotation and sludge separation in one single reactor with iron electrode. However, it did not qualify when Al was used as the electrode.

Results indicated that the efficiency of the electrochemical systems did not change when the biotreated effluent was of much lower quality, emphasizing the robustness of electrochemical process as a “buffer” stage between secondary and tertiary treatment.

A detailed cost evaluation in terms of operating expenses was also undertaken for all investigated systems.

ÖZET

Tekstil boyama endüstrisi atıksuları, yoğun renk, yüksek oranda çözünmüş ve askıda katı madde içerdiğinden dolayı kaliteli proses suyu geri kazanımı için son aşamada membran teknolojilerinin uygulanması kaçınılmazdır. Birçok kimyasal arıtma prosesinin ortak dezavantajı olarak arıtılan suyun tuzluluğunun artması nedeni ile bu yöntemlerin pratikte geri kazanım için uygun olmadığı kabul edilir. Tekstil atıksularının geri kazanımı sağlayacak membran içeren bir sistemin güvenilir ve dengeli şekilde işletilebilmesi için kurulacak ideal sistemin biyolojik arıtmada meydana gelebilecek ani değişikliklere karşı dayanıklı olması gerekir. Sonuç olarak, kurulacak olan arıtma ünitesinin mevcut arıtma sistemi ile uyum içinde çalışabilecek kadar esnek olması beklenir.

Bu deneysel çalışma, biyolojik olarak ön arıtılmış tekstil endüstrisi atıksularının ($KOİ_o$= 370 mg/L; $BOİ_5$ < 20 mg/L; Askıda Katı Madde (AKM) = 130 mg/L; Çözünmüş Katı Maddeler (ÇKM) = 10.000 mg/L; 436 nm dalga boyundaki absorbans olarak Renk = 0.280 1/cm; pH = 7.5; SO_4^{2-} = 1250 mg/L) verimli ve ekonomik bir şekilde geri kazanımı için ileri kimyasal arıtma yöntemlerinin (elektroliz, ozonlama), faz transferine dayalı çok kademeli filtrasyon prosesleri yerine önerilmesini amaçlamıştır. İlave olarak, son zamanlarda gelişmekte olan bir ileri oksidasyon prosesi (sonokimyasal arıtma), tekstil boyama ve terbiye sektöründen kaynaklanan en problemli atıksu olan boya banyo atıksularına uygulanmıştır. Sonokimyasal arıtmanın, kullanılmış boya banyolarında bulunan yardımcı kimyasalların varlığında boyarmaddelerin renk giderimine ve ayrışmalarına olan etkisini araştırmak için boya banyo atıksuları taklit edilmiştir.

Biyolojik olarak arıtılmış boyahane atıksularının en iyi işletme koşulları (pH, akım, temas süresi) ve elektrod tipi (demir, alüminyum, demir/alüminyum) ile elektrokimyasal olarak arıtımı KOİ, renk ve AKM parametreleri açısından verimli bulunmuştur. Ayrıca, farklı elektrod malzemeleri ile farklı renk giderim mekanizmalarının varlığı kanıtlanmıştır. Renk giderimi, demir elektrodlar ile dolaylı redoks reaksiyonlarından kaynaklanırken, alüminyum elektrod kullanıldığında ise fiziksel adsorpsiyon ile meydana gelmektedir.

Gerçek elektrokimyasal arıtma koşullarını taklit edebilmek ve işletme maliyetlerini ortaya çıkartabilmek için sürekli elektrokimyasal arıtma sistemi geliştirilmiştir. Bu sistem demir elektrod kullanıldığında tek reaktör içinde tatmin edici flok oluşumu, koagülasyon, yüzdürme ve çamur ayırımı sağlarken, alüminyum elektrod kullanıldığında bu performans sağlanamamıştır.

Sonuçlar, elektrokimyasal sistemlerinin arıtma verimlerinin biyolojik arıtmadan düşük kalitede atıksu geldiğinde değişmediğini, bu nedenle elektrokimyasal prosesin ikincil ve üçüncül (ileri) arıtma arasında tampon görevini üstlenecek kadar dayanıklı olduğunu açıkça göstermektedir.

Tüm incelenen sistemlerin işletim giderleri için ayrıntılı bir maliyet analizi yapılmıştır.

TABLE OF CONTENTS

LIST OF FIGURES

LIST OF TABLES

ELECTROCOAGULATION AND ADVANCED OXIDATION AS INTERMEDIATE EFFLUENT TREATMENT STEPS FOR WATER REUSE IN A TEXTILE DYEING PLANT

Gilbert İzzet Alaton
Environmental Technology Ph.D. Thesis, 2005
Advisor: Prof. Dr. Nilsun İnce

Keywords: Dyehouse effluent, electrocoagulation, ozonation, sonolysis, reuse

Dyehouse effluents are highly colored and contain significant amounts of dissolved and suspended solids so that in most cases the use of membrane separation technologies as a final treatment stage becomes inevitable to achieve high quality process water for reuse purposes. The inherent disadvantage associated with most chemical treatment processes is that they increase the salinity of the final, treated effluent and hence chemical intense methods are generally considered as impractical or impossible to prepare water for reuse. A successful reuse plant for textile dyehouse effluent should ideally involve a system, which will compensate for all sudden changes in the biotreated effluent in order to ensure safe and stable operation of the membrane units. Consequently, the treatment unit that is going to be implemented has to be flexible enough to comply with the existing treatment units.

The present experimental work aimed at proposing advanced chemical treatment schemes (eletrolysis and ozonation) for the effective and economical remediation of biologically pre-treated textile industry wastewater (average COD_o = 370 mg/L; BOD_5 < 20 mg/L; Suspended Solids (SS) = 130 mg/L; Dissolved Solids (DS) = 10,000 mg/L; Color as absorbance at 436 nm = 0.280 1/cm; pH = 7.5; SO_4^{2-} = 1250 mg/L) instead of the more commonly applied “phase – transfer” – limited multi-stage filtration processes. In addition, a more recently developed advanced oxidation process (i.e. sonochemical treatment) was employed for the degradation of the most problematic effluent stream of the textile dyeing

and finishing sector, namely the dyebath effluent. Spent dyebaths were simulated to explore the effect of ultrasound on decoloration and degradation of dyes in auxiliaries present in spent dyebaths under varying reaction conditions.

Electrolysis of biotreated dyehouse effluent appeared to be effective in terms of COD, color and SS once optimized for operating conditions (pH, current, contact time) and electrode materials (iron, aluminum, iron/aluminum). It was also shown that different color removal mechanisms existed for different electrode materials. Indirect redox reactions were found to be responsible for color abatement during electrolysis using iron electrodes, whereas color removal with aluminum electrodes occurred via physical adsorption.

It was found that sulphate could be removed with aluminum or iron/aluminum electrodes indicating that adsorption on the positively charged aluminum hydroxide complexes was the dominant removal mechanism for sulphate. No sulfate removal could be achieved using iron electrode alone.

A continuous electrochemical system was also developed to simulate real electrochemical treatment conditions and estimate operating costs. The system enabled satisfactory floc formation, coagulation, flotation and sludge separation in one single reactor with iron electrode whereas the system failed to operate properly when aluminum electrodes were employed.

Results indicated that no deterioration of the electrochemical treatment efficiency was observed for both batch and continuous electrolysis under stressed biotreatment conditions, emphasizing the robustness of electrochemical treatment acting as a “buffer” stage between secondary and tertiary treatment.

The effect of electrolysis performance ozonation was also examined. The highest improvement in color removal via ozonation occurred when biotreated effluent was first subjected to electrolysis using aluminum electrodes. Almost complete decolorization was achieved during all electrolysis + ozonation experiments, and final effluent color and COD were found suitable for reuse in dyeing processes.

Sonolysis, a more recently developed type of AOP, was applied to assess the reuse potential of simulated spent dyebaths after being subjected to advanced oxidation. H_2O_2 addition resulted in an appreciable increase in COD removal, but did not have any positive effect on color abatement rate.

A detailed cost evaluation in terms of operating expenses was also undertaken for all investigated systems.

TEKSTİL BOYAMA TESİSİNDE SU GERİKAZANIMI İÇİN ARA ARITMA KADEMELERİ OLARAK ELEKTROKOAGÜLASYON VE İLERİ OKSİDASYON

Gilbert İzzet Alaton
Çevre Teknolojisi, Doktora Tezi, 2005
Tez Danışmanı: Prof. Dr. Nilsun İnce

Anahtar Kelimeler: Boyahane atıksuları, elektrokoagülasyon, ozonlama, sonoliz, gerikazanım

Tekstil boyama endüstrisi atıksuları, yoğun renk, yüksek oranda çözünmüş ve askıda katı madde içerdiğinden dolayı kaliteli proses suyu geri kazanımı için son aşamada membran teknolojilerinin uygulanması kaçınılmazdır. Birçok kimyasal arıtma prosesinin ortak dezavantajı olarak arıtılan suyun tuzluluğunun artması nedeni ile bu yöntemlerin pratikte gerikazanım için uygun olmadığı kabul edilir. Tekstil atıksularının gerikazanımı sağlayacak membran içeren bir sistemin güvenilir ve dengeli şekilde işletilebilmesi için kurulacak ideal sistemin biyolojik arıtmada meydana gelebilecek ani değişikliklere karşı dayanıklı olması gerekir. Sonuç olarak, kurulacak olan arıtma ünitesinin mevcut arıtma sistemi ile uyum içinde çalışabilecek kadar esnek olması beklenir.

Bu deneysel çalışma, biyolojik olarak ön arıtılmış tekstil endüstrisi atıksularının ($KOİ_o$= 370 mg/L; $BOİ_5$ < 20 mg/L; Askıda Katı Madde (AKM) = 130 mg/L; Çözünmüş Katı Maddeler (ÇKM) = 10,000 mg/L; 436 nm dalga boyundaki absorbans olarak Renk = 0.280 cm^{-1}; pH = 7.5; SO_4^{2-} = 1250 mg/L) verimli ve ekonomik bir şekilde gerikazanımı için ileri kimyasal arıtma yöntemlerinin (elektroliz, ozonlama), faz transferine dayalı çok kademeli filtrasyon prosesleri yerine önerilmesini amaçlamıştır. İlave olarak, son zamanlarda gelişmekte olan bir ileri oksidasyon prosesi (sonokimyasal arıtma), tekstil boyama ve terbiye sektöründen kaynaklanan en problemli atıksu olan boya banyo atıksularına uygulanmıştır. Sonokimyasal arıtmanın, kullanılmış boya banyolarında

bulunan yardımcı kimyasalların varlığında boyarmaddelerin renk giderimine ve ayrışmalarına olan etkisini araştırmak için boya banyo atıksuları taklit edilmiştir.

Biyolojik olarak arıtılmış boyahane atıksularının en iyi işletme koşulları (pH, akım, temas süresi) ve eletrod tipi (demir, alüminyum, demir/alüminyum) ile elektrokimyasal olarak arıtımı KOİ, renk ve AKM parametreleri açısından verimli bulunmuştur. Ayrıca, farklı elektrod malzemeleri ile farklı renk giderim mekanizmalarının varlığı kanıtlanmıştır. Renk giderimi, demir elektrodlar ile dolaylı redoks reaksiyonlarından kaynaklanırken, aluminyum elektrod kullanıldığında ise fiziksel adsorpsiyon ile meydana gelmektedir.

Sülfatın, alüminyum ve demir/alüminyum elektrodları ile giderilebilmesi, baskın giderim mekanizmasının sülfatın pozitif yüklü alüminyum hidroksit kompleksleri üzerine adsorpsiyonu olduğunu göstermektedir. Demir elektrod tek başına kullanıldığında ise sülfat giderimi sağlanamamıştır.

Gerçek elektrokimyasal arıtma koşullarını taklit edebilmek ve işletme maliyetlerini ortaya çıkartabilmek için sürekli elektrokimyasal arıtma sistemi geliştirilmiştir. Bu sistem demir elektrod kullanıldığında tek reaktör içinde tatmin edici flok oluşumu, koagülasyon, yüzdürme ve çamur ayırımı sağlarken, alüminyum elektrod kullanıldığında bu performans sağlanamamıştır.

Sonuçlar, kesikli ve sürekli elektroliz sistemleri arıtma verimlerinin olumsuz biyolojik arıtma koşullarından etkilenmediğini, bu nedenle elektrokimyasal arıtmanın ikincil ve üçüncül (ileri) arıtma arasında tampon görevini üstlenecek kadar dayanıklı olduğunu açıkça göstermektedir.

Elektrokimyasal arıtma performansının ozonlamaya etkisi incelenmiştir. Ozonlama ile renk gideriminde en yüksek artış, biyolojik olarak arıtılmış atıksuyun önce alüminyum elektrod kullanılarak elektrolizi ile meydana gelmiştir. Renk, tüm elektroliz + ozonlama deneylerinde tamamen giderilebilirken, elde edilen son suyun, renk ve KOİ değerleri bakımından boyama prosesinde tekrar kullanılabilecek kaliteye ulaştığı görülmüştür.

Yeni gelişmekte olan İleri Oksidasyon Prosesleri arasında yer alan Sonoliz, taklit edilmiş boya banyo atıksularının geri kazanım potansiyellerini incelemek üzere denenmiştir. H_2O_2 ilavesi ile renk giderim hızı etkilenmezken, KOİ giderim veriminde önemli bir artış sağlanmıştır.

Tüm incelenen sistemlerin işletim giderleri için ayrıntılı bir maliyet analizi yapılmıştır.

1. INTRODUCTION

In spite of numerous developments and technical advances in textile dyeing machinery and dyestuff technology, the textile industry is still one of the major water consumers among all industrial sectors. This has turned Research & Development studies on water reuse technologies extremely important, and fortunately much progress has been lately achieved in this field. However, the complexity of textile dyeing mill effluents both in terms of composition and the variability of flow rates makes the use of manufacturer - designed water reuse technologies rather ineffective. In addition, the cost of wastewater segregation in an operating dyehouse is nearly equal to the cost of a reuse system itself, such that in this case proper "end-of-pipe" treatment seems to be the only and most effective method of water reuse.

The design of the recovery system is mostly affected by the level of water quality requirement of the dyehouse, which differs, depending on the types of finishing applications, chemicals used and fabrics processed. In this respect, a commission dyehouse must be supplied with the best water quality among all textile processors since the highest variety of finishing applications and fabric types are observed in this sector. Therefore, the water obtained must be clean enough to meet the desired level of quality for every individual application not to fail in the quality of finished goods. In most cases it becomes evident that the use of membrane separation technologies as a final treatment stage is inevitable to achieve this high quality.

Textile wastewaters are usually treated in a chemical – physical or more commonly in an activated sludge biochemical plant in order to meet legislative requirements. The inherent disadvantage associated with most chemical units is that they are "additive", i.e. "chemicals intense" processes. The addition of coagulants such as alum, ferric chloride, ferric sulfate, ferrous sulfate and hydrated lime ends up with a considerable increase in dissolved constituents in the effluent, which makes it impractical or impossible to reuse. Most of the time the high amounts of auxiliaries that are used as sequestering and dispersing agents in textile preparation and dyeing processes reduce the efficiency of chemical settling considerably. Although these systems are known to be very cost effective

for pretreatment purposes, when considering reuse applications, biological treatment becomes much more practical than chemical coagulation. On the other hand, troubles encountered during biological treatment operation such as poor settling, fluctuations in the quality and quantity of incoming wastewater may cause serious problems for the proceeding membrane filtration units. Therefore, a successful reuse plant for textile dyehouse effluent should involve a system which will compensate for all sudden changes in the biotreated effluent character to ensure safe and stable operation of membrane units.

The purpose of this research was to investigate the feasibility of various physical/chemical processes as alternative options to the reusability of textile dyeing and finishing process effluents. The experimental work presented covers lab scale application of ozonation, electrochemical and sonochemical processes and their performance analysis for reusing of dyeing/finishing effluents.

The study scheme is as outlined in the following:

1. Electrolysis:

i. Batch electrolysis of biotreated effluent:

Electrochemical processes offer several advantages in wastewater treatment such as high flexibility and robustness, relatively low operational and capital costs, no or minimum requirement of externally added oxidants/catalysts, as well as the possibility/ease of combining with other unit operations. They have already been successful for the treatment of a variety of difficult to degrade, recalcitrant industrial pollutants. The first part of this study was concerned with the optimization of electrochemical process conditions such as electrode material, reaction time, initial pH and applied current. The performance of the system was evaluated in terms of color, suspended solids (SS), chemical oxygen demand (COD), conductivity, dissolved solids (DS) and sulfate removal efficiencies. In addition, for a better understanding of the prevailing color removal mechanism during electrolysis, the reduction potential was continuously monitored.

ii. Continuous electrolysis of raw and biotreated effluent (CET):

This part of the study is focused on a continuous operation of an electrochemical process on biotreated effluent. Additionally, the continuous mode has also been tested on raw (untreated) textile effluent to investigate the possibility of eliminating a preceding biotreatment step.

iii. Effect of biological treatment performance on electrochemical process:

Biological treatment process operating parameters such as aeration (reaction) and/or settling time were deteriorated to simulate operational problems encountered during biological treatment of the studied textile effluent. The efficiency of batch, as well as continuous mode electrochemical process under poor biological treatment conditions (low-rate aeration, poor biosludge settling and their combination) were examined in order to evaluate the response of electrolysis.

2. Ozonation

i. Ozonation of biotreated effluent: In this part of the study biotreated dyehouse effluents were ozonated at various conditions and impacts of pH, and ozone dose were investigated. In addition color and COD decay profiles comparatively evaluated, and process efficiency was assessed in terms of oxidant consumption.

ii. Ozonation of biologically + electrochemically pre-treated textile effluent: In this part of the study, biologically pretreated textile effluent was subjected to sequential electrolysis and ozonation in order to assess the influence of electrochemical process on post ozonation. In this treatment train ozonation was considered as an intermediate polishing step prior to membrane filtration. For this proposed treatment scheme, electrochemical process conditions such as the electrode material and operating pH were varied to establish optimum treatment conditions.

3. Sonochemical Destruction of Textile Dye-bath Effluent:

Sonochemical techniques are comparatively more novel means of destroying recalcitrant compounds such as dyestuffs. In this part of the study, treatability of some common dyeing process effluents in a commission-dyeing mill was evaluated by sonochemical technique. A more thorough research and development was found necessary to assess the applicability of such systems on water reuse from spent dyebaths.

4. Economic analysis:

Finally, the operating costs of the investigated advanced treatment processes (ozonation, electrochemical and sonochemical processes) were compared with each other to achieve the target effluent qualities and process performances.

2. THEORETICAL BACKGROUND

2.1. Electrochemistry and Practical Application

2.1.1. The Electrochemical Cell

An electrochemical cell can be formed when any two electronically conducting materials are put into an electrolyte solution. The conducting materials, which are typically metal or carbon (semiconductors and polymers are also used), are referred to as the electrodes. The electrolyte solution is an ionically conducting liquid containing a proportion of dissociating salt or acid. A simple example is an electrolyte of an aqueous solution of copper (II) ions in sulfuric acid with a copper electrode and an iron electrode placed in solution. If the electrodes are connected by an external circuit then two processes will occur at the electrodes:

$$Fe \longrightarrow Fe^{2+} + 2\,e^{-} \qquad (2.1)$$

The iron will dissolve into the solution and this electrode is called the anode.

The following electrochemical reaction occurs at the copper electrode:

$$Cu^{2+} + 2\,e^{-} \longrightarrow Cu \qquad (2.2)$$

The copper is deposited onto the surface of the copper electrode that is hence called the cathode. These two processes give rise to the flow of current, I, in the external circuit. By this convention it is evident that the anode withdraws electrons from the cell and the anode reaction is therefore oxidation and conversely the cathode supplies electrons to the cell and the reaction is therefore reduction. The above example of iron dissolution and copper electrodeposition is in fact the industrially used system referred to as cementation, in which metals such as copper are extracted from liquors, containing relatively low concentrations of copper (metal) ions, by the dissolution of iron.

If in the above example cell a direct current (d.c.) power supply is placed in the external circuit and current is made to flow externally from the iron electrode to the copper electrode, then the copper electrode becomes the anode and the reverse reaction of (2.2) occurs. At the iron electrode, which is now the cathode, reaction (2.2) occurs, in which copper is deposited onto the iron cathode. This type of cathode reaction is commonly used in the recovery of metal ions from aqueous solutions in effluent treatment and electrowinning.

It is apparent in the above cell that copper ions are moving from the anode to the cathode and there is no accumulation of charge, as the amount of oxidation is equal to the amount of reduction. The movement of the ions is therefore responsible for the transfer of charge in solution from one electrode to the other. In practice the charge is carried by several ions, both cations (positively charged) and anions (negatively charged). The rate of charge transfer in the cell is therefore the total rate of the electrode reactions, which is conveniently measured by the current. The relationship between the charge passed and the amount of reaction is described by Faraday's Law (Scott, 1995).

2.1.2. Faraday's Law and Current Efficiency

In an electrochemical cell the amount of charge passed, q, in a time interval, t, is given by the following empirical equation;

$$q = \int I \, dt \qquad (2.3)$$

I stand for the electric current. Referring to reaction (2.2.), the amount metal deposited (in mols) is calculated from Faraday's Law of electrolysis as indicated below:

$$m = q/nF = I.t/nF \qquad (2.4)$$

where F is the Faraday constant and equal to 96485 C/mol.

The processes at individual electrodes frequently involve more than one reaction and this brings in the concept of current efficiency, which is a major criterion for measuring the performance of electrochemical systems.

The current efficiency (CE) is the yield of a process based on the charge passed and can be defined as the charge consumed in forming an electrochemical product/total charge consumed.

Experimentally, CE is obtained from the measure of the amount of product formed, or reactant consumed, m_{act}, and the theoretical amount of reactant, i.e. m as indicated below;

$$CE = m_{act}/m \tag{2.5}$$

According to Faraday's Law, the following expression is obtained:

$$CE = m_{act}nF/q \tag{2.6}$$

The total current I at an electrode is the sum of the currents, I_j, of the individual reactions;

$$I = \sum I_j \tag{2.7}$$

and the CE at any instant can thus be expressed in terms of current I as described below;

$$CE = I_j/I \tag{2.8}$$

2.1.3. Electrode Potential and Current Density

The example in equations (2.1) and (2.2), of the dissolution of iron coupled with the formation of metallic copper is a Galvanic process in which the free energy of the overall reaction

$$Cu^{2+} + Fe \longrightarrow Fe^{2+} + Cu \tag{2.9}$$

has a negative value. From the general definition of the Gibbs free energy;

$$\Delta G = -nFE_o \tag{2.10}$$

the equilibrium cell potential, E_o (or the open cell voltage), has a positive value. The equilibrium cell potential is made up from two components, the cathode and anode equilibrium (half-cell) potentials $(E_e)_c$ and $(E_e)_a$, respectively:

$$E_o = (E_e)_c - (E_e)_a \tag{2.11}$$

When a current flows, the electrode is said to be polarized and the electrode potential E departs from its equilibrium value and takes up a value E. The degree of polarization is measured in terms of the overall potential, η, which is defined as follows;

$$\eta = E - E_e \tag{2.12}$$

The electrode potential E is defined as the difference in the potential of the electrode surface, E_m, and the potential of the solution adjacent to the electrode surface, E_s.

$$E = E_m - E_s \tag{2.13}$$

By convention, cathode potentials have negative values and anode potentials have positive values. In practice, however, it should be noted that there is in fact a distribution of potential in solution at the electrode interface, which decays rapidly a short distance into the solution.

It is usual to normalize the rate of an electrode reaction with regard to the surface area of an electrode, A, and thus the term current density, j, is introduced:

$$j = I/A \tag{2.14}$$

The rate of an electrode process can be defined as follows;

$$r_j = I/AnF = j/nF \tag{2.15}$$

and has the units of $1/m^2$ s.

The current density of simple reactions increases with the over-potential and is typically represented as a 'polarization' curve in which the logarithm of current density j is plotted against the over potential η as shown in Figure 2.1. (Scott, 1995).

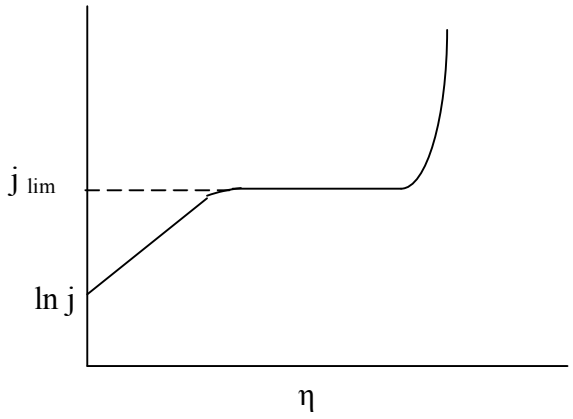

Figure 2.1. A typical polarization curve at an electrode

It is seen that current density and over-potential are exponentially related and the rate of reaction is controlled by kinetics and is said to be under activation control. Departure from this behavior occurs at low potentials when equilibrium is approached and at high over-potentials where the influence of mass transport of reactants becomes an important factor and other reactions will possibly occur.

2.1.4. Types of Electrochemical Processes

When two electrodes are placed in an ionic conducting solution and are connected externally they become charged. Thus, locally at the solution-electrode interface, there is a large potential difference over a molecular scale of a few nanometers. A simple model of this situation consists of a double layer, comprised of a plane of closest approach, i.e. the inner Helmholtz plane, IHP, and a diffuse layer or outer layer as shown in Figure 2.2. The equilibrium established at the interface is electrostatic, somewhat analogous to that in a capacitor. The electrostatic interactions determine the distribution of the potential and the potential difference, which constitutes the driving force for electrochemical (Faradaic) reaction when a current flows through the circuit. An increase in magnitude of the potential

applied between two electrodes increases this potential difference at the interface. This interfacial potential difference is the driving force for the electrochemical reaction.

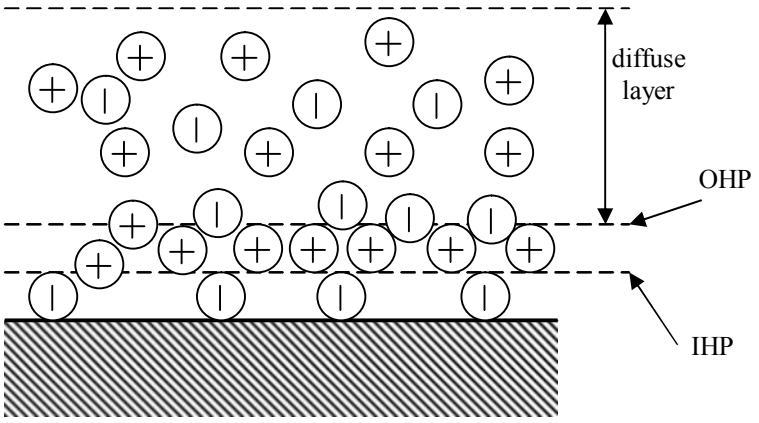

Figure 2.2. Model of the electrode-solution interface and simple electrochemical process (OHP: outer Helmholtz plane; IHP: inner Helmholtz plane)

The types of electrochemical processes, which can occur at the electrode solution interface, can be divided into three general headings:

- Electrochemical reaction
- Electrocatalysis
- Heterogeneous electrocatalysis

2.1.4.1. The Electrochemical Reaction. A simple electrochemical process, shown in Figure 2.3, is established when a reactant undergoes a transformation to a product by the transfer of an electron from the electrode to the species (S) in solution, without contacting or interacting with the surface in any significant way.

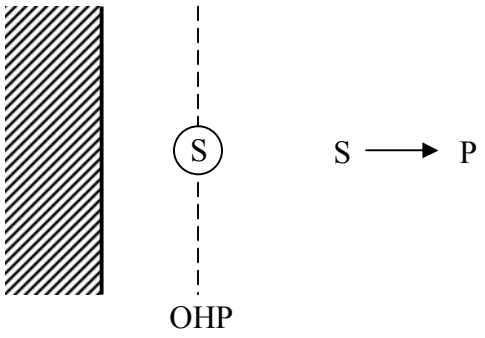

Figure 2.3. Schematic representation of an electrochemical reaction

The role of the electrode is essentially that of a source or sink for electrons, and it does not influence the type of final product species. The nature of the product species is thus determined by the chemistry, which occurs between the species, which has undergone charge transfer, and the electrolyte solution.

2.1.4.2. Electrocatalysis. In heterogeneous catalysis the strong adsorption of a starting material (reactant) at the surface reduces the activation barrier for the reaction to proceed via an intermediate species as shown in Figure 2.4.

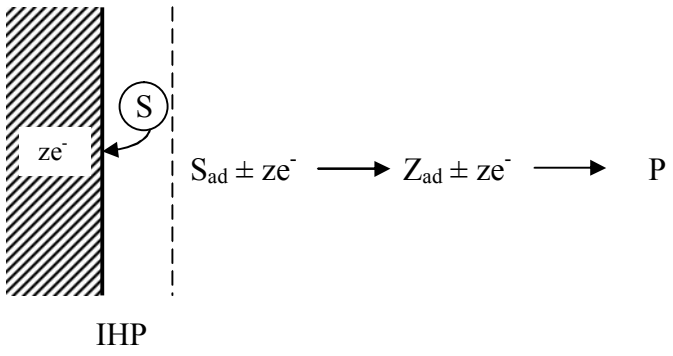

Figure 2.4. Schematic representation of electrocatalysis

The chemical steps in the process, rather than the electrochemical steps, are catalyzed by the interaction with the surface. This, therefore, distinguishes the electrochemical reaction, which is directly affected by the adsorbed species, from the electrocatalytic reaction, where the adsorbed electroactive intermediates are directly involved. The rate constants of electrocatalytic reactions exhibit a wide variation with the type of electrode (electrocatalyst) used. This has also been observed in the case of hydrogen evolution reactions.

The enthalpy of adsorption of hydrogen on a given electrode metal is related to the ease with which the hydrogen evolution reactions (Equation 2.16.) for alkaline and acidic solutions proceed at the respective metal/electrolyte interface. Three different reaction steps can be distinguished and may become rate limiting;

a. Electrochemical adsorption/desorption of electrosorbed hydrogen, the so-called "Volmer Reaction":

$$H^+ + e^- \rightleftharpoons H_{ad} \qquad (2.16)$$

b. Chemical desorption/adsorption of adsorbed hydrogen atoms, i.e. the "Tafel Reaction":

$$2H_{ad} \rightleftharpoons H_{2,\,ad} \rightleftharpoons H_2\,(g) \qquad (2.17)$$

c. Electrochemical desorption/adsorption of adsorbed hydrogen atoms, i.e. the "Heyrovsky Reaction":

$$H_{ad} + H^+ + e^- \rightleftharpoons H_2\ (g) \qquad (2.18)$$

For instance, on nickel electrodes at high current densities all three reactions steps are taking actively part in controlling the overall rate of hydrogen release. The overpotential for a given cathodic current density or the logarithm of the cathodic current density at a given overpotential is a measure of the catalytic activity of a cathode material. Plotting

these values versus the heat of hydrogen adsorption at the respective electrode material, gives the "volcano curve" (Figure 2.5.). This figure indicates that an intermediate adsorption enthalpy for hydrogen is optimal because adsorption is favored, but associative or electrochemical desorption is not yet hindered for moderate adsorption enthalpies of approximately 50 $kJmol^{-1}$ or M - H bond strengths of roughly 240 kJ/mol. This condition is optimally fulfilled at platinum electrodes that are the best H_2 catalyst known (Wendt and Kreysa, 1999).

The formation of adsorbed hydrogen is also responsible for many reduction reactions of organic species. These reactions occur between the adsorbed hydrogen and the organic molecule (probably also adsorbed on the electrode surface) and are only possible on electrode materials which, exhibit a significant coverage of hydrogen atoms. The materials employed are usually Pt, Ni, Rh, Co and Fe.

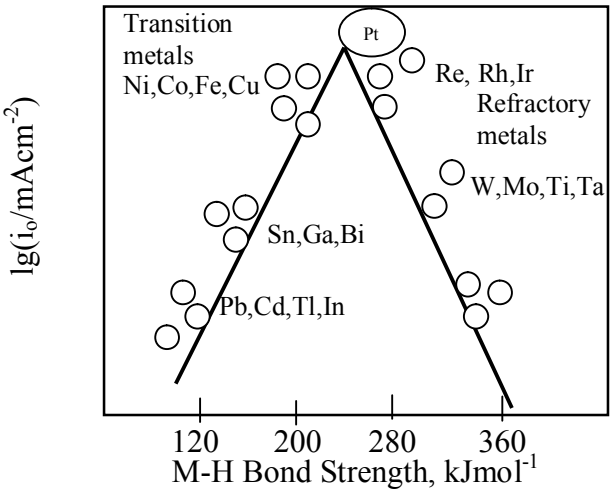

Figure 2.5. The Volcano Curve

2.1.4.3. Heterogeneous Electrocatalysis. The performance of electrochemical processes can be significantly affected if the electrode surface is modified by a layer, at least a monolayer, of a redox system. This redox system can serve as a mediator for the reactant, S, as well as a new surface for adsorbed interactions with reagents and other molecules. The mediator, R, exhibits a typical catalytic behavior, and is continuously regenerated as the reaction occurs (Figure 2.6.). This type of catalysis is termed "redox catalysis" and is

an inner Helmholtz plane process between the adsorbed reactant and the immobilized redox mediator.

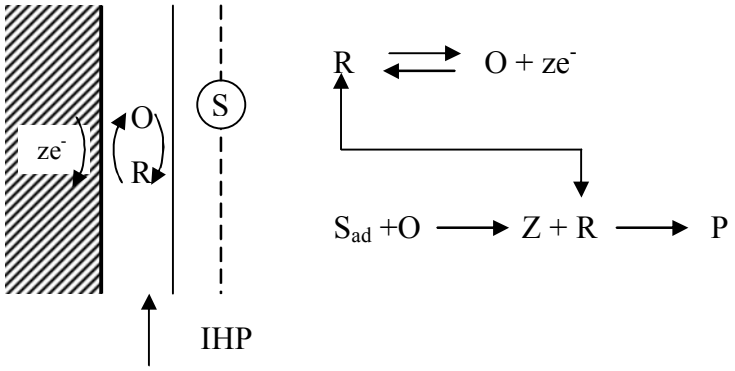

Figure 2.6. Schematic presentation of heterogeneous electrocatalysis reactions

2.1.5. Electrode Materials

A crucial aspect of an electrochemical process is the selection of the appropriate materials for the electrodes. Working electrode and counter electrode materials cannot always be selected independently as there will be important interactions of the cell chemistry to consider. The choice of materials for electrodes is dictated by their corrosion resistance, high conductivity and material strength together with considerations concerning the price of the material and methods applied for shaping and processing the metals and their respective costs. Table 2.1. summarizes the criteria for electrode material selection (Scott, 1995).

Table 2.1. Criteria for electrode material selection

1	Suitable electrocatalytic and electrochemical properties
2	Chemical and electrochemical stability
3	Physical and thermal stability
4	Suitable physical form and fabrication
5	Good electrical conductivity
6	Low over-voltage
7	Environmentally suitable (non-polluting/non-contaminating)
8	Low cost

2.1.5.1. Titanium. Titanium electrodes are state of the art as anodes for chloralkali electrolysis. The reasons are:

- The excellent stability of titanium against surface and pitting corrosion in acidic and slightly basic aqueous solution cannot be met by any steel or nickel alloy.

- The application of RuO_2 coatings or other coatings containing metal oxides or metals of platinum group allows to reduce remarkably the overpotential for anodic chlorine and anodic oxygen evolution.

Titanium cannot be used as cathode material for H_2 evolution because of hydrogen embrittlement of this metal under cathodic H_2 evolution.

2.1.5.2. Lead. Lead is particularly suited for oxygen-evolving anodes in strongly acidic aqueous solutions particularly in aqueous sulfuric acid solutions. Still silver-alloyed Pb/PbO_2 anodes are preferred for metal electrowinning from aqueous sulfuric acid solutions. O_2–evolution overpotential is, however, particularly high on PbO_2 and can be sizably reduced by alloying silver to the lead. Unalloyed Pb/PbO_2 anodes are preferred for some anodic oxidations of organic substrates or inorganic redox couples serving as anodic mediators where O_2 evolution is an undesired side reaction.

2.1.5.3. Nickel. Nickel electrodes are much more expensive than steel electrodes. Therefore nickel is used as a material for electrodes or electrode supports only in cases of enhanced passivity demands. Nickel coated steel electrodes are sometimes a cost efficient compromise but this option does not meet very high quality demands because such coatings are always somewhat porous so that the steel as base-material is still exposed to some extent to the electrolyte. Nickel anodes form NiOOH in alkaline solution on their surface prior to O_2 evolution, which mediates anodic oxidation of organic substrates very effectively, so that Ni anodes are today more and more used for anodic electrosynthesis processes.

2.1.5.4. Noble Metals. Noble metals, in particular platinum metals, are too expensive to be used as bulk materials for electrodes, except for very special applications. It is more appropriate to apply the respective noble metal as a coating to a suitable support. Noble metals and Pt in particular may also be used in the form of thin sheets, i.e. on carbon electrodes fixed to the carbon surface by special conducting glues. Such electrodes are applied, for instance, for the synthesis of dicarbonic acids (Wendt and Kreysa, 1999).

2.1.5.5. Iron, Steel and Aluminum. Iron, steel and aluminum electrodes are the cheapest choice for cathodes and anodes for electrocoagulation and electrofloatation purposes and hence more commonly used in different application. In addition to the adsorption of the contaminants on the resultant metal hydroxides, in case of iron and steel there is evidence for partial direct oxidation at the anode and reduction at the cathode. Aluminum electrodes cannot act as reducing agents since aluminum enters solution in a single valence state as shown in Equation 2.19. In contrast, the iron electrode causes ferrous iron release, which is capable of acting as a reducing agent (Eqn. 2.20.) (Reife and Freeman, 1996);

Anode: $Al \longrightarrow Al^{3+} + 3e^-$ (2.19)

Cathode: $2H_2O + 2e^- \longrightarrow 2OH + H_2$ (2.20)

2.1.5.6. Graphite. For more than 80 years graphite had been used as chlorine evolving anode material. Due to its instability to towards anodic oxidation, which renders this material dimensionally unstable as an anode material, carbon anodes are now substituted by ruthenium dioxide coated titanium anodes in the chloralkali and chlorate industries.

2.1.6. Industrial Applications

2.1.6.1. Treatment of Organic Compounds. The electrochemical treatment or destruction of organics in wastewaters is potentially a powerful method of pollution control. In many cases no other chemicals are released into the wastewaters. Owing to the nature of the process streams and the implications of the electrochemistry, the methods, which are applied, either partially or completely detoxify or decompose the organic species. Complete destruction often means the extended oxidation of the organic species to carbon dioxide (mineralization). This oxidation can be achieved either directly or indirectly at the anode, or indirectly using appropriate anodically generated reagents.

In certain cases the complete destruction of an organic molecule by anodic oxidation is not an appropriate or easy process to perform and a partial transformation may be more desirable. The complete oxidation of large organic molecules requires a large number of electrons and energy consumption can be relatively high, as in the case of the hardware costs. Ideally, current efficiencies for the electrochemical pre - or post - treatment process should be high, but more importantly, any products from the treatment should be either non-toxic, readily biodegradable, or in sufficiently low concentrations to satisfy environmental legislative requirements.

- direct anodic oxidation

Complete conversion of phenol and p-benzoquinone can be achieved with optimum conditions of pH, temperature, and current density. The rate of phenol oxidation is higher on lead dioxide than on either graphite, platinum or nickel (Scott, 1995).

Comninellis (1988) has studied the oxidation of approximately two dozen organic compounds, and proposed two measures for estimating the electrochemical oxidation of

organics (Table 2.2.): The electrochemical oxidation index (EOI) and the electrochemical oxygen demand (EOD).

Table 2.2. The electrochemical oxidation index for various organic compounds

Compound	Pt anode	SnO_2 anode
Ethanol	0.02	0.49
Acetone	0.02	0.21
Acetic acid	0.00	0.09
Formic acid	0.01	0.05
Tartaric acid	0.27	0.34
Oxalic acid	0.01	0.05
Malonic acid	0.01	0.21
Maleic acid	0.00	0.15
Benzoic acid	0.10	0.79
Naphtalene-2-sulfonic acid	0.04	0.51
Naphtalene-1-sulfonic acid	-	0.41
Phenol	0.15	0.60
Aniline	0.56	0.43
Benzenesulfonic acid	<0.05	0.28
Orange-II (Acid Orange 7)	-	0.58
Anthraquinone sulfonic acid	-	0.18
Nitrobenzene	-	0.80
Nitrobenzenesulfonic acid	-	0.46
EDTA	0.03	0.30
4-Chlorophenol	-	0.35

The EOI relates to the evolution of oxygen during electrolysis and is defined as indicated below:

$$EOI = ICE\ dt/t \qquad (2.21)$$

where t is the time of electrolysis and ICE is the instantaneous current efficiency of phenol calculated from the following relationship;

$$ICE = (v-v_{org})/v \quad (2.22)$$

where v is the volumetric rate of oxygen evolved in the absence of the organic species and v_{org} is the oxidation rate in the presence of an organic compound.

The EOD (g O_2/g organic) is calculated from the below relationship as follows:

$$EOD = 8(EOI \cdot I \cdot t)/F\ [PhOH] \quad (2.23)$$

where [PhOH] is the initial molar concentration of the organic species.

Platinum anodes have a limited range of oxidation potentials and thus attention has focused on SnO_2 coated titanium materials. The tin oxide material, particularly when doped with Sb to impart the appropriate electrical conductivity, exert oxygen overpotentials some 600 mV greater than those of platinum.

Tin oxide is a superior anode material to platinum in removing TOC during the oxidation of phenol. With SnO_2, only residual amounts of intermediates (hydroquinone, cathecol, benzoquinone) remain after oxidation. Aliphatic acids (oxalic, fumaric and maleic) are rapidly oxidised at a SnO_2 anode, are almost inactive at platinum.

Tin oxide has also been proposed as a material for electrochemical oxidation of biorefractory organics in wastewater (Kotz et al., 1991). This electrochemical oxidation is seen as an alternative to chemical treatment, using powerful oxidants such as ozone or hydrogen peroxide, prior to discharge to a biological treatment plant.

Other applications of anodic oxidation reactions are listed below;

- spent wash water from distillery effluent containing high biological oxygen demand (BOD), high COD and dark-brown color,
- wastewaters containing alcohols and sugars,

- effluents originating from the production of amino ether,
- treatment of dyes and surfactants,

- indirect oxidation processes

There are three general categories of indirect oxidation, namely heterogeneous oxidation at oxide anodes, generation of "active" chlorine, generation of short life species like ozone and hydroxyl radicals and regenerable solution redox couples.

(i) ozone production

Among other chemical oxidation methods, ozonation is an attractive alternative for water treatment, as it does not release any additional reagents into the waters. Ozone can be generated electrochemically from relatively pure water according to the reaction:

$$3\ H_2O \longrightarrow O_3 + 6H + 6e^- \qquad (2.24)$$

An inherent advantage of electrochemical generation is the on-site, on-demand production of ozone at a concentration much higher than can be achieved by other methods.

(ii) redox couples

Silver in the +II oxidation state is a powerful oxidizing agent. This specie can be produced by the anodic oxidation of Ag(I) ions:

$$Ag^+ \longrightarrow Ag^{2+} + e^- \qquad (2.25)$$

In nitric acid, the following (dark brown) complex is formed:

$$Ag^{2+} + NO_3^- \longrightarrow AgNO_3^+ \qquad (2.26)$$

which then reacts with water or with an oxidizabe pollutant. At the end of the reaction the dark brown color fades away, signaling the reduction of Ag(II) to Ag(I) .

Table 2.3. contains a listing of the redox reagents that have been successfully used for pollutant treatment, and the corresponding redox potentials.

Table 2.3. Redox mediators for the indirect electrolysis of pollutants

Mediator Couple	Standard Reduction Potential, V
Ag(I/II)	1.98
Co(II/III)	1.82
Ce(IV/III)	1.44
Fe(II/III)	0.77

Relative to the Ag(I/II) couple, the Fe(II/III) couple has a much less positive reduction potential (i.e. 0.77 V), which should substantially lower the electrical (operational) cost that accounts for up to 90% of the total operating cost. Cellulosic materials, fats, urea, sewage sludge, meat packing wastes, ethylene glycol and the like have been treated. Electrolytic grade H_2 gas is produced at the cathode with efficiency up to 99%; this can be used in a fuel cell to generate electricity (Rajeshwar and Ibanez, 1997).

2.1.6.2. Treatment of Wastewaters Containing Inorganic Compounds.

- cyanide removal

Several methods for cyanide destruction have been adopted and proposed based on the oxidation of the cyanide to cyanate, which then decomposes further to innocuous products such as carbonate and nitrogen. Electrochemical methods of cyanide treatment use direct oxidation and indirect oxidation. The electrochemical method offers the advantages of reduced handling of reagents and in many applications the possibility of simultaneous recovery of dissolved metal ions.

The overall reaction proposed is:

$$CN^- + 2OH^- \longrightarrow CNO^- + H_2O + 2e^- \quad (2.27)$$

The produced cyanate ions, CNO^-, are approximately 1000 times less toxic than CN^- ions.

When NaCl is added to the electrolyte to increase its conductivity, the mechanism switches to an indirect oxidation since Cl_2 is produced and it oxidizes cyanide (Ogutveren et al., 1993).

• chromium removal

Liquors containing dissolved chromium are used in a number of sectors of the process industries in applications such as plating and coating, metal finishing and as oxidizing and reducing agents. The most common form is hexavalent chromium, which is highly toxic to man and to aquatic life.

Precipitation is used to remove the chromium originating from metal-finishing streams and cooling waters using undivided cell with steel electrodes. The anode side dissolves to form Fe(II) ions, and the cathode side of the electrodes generates hydroxide ions through the formation of hydrogen gas. The Fe(II) and OH^- ions combine in the overall process, which involves the reduction of Cr(VI) to Cr(III) by Fe(II) with the subsequent precipitation of the insoluble hydroxides of chromium, Fe(II) and Fe(III);

$$3\ Fe^{2+} + CrO_4^{2-} + 4H_2O \longrightarrow 3Fe^{3+} + Cr^{3+} + 8OH^- \quad (2.28)$$

2.1.6.3. Electrochemical Fenton Processes. The combination of H_2O_2 and a soluble ferrous salt, i.e. “Fenton’s reagent,” is an effective oxidation process that has been applied for a wide variety of organic substrates. The Fenton reaction involves the following sequence of major steps;

$$Fe^{2+} + H_2O_2 \longrightarrow Fe^{3+} + OH^- + OH^\bullet \quad (2.29)$$

$$Fe^{2+} + OH^{\bullet} \longrightarrow Fe^{3+} + OH^{-} \quad (2.30)$$

$$H_2O_2 + OH^{\bullet} \longrightarrow HO_2^{\bullet} + H_2O \quad (2.31)$$

$$Fe^{2+} + HO_2^{\bullet} \longrightarrow Fe^{3+} + HO_2^{-} \quad (2.32)$$

Of these, only reaction (2.29) is desirable from the point of view of $OH^{\cdot}$ production. On the other hand, reactions given in Eqn.s 2.30. to 2.32. are H_2O_2 consuming, and thus a substantial portion of the theoretical oxidation equivalent of the H_2O_2 is unavailable for oxidation of the organic substrate. A further difficulty is that Fe^{3+} accumulates in the system via reactions 2.29., 2.30., and 2.32., and the Fe^{2+} ion catalyst is therefore not efficiently regenerated.

There are two main types of Fenton processes involving the use of in-situ electrochemically produced reagents. They differ mainly in the form in which the iron enters the system. In the cathodic Fenton processes, the iron is added as an Fe(II) salt or Fe(III) salt, whereas in anodic Fenton processes the source of the iron is a sacrificial iron anode.

- the cathodic Fenton process

In cathodic processes there are several possibilities in which one or both of the reagents Fe(II) and H_2O_2 are produced in-situ. The source of Fe(II) may be direct Fe(II) addition or it may be produced by reduction of Fe(III) at the iron cathode. The source of H_2O_2 may be either direct H_2O_2 addition or it may be produced by reduction of dioxygen at the cathode (Eqn. 2.33.);

$$O_2 + 2H^{+} + 2e^{-} \longrightarrow H_2O_2 \quad (2.33)$$

Simultaneous Fe(III) and O_2 reduction can take place at the cathode at comparable rates. Since Fe(II) and H_2O_2 are continuously produced at controlled rates, this leads to a more efficient and complete degradation of the contaminant as compared with the classic Fenton systems where all the reagents are typically added at the beginning of the reaction. This is because there are less competitive reactions, which consume reagents without producing hydroxyl radicals.

The electrochemical cell is undivided and has an anode made from inert material such as platinum, platinised titanium or dimensionally stable anode (DSA). The cathode is made from carbon-containing materials such as carbon felt or carbon polytetrafluoroethylene (PTFE) and is supplied with oxygen.

The electro-Fenton systems may also be exposed to irradiation by UV/visible light, leading to the photoelectro-Fenton process.

- the anodic Fenton process

In the anodic Fenton process, an iron electrode is used as the anode and becomes the Fe(II) source. The system consists of two electrochemical cells, with a salt bridge providing electrical connectivity between the cells and a graphite electrode used as a cathode. The anodic Fenton treatment (AFT) has several advantages over the classical Fenton processes. These are listed below;

- The AFT occurs under acidic conditions (pH 2 to 3), unlike the cathodic Fenton treatments, which operate under neutral conditions, hence it has a higher efficiency. The pH of the final treated effluent can be partially neutralized by combining the solutions from the anodic and cathodic half-cells.

- Since Fe(II) is produced by controlled electrolysis using a sacrificial iron electrode, consequently, there is no need to handle Fe(II) or Fe(III) salts.

A modification of the electro-Fenton process involving the use of a sacrificial iron anode makes use of an undivided electrochemical cell. Since the solution cannot be maintained in the acidic pH range, this process is characterized by precipitation of iron hydroxides (Wadley and Waite, 2004).

2.1.6.4. Electrofloatation, Electrocoagulation and Electroflocculation. Electrofloatation involves the electrolytic production of gases that can be used to attach pollutants to the gas bubbles and carry them up to the solution where they can be more easily collected and removed. Electrocoagulation refers here to the electrochemical production of destabilization agents that bring about charge neutralization for pollutant removal. Electroflocculation is the electrochemical production of agents that promote partical bridging or coalescence.

If hydrogen gas is produced on the cathode and Fe or Al are used as anodes, the Fe^{2+}, Fe^{3+} or Al^{3+} ions resulting from the oxidation of the anode can react with the OH^- ions produced at the cathode and yield insoluble hydroxides that will precipitate, adsorbing pollutants out the solution. This reaction mechanism will contribute to the coagulation – flocculation processes. Since Fe(III) hydroxide precipitates more easily than Fe(II) hydroxide, air or oxygen may be injected into the solution to oxidize Fe(II) to Fe(III) and aid in the flotation process.

In case of iron or steel anodes, two mechanisms for the production of the metal hydroxide have been proposed; shown as Mechanism I and II (Wilcock et al.,1992);

Mechanism I:

Anode: $4Fe(s) \longrightarrow 4Fe^{2+} + 8e^-$ (2.34)

Chemical: $4Fe^{2+}(aq) + H_2O(l) + O_2 \longrightarrow 4Fe(OH)_3(s) + 8H^+(aq)$ (2.35)

Cathode: $8H^+ + 8e^- \longrightarrow 4H_2(g)$ (2.36)

Overall: $4Fe(s) + 10\ H_2O(l) + O_2 \longrightarrow 4Fe(OH)_3(s) + 4H_2(g)$ (2.37)

Mechanism II:

Anode: $Fe(s) \longrightarrow Fe^{2+} + 2e^-$ (2.38)

Chemical: $Fe^{2+}(aq) + 2OH^- \longrightarrow Fe(OH)_2(s)$ (2.39)

Cathode: $2\ H_2O(l) + 2e^- \longrightarrow H_2(g) + 2OH^-(aq)$ (2.40)

Overall: $Fe(s) + 2H_2O(l) \longrightarrow Fe(OH)_2(s) + H_2(g)$ (2.41)

Electrocoagulation offers several advantages, including the following (Rajeshwar and Ibanez, 1997):

- The formation of extremely fine dispersed gas bubbles (diameter = 8-15 μm), allows the flotation and removal of very fine particles. Furthermore, such motion avoids the need for mechanical agitation, which (if uncontrolled) may destroy precipitates as soon as they are formed.
- The creation of a very wide range of bubble concentration is possible by varying the current density. Thus a gas medium with an overall large surface area is formed during flotation, increasing the probability of bubble/particle collision and adhesion.
- The amount of required chemicals is much lower as compared to conventional coagulation.
- A smaller amount of sludge is produced, due to the higher content of dry solids. In addition, the sludge produced by electrochemical treatment is more hydrophobic, which lead to more compact residues ultimately leading to shorter decantation times.
- No mixing of chemicals required.
- The durability of electrodes translates to low "down times" for maintenance or replacement.
- Organic matter removal (including nonbiodegradable organics) is more effective, which facilitates subsequent biological treatment.
- Coagulant dosing as well as required overpotentials can be easily calculated and controlled
- A pH increase is normally observed, which aids in the removal of heavy metal ions by their precipitation as hydroxides or by adsorption into other flocs or precipitates.
- Often, pH control is not necessary, unless this parameter acquires extreme values; this facilitates process design and operation.
- High current efficiencies (90%) can be achieved in well-designed systems.
- Only very short contact times (a few min) are required.
- Operating costs are much lower when compared with most of the conventional technologies.

- clean-up of oil/water emulsions

The main interacting forces between emulsion droplets can be both van der Waals and electrostatic in nature. Oil colloidal particles generally have negative charges on their surface due to the frictional charging or the ionization of the hydrophilic carboxylic groups. These charges are mainly responsible for the repulsion forces that prevent the particles from colliding and having a chance to flocculate or coalescence. Addition of positively charged cations neutralize the colloids and enable flocculation or coalescence to occur. Organic and inorganic coagulants such as polyamines, $AlCl_3$ or $FeSO_4$ are usually employed. Unfortunately, these processes require relatively large amounts of chemicals as well as long periods of time for their handling, produce considerably large amounts of sludge, and are unable to coagulate the finest and smallest colloids (Pouet et al., 1992).

The addition of metallic ions with high charge densities by the controlled electrodissolution of soluble metal anodes like Fe, Al and steel, is a very effective alternative. Here, the potential at the anode must be controlled; if this anode becomes too positive it can become passivated and its dissolution will stop. On the other hand, if the applied potential is not positive enough the metal dissolution will not feasible (Weintraub et al., 1983)

The corresponding cathodic reaction is normally the reduction of H_3O^+ at an inert cathode. Here, H_2 gas evolves and carries upward flocs or precipitate that provide a large surface area for the adsorption of oil particles and other impurities that may be contained in the aqueous solution. The concomitant pH increase facilitates the flocculation or precipitation of hydroxides of metallic ions as sludge. The oil layer and the solid sludge produced in this electrocoagulation-electrofloatation process can then be mechanically removed. Oil removal efficiencies of up to 96-99% can be achieved (Biswas and Lazarescu, 1991).

- dye removal

Aluminum and iron anodes have been used for the electrogeneration of hydroxide flocs that adsorb and remove disperse, metal complex, and acid dyes and other pollutants (such as metal ions or compounds) from the wastewater. The aluminum based process seems to remove dyes by adsorption mechanism without chemically altering their structure, whereas iron anodes were found to additionally yield other degradation products, possibly due to the action of reducing Fe^{2+} ions. Likewise, the iron process seems to be more effective for reactive dyes, whereas the aluminum process is superior for disperse dyes. Addition of oxidizing agents favors the formation of Fe(III) hydroxide, which is more effective than Fe(II) hydroxide for color removal. Nevertheless, high decolorization rates are achieved in all cases as well as a considerable lowering of toxicity.

In addition to the pollutant removal mechanisms with electrogenerated metal hydroxides, chemical modification may occur here by direct or indirect electron transfer to or from the electrodes. For example, -C=C- and -N=N- bonds are susceptible to catalytic hydrogenation or reduction in the presence of H_2 and a catalyst.

- other uses of electrocoagulation and electrofloatation

(i) Phosphorus removal: Phosphate can be removed from aqueous media by anodic dissolution of Fe or Al to yield insoluble $AlPO_4$ or $FePO_4$ with simultaneous phosphate adsorption on the corresponding insoluble hydroxides. Phosphates and organic nitrogen have been simultaneously removed by this method.

(ii) The treatment of waters containing food, protein wastes, synthetic detergents, and fluorides.

2.1.7. Electrochemical Treatment of Textile Wastewaters

2.1.7.1. Direct Oxidation. Chen et al. (2003) examined the physicochemical and electrochemical properties as well as the activity of Ti/B-diamond electrodes for anodic oxidation of various dyes. They found that the Ti/B-diamond electrodes were much more active than Ti/Sb_2O_5-SnO_2. 17 reactive dyes were found to be mineralized at Ti/B-diamond, with current efficiencies of 51.0-90.2% and with energy consumption ranging between 8.9 to 17.9 kWh/m^3. The COD of 1000 mg/L solutions of Orange II and reactive red HE-3B were found to be reduced from 1120 mg/L to 100 mg/L and from 920 mg/L to 50 mg/L respectively at 100 A/m^2 current density and pH of 4.7-6.73.

2.1.7.2. Electro-coagulation/flocculation. Lin and Peng (1993) investigated the treatment of textile wastewaters from several dyeing and finishing mill by electrochemical method using sacrificial iron electrodes. The wastewater conductivity, pH, power requirement and addition of polyelectrolyte were explored to determine their on the treatment efficiency. They found that there is no need to adjust the pH of the most of the wastewaters as it is in the range between 5 and 10. In addition the conductivity of the wastewaters were found to be within the optimum range. Addition of PAC up to 40 mg/L has been observed to significantly enhance the treatment efficiency. A current density of about 92.5 amp/m^2 was found to yield a maximum COD removal (62%). The COD removal of the continuous runs operating at the optimum conditions obtained from batch experiments fluctuated around 51% and the transparency of the treated wastewater was above 20 cm.

Do and Chen (1994) studied the electrocoagulation of Drimarene Discharge x-3LG (R12S) and Samaron Yellow 4 (D05H) dyes and tested the effects of sacrificial anodes, initial pH, rate of stirring on the treatment performance. The experimental results showed that the color of dyes in aqueous solution were effectively removed using iron and aluminum electrodes. Iron was found to be a more suitable sacrificial anode than aluminum, when the concentration of R12S exceeded 300 mg/L. In case of D05H, aluminum was found to be superior to iron when the concentration of D05H exceeded 300 mg/L. They found that using iron electrode as sacrificial anode, the residual fraction of R12S was decreased below 10% when the initial concentration of R12S and charge passed

were 500 mg/L and 120 C, respectively. The decolorization fraction of D05H was found to be 99% when aluminum was used as sacrificial anode.

Chua et al. (1998) examined the treatability of textile dyeing and finishing wastewater composites by electrocoagulation under different operating conditions (i.e. dyestuff type & concentration, electric current, temperature, pH, sodium salt type, electrode type, spacing & surface area). Both batch (jar test) and continuous (4-stage pilot scale plug flow) type electrocoagulation systems could be used effectively for almost complete color removal from the dyeing wastewaters. The proposed system is particularly suitable for cost effective and simple textile wastewater treatment in areas with lack of space (South – East Countries) Electrocoagulation in the sequential, continuous flow pipe reactor was optimized for color removal (pH 6-9; electrode spacing 2 cm; electrode surface area 0.36 m^2) that was around 80 % at 4 A, a wastewater flow rate of 1 L/min (HRT = 20 min) using iron electrodes.

Ciarelli and Ranieri (2000) investigated the treatability of biologically pre-treated wastewaters coming from several finishing and dyeing plants with ozone (20-50 mg/L) and pilot-scale electroflocculation (water flow up to 2 m^3/h; 40-60 A alternating and constant current; iron/aluminum electrodes). Results have indicated that practically complete color removal (95 – 99 %) and up to 60 % COD removal can be achieved via ozonation. Despite the fact that COD removal was rather incomplete, satisfactory dyeing of even light colors with the treated effluent was possible. Electrochemical treatment showed also promising results in terms of color (80 – 100 %) and COD (70 – 90 %) removal. Moreover, significant reduction in chloride and sulphate ion concentrations was also obtained. The authors note that biological pre-treatment and sand filtration are essential prior to ozonation for high efficiency and low operating costs whereas in the case of electrochemical treatment post – treatment (i.e. removal of flocculated material) is required to establish a correct cost-benefit ratio for real – scale implementation.

2.1.7.3. Photoelectrochemical treatment. Hepel and Luo (2001) investigated the photoelectrochemical degradation of Naphtol Blue Black (NBB) dye using nanocrystalline WO_3 electrodes. A strong pH dependence of the NBB dye degradation rate has been found in chloride media. In the low pH range (1.0-4.5), dye degradation occurred due to the formation of $Cl^{\cdot}$ and $Cl_2^{\cdot}$ radicals, whereas in alkaline solutions the formation of $OH^{\cdot}$ radicals was dominant. Therefore, NBB dye degradation rate has been found to be much slower in acidic media. In chlorine solutions NBB degradation rate has been found to be much faster than in sulfate solutions due to the lower oxidizing power of the dipersulfate ion ($S_2O_8^{2-}$).

2.1.7.4. Indirect Oxidation. Szpyrkowicz et al. (2001) have reported an experimental study on the destruction of a synthetic disperse dye-bath (COD_o = 1425 mg/L) electrolytically supported with chloride (7140 mg/L as NaCl) and sulphate (8250 mg/L) using ozone at pHo = 8 (applied dose = 0.36 g/h), Fenton reagent (250 mg/L Fe^{2+} and 300 mg/L H_2O_2 at pH_o = 3), hypochlorite (744 – 5955 mg/L Cl_2 at a fixed pH of 8.5) and electrochemical oxidation under a constant current of 2 mA/dm^2, using seven different anodic materials (such as Ti/Pt, Ti/RuO_2, $Ti/MnO_2 – RuO_2$ etc.). The work aimed to compare the effectiveness of indirect/direct electro-oxidation of disperse dyes with that of conventional chemical oxidation methods. It could be demonstrated that hypochlorite oxidation did not give satisfactory results in terms of color removal and that ozonation enabled 90 % color removal at a dose of o.5 g/L wastewater but only low (10 %) COD reduction. Much more efficient was electrochemical oxidation (at pH = 4, 40 min electrolysis time) using the Ti/Pt-Ir electrode, for which the highest COD removal efficiency could be obtained together with 90 % reduction in color. The pre-dominating oxidation process leading to COD and color abatement has been proven to be “indirect oxidation” by means of chlorine derivatives. However, electrochemical treatment was not able to outperform the performance of the Fenton’s process that resulted in complete color abatement and COD removal down to 100 mg/L levels.

2.1.7.5. Catalytically assisted electrochemical oxidation. Shen et al. (2002) studied the degradation of the textile dye Acid Red B (60 mg/L) in a catalytically assisted electrochemical oxidation system with rutile $_{type}$ TiO_2 semiconductor suspended in an electric field (anodes: graphite and Ti/PbO_2; cathode: activated carbon felt; electrode surface area: 50 mA/cm^2). The addition of catalyst enhanced color removal to 100 % instead of 75 % in its absence, whereas TOC removal kinetics were accelerated by a factor of 2 (to about 75%) in the presence of catalyst provided that Ti/PbO_2 was employed as the anodic material. Biodegradability as also improved after catalytic electrolysis. Results of the IR analysis have revealed that the -N=N- (azo) bond of the dye must be cleaved by OH radical attack and oxidized to nitrate.

2.1.7.6. Electro-Fenton, Photo-Electro-Fenton. Lin and Chen (1997) studied the treatment and reuse of wastewater from the secondary wastewater treatment plant of a dyeing and finishing mill using electrochemical method with steel electrodes, chemical coagulation and ion exchange. The electrochemical method was used to remove color, turbidity and COD of the wastewater while ion exchange was employed to further lower the COD, Fe ion concentration, conductivity and hardness. The addition of hydrogen peroxide was found to significantly enhance the treatment process in terms of COD and color removal. The COD and color removal improved from 33% to 78% and 83% to 92% with an addition of 100 mg/L H_2O_2. The enhancement in the efficiency of electrochemical treatment was explained by the combined effects of H_2O_2 and Fe ion. The settling efficiency of the electrochemical treatment has been improved by the addition of 100 mg/L polyaluminum chloride (PAC) and 1 mg/L polymer. Cationic and anionic ion exchange resins have been used in order to further elevate the water quality to the reuse standard. The total hardness was found to be reduced from 50-75 mg/L to 10 mg/L while the Fe ion concentration was reduced from 1 mg/L to 0.1 mg/L.

Bandara et al. (1998) studied the degradation of the acid dye Orange II (Acid Orange 7; 450 mg/L and 60 mg/L in C) by 0.92 mM Fe^{3+}/ 10 mM H_2O_2/near-UV (photo-Fenton at pH_o = 2-10) and electrochemical methods (pH = 2.9; Pt anode and Zr cathode; 100 mA/cm^2; 3.2 V; in the presence of 50 mg/L Na_2SO_4 added as the electrolyte). Practically complete decolourization and mineralization was reached in a few min and

approximately 7 h irradiation during the photo-Fenton process, whereas the rate of color and TOC removal was rather poor for electrochemical treatment. The main organic intermediate found during electrochemical oxidation of Orange II was sulfanilic acid.

2.2. Ozonation and Environmental Applications

2.2.1. Physical Properties of Ozone

Ozone (O_3, molecular weight: 48 g/mol) with its characteristic pungent odor is colorless at room temperature and condenses to a dark blue liquid. It is generally encountered in dilute form in a mixture with oxygen or air. Liquid O_3 is very unstable and will readily explode. Concentration of O_3 in air-oxygen mixtures above 30% are easily exploded. Explosions may be caused by trace catalysts, organic materials, shocks, electric sparks, or sudden changes in temperature or pressure. Ozone absorbs light in the infrared, visible, and ultraviolet at certain wavelengths.

Ozone is more soluble in water than is oxygen, but, because of a much lower available partial pressure, it is difficult to obtain a concentration of more than a few milligrams per liter under normal conditions of temperature and pressure. Figure 2.7. depicts the theoretical solubility of O_3 in water under standard conditions. Ozone promptly decomposes in water, but this is probably due to its strong oxidizing ability rather than a simple decomposition phenomenon. Inorganic, organic salts and hydroxyl ions accelerate its decomposition. Ozone is much more soluble in acetic acid, acetic anhydride, propionic acid, propionic anhydride, dichloroacetic acid, cloroform, and carbon tetrachloride than it is in water.

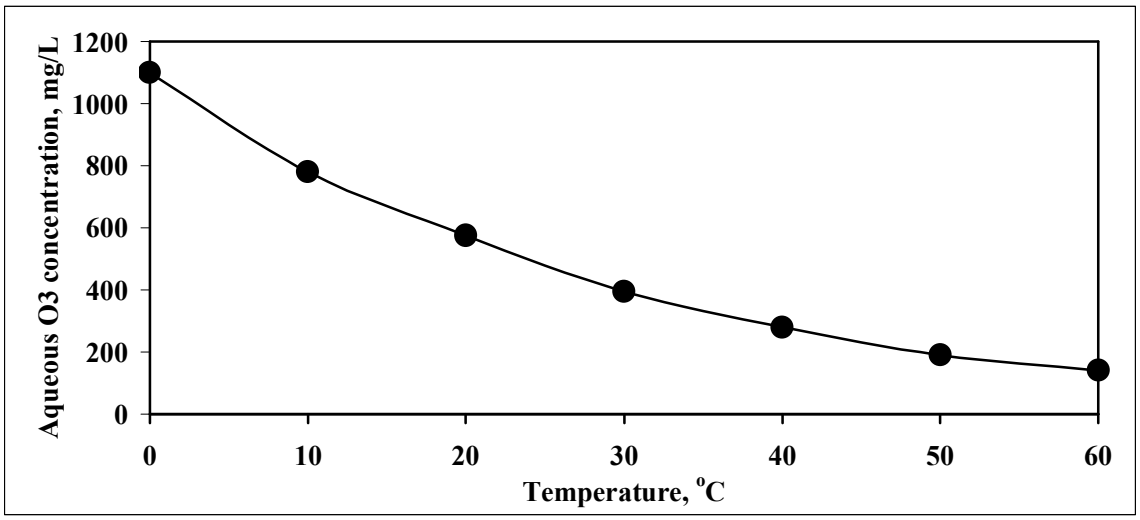

Figure 2.7. Solubility of ozone in water (Sotelo et al., 1989)

2.2.2. Chemical Properties of Ozone

Ozone is naturally unstable and readily decomposes to oxygen. Heat accelerates its decomposition, which is instantaneous at temperatures of several hundred degrees C. Moisture, silver, platinum, manganese dioxide, sodium hydroxide, soda lime, bromine, chlorine, nitrogen pentoxide catalyzes decomposition. Ozone is also decomposing photochemically. From a practical standpoint, decomposition is slow enough to permit the use of ozonized air or oxygen streams for water disinfection. Ozone is a powerful oxidant. Only fluorine, F_2O, atomic oxygen and rather unstable free radicals such as •OH have higher electronegative oxidation potentials. Ozone retains this strong oxidizing ability in aqueous solution. It attacks most metals except gold and platinum. The presence of trace reducing agents may account for the instability of aqueous O_3 solutions.

Ozone behaves as a selective oxidizing agent in many reactions. However, temperature, pH, accumulation of reaction products, the presence of solvents, etc. may alter the predicted reaction in aqueous solution. Ozone may react with activated carbon to form explosive end products and this fact should be kept in mind in tertiary treatment applications. Probably ozone's great ability to oxidize organics accounts for its widespread use in removing color, odor and tastes. This same ability can and has been used to kill pathogens in water (disinfection).

2.2.3. Ozone Kinetics

Ozone's high level of chemical energy is the driving force for its decomposition. The ozone molecule readily reverts to elemental oxygen during the oxidation-reduction reaction (Montgomery, 1985).

When ozone gas is introduced into the water different mechanisms affect its absorption in water and its reactions with aqueous contaminants. Many studies have been accomplished concerning the decomposition kinetics of aqueous ozone. Hoigné and Bader (1976) as well as Glaze and Kang (1992) have already demonstrated that the rate of O_3 decomposition is a complex function of temperature, pH and concentration of organic solutes and inorganic constituents.

In water, ozone may react directly with dissolved substances, or it may decompose to form secondary oxidants such as $OH^{\bullet}$ radicals, which then themselves immediately react with solutes. The decomposition of aqueous ozone is generally due to chain reactions involving $OH^{\bullet}$ radicals. Different reactions pathways lead to different types of kinetics (Staehelin and Hoigné, 1985).

Ozone's high level of chemical energy is the driving force for its decomposition. Staehelin and Hoigné (1986) showed that the mechanism of ozonation specially changes at elevated pH (> 11). A chain reaction mechanism was postulated which involves the intermediacy of $OH^{\bullet}$. The reaction mechanism of ozone with another substrate may involve both direct, selective reaction of ozone with the substrate (typically electrophylic addition reactions) and that of the substrate with $OH^{\bullet}$, even at neutral pH the relative proportions of which will depend on various organic and inorganic species present or added;

$$O_3 + OH^- \longrightarrow HO_2^- + O_2 \qquad k_1 = 70\ 1/M.s \qquad (2.42)$$

$$HO_2^- + O_3 \longrightarrow O_3^{\bullet-} + HO_2^{\bullet} \qquad k_2 = 2.8 \times 10^6\ 1/M.s \qquad (2.43)$$

$$HO_2^{\bullet} \longrightarrow O_2^{\bullet-} + H^+ \qquad pK_3 = 4.8 \qquad (2.44)$$

$$O_2^{\bullet-} + O_3 \longrightarrow O_3^{\bullet-} + O_2 \qquad k_4 = 1.6 \times 10^9\ 1/M.s \qquad (2.45)$$

$$O_3^{\bullet-} + H^+ \longrightarrow HO_3^{\bullet} \qquad k_5 = 5 \times 10^{10}\ 1/M.s \qquad (2.46)$$

$$HO_3^{\bullet} \longrightarrow OH^{\bullet} + O_2 \qquad k_6 = 1.4 \times 10^5\ 1/M.s \qquad (2.47)$$

$$HO_2^{\bullet} + O_2^{\bullet -} \longrightarrow HO_2^{-} + O_2 \qquad k_8 = 8.7 \times 10^7\ 1/M.s \qquad (2.48)$$

$$OH^{\bullet} + R \xrightarrow{k_9} ROH^{\bullet} \longrightarrow RO_2^{\bullet} \longrightarrow P \quad k_9 = 10^8 - 10^{11}\ 1/M.s \qquad (2.49)$$

The net overall reaction for OH^- - initiated O_3 decomposition is;

$$3\ O_3 + OH^- \longrightarrow 2OH^{\bullet} + 4O_2 \qquad (2.50)$$

Figure 2.8. shows reaction pathways of ozone as they have been described by Glaze et al. (1987). Once ozone enters solution, it follows two basic modes of reaction; i.e. direct oxidation, which is rather slow and extremely selective, and auto-decomposition to less selective and short-lived reactive free radicals. Decomposition to hydroxyl radicals is catalyzed by the presence of high concentrations of hydroxide ions (high pH), hydrogen peroxide, UV-light, or organic radicals. The hydroxyl radical is extremely fast and nonselective in the oxidation of organic compounds. These compounds all act as free radical chain initiators and promoters. At the same time, hydroxyl radicals are scavenged by carbonate and bicarbonate ions to form carbonate ($CO_3^{\bullet}$) and bicarbonate ($HCO_3^{\bullet}$) radicals. Thus, conditions of low pH or high alkalinity favor the slow direct oxidation reactions (surpression of ozone decomposition), whereas elevated pH conditions or high concentrations of organic matter favor the autodecomposition route (Hoigne and Bader, Glaze and Kang).

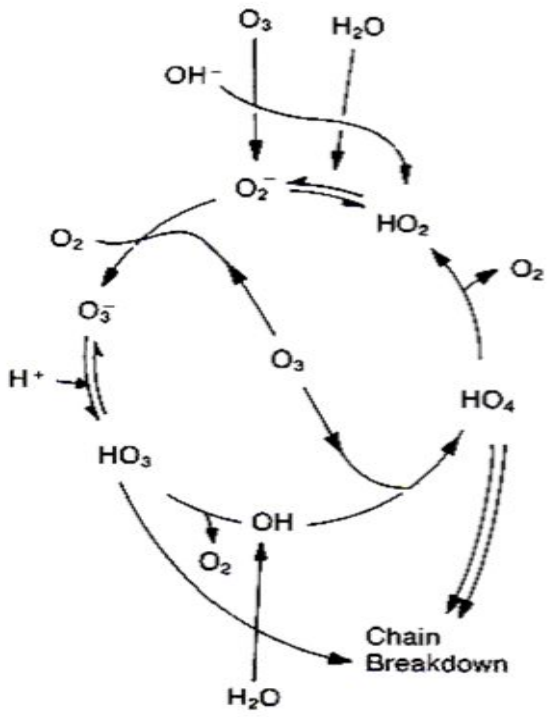

Figure 2.8. Reaction pathways of ozone (Hoigne and Bader, 1985)

Ozone is capable of oxidizing a variety of organic materials in aqueous solution. The major mechanisms contributing to the removal of organic pollutants can be identified as physical stripping and chemical oxidation by ozone molecules (direct bimolecular oxidation) and by free radicals (indirect oxidation) (Gurol, 1985). Gurol and Singer (1983) described the process of oxidation by ozone in an ozone contactor involving the phenomenon of mass transfer with simultaneous reactions. They have pointed out the following for the understanding of the process:

- The interrelationship between partial pressure of the gaseous ozone and the solubility on water and the rate of mass tranfer of ozone from the gas phase into solution,
- The kinetics of auto-decomposition of ozone in water,
- The kinetics of the oxidation of the substrate and their oxidation products by molecular ozone.

2.2.4. Toxicity of Ozone

The effects of O_3 breathing on human health can vary from coughing and sneezing to nausea and even death, depending upon the concentration of O_3 and the duration of exposure. Since people can begin to detect the odor of O_3 at about 0.01 ppm in air, plant operators can easily leave the area or take corrective action when they encounter this odor. In practice, men's health is seriously affected if the O_3 level reaches 1.0 ppm in air.

2.2.5. Generation of Ozone

O_3 must be generated on-site where it is to be used. In general, it is produced by one of the following techniques (Saupe and Wiesmann, 1998):

- electrical (corona) discharge,
- electrolysis of perchloric acid
- irradiation with ultra violet (UV-C) lamps.

Relatively high concentrations of ozone can be produced by the first two methods. The only practical method of large-scale O_3 production is the electrical discharge method. Ozone is produced according to the following endothermic reaction (Gottschalk and Saupe, 2000):

$$3O_2 \xrightarrow{\text{Silent electrical discharge}} 2O_3 \qquad (2.51)$$

Ozonized air contains some nitrogen pentoxide (N_2O_5) and also nitrous oxide (N_2O), which is inert. The more moisture in the air the higher the concentration of N_2O_5. More research is needed to find better ways to produce and dissolve O_3 in water or wastewater that is to be treated.

2.2.6. Determination of Ozone

One of the problems encountered in the use of O_3 for water disinfection has been the difficulty of accurate determination of aqueous O_3 remaining in water. The present standard quantities method (IOA,1987a) for O_3 in water involves the oxidation of KI to I_2 in the presence of excess iodide. However, new methods for determining O_3 in air and water have appeared regularly in the literature. This fact suggests some limitations are connected with all of the existing methods. When the O_3 concentration is less than about 1.0 mg/L, some methods may not be accurate. The most often used analytic procedures are the colorimetric indigotrisulfonic acid and the iodometric methods.

In neutral or alkaline solutions, O_3 reacts with iodide according to the following reactions:

$$H_2O + O_3 + 2I^- \longrightarrow O_2 + I_2 + 2OH^- \qquad (2.52)$$

In acidic solutions the ratio of iodide released increases so that in concentrated potassium iodide solutions the following reaction occurs (IOA, 1987a):

$$6KI + 6H^+ + O_3 \longrightarrow 3H_2O + 3I_2 + 6K^+ \qquad (2.53)$$

Special precautions must be taken to apply the starch iodide method when working in the sub-mg/L concentration range of aqueous phase O_3. In this case more sensitive analytical methods or ozone probes have to be used.

The indigotrisulfonic acid analysis is another colorimetric method being very sensitive to residual aqueous phase ozone concentrations (IOA, 1987b). The underlying principle is that ozone decolorizes indigo and the remaining color is determined as the absorbance difference at 600 nm.

O_3 - sensitive probes are the best preferable options of liquid phase ozone determination provided that the wastewater is not oily or turbid.

2.2.7. The Use of Ozone as an Oxidizing Agent

Ozone, an allotropic form of oxygen, is a powerful oxidizing agent, the oxidation-reduction potential being + 2.07 eVolts as compared with that of HOCL which is only +1.49 eVolts (Table 2.4.).

Table 2.4. Oxidation potentials of certain disinfectant species compared to the hydrogen electrode at 25 ^{o}C and unit hydrogen - ion activity (EPA, 1991)

Oxidant	Oxidation Potential (eVolts)
O_3	-2.07
HOBr	-1.59
HOCl	-1.49
HOI	-1.45
Cl_2	-1.36
Br_2	-1.07
NH_2Cl	-0.75
NH_2Br	-0.74
I_2	-0.54

Advantages of ozone in environmental applications are (Nriagen and Simmons, 1989):

1. Ozone is a powerful oxidizing agent, which has twice the chemical oxidation potential of chlorine in its reactive form of hypochlorite ion. As a result more complete oxidation can be expected from ozonation than from chlorination.

2. Many ozone reactions are very rapid. Unlike chlorine, ozone does not always have to go into solution before reacting. In the case of disinfection, there is some evidence that the lysing reaction occurs between gaseous ozone and microorganism. Faster reaction times can mean shorter contact times to reach required effluent contaminant levels and, as a result, reduce capital for contactors.

3. Ozone is a highly efficient germicide. This result in a more efficient bacterial and virucidial action with shorter contact times and less sensitivity to pH and temperature than for chlorine. The reactions with viruses are so rapid and sure kill of viruses than of bacteria by ozone. In both cases, ozonation was an improvement over chlorination in terms of rate and efficiency of disinfection.

4. It leaves beneficial oxygen residual as a decomposition product. Ozonation for COD reduction, as demonstrated in the Blue Plains Pilot Plant (McNabney,1971) with oxygen feed and recycle to the ozone generator, showed a dissolved oxygen (DO) concentration of almost 40 mg/L in the effluent. The use of air as the ozonator feed would leave an appreciably lower residual but would still increase the DO content of the effluent.

5. Completely and/or or partially oxidized products are generally less toxic than chlorinated or unreacted species. This is a generality, which requires further testing. However, comparison of the toxicity of ozonized versus chlorinated effluents (Arthur,1971) tends to support the generality.

As an oxidizing agent, less reaction time is usually required for ozone than for other chemical oxidizing agents in a particular application because of its higher reactivity. However, this efficiency is partially offset by the decomposition reactions of ozone in aqueous solutions, which has a half-life of approximately twenty minutes in pure water. Since many oxidation and disinfection reactions are very rapid, the efficient use of ozone must be guaranteed with short contact times and minor loss due to decomposition.

A major advantage results from the use of ozone as compared with other oxidizing agents or disinfectants. A wastewater with low toxicity and AOX levels and a high DO concentration is produced during ozonation. Chlorination may produce highly toxic chlorinated organics and chloramines as a contaminant class with carcinogenic character while ozone produces fully or at least more hydrophilic, partially oxidized organics and oxygen.

2.2.8. Ozone Applications in Wastewater Treatment

Ozone can be used in various locations of a wastewater treatment plant (Rice, 1980; Singer, 1990). These may include:

- Disinfection of effluents
- Tertiary treatment (removal of micropollutants)
- Reduction of COD and removal of BOD
- Increasing DO content
- Control of color, taste and odor
- Reduction of turbidity
- Sludge disinfection and treatment

    - Oxidation of secondary sludge for partial or complete volatilization of organics.
    - Partial oxidation and lysing to make bacteria and other organics available as food in recycle to activated sludge.
    - Breaking up filamentous bacterial growth and colloid structure to allow easier dewatering.

- Combined treatment with activated carbon, filtration, ultrasonic and/or oxidizing agents.
- Pre-treatment of industrial wastewater to enhance biocompatibility

2.2.8.1. Tertiary Treatment (Post – Treatment) of Secondary Wastewater. Final polishing with ozone produces almost potable water with the primary exception on the removal of some dissolved and suspended solids. Reduction of BOD, COD, TOCC, disinfection and aeration is provided in the final, ozonized effluent. Significant COD reductions to below 15 mg/L and TOC abatement to below 5 mg/L can be achieved at initial ozone dosages of 0.7 to 3.0 mg ozone per mg COD removed (0.3 to 1.0 mg TOC removed). In most cases, BOD fell down to practically zero mg/L such that complete disinfection was accomplished accompanied with a high DO of the tertiary treated effluent.

On the basis of these laboratory scale investigations, it was concluded that tertiary treatment with ozone offers the following advantages:

- There is a major reduction in COD, TOC and BOD of the effluent. The organic material is destroyed, not simply separated; hence, there are no problems of solids handling or sludge disposal.
- There is pronounced reduction in odor, color, turbidity, toxicity, AOX and surfactants.
- The ozonation by-products are usually harmless or even beneficial.
- The final (product) water has a high DO concentration. Especially when using pure oxygen to generate ozone, the DO is generally greater than the residual BOD or COD. In other word, the effect of such an effluent on receiving streams would be that of a negative BOD.

2.2.8.2. SludgeTreatment. Partial oxidation to remove volatile organic contaminants makes the sludge more desirable for landfills and allows its application on the land to depths of several feet rather than several inches for untreated sludge. A second potential use in activated sludge is the partial oxidation of organics and lysing bacteria. The desired result of this process is to make the degraded material available as food through a recycle to the activated sludge process, thereby achieving a net reduction in solids for disposal. A third application in sludge treatment is the attack of the filamentous bacterial growth which makes sludge difficult to de-water. Small dosages of ozone applied selectively could destroy the colloidal structure that holds so tightly.

2.2.8.3. Ozone Combined with other Unit Processes. In some instances, where COD consists of more difficult to oxidize organics, ozone in combination with activated carbon to polish, disinfect and/or deodorize is another possibility. The capacity of activated carbon columns decreases when some biological growth occurs, that in turn may cause production of hydrogen sulfide. Ozone can be used to control biological growth and eliminate odors due to H_2S formation. In cases where the BOD and COD of a secondary effluent are too high, it would probably be more economical to consider a chemical pre-clarification step before applying ozonation. In other cases, ozone in combination with a mechanical filtration step such as microstaining will be sufficient. Recent studies reported the combination of ozone with ultrasound to remove phosphorus and nitrogen from aqueous

solution by a yet unknown mechanism. In other experimental work ozone was combined with ultrasonics and catalysts for phenol and benzene oxidation as well as with foam flotation for disinfection and clarification (Foulds et al., 1971).

2.2.8.4. Odor Control. Odor control with ozone is a well established process. Ozonation is applied for this purpose in many municipal and industrial wastewater treatment plants all over the world for many decades (Rice, 1997).

2.2.8.5. Biodegradability Improvement of Recalcitrant Wastewater. In some cases organic compounds can be oxidized down to CO_2, H_2O and inorganic salts with ozone that is called mineralization. However, full oxidation is not very common in water and wastewater treatment plants using relatively short ozone contact times and relatively low ozone dosages (1-10 ppm). In most cases, organic compounds are partially oxidized to intermediates in which more and more oxygen atoms are incorporated into the contaminant structure, such that pollutants become more oxygenated and hence more polar prior to ozonation. Significant reduction in COD but not in TOC has thus been observed upon ozonation.

Generally speaking ozone oxidation introduces more and more oxygen into the original (parent) compound implying that ozonized organics should be more easily biodegradable than the starting (initial) material. The magnitude of the increase in the BOD_5/COD (biodegradability) ratios after ozone oxidation indicates the relative increase in the 5-day biodegradability of many organic materials (Rice, 1980; Gilbert, 1985; Alvares et al., 2001).

This property of an organic material becoming more biodegradable upon ozone oxidation now suggests the treatment concept or ozonation followed by a biological treatment step, as opposed to considering ozone to be merely a terminal oxidant. In fact, with the production of refractory organic materials, such as those which require catalytic agents (UV-C irradiation, H_2O_2, ultrasound, transition metal oxides, etc.) to oxidize at any reasonable rate, this behavior suggests that rather than trying to completely destroy a hazardous refractory material by ozone (which would require considerable quantities of ozone and hence is economically not feasible), a more practical, cost-effective approach

would be to utilize sufficient ozone to convert the original organic material into a substrate which thereafter can be readily biodegraded. Thus an integrated approach (ozonation followed by biological treatment) step should be considered, especially if ozonation alone is insufficient to remove the particular contaminant from water or wastewater.

2.2.9. Ozonation of Textile Wastewater

Radetski et al. (2002) evaluated the performance of ozonation as a technique to treat textile effluents. This evaluation was made using physico-chemical parameters and phytotoxic endpoints (i.e. biomass growth and enzyme activities - catalase and peroxidase). After ozonation, the color absorbance was reduced by 81 % while COD reduction reached nearly 87 %. Phytotoxicity tests were carried out with three plant species (i.e. soybean, rice and wheat) to compare the toxicity of raw and ozonated effluents. Reduction in the phytotoxicity of textile effluent samples after ozonation is likely due to the elimination of the toxic organic fraction oxidized during this process. Ozonation was relatively effective in reducing physico-chemical parameters and phytotoxic effects of textile effluents.

Hassan and Hawkyard (20002) investigated the effect of six dyebath additives (sodium chloride, sodium sulfate, EDTA, sodium dithionite, a optical brightener and a dispersing agent) on the decolorization efficiency of ozone. The addition of sodium chloride, sodium dithionite and the dispersing agent markedly improved decolorization efficiency, but EDTA and the optical brightener showed a negative effect. Sodium sulfate did not affect the decolorization efficiency.

Lopez et al. (2004) used ozone and the H_2O_2/O_3 oxidation systems to decolorize aqueous solutions of Orange II (AR-7) and Acid Red 27 (AR-27) in a semi-batch bubble column reactor. Molecular and radical kinetics were compared: A radical scavenger, t-butanol, was added to ensure the mere molecular reaction of ozone. Results revealed that color removal was ensured by direct ozone attack, whereas TOC removal efficiencies of 50 – 60 % were obtained by the free radical reaction. Both mass transfer and the ozone reactivity were considered to evaluate the kinetic parameters for the molecular pathway.

Muthukumar et al. (2004) used the central composite design experiment to study the effect of ozone treatment for acid dye effluents and to optimize the variables such as salt concentration, pH and treatment time. Acid Red 88 dye was used for this study and the additive was sodium sulphate. At neutral pH, the efficiency of ozone was low in terms of decoloration when compared with that at acidic and alkaline pH. Lower salt concentration resulted in faster decoloration while increasing the salt concentration inhibited decoloration efficiency.

Kos and Perkowski (2003) examined the efficiency of advanced oxidation processes for the decoloration of different types of textile wastewater taken from textile plants in Lodz. The wastewater had different compositions and concentrations of pollutants, and the dyeing wastewater was of intense color. The advanced oxidation processes with the use of ozone, gamma radiation, hydrogen peroxide and UV radiation gave good decoloration results. The efficiency of color removal depended on the type of wastewater and concentration of pollutants contained therein. Considering both the experimental results and technological problems, it can be presumed that advanced oxidation with a simultaneous application of ozone and hydrogen peroxide is a very promising technique for potential industrial implementation.

Wang et al. (2003) investigated the effect of ozonation on the degradation of the azo dye Remazol Black 5 (RB5). Conventional parameters such as COD, TOC, pH, conductivity, color removal, biodegradability (BOD_5 or BOD_{28}), and toxicity were monitored during the process. Ozonation was a very effective way to remove the color, however, a considerable organic load still remained as indicated by high COD and TOC residues. The COD, TOC reductions were about 40% and 25% after 6 h ozonation of 2 g/L RB5 aqueous solution. The BOD_{28} revealed that partial ozonation (10-150 min) of RB_5 resulted in products that were more biodegradable than the parent compound. During the first 150 min of 360 min ozonation, the formation of highly toxic dye intermediates took place as could be confirmed by two acute toxicity-screening tests. A negative correlation existed between ozonation time and biodegradability.

Khraisheh (2003) investigated the use of ozone for the decolorization of reactive dyes from textile effluent. Several variable including dye concentration, pH, dye structure,

salt concentration, ozone concentration and treatment time were assessed to optimize the dye degradation. A higher rate of color degradation and higher degree of total color removal was achieved at high pH. Ozone removed more than 50% COD from Remazol Black B solutions at high ozone doses. Under similar experimental conditions COD removal from Remazol Red RB and Remazol Golden Yellow RNL solutions was less than 15%.

Dogruel et al. (2003) ozonated streams of cotton finishing textile plant wastewater for optimizing chemical oxygen demand (COD) removal. For this purpose, significant COD fractions in the wastewater were experimentally identified and the effect of ozone on these fractions was investigated. After 30 min ozonation at a rate of 1 g/h, the removal of the readily biodegradable COD was 60%, but soluble inert COD reduction remained at 16%, indicating selectivity of ozone for simpler compounds. Longer ozonation times (higher ozone doses) resulted in the solubilization of the particulate COD fractions. Pre-ozonation of the dye-house wastewater rendered the overall plant effluent more amenable to biological treatment.

Karahan et al. (2002) evaluated the effect of ozonation on the quality of wastewater from a textile mill involving bleaching and reactive dyeing of cotton and synthetic knit fabric. The results indicated that the applied ozone dose greatly affects the remaining organic carbon composition in the wastewater. The relative magnitude of different COD fractions varied as a function of the ozone dose. Ozonation did not exert a measurable impact on the rate of major biological processes.

Marcucci et al. (2002) described the experimental results of a pilot scale application of different membrane technologies, supported by clariflocculation and ozonization for the treatment and reuse potential of a secondary effluent coming from a biological activated plant and a wastewater coming directly from several textile departments. In the first case the pilot plant used sand filtration and microfiltration (MF) as pre-treatments for nanofiltration (NF). The NF permeate was reusable in all production steps, including dyeing with light coloration. The most interesting experimental results were obtained from the treatment of wastewater from the carbonising process. A treatment scheme in which

ultrafiltration (UF) sheets operating under vacuum are placed downstream of an ozonization treatment has been proposed.

Hassan and Hawkyard (2002) studied combined oxidation with ozone and Fenton's reagent ("Fentozone" process) for decolorization of aqueous dyes and compared the results with traditional Fenton's reagent. Although the 'Fentozone' process was found to be effective at a wide range of pH values, the maximum color removal was achieved at pH 4. The effect of pre-ozonation on color removal efficiency of aqueous dyestuffs in the subsequent treatment with Fenton's reagent was investigated. The reaction rates increased with increasing ferrous sulfate.

Ciardelli et al. (2001) described the treatment of textile wastewaters by means of an ozonation pilot plant. Wastewaters used were produced by a dyeing and finishing factory and were first treated in an active sludge plant and filtrated through sand. In the appropriate conditions very high color removal (95-99%) was achieved and the effluent could be reused in production processes requiring water of high quality as dyeing yarns or light colorations. Even if the chemical oxygen demand of treated waters was still in a range (75-120 mg/l, a decrease of up to 60%) that was usually considered to be too high for recycling purposes, recycling experiments were successful.

Balcioglu and Arslan (2001) investigated the ozonation and O_3/H_2O_2 oxidation of reactive dyestuffs and simulated textile dye-bath. Considerable improvement both in COD and color removal rates were obtained at pH=11, whereas increasing the initial dyestuff concentration had an adverse effect upon oxidation rates. Removal of color, COD and TOC were found to be fairly sensitive to the introduction of soda ash being frequently applied as an auxiliary chemical during the reactive dyeing process. The addition of H_2O_2 had negligible effect on COD removal and decolorization. A three-fold enhancement in BOD_5 was observed after 5 min ozonation accompanied by a decrease in the inhibition of oxygen uptake rates for the same reaction period.

Arslan and Balcioglu (2000) studied the ozonation of two commercially important reactive dyes, i.e. Procion yellow HE4R (Reactive Yellow 84) and Remazol Black SB (Reactive Black 5) in actual dye rinse waters and simulated exhausted dye bath. The effect

of common dye auxiliaries (NaCl and Na_2CO_3) and initial dye was investigated. It was found that NaCl did not affect the ozonation efficiency, whereas the addition of Na_2CO_3 resulted in a significant inhibition of COD removal. A simple kinetic model describing the effect of inhibitor concentrations on COD and/or color removal rate constants was proposed.

Bes-Pia et al. (2003) focused on the advanced treatment of the biologically treated wastewater of a textile plant for reuse purposes. Both nanofiltration experiments at different operating conditions and oxidation reactions with ozone and ozone/UV irradiation were performed to evaluate the final water quality.

2.3. Sonochemistry and Practical Applications

2.3.1. Basic Principles

Ultrasound is defined as any sound of a frequency above that to which the human ear has no response (i.e. above 16 kHz). In practice, three ranges of frequencies are reported for three distinct uses of ultrasound:

- diagnostic or high frequency ultrasound (2-10 MHz)
- low frequency or conventional power ultrasound (20 -100 kHz), and
- medium frequency, or "sonochemical-effects" ultrasound (300 - 1000 kHz).

It is the latter range, where chemical reaction processes are uniquely catalyzed through very "extreme" temperatures and pressures generated by the formation, growth and collapse of cavitation bubbles.

2.3.1.1. Acoustic Cavitation. When a liquid is exposed to an acoustic field, the pressure waves of the sonic vibrations create a time/frequency dependent acoustic pressure, consisting of alternating compression and refraction cycles (Mason, 1990). If the applied pressure is equal to the negative pressure developed in the rarefaction cycle of the wave such that the distance between the molecules of the fluid exceeds the critical molecular distance to hold it together, the liquid breaks apart to form cavities made of vapor and gas-

filled microbubbles. The phenomenon called “acoustic cavitation” consists of at least three distinct and successive stages (Neppiras, 1984):

- nucleation,
- bubble growth (expansion), and
- implosive collapse (under proper conditions).

The first stage is a nucleated process, by which cavitational nuclei are generated from microbubbles trapped in micocrevices of suspended particles within the liquid. In the second stage, the bubbles grow and expand in a manner restricted by the intensity of the applied sound wave. With high-intensity ultrasound, a small cavity grows so rapidly through inertial effects, whereas at lower intensities the growth occurs through “rectified diffusion”, proceeding in a much slower rate, and lasting many more acoustic cycles before expansion (Neppiras, 1984). The third stage of cavitation occurs only if the intensity of the ultrasound wave exceeds that of the “acoustic cavitational threshold” (typically a few Watts/cm^2). At this condition, the microbubbles overgrow to the extent where they can no longer efficiently absorb energy from the sound environment to sustain themselves, and implode violently, therefore, in a so called “catastrophic collapse” (Mason, 1990; Mason 1999; Suslick, 1989)

During this collapse stage, the temperatures and pressures released are in such extremes that the entrapped gasses undergo molecular fragmentation, which is the underlying phenomenon in homogeneous sonochemistry (Kang and Hoffmann, 1998) Furthermore, it has been observed that just before the catastrophic collapse of compressed gas-filled cavities in water, the bubbles produce a flash of light called “sonoluminescence”, as detected by a peak at 310 nm and a broad continuum throughout the visible. The spectrum of sonoluminescent water was associated with the formation of high-energy species (excited hydroxyl radicals) from molecular fragmentation of compressed gasses, rather than with black body radiation. Hence, like photochemistry, sonochemistry involves the introduction of very large amounts of energy in a short period of time, but the type of molecular excitation is thermal, unlike the electronic excitation felt by molecules in photochemical processes (Suslick, 1989).

2.3.1.2. Collapse Phase. At present, no consensus exists for the physical explanation of the collapse phase, except that "extreme and non-equilibrium" conditions exist during the implosion. The most highly favored explanation is that given by the "hot spot theory", which suggests that the collapse is so rapid that the compression of the gas and vapor inside the bubble is adiabatic (Noltingk and Neppiras, 1950). Consequently, the temperatures and pressures within a collapsing microbubble can reach values as high as 4200-5000 ^{o}K and 200-500 atm, respectively, just before fragmentation. The localized "hot spot" generated by the rapid collapse of acoustic cavities is very short lived (<10μs), implying the existence of extremely high heating and cooling rates in the vicinities of 10^{10} ^{o}K/s. Hence, sonochemistry is generated by short lived cavitational heating is found similar to shock-tube chemistry or multi-photon infrared laser photolysis, but is unique in that acoustically induced cavitational heating occurs only at condensed phases of the fluid (Mason and Lorimer, 1989)

2.3.2. Physicochemical Aspects of Sonochemistry

2.3.2.1. Heterogeneous Sonochemistry. A great majority of sonochemical systems with industrial applications are heterogeneous, where enhancement of chemical reactivity is associated with the physical effects of ultrasound such as heat and mass transfer, surface activation, and phase mixing (Mason and Cordemans, 1998). Sonocatalysis of liquid-liquid heterogeneous reactions is based on the mixing of acoustic streaming, which promotes the emulsification of non-miscible liquids by enhancing reaction rates upon increased interfaces. When the system is made of a solid-liquid medium catalysis is a consequence of the disruption of the solid by the jetting phenomenon associated with the collapse of cavitation bubbles. It is important to note that many of such effects are observed when the heterogeneous medium is irradiated with low frequency, or power ultrasound are the 20-100 kHz range.

2.3.2.2. Homogeneous Sonochemistry. Homogeneous sonochemistry is induced directly by the outcome of "extreme" conditions in collapsing microbubbles. Such extremes are reported to produce very unique catalytic effects, arising from inherent advantages of the system such as:

- the ability to generate high-energy species, and
- the mimicry of autoclave reaction conditions (high temperatures and pressures) on a microscopic scale (Suslick, 1989).

These effects start in the cavities, which are made of microbubbles filled with vapor of the liquid medium and/or dissolved volatile solutes and gasses diffused into them. During the collapse of the cavities in pure aqueous systems, gaseous water molecules entrapped in expanded microbubbles are fragmented as in pyrolysis to generate highly reactive species, such as hydroxyl radicals (Serpone et al., 1994). In non-aqueous organic solvents or aqueous media containing volatile organic gasses and solutes, cavitational collapse not only results in the fragmentation of water molecules to hydroxyl and hydrogen radicals, but also in the formation of organic radicals (Seghal et al., 1980).

The hydroxyl radicals generated by water sonolysis may either react in the gas phase or recombine at the cooler gas-liquid interface and/or in the solution bulk to produce hydrogen peroxide and water as shown in (Fischer et al., 1986).

$$H_2O \longrightarrow {}^{\bullet}OH + {}^{\bullet}H \qquad (2.54)$$

$${}^{\bullet}OH + {}^{\bullet}H \longrightarrow H_2O \qquad (2.55)$$

$$2\,{}^{\bullet}OH \longrightarrow H_2O \qquad (2.56)$$

$$2\,{}^{\bullet}OH \longrightarrow H_2O_2 \qquad (2.57)$$

$$2\,{}^{\bullet}H \longrightarrow H_2 \qquad (2.58)$$

If the solution is saturated with oxygen, peroxyl and more hydroxyl radicals are formed in the gas phase (upon the decomposition of molecular oxygen), and the recombination of the former at the cooler sites (interface or the solution bulk) produces additional hydrogen peroxide, as shown in (Makino et al., 1983; Pétrier et al., 1994):

$$O_2 + \dot{H} \longrightarrow H\dot{O}_2 \quad (2.59)$$

$$O_2 \longrightarrow O + O \quad (2.60)$$

$$O + H_2O \longrightarrow \dot{O}H + \dot{O}H \quad (2.61)$$

$$H\dot{O}_2 + H\dot{O}_2 \longrightarrow H_2O_2 + O_2 \quad (2.62)$$

Experience in homogeneous sonochemistry has shown that there are three potential sites for chemical reactions in ultrasonically irradiated liquids, as illustrated in Figure 2.9:

- the cavitation bubble itself,
- the interfacial sheath between the gaseous bubble and the surrounding liquid, and
- the solution bulk (Weavers et al., 1998).

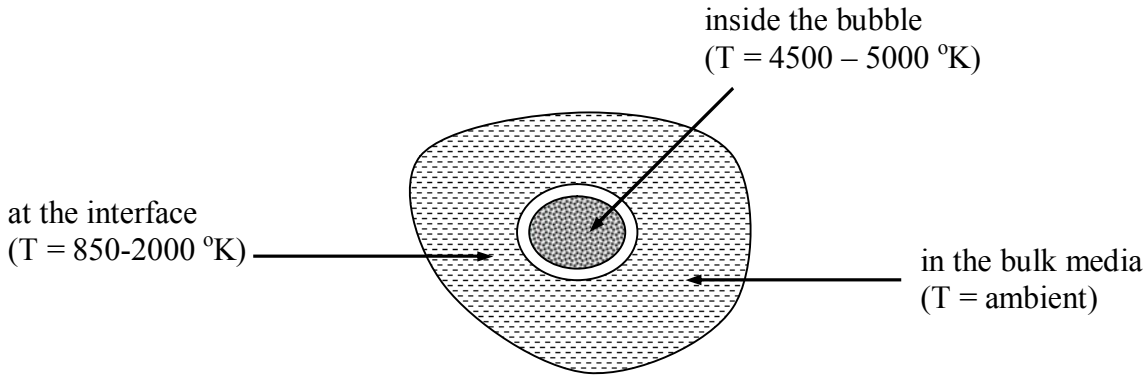

Figure 2.9. Possible sites of chemical reactions in homogenous reaction media

In water or effluent treatment practices, organic pollutants may be destroyed either at the first two sites upon combined effects of pyrolytic decomposition and hydroxylation, or in the solution bulk via oxidative degradation by hydroxyl radicals and hydrogen peroxide. The extent of oxidation in the latter site is limited by the quantity of uncombined hydroxyl radicals available in solution, which in turn is a matter of the lifetime and collapse duration of the bubbles, as well as the geometry of the reactor.

2.3.3. The Effects of Cavitation

The more important cavity effects are reported to occur when the frequency of the wave is equal to the resonating frequency of the bubble (Mason and Lorimer, 1988). The resonance radius of a bubble excited by low frequency waves is reported to be ~ 170 μm (at 20 kHz), and the cavities entrapping such bubbles are said to be "stable" or long lived, with average life times of 10 μs (Pétrier et al., 1994). In this kind of cavitation, the collapse stage is delayed till after the elapse of a number of compression and rarefaction cycles, during which sufficient volumes of volatile solutes and solvent vapors in the liquid may flow into the gas phase. The delayed growth and long collapse duration of gas-filled bubbles allow radical scavenging and recombination reactions at the interfacial sheath, thus inhibiting the mass transfer of hydroxyl and other reactive species into the solution. Hence, low frequency ultrasound is expected to induce destructive effects only for hydrophobic solutes, which easily diffuse into the cavity bubbles to undergo pyrolytic destruction inside the collapsing bubble, or hydroxylation and thermal decomposition at its interfacial sheath, where pressure gradients and temperatures are still high enough to induce thermal effects (Makino, 1983).

On the contrary, the resonance radii of bubbles excited by medium frequency (300-1000 kHz) ultrasound waves are extremely small (4.6 μm at 500 kHz), giving rise to very short-lived (0.4 μs on the average) and mainly void or vapor-filled "transient" cavitations. The pressures and temperatures developed in such cavities are much higher that found in "stable" cavities, and larger energies are released into the surrounding liquid during their more rapid and violent collapse (Mason and Lorimer, 1988; Henglein, 1987). Furthermore, such cavitations are so short lived and the collapse is so rapid that the time for appreciable degrees of radical scavenging reactions in the hot bubble or at its interface is insufficient. As a consequence, medium frequency ultrasound waves are highly effective for catalyzing advanced oxidation processes, which are aimed to destroy non-volatile organic solutes in solution. The destructive effect of ultrasound in this condition is due to the high probability of hydroxyl radical transfer into the surrounding liquid during the collapse stage of acoustic cavitations (Pétrier et al., 1992).

2.3.4. The Effect of Frequency on Sonochemical Destruction

It is obvious that the selection of the right frequency range is of utmost significance for achieving appreciable degrees of decontamination. The choice is based primarily on the physicochemical properties of the contaminating species, such as vapor pressure (or Henry's constant), solubility and octanol-water partition coefficient (Suslick, 1986; Hua and Hoffmann, 1997). Hydrophobic chemicals with high vapor pressures have a strong tendency to diffuse into the gaseous bubble interior, and the most effective site for their destruction, therefore, is the bubble-liquid interface and/or the bubble itself. Hence, aqueous solutions contaminated with volatile pollutants preferably be exposed to power ultrasound (whereby long-lived "stable" cavities are generated) for thermal and oxidation effects in the gas phase and the gas-liquid interface (Weavers et al., 1998). In contrast, hydrophilic compounds with low vapor pressures and low concentrations tend to remain in the bulk liquid during irradiation, due to the repulsive forces exerted to-and-from the slightly hydrophobic bubble surfaces. The major reaction site for these chemical, therefore, is the liquid medium, where they may be effectively destroyed by oxidative degradation, provided that sufficient quantities of hydroxyl radicals are ejected into the solution during cavity collapse. As stated previously, maximum radical transfer into the bulk medium occurs when the collapse is "transient", or when sonication is carried out via medium frequency ultrasound waves. Moreover, at this frequency and high solute concentrations, an additional destructive pathway via thermal decomposition was observed. As demonstrated by the formation of pyrolysis products along with hydroxylated intermediates during sonolysis at 300-500 kHz. The extent of destruction by pyrolytic fragmentation of nonvolatile contaminants is directly related to their concentration and hydrophobicity, which dictates their ability to migrate towards the bubble and/or to accumulate at the bubble-liquid interface (Serpone et al., 1994). Consequently, the probable site for thermal decomposition of nonvolatile solutes is the bubble interface, at which solutes may accumulate via adsorptive processes during the formation and growth of acoustic cavities. At appreciable concentrations, the adsorptive tendency of nonvolatile solutes on nonpolar surfaces of cavity bubbles was verified by the exhibition of saturation type kinetics, typical of Langmurian behavior, which is commonly proposed for describing photocatalytic process kinetics.

2.3.5. Optimization of Sonochemical Reaction Systems

The main concern of scientists and engineers working with ultrasonic systems is to accomplish maximum reaction yields and/or maximum pollutant destruction at optimal conditions. Research and development in sonochemical systems exposed the significance of two basic strategies for maximizing reaction efficiencies:

- optimization of power and reactor configuration, and/or
- enhancement of cavitation (Mason and Cordemans, 1998; Hua and Hoffmann, 1997).

The first strategy requires a mechanistic approach with features such as:

- selection of the transducer (piezoelectric or magnetic material that converts electrical impulses to mechanical vibrations) and generator (probe types for low-frequency, and plate types for high frequency effects),
- configuration and dimensioning of the reaction cell,
- optimization of the power efficiency (the effective power density delivered to the reaction medium).

The second strategy to enhance cavitation is to maximize chemical reactivity involves the addition of different gasses and solids into the system to test and compare their effectiveness in increasing reaction yields and/or reaction rates.

Aqueous media free of impurities are well known with their tremendously high cavitation threshold, so that any kind of interference to create “liquid defects” in the structure is reported to favor cavitation events. The easiest way of creating impurities in sonicated water is by saturating the solution with a soluble gas, which speeds up the initialization of cavity formation via provision of excess nuclei (Mason and Cordemans, 1998), while enhancing the collapse conditions by increasing the temperature within cavity bubbles (Pétrier et al., 1992; Riesz et al., 1990). However, since the first effect of cavitation is degassing, the solution will rapidly be free of dissolved gases if gas entertainment is ceased during sonication. It is common practice, therefore, to bubble the

liquid incessantly with a gas throughout the sonication period to maintain a constant gas flow into the bubbles so as to sustain the "extreme" conditions of collapse. The selection of this gas is also of significance, because the final temperature of a collapsing bubble is closely related (by a power function) to a gas parameter, called the "polytropic γ ratio", i.e. the ratio of specific heats (C_p/C_v) of the ambient gasses entrapped in the bubble (Noltingk and Neppiras, 1950, Riesz et al., 1990). The nature of the saturating gas is further important, due to the inverse relationship between thermal conductivity of a gas and the temperature build-up in a cavity bubble (Pétrier et al., 1992; Hua and Hoffmann, 1997). Sonoluminescence studies with rare gases have shown that as the thermal conductivity decreases in order:

Xe<KR<Ar<Ne<He,

the amount of heat loss to the surrounding liquid (due to heat conduction in the gas) also decreases, the collapse approaching perfect adiabatic conditions (Riesz, et al., 1990, Hua and Hoffmann, 1997). Hence, sonolytic radical yields increase with increasing effective temperature of collapsing bubbles, i.e. with increasing γ ratios, but decrease with increasing thermal conductivities of ambient gases (Hua and Hoffmann, 1997). Furthermore, rare gases are more effective than diatomic gases (and air), owing to higher γ ratios obtained with monoatomic gases in water (Hung and Hoffmann, 1998; Riesz et al., 1990). However, despite the equal γ ratios of Ar and He in water, much higher yields of pyrolysis products were detected with Ar, as attributed to its tenfold lower thermal conductivity (Hua and Hoffmann, 1997).

The addition of solid catalysts such as glass beads, ceramics, SiO_2, Al_2O_3, and talk into the reaction medium is another common method for enhancing cavitation effects. The presence of such material is reported to be useful for micronization of species (in ultrasonic cell disruption), and for the abrasion, activation and alteration of the chemical properties of catalyst surfaces during ultrasonic irradiation of liquid media (Mason and Cordemans, 1998).

2.3.6. Sonochemistry for Textile Wastewater Treatment

The use of ultrasound in environmental remediation is an emerging technology, and a thorough review of all related studies has been made during this study and published Ince et al. (2001).

Textile industry produces huge amounts of wastewater heavily charged with dyestuffs and auxiliaries. Most textile chemicals (i.e. dyes, sequestering agents, carriers, tannins, wetting agents, tannins, etc. cannot be treated via conventional methods (adsorption, coagulation, biological activated sludge reactors) leave the treatment plant without being subjected to any significant structural changes. In particular exhausted dyes may cause serious aesthetic and environmental problems in receiving water bodies (inhibition of plant activity due to interference with light transmission, formation of potentially carcinogenic aromatic amines under anoxic conditions). So far, hundreds of papers have already been published dealing with the advanced chemical oxidation of dyes and other recalcitrant chemicals present in dyehouse effluent. Among them, ultrasonic irradiation has most recently been explored and applied for the degradation of a variety of dyestuffs and spent dyebaths. Although several studies have reported the beneficial use of ultrasonic irradiation for decolorization of several types of textile dyes. However, as has also been evidenced for other advanced chemical oxidation technologies such as ozonation, H_2O_2/UV-C treatment and TiO_2-mediated photocatalysis, mineralization to ultimate oxidation end products (i.e. CO_2, H_2O and mineral acids or salts) is rather difficult and only possible upon extended irradiation times if ultrasound is used alone. For this reason, the combination of ultrasound with oxidants (O_3, H_2O_2) or advanced oxidation systems (H_2O_2/UV-C/O_3, Fe^{2+}/H_2O_2) appears to be a more convenient and economically feasible approach for effective dyehouse effluent treatment. Some scientific papers reporting ultrasound assisted decoloration and mineralization of textile dyes and dyebaths are addressed below.

2.3.6.1. Application of Sonolysis alone. Rehorek et al. (2004) investigated the sonolytic treatment of several acid, direct and reactive dyes at 850 kHz and varying power input rates. The changes in toxicity of the treated dyes were followed with a respiratory inhibition test using *Pseudomonas putida*. Results have indicated that increasing the power from 90 to 120 W increased the degradation and detoxification rates for all tested dyes. Free radicals were rather formed at the higher end of studied power input values.

Tezcanli-Guyer and Ince (2004) examined the degradation of different reactive and basic dyes with power ultrasound at 520 kHz. Changes in acute toxicity during decoloration of the dye solutions were traced using luminescent bacteria (*Vibrio fischeri*). Results have indicated that more than 80 % color removal was achieved within 120 min and that the reactive dyes showed non-toxic character after complete decoloration was achieved.

2.3.6.2. Sonolysis Combined with Ozone. Ince and Tezcanli (2001) studied the decolorization and mineralization of Reactive Black 5 (RB5) using sonolysis combined with ozonation (US/O_3) using 520 kHz and 3.36 g/L ozone. Color removal was faster for US/O_3, and TOC removal for 20 μM RB5 was obtained as 2%, 50% and 76% for US, O_3 and US/O_3, respectively after treatment for 1 h.

2.3.6.3. Sonolysis Combined with Electrolysis. Lorimer et al. (2000) applied sonolysis together with electrolysis (US/EC) for different commercial dyestuffs at 20 and 510 kHz in a sealed electrolysis cell. The effects and functions of electrode material, current density, electrolyte type, sonolysis frequency and reaction temperature were assessed and evaluated in this study.

2.3.6.4. Sonolysis Combined with H_2O_2/UV. Poon et al. (1999) studied the combined $US/H_2O_2/UV$ system for the decoloration and degradation of Cuprophenyl Yellow RL at varying pH and H_2O_2 doses. Higher color and TOC removal efficiencies were obtained at pH =11 and H_2O_2 doses between 0.1 – 1.0 mL/L (source: 30 % w/w H_2O_2).

2.3.6.5. Sonolysis Combined with γ - Radiolysis. Vinodgopal and Peller (2003) investigated the combination of sonolytic and radiolytic irradiation for the treatment of 82 μM purified Acid Orange 7 (AO7) at 640 kHz. Hyrdoxybenzenesulfonic acid, 1,2 naphtaquinone were identified as AO7 intermediates leading most probably to the end products oxalate and formate after 6 h treatment.

2.3.6.6. Sonolysis Combined with Photocatalysis. Mrowetz et al. (2003) combined sonolysis and photocatalysis (named sonophotocatalysis) to degrade purified 20 to 70 μM Acid Orange 1 and Acid Orange 8 at 20 kHz and different photocatalyst (TiO_2) concentrations. The effect of Fe^{3+} addition on mineralization rates was also examined. It could be established that sonolysis induced catalyst de-aggregation and accelerated solid (photocatalyst surface) – liquid (dye solution) mass transfer rates.

2.3.6.7. Combined Systems of Sonolysis, Ozone and UV. Tezcanli-Guyer and Ince (2004) investigated the combinations of US/O_3, US/UV and US/O_3/UV for the degradation of 57 μM AO7 at 520 kHz. The combined systems were optimized for ultrasonic power density, ozone flow, UV intensity and gas (Ar, O_2) flowrate. No significant improvement was obtained for the triple combination. The highest mineralization rate was achieved as 40 % for US/O_3/UV resulting in a considerable increase in biodegradability (measured as BOD_5).

2.4. Textile Industry

2.4.1. Turkish Textile Industry: Recent Figures

Industrialization efforts of the 1960's and 1970's in Turkey have resulted in the modern textile industry in Turkey. At the beginning, this sector operated in the form of small workshops. Thereafter, it showed rapid development and during the 1970's and 1980's it began exporting. Currently it is one of the most important sectors in the Turkish economy in terms of GDP, employment and exports. In the 1990's, the share of this sector in the country's GDP was around 10 % and the sector's share of employment in the country's total employment was 20 %. Its share in the total industrial production of the

country was around 40 % during the same period. Nowadays, Turkey is one of the most important textile and clothing producers and exporters in the world. For instance, Turkey ranked number 6 in world exports of clothing in 1997 (The General Secretariat of Istanbul Textile & Apparel Exporters' Association; ITKIB, 1998).

As a quality cotton-producing country, Turkey has an integrated and diversified production in all sub-sectors of the textile industry, produces and exports all types of yarn, fabric, clothing, household textiles and other ready-made products. Turkey, as a traditional cotton grower has a great advantage in the production of textile and clothing. In 1998 the amount of cotton grown in Turkey was 806 000 metric tons. In the year 2000, with the completion of the South-eastern Anatolian Project (GAP), Turkey's cotton production increased tremendously. The GAP is one of the largest projects that have ever been attempted in Turkey. It was estimated that upon completion of the project nearly 1.7 million hectares of land will be irrigated. Irrigation of the Harran Plain Region began in 1994 and since then approximately 200 000 tons cotton, which is almost around one fourth of Turkey's total cotton production, are cultivated every year.

As a consequence of the availability of raw cotton in huge amounts, the Turkish spinning and weaving industries have also shown progress. In 1998 the amount of cotton yarn produced in Turkey was around 790 000 tons and cotton fabric production was 1 455 million meters. The export value of cotton textile products was 781 million dollars in 1998. The values of cotton, cotton yarn and cotton fabric exported were 92, 293 and 396 million dollars in 1998, respectively. Main destinations for cotton yarn exports are Italy, Belgium, the UK, Israel, the USA, Germany and Egypt. Main destinations for cotton fabric exports are the UK, Italy, the USA and Iran.

Turkey also has a strong woollen textile and clothing industry as Turkey is at the same time one of the leading producers of wool. Turkey is also the third largest mohair producer in the world. The majority of woollen products meets the demands of clothing producers and exporters and part of them are being exported at a value of wool, fine hair, yarn and fabric was 97 million dollars according to 1998.

The man-made fibers industry started in Turkey with the production of regenerated cellulose in 1938. Polyamide was first produced in Turkey in 1964, polyester in 1968, acrylic in 1974 and polypropylene in 1975. Turkey now has the ninth largest synthetics capacity in the world. Most of the raw materials for synthetic fibers and yarns are procured locally, but the main raw material for acrylic fibers is still being imported. The total value of man-made fibers, yarns and fabrics exported was 1 billion dollars in 1998. The main destinations for synthetic filament yarn exports are the UK, Italy, Syria, Spain, Hungary, Romania, Bulgaria, Germany and France, whereas the main destinations for synthetic filament fabric exports are Hungary, Romania, Bulgaria, Germany and France. The main destinations for artificial filament fabric are France, Bulgaria, the UK, Germany and the USA.

Besides the Turkish textile industry, the Turkish home textile industry has also shown a considerable growth in terms of production and exports. In the recent years the production of home textiles has shown a stable increase due to the rise in domestic and external demand for home textiles. Almost all kinds of home textiles are produced in Turkey. These may be listed as follows in order of their export values; bed linens & spreads, table linens, towels, bathrobes, voiles, curtains, lace, interior blinds, curtain or bed valances, blankets, cushions, pillows, quilts, eiderdowns. In home textile sector, there are many small and medium sized firms scattered all around the country besides large, integrated plants. Turkish home textile manufacturers are mainly located in Istanbul, Bursa, Denizli, Izmir, Kayseri, Gaziantep and Usak. Towel and bathrobe producers are mainly concentrated in Denizli and Bursa, voile producers in Istanbul and Bursa and blanket producers in Usak. In some rural areas of cities such as Denizli, Mugla and Kastamonu the production of traditional cloths is still widespread and recently they have been used in the production of specific home textiles.

2.4.2. General Properties of Textile Industry Wastewater

Considering both the volume and chemical composition of the discharged effluent, the textile industry is one of the major polluters among all industrial sectors. The typical wastewater volume produced per kg of knit finished goods ranges from 83.4 to 135.9 L (UNEP, 1994).

Effluents from textile dyeing, washing and rinsing operation stages can be classified as high volume ($Q \geq 1000$ m^3/day), varying pH (4 - 12, mostly alkaline), medium strength effluents (COD range = 1000 – 5000 mg/L; BOD_5 = 200 – 2000 mg/L) that contain high concentrations of dissolved solids (DS range = 1000 – 10000 mg/L), and are strongly colored due to the presence of refractory and polyaromatic dyestuffs (Easton, 1995). These properties make the decolorization and effective oxidation of textile wastewater via conventional treatment methods such as biological oxidation, coagulation, and adsorption quite inappropriate (Reife and Freeman, 1996). Moreover, applying physicochemical treatment technologies results in a phase transfer of pollutants thus creating another source of waste. Consequently, appropriate “destructive” chemical technologies should be preferred for the fast and effective treatment of pollutants present in textile industry wastewater.

As mentioned above, the textile industry is associated with a strong, persistent color (Correa et al., 1994) since textile dyes are intentionally designed to withstand microbial, chemical and photolytic degradation to satisfy the consumers’ requirements (Reife, 1993). Commercial textile dyes such as acid, direct and reactive dyes are hardly biodegradable and hence pass untreated through the sewage works due to their high water solubility and relatively low molecular weight (Reife and Freeman, 1996). General characteristics of major types of textile dyes together with their fixation degree for different dye and fiber combinations are presented in Table 2.5. The table shows that fiber reactive dyes possess rather low fixation rates while the highest fixation is achieved by basic dyes.

It has been reported that after the reactive dyeing process is complete up to 800 mg/L of unfixed and hydrolyzed dye may remain in the spent textile bath and cannot be reused. Therefore, up to 50 % of the applied reactive dye is usually discharged as a deeply

colored effluent. This rate is closely followed by disperse and sulphur dyes whose popularity can be verified by examining their appearance in textile wastewater (Easton, 1995).

An important factor that has directed research on color removal from dyehouse effluent towards “destructive” chemical oxidation processes is the fact that conventional physicochemical “phase transfer” methods such as activated carbon adsorption, coagulation, flocculation or precipitation no longer give satisfactory treatment results in terms of color consents (Slokar and Le Marechal, 1998; Vandevivere et al., 1998). Sludge formation after coagulation creates another source of waste problem. Moreover, among the oxidation techniques chlorination, hydrogen peroxide treatment, direct short UV (UV-C) photolysis, and in some instances even ozonation are insufficiently powerful to decolorize most of the commercial textile dyes at ambient reaction conditions (Marechal et al., 1997; Arslan, 2001).

Table 2.5. Classification of dyestuffs, their associated fibers and fixation rates (Buckley, 1992)

Dyestuff	Characteristics	Attachment mechanism and associated fibers	Loss to dyehouse effluent (%)
Acid	Anionic, highly water soluble, poor wet fastness	Ionic bond, nylon, wool	5-20
Metal (Cr, Co, Cu) Complexed Acid	Anionic, low water solubility, good wet fastness	Ionic bond, nylon, wool	2-10
Direct	Anionic, highly water soluble, poor wet fastness	ionic bond cotton, viscose	5-30
Basic and Cationic	Cationic, highly water soluble	Ionic bond, Acrylics	0-5
Disperse	Colloidal dispersion, very low water solubility, good wet fastness	Colloidal impregnation & adsorption Polyester, nylon, acrylic, cellulose acetate	0-10
Reactive	Anionic, highly water soluble, good wet fastness	Covalent bonds, Cotton, viscose, wool	10-50
Sulfur	Colloidal after reaction in fiber, insoluble	dye precipitated in-situ in fiber, cotton, viscose	10-40
Vat	Colloidal after reaction in fiber, insoluble	dye precipitated in-situ in fiber, cotton, viscose	5-20
Azoic	Colloidal after reaction in fiber, insoluble	dye precipitated in-situ in fiber, cotton, viscose	2-3

Research on textile effluent treatment has focused on color removal and in particular on the degradation of reactive dyes for the following reasons. First, reactive dyes represent an integral market share (almost 45 % of all textile dyes produced annually are belonging to the fiber reactive class) due to the appreciable use of woollen, cotton and viscose rayon fibers. Second, these dyes have low fixation rates which results in highly colored spent dye-baths whose treatment is inadequate in conventional wastewater treatment plants (Easton, 1995). Third, of special concern is the reactive dyeing process, where in the average 10 times more water is consumed for the preparation, dyeing, washing and rinsing stages than for dyeing with other dye types.

2.4.3. Recovery and Reuse in the Textile Industry

From the above sections it is obvious that energy & material recovery of such a chemical and process intense sector is very critical for its sustainable development. For instance, by the use of heat exchangers considerable amounts of energy can be saved, and some process chemicals can be recovered, such as solvents, some dye types and caustic. Below, some typical examples for process recovery & reuse in the textile industry using different applications of Ultrafiltration (UF) operations of were given.

2.4.3.1. Polyvinyl Alcohol (PVA) Recovery. Sizing chemicals that are resistant to biodegradation, such as PVA, can be recovered, when they are washed from the fabric prior to dyeing, and hence reused. Sizing chemical and treatment costs are significantly reduced when this is done. The first recycle - recovery application of sizing materials used and UF unit that was installed for PVA recovery in 1971 in Clemson, S.C., U.S.A. (Aurich, 1975). The system is still in operation and has brought the company considerable savings in water, chemical and energy costs. The economics of PVA recovery can be over 5700 USD/day, when the feeding speed is 100 yards/min. Automatic process control has increased the range speed to 200 yards/min and hence the value of the recovery process exceeds 11000 USD/day now. UF and process automation will become an integral part of the desizing process when the increased use of synthetic sizes necessary for high speed weaving will continue. When the size is recovered and the permeate water is used to wash out more sizing chemical, over 60000 gallons of wastewater per day from the biological wastewater treatment system and the influence of governmental regulations. Recycling will

become more and more attractive because sizing material, fresh water and waste treatment prices are increasing every day. In some installations the permeate water from the UF unit is not recycled but discharged as an effluent to the wastewater treatment system because of the risk of solids build – up and fabric contamination. Here, still chemical savings can be realized even if process water needs do not diminish. To overcome solids buildup and contamination problems, it is necessary to replace the recycle water in the system periodically with fresh water.

2.4.3.2. Caustic Recovery. To improve luster and adsorption of cotton fiber, recovery of caustic (NaOH) from the mercerization process is commonly practiced in textile manufacturing plants. In large textile mills, the requirement of caustic for mercerization is tremendous and hence multistage evaporation units are used to re-concentrate dilute NaOH rinse water for process economy. Care must be taken that the NaOH concentration in the wash boxes never fall below 2 - 4 %, otherwise the recovery of NaOH becomes economically impractical. In other words, if the caustic concentration falls below 2%, the rinse water (caustic solution) must be discharged to the wastewater treatment unit. The rinse water fed to the evaporator is usually concentrated up to 50 % NaOH (Gaddis et al., 1988).

The major limitation of efficient caustic recovery for the mercerization process is the buildup of fabric impurities in the caustic concentrate after repeated evaporations. At this stage, the contaminated caustic solution becomes discarded. This can be avoided if an UF unit is unit is used to periodically remove impurities from the caustic solution prior to evaporation. One textile finishing plant has reported that the UF system has paid itself back in 1.5 years and has been operating for 8 years with an annual savings of 1.5 million USD in NaOH cost (Johnston and Wett, 1989). The recovery of NaOH also contributes to the cost of neutralization with acid and reduced salinity in the discharged effluent.

2.4.3.3. Indigo Dye Recovery. Indigo dyes are usually present in vat dyes together with dye auxiliaries such as sodium hydroxide and lint fibers. Indigo dye is recalcitrant and hence passes through conventional activated sludge treatment systems. Vinyl sulfone UF units are generally used for indigo dye recovery (Leonard, 1981). Important is to design the dyeing process in such a way that the indigo dyeing operation is complete before sulfur

dye application to prevent the contamination with sulfur dyes. Three-stage UF units are used to provide more circulation velocity and to prevent membrane fouling. Each stage automatically establishes a steady state indigo concentration increase from 800 to 20000 mg/L dye in the retentate and unwanted, residual water and chemicals in the permeate. The resulting, recovered solution is then filtered through a 74 μm basket strainer and thereafter stored in a holding tank for up to 4 days prior to its supply. Ratios of concentration flow rate to feed water flow rate is generally varying between 1:25 and 1:50 and depends on the particular dye concentration or strength used. The permeate containing dye residues, NaOH, sodium sulfite and surface active agents, is of no value and has to be discarded as effluent. High rinse water flow rates applied after indigo dyeing increases capital costs (i.e. size) of membrane modules used for indigo dye recovery. Hence rinsing at low flow rates (via counter-current rinsing techniques) giving low volume high concentration rinse water is economically more practical and may reduce treatment costs to almost one third of that required for conventional indigo dyeing operations. This again points out the importance of automatic process control for regulating process variables to achieve optimum recovery conditions.

2.4.3.4. Applications of Reverse Osmosis. It is not always possible to isolate the spent dyestuffs from the waste stream. However, when specific mixtures of dyes are used to formulate a specific recipe for the dyeing process, it may be possible to recover the spent dyes. This has been reported by a plant that recovered from the reverse osmosis (RO) concentrate (Brandon, 1980). The concentrate was thereafter used for dyeing and if needed, additional dye was added to the recovered spent dye-bath if needed. Almost identical shades were produced when a relatively small amount of dye was added to complement the recipe. RO units enabled the reclamation and reuse of hot rinse water (permeate) as well as cationic, anionic dyes (forming the concentrate) for cotton, polyester, acrylic and rayon fibers. In automated dyeing systems it is possible to discharge those exhausted dye-baths causing technical problems for the filtration systems, to the wastewater treatment plant, bypassing the filtration system. Only recovery of the dye concentrate of very dark shades caused operating problems, i.e. it was only rarely possible to obtain a shade identical that of a conventional production. However, this problem can also be overcome by scheduling the dyeing in such a way that the dark shadings follow the

light one and never vice versa. Such a procedure of right scheduling would also minimize the need for extensive equipment cleaning.

Table 2.6. shows the cost savings generated by a recovery system with which it was possible to recover over 332400 USD/year from energy, water and wastewater treatment savings (Brandon, 1980). The system was able to recover soluble dyes and could pay for itself in 1.5 years. Presently, one of the few RO membranes capable of handling wastewater above 100 ^{o}C is manufactured by Dupont Separation Systems in Seneca, SC, USA.

Table 2.6. Annual cost savings obtained from the filtration and recycling of dyeing wastewater

Assume 300 Working Days/year and 3 Shifts/day	Savings (USD)
1. Reduction in water use from 100 gal/min to 5 gal/min	
a. process water savings (1 USD/1000 gal)	41000
b. wastewater treatment (2 USD/1000 gal)	82000
2. Reduction in energy consumption	
a. hot water (60 - 180 ^{o}F) at 5 USD/10^{6} BTU	205400
b. boiler chemicals	4000
3. Dyes and auxiliary chemicals	Depends on the case
Total Savings	332400

2.4.3.5. Effects of Water Recycling on Wastewater Treatment. When the total water consumption is decreased by process automation and recycle systems, not only are water, waste treatment, and energy costs reduced, a considerable improvement in the biological wastewater treatment performance may also be expected. There will be additional treatment time (time for equalization, or settling) left as the water flow to the same volume of treatment unit is decreased. The additional treatment time (hydraulic retention time) should increase the overall organic matter removal efficiency and decrease the power requirement for aeration. However, the treatment process has to be carefully monitored such that chemical feed, mixing, aeration and settling rates are adjusted to the new flow conditions. The same is valid if chemical/physical treatment is practiced at the textile

manufacturing plant. Other factors may also affect the treatment efficiency, for instance not only the quantity, but also the quality of the effluent will change (Sundstrom and Klei, 1979).

In summary, the potential for savings seems very good provided that the processes are fully automated, i.e. the human element that generally takes much longer time to respond and has a higher probability for errors. Many textile plants use automation particularly for quality control rather than for recovery and reuse purposes.

There are several recycle systems in operation today. It should always be considered that some membranes are sensitive to high temperatures (nylon dyeing), and some to specific chemicals. Therefore, a membrane or filter that has the least limitation has to be selected for recovery systems and not the most economical one (Reife and Freeman 1996).

2.4.4. Significance of Textile Dyehouse Wastewaters Recovery and Reuse in the Turkish Textile Industry

In the last 20 years, textile production became an important part of our exportation. The most important reasons for the shifting of textile production from developed to developing and undeveloped countries are high labor costs, high consumption of raw material/natural resources and strict environmental legislations. Turkey, as one of those countries who did not face such problems in the past, has continuously increased its activity and investments considerably in this sector. However, the factors that led Turkey to be one of the leaders among textile manufacturers have started to disappear in the recent years. Consequently, it becomes evident that we will loose an important part of our textile production in the next 5 or 10 years if necessary precautions are not taken.

The reason why some of the European countries can still maintain their market share in textile production is because they have foreseen this threat in time and taken critical measures by focusing on:

- the production of textile finishing machineries, highly complicated machinery/process controllers and software,
- chemical and dyestuff development technologies,
- technical textile production,
- right first time production,
- leading fashion instead of following others

Although those efforts have proven their success, European countries have definitely failed to hold their position in the textile wet processing sector. The most important factors for this situation may be attributable to the dramatic increase in process water costs due to the more stringent environmental legislations and the reduction in water resources. Their inability in solving the water problem (shortage and increasing costs) could be due to facts that

- technology and pollution prevention did not go hand with each other (lack of advanced machinery with low rate water consumption without reducing product quality),
- the cost of wastewater recovery was still much higher than the supply of fresh water.

In Turkey similar problems seem to appear as a result of

- unconscious water usage techniques leading to reduction of both quality and quantity of water resources,
- the difficulties to get license from municipalities to drill and operate new wells,
- increasing costs of water supply by tracks,
- the high fees that have to be paid to discharge partially pretreated waste water
- the continuous increase in the number of pollution parameters for the requirements of European discharge standards.

It is evident that all these factors stimulate dyers to pay more attention to apply best available technologies to reduce water consumption but sooner or later water recovery and

reuse will be unavoidable. Fortunately, the increased application of membrane technologies has led to a tremendous reduction in membrane unit costs. In addition development in chemical and dyestuff technologies made the treatment, recovery and reuse of dyehouse effluent easier. On the other hand, since there is not a single, complete solution for all dyehouses, more attention should be paid to enable textile dyehouse wastewater reuse technically and economically feasible.

2.4.5. Introducing the Textile Mill under Investigation

The raw and biotreated textile wastewater was obtained from a local textile dyeing and finishing company located in Yenibosna, Istanbul, Turkey. The process flow scheme of the mill is depicted in Figure 2.10. The company works three shifts (8 h each) as a commission dyer treating only knit qualities with a capacity of 20 tones finished fabrics per day. As a typical commission dyeing and finishing mill, all kind of cellulosic (cellulose and regenerated cellulose) and synthetic fabrics (polyester, polyamide, acetate) are processed. The production consists of:

- Pretreatment and Dyeing: 12-13 t/d (60 percent cellulosics and 40 percent synthetics)
- Mercerization: 3-4 t/d (only cotton)
- Washing and Softening: 1-1.5 t/d
- Optical Whitening: 1-1.5 t/d (only cellulosic fabrics)

In addition to wet processing of the knit goods some physical processes are also being practiced at the plant. The physical processes are:

- Singeing (burning of the pills on the surface of the fabrics)
- Brushing, raising (giving special handling effects such as peach handle)

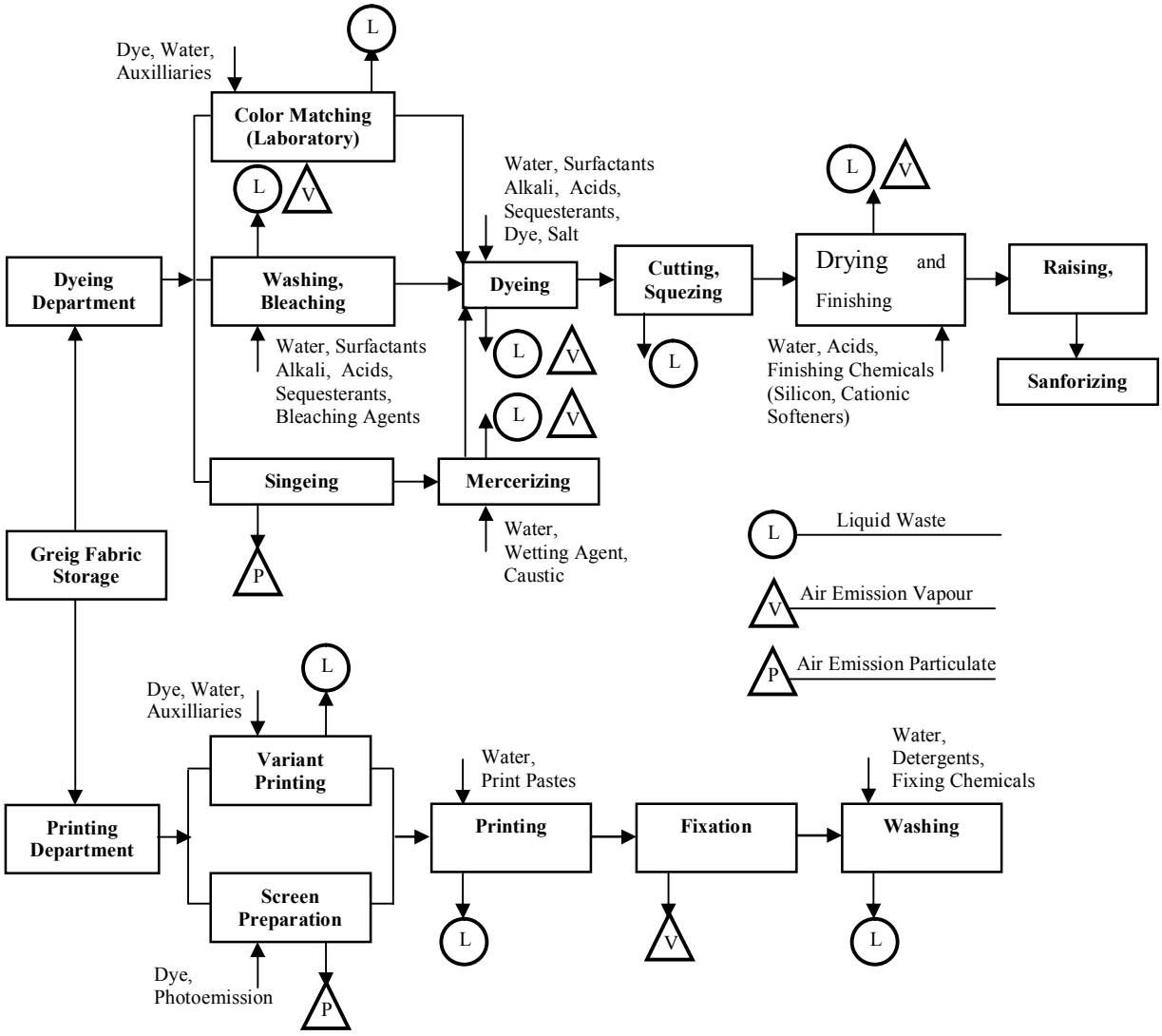

Figure 2.10. The process flow scheme of the textile dyehouse under investigation

Table 2.7. shows the relationship between process and pollution profile of the selected textile factory.

Table 2.7. Process and pollution profile of the selected mill (Ince, 2004)

Process (Source of Pollution)	Environmental Impacts
Sample dyeing	Water and energy consumption, dyestuff and chemicals consumption, vapor emissions from the dyeing and washing processes (volatile organic emissions, such as acetic acid, formic acid, polyglycol ether emissions), discharge of highly colored and high temperature effluent
Bleaching, dyeing and washing-off	Water and energy consumption, dyestuff and chemicals consumption, emissions of toxic vapors such as sulfur, alcohol, trichloroethylene, formic acid, nonyl phenol vapors, highly colored, high temperature, pH & COD effluent discharge
Drying, thermo-fixation, finishing	Water and energy consumption, emissions of vapors such as acetic acid, formic acid, ammonia, isopropanol, methanol, trichloroethylene, perchloroethylene vapors, high temperature, pH & COD effluent discharge
Printing	Water and energy consumption, dyestuff and chemicals consumption, emissions of volatiles such as acetone, toluene, ethylene glycol etc.)
Fixation and washing of the printed fabric	Water and energy consumption, dyestuff and chemicals consumption, emissions of toxic volatiles such as ammonia, acetone, methanol, acetic acid, methyl acrylate, isopropanol, noise & odor emissions, high COD effluent
Energy generation and maintenance	Water & energy consumption, hazardous gas emissions (nitrogen, carbon monoxide, carbon dioxide), liquid waste effluent at high pH & T, hazardous solid waste discharge (mineral oils, accumulators, contaminated vessels & containers)

The total wastewater production of the textile mill is about 2000 m^3/day and for its secondary treatment a 1000 m^3 capacity sequencing batch reactor (SBR) is operated to fulfill secondary treatment goals. The SBR unit features the following 8 h cycle:

1. Filling of wastewater and aeration (4.5 h)
2. Aeration (1 h)
3. Settling of the bacteria (1 h)
4. Draining of the biotreated effluent (1.5 h)

3. MATERIALS AND METHODS

3.1. Characteristics of Effluent Samples

3.1.1. Raw and Biotreated Effluent

All effluent samples used in the batch, continuous electrolysis and ozonation experiments were obtained from the local textile dyeing and finishing company introduced in section 2.4.5. In the batch electrolysis and ozonation experiments, biologically pretreated textile effluent was used as wastewater samples, whereas in the continuous mode electrochemical treatment, both biotreated and raw (untreated) were employed.

The characterization of the raw and biologically pretreated textile effluent is given in Table 3.1. All effluent samples were stored in 8 L plastic carboys at 4 ^{o}C prior to use.

Table 3.1. Environmental characterization of raw and biologically pre-treated textile effluent samples

Parameter	Raw Effluent	Biotreated Effluent
COD (mg/L)	1450	350
BOD_5 (mg/L)	560	80
A_{436} (1/cm)*	1.356	0.350
A_{525}(1/cm)*	2.155	0.230
A_{620} (1/cm)*	0.776	0.161
Sulphate (mg/L)	420	1250
Total Alkalinity (mg/L)	650	350
pH (-)	10	7.5
Dissolved Solids (mg/L)	10000-14000	6000-8000
Suspended Solids (mg/L)	450	140

*Absorbance measured in 1 cm path length cells

3.1.2. The Dyebath Effluent

Sonication experiments were conducted with simulated dyebath effluent formulations (Tezcanli-Guyer et al., 2003). For that purpose, dyeing auxiliaries were obtained from the dyeing mill under investigation whereas the dyes used in the study (CI Reactive Blue 19, CI Basic Blue 16 and CI Basic Brown 4) were purchased from Aldrich in 45, 70 and 40 percent purity, respectively. Upon preparation of the dyebaths in accordance with the provided recipes, the bath containing Reactive Blue 19 was heated to 90 ^{o}C, following pH adjustment to 11, and maintained at its temperature for 6 h to complete hydrolysis and simulate reactive dyebath effluents. Stock solutions were prepared by 67 fold (v/v) dilution of the initial simulated dyebath with tap water to mimic effluents from the washing operations. The dilution water contained 65.5 mg/L calcium carbonate alkalinity and 33.6 mg/L chloride. All stock solutions following 2 h aeration were transferred to glass bottles, kept and maintained in the dark at 4 ^{o}C. The composition of aerated reaction solutions of simulated dyebath effluent is given in Table 3.2.

Table 3.2. Composition of the simulated dyebath effluent following 2 h aeration

Dyebath	Dye Auxiliary	Concentration (mg/L)
DB1[a]	Sequestering agent (Verolan NBO)	7.5
	Anticreasing agent (Slipper)	15.0
	Acetic acid	4.5
	Sodium chloride	900.0
	Sodium carbonate	300.0
	Calcium carbonate	65.5
	Chloride	33.6
DB2 and DB3[b]	Leveling agent (Avolan IV)	15.0
	Acetic acid	22.4
	Sodium sulphate	90.0
	Calcium carbonate	65.5
	Chloride	33.6

a: DB1 contains 0.048 mM Reactive Blue 19

b: DB2 contains 0.059 mM Basic Blue 16 and 0.065 mM Basic Brown 4

Hydrogen peroxide (35% w/w) used in the sonication experiments was obtained from Merck whereas H_2SO_4, NaOH used for pH adjustment purchased from Fluka Chemicals Corp., and of high purity grade. Potassium iodide employed for the determination of feed and off gas ozone was obtained from Riedel. All other chemicals were of high purity and obtained from the companies indicated above.

3.2. Experimental Setup

3.2.1. Batch Electrolysis

Batch tests were conducted in a 6000 mL electrolytic cell. The experimental setup is schematically shown in Figure 3.1. The electric power required during these experiments was established to provide a direct current (DC) output of 0-60 A and 0-24 V. The polarity reversing time was alternated through the microprocessor to prevent electrode passivating and increase service life.

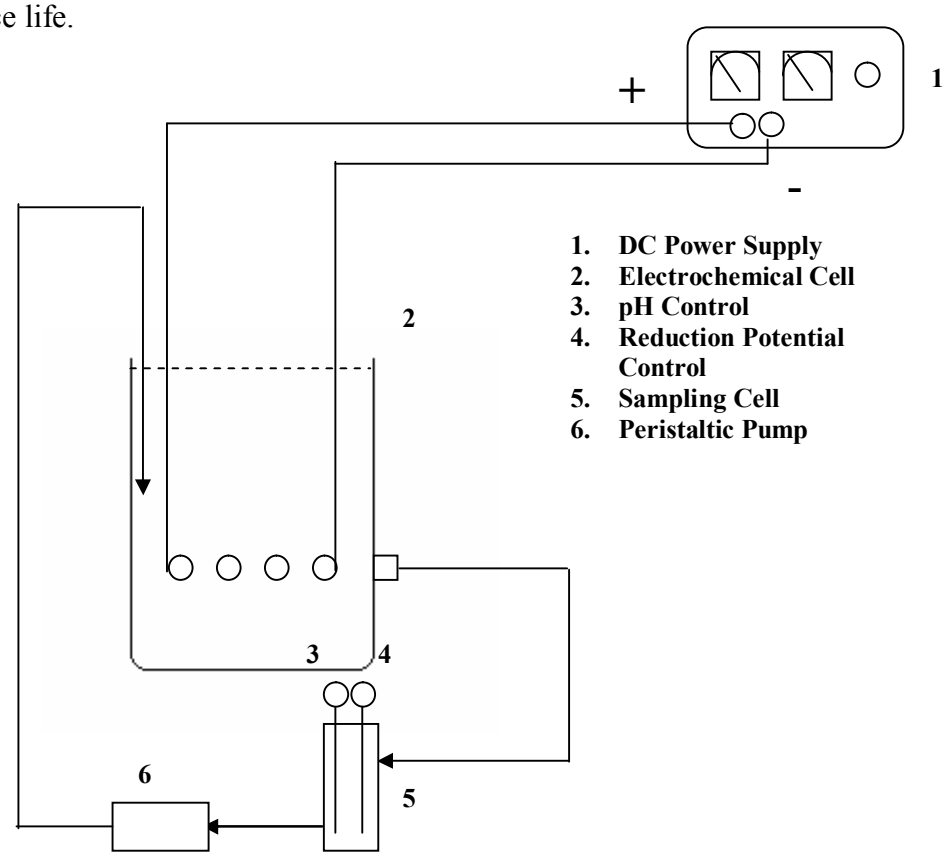

Figure 3.1. Schematic representation of the batch electrochemical setup

During the electrolysis experiments three different electrode systems were analyzed. These systems are schematically represented in Figure 3.2. In Figure 3.2.a. four iron electrodes were utilized as both anode and cathode materials, whereas in 3.2.b. four aluminum electrodes were used as both anode and cathode. On the other hand, in the third configuration iron and aluminum electrodes were connected to each other and used as sacrificial anodes to be consumed simultaneously. The aim of the third system is to benefit from the existence of the both metal anions in the electrolysis solution at the same time. All tested electrodes were of cylindrical, rode shape and had a geometric surface area of 44 cm^2. The electrode spacing was adjusted to 5 mm and separated with silicone at both ends. During all experiments polarization time was set as 5 min, i.e. the time when coating of the electrode surface became apparent.

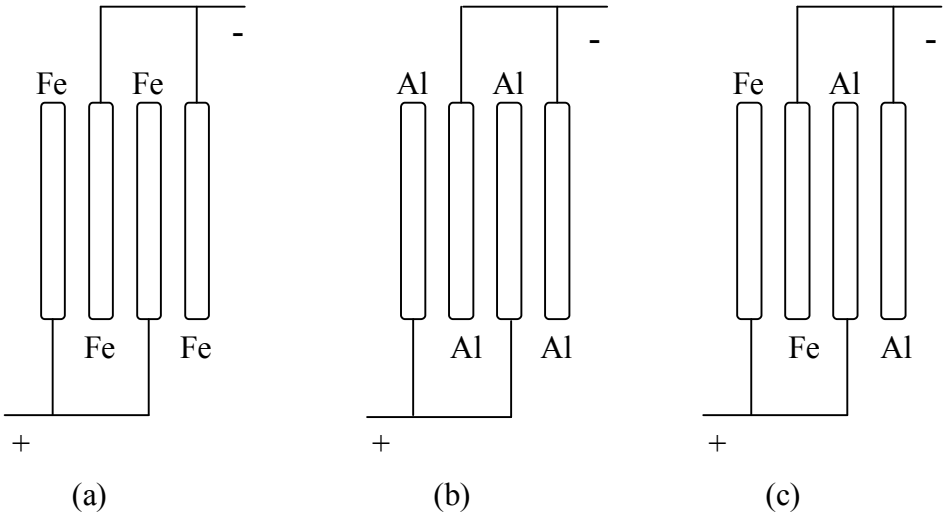

Figure 3.2. Electrode material configurations used during electrolysis experiments a. Iron electrodes as anode and cathode; b. Aluminum electrodes as anode and cathode; c. Iron/aluminum electrodes as anode and iron/aluminum electrodes as cathode

3.2.2. Continuous Electrolysis (CET)

The experimental setup consisted of a 25 L capacity plexi-glass electrochemical cell (Figure 3.3.) divided into two regions. The four iron electrodes, each 25 mm in diameter and 400 mm in length, were placed in the upper region of the reactor, where the coagulation and flotation processes occurred simultaneously. Below this region, the heavy sludge was separated from the treated wastewater by passing it through four parallel plates with 45^{o} inclination. The electrodes were attached to a direct current (DC) power supply through a microprocessor.

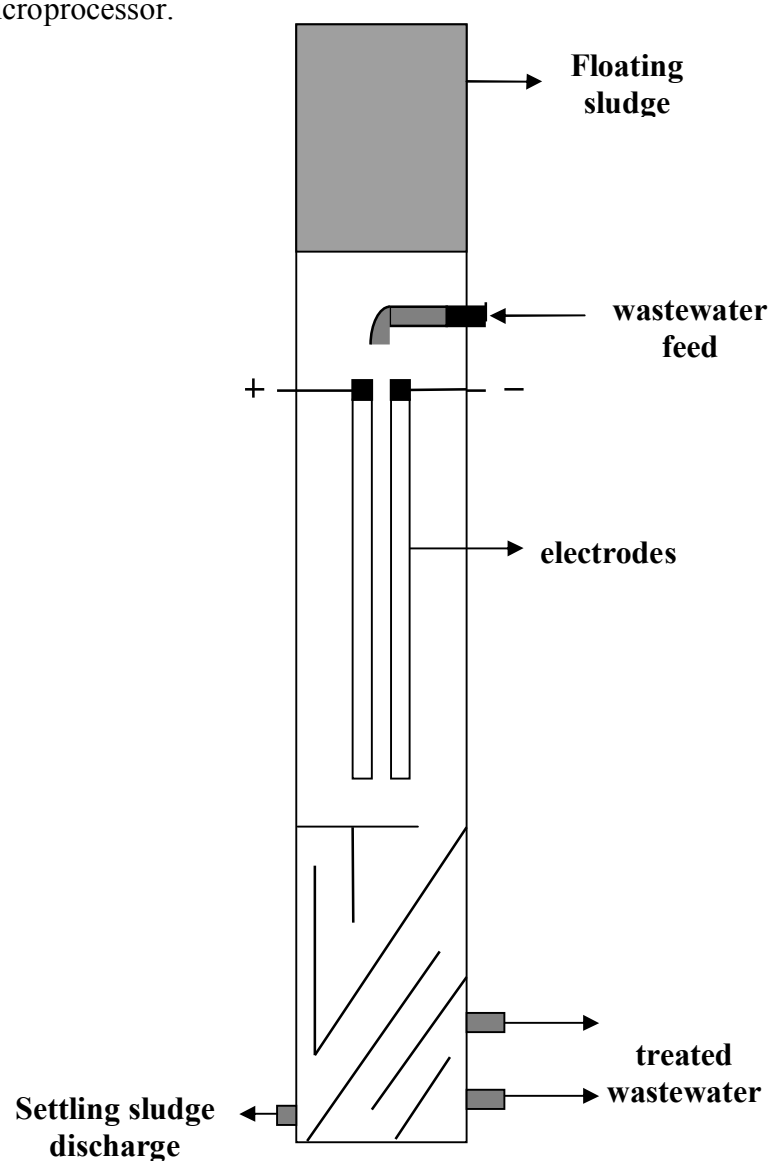

Figure 3.3. Schematic representation of the continuous electrochemical setup

Since there was a constant flow of wastewater passing through the electrodes the coating of the electrodes started after 10 min of electrolysis. Therefore in continuous electrolysis tests the polarity reversing time was set as 10 min.

3.2.3. Ozonation

The ozonation system comprised of a 1000 mL - capacity borosilicate glass bubble column used as the reactor unit as presented in Figure 3.4. A course sintered gas dispersion disc continuously delivered an O_3 gas + air mixture from the reactor bottom at a flow rate of 1.3 mL/min. Ozone was generated from air using a Air Purification Technologies Inc. WPN-05 model pilot scale ozone generator with a maximum production capacity of 6 g/h O_3. The applied ozone dose was set to a constant value as 1440 mg/h, corresponding to an ozone input rate of 1440 mg/L of wastewater.

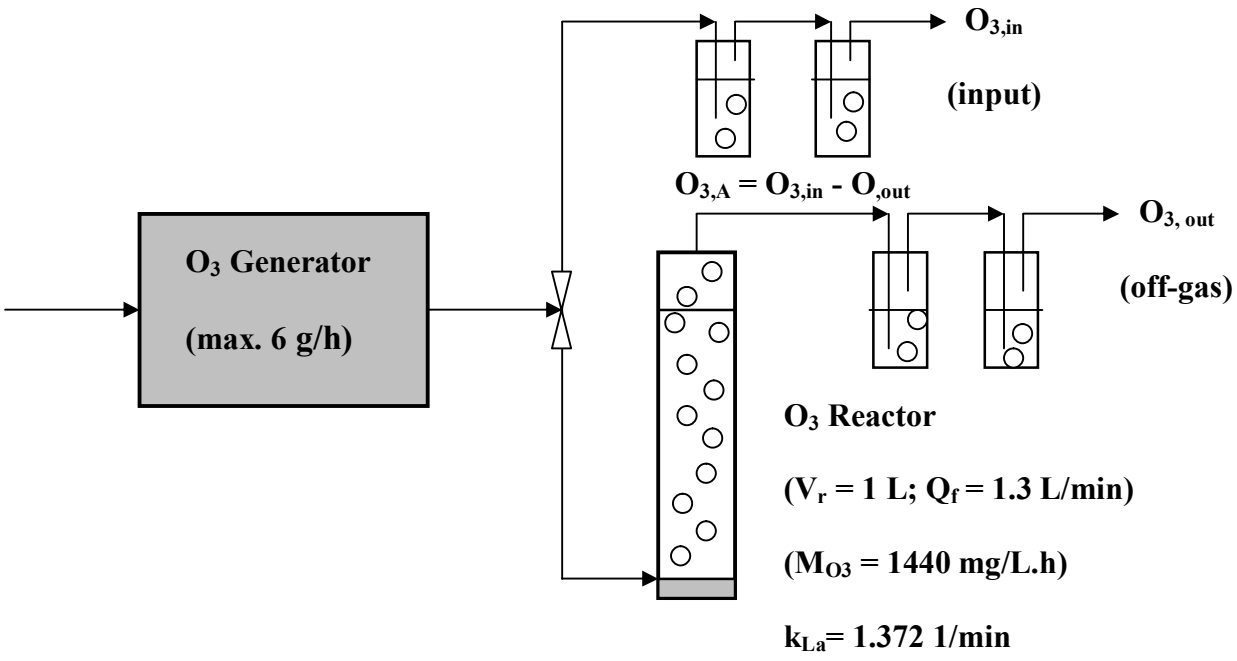

Figure 3.4. The ozone contactor

3.2.4. Ultrasonic Setup

The reactor contained a 150 mL glass cell surrounded by a water-cooling jacket to keep its contents at constant temperature (20 ± 0.5 ^{o}C), a plate-type piezoelectric transducer emitting ultrasonic waves at 300 kHz, and a 25 W generator to convert electrical power input into mechanical energy (Undatim Ultrasonics). The schematic representation of the reactor is presented in Figure 3.5.

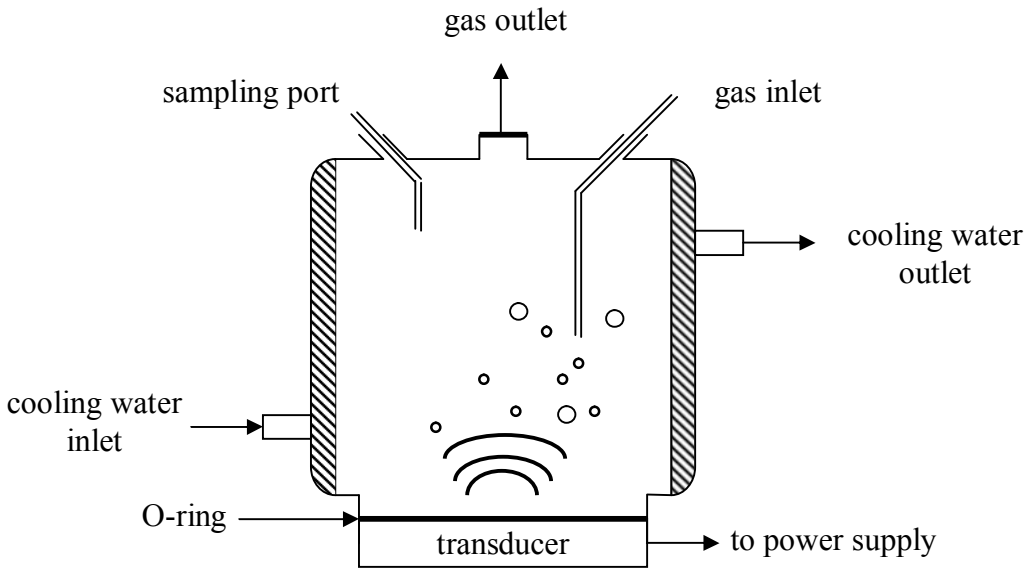

Figure 3.5. Schematic representation of the ultrasonic reactor

3.3. Experimental Procedures

3.3.1. Batch Electrolysis Experiments

A typical electrolysis experiment run was conducted by the following protocol:

- Electrode surface cleaning with 6 N HCl solution, rinsing with deionized water, emerizing of the surface (when necessary), final rinsing with deionized water and drying of the electrode,
- Filling of the electrolysis cell with 5 L of wastewater after pH adjustment,

- Starting to reaction by opening the direct current (DC) power supply and adjustment of the current,
- Closing of the power supply and leaving the solution for 1 h for degassing and settling
- Sampling from 3 cm above the reactor bottom.

The pH, and the redox potential were continuously monitored outside the electrolytic cell by circulation of the reaction solution by means of an electrostatic pump when necessary.

3.3.1.1. Determination of the Optimum Electrolysis Time. The effluent of the biological treatment plant in the textile dyeing mill was used for determination of the optimum reaction time. Contact time was optimized at 20 A current for iron, aluminum and iron/aluminum electrodes and for each initial pH selected. Since degassing and settling were necessary at the end of each set, separate experiments were conducted for 5, 10, 15, 20, 25 and 30 min. The efficiency of electrolysis was evaluated in terms of chemical oxygen demand (COD) and suspended solids (SS).

3.3.1.2. Evaluation of the Effect of Applied Current. The effect of current input (5, 10, 20, and 30 A) was investigated for each electrode material and initial pH at fixed electrolysis time of 15 min. The electrolysis efficiency was evaluated in terms of COD, Color, SS, SO_4^{2-} and dissolved solids (DS) reduction. In addition, for better understanding the mechanism of color removal, the reduction potential was monitored during electrolysis for each run. Finally, the change in conductivity of the effluent was measured after each electrolysis experiment to assess the effluent's potential for reuse.

3.3.2. Continuous Operation of Electrochemical Process

Pilot scale electrochemical treatment of raw and biologically pretreated textile dyehouse wastewater was investigated. After filling the reactor with 25 L of wastewater, the DC power was supplied to the electrodes for 15 min without any wastewater flow inside and outside to the reactor. At the end of 15 min electrolysis, i.e. the time at which the color of the reactor content disappeared, the reactor was fed with fresh wastewater at a

flow of 150 L/h. The flow was adjusted to obtain a minimum level of reduction potential to maintain constant decolorization efficiency. Treated effluent samples were collected after 1 h of operation for the evaluation of the treatment performance in terms of COD, color, conductivity, SS, Fe^{2+}, Fe^{3+} and pH.

3.3.3. Evaluation of the Treatment Performance of Biological Treatment System on Electrochemical Process

The effect of biological treatment performance on the effectiveness of electrolysis was evaluated for the case of batch and pilot electrochemical systems. For that purpose the wastewaters were collected from the operating sequencing batch reactor (SBR) under three different conditions of:

- Case I: Reduced Aeration (30 min instead of 60 min),
- Case II: Reduced Settling (30 min instead of 60 min),
- Case III: Reduced Aeration and Settling.

The effluents of the biological treatment plant were used as the wastewater for electrolysis. The efficiency of electrolysis was re-evaluated with different electrodes in terms of COD and SS removal under the above conditions of biological treatment without increasing the electrical current (20 A) and electrolysis time (15 min).

3.3.4. Ozonation Experiments

For a typical run, the reactor was initially charged with the biotreated or biotreated + electrochemically pre-treated textile effluent and ozonated for 1 h in “semi-batch mode” with respect to ozone gas flow. Teflon tubing was used for all connections from the ozone generator to the reaction vessel. All excess (unreacted) gaseous ozone leaving from the reactor top was collected in two gas washing bottles connected in series and filled with 10% KI solution in order to determine the amount of off-gas ozone production. Two other gas washing bottles filled with only 2% KI solution were placed in another ozonation line in order to determine the exact ozone input rate prior to adjustment of the appropriate

ozone dose. Ozone was fed to one of the lines (input line or ozonation line) by means of a three-way valve.

3.3.5. Ozonation of Biotreated and Biotreated + Electrochemically Treated Effluent for COD and Color Removal

In the first stage of experiments, the performance of ozonation was evaluated for the biological treatment effluent at varying initial pH (4.5, 7.5, and 9.5) and contact time (ozone dose) in terms of color and COD removal. In the second stage, biotreated effluents were electrolysed in the batch electrochemical cell for 15 min at 20 A using iron, aluminum and iron/aluminum electrodes at varying initial pH. After allowing enough time for degassing and settling, the effluents of electrolysis were collected and used as the wastewater for ozonation. The performance of ozonation was re-evaluated in terms of color and COD removals.

3.3.6. Sonolysis Experiments

Two 100 ml of test samples with different pH (4.5 and 3.0) were prepared from the dyebath stocks. The experiments involved 1 h sonication of the aliquots in the absence and presence of 7 mM hydrogen peroxide during argon bubbling at 2 L/min. Effluent samples were collected at 0, 3, 5, 10, 15, 20, 30, 45 and 60 min to run spectrophotometric analysis. In addition initial and final COD of effluent samples were also determined.

3.4. Analytical

All samples collected during the experiments were filtered through Whatmann No. 40 (8 μm) filter paper prior to analysis of collective environmental parameters, which accurately simulates the results of multimedia filtration (Wilcock et al., 1996).

The pH of sample solutions was detected by a pH-mV-meter (WTW-pH 330, Germany). COD, ferric iron, ferrous iron and total iron measurements were carried out

using appropriate test kits colorimetrically. Suspended solids (SS), sulphate and total alkalinity analyses were conducted according to Standard Methods (APHA, 1998). Dissolved solids and conductivity were determined by employing a WTW-LF 330 model conductivity meter. The changes in reduction potentials were monitored by Hanna (HI-98201) ORP electrode.

Color was analyzed by a single beam UV-VIS spectrophotometer in 1 cm path length quartz cuvettes. For that purpose, the absorbance of filtered, raw and treated effluent samples were determined at three different wavelengths, namely at λ = 436, 525 and 620 nm wavelengths, for yellow, red and blue color, respectively. These wavelengths have been specially selected due to the following reasons:

i. textile wastewater samples are always trichromatic mixtures of the above mentioned colors,
ii. measurements at these three wavelengths are currently practiced in accordance with regulations and limits set for textile wastewater discharge in many EU countries (Gaehr, 1994).

Each effluent samples were also scanned in the near-UV and VIS spectrum (i.e. between 300 and 700 nm) to observe changes in characteristic absorption bands and chromophoric groupings after treatment.

The input and off-gas ozone concentrations were determined iodometrically (IOA, 1987) to calculate ozone absorption rates (O_{3A} values) for each run as follows;

$$O_{3A}\ (mg/L) = \text{applied } O_3\ (mg/L) - \text{off - gas } O_3\ (mg/L) \quad (3.1)$$

$$O_{3A}\ (\%) = \{\text{absorbed } O_3\ (mg/L)/\ \text{applied } O_3\ (mg/L)\} \times 100 \quad (3.2)$$

The volumetric ozone mass transfer rate constant k_{La} was determined as L/min at an ozone feeding rate of 10 mg/min and pH = 2.0 employing the indigo colorimetric method (Bader and Hoigné, 1981).

4. RESULTS AND DISCUSSION

4.1. Application of Batch Electrolysis

As mentioned in 3.3.1, samples for this section were collected from the biological treatment plant in the dyeing mill under investigation. During the experiments iron, aluminum and iron/aluminum electrodes were slowly consumed at anode, as the metal hydroxide matrix was generated to bring about charge neutralization (electrocoagulation). The coagulated flocs were simultaneously floated by the electrolytic production of the hydrogen gas evolved from the cathode (electrofloatation).

4.1.1. Optimization of Reaction Time

Contact time was optimized at 20 A, the current at which hydrogen gas production and mixing of the reactor contents could be monitored most efficiently, for each electrode material (iron, aluminum, and iron/aluminum) and each initial pH (4.5, 7.5, 9.5) in accordance with the following considerations:

i. COD Reduction,
ii. SS Reduction.

Reaction time intervals were selected as 5-10-15-20-25, and 30 minutes and for each reaction time a separate experiment was conducted in order to allow enough time for degassing and settling of the electrolysis cell content.

4.1.1.1. COD Reduction. The operation of the biological treatment plant in the mill is such that approximately 70% of total COD is removed. The remaining organic carbon content of the dyehouse effluent is defined as a mixture of slowly biodegradable and practically inert COD that has to be removed using advanced physicochemical treatment methods. Consequently, during the optimization of the operating conditions of the method

proceeding biotreatment, one of the major criterion is the removal of remaining, "difficult-to-degrade COD".

• iron electrode

Changes in COD of biotreated effluent during 30 min electrolysis using iron electrode at three different pH is presented in Figures 4.1.

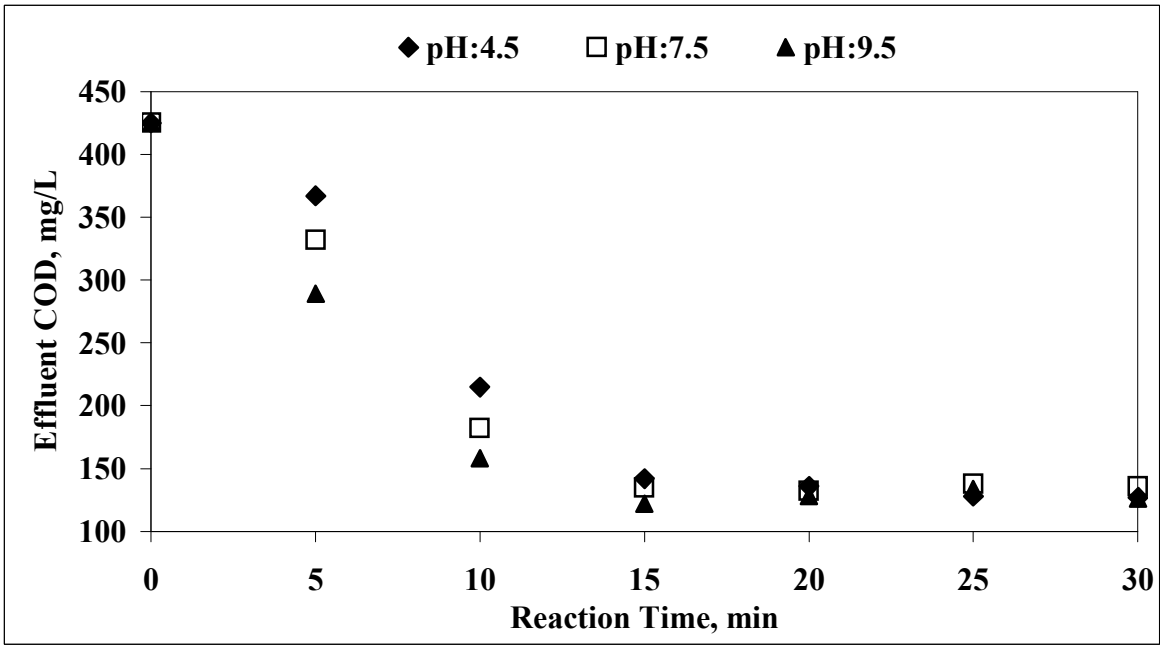

Figure 4.1.The effect of electrochemical reaction time on COD removal at varying pH (COD_0 = 425 mg/L; electrode material: iron)

As can be seen in Figure 4.1, similar trends in COD reduction have been obtained for all studied initial pH values. Increasing the reaction time over 15 min did not cause further reduction in COD. Therefore 15 min was selected as the optimum electrolysis time for all pH values. COD removal efficiency obtained after 15 min was 67%, 68%, and 71% at pH = 4.5, pH = 7.5, and pH = 9.5, respectively.

• aluminum electrode

It was found that COD removal was more pH sensitive when aluminum was used as the electrode material than iron. The effluent COD against contact time at different initial pH using aluminum electrode is plotted in Figure 4.2. Effluent COD remained constant after 15 min for all tested pH. 58% COD removal efficiency was obtained in 15 min with the starting pH of 4.5, whereas lower efficiencies were observed at pH of 7.5 and 9.5 (49% and 43% respectively). In general, higher COD efficiencies were obtained when iron was used as electrode material, which will be discussed in later sections in more detail.

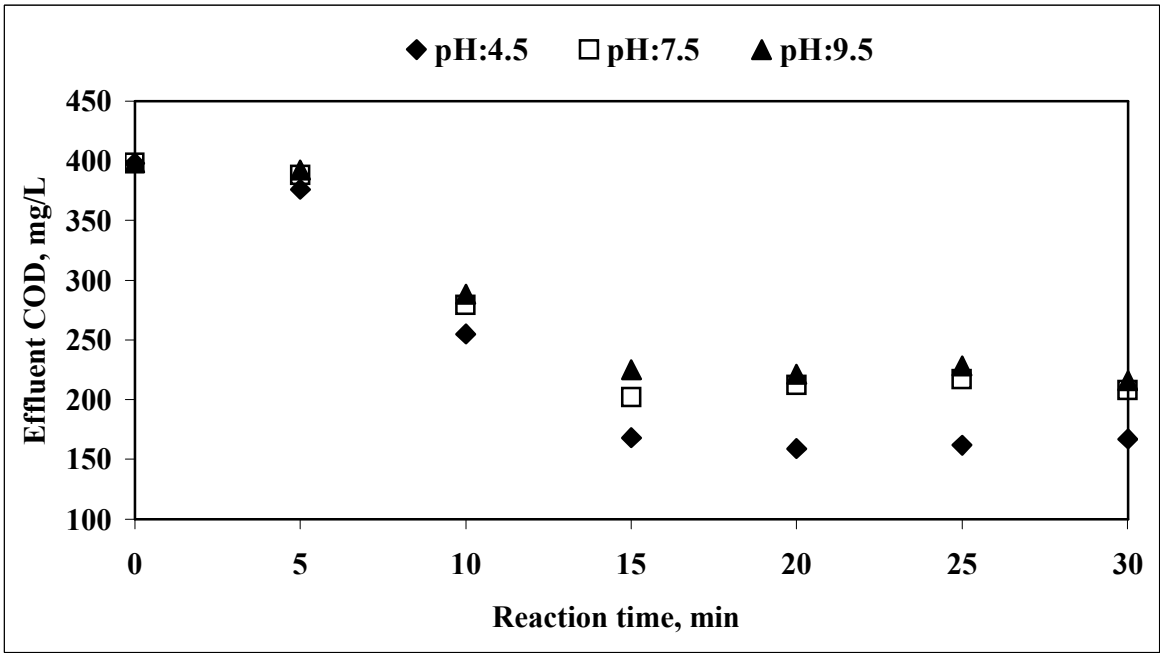

Figure 4.2. The effect of electrochemical reaction time on COD removal at varying pH (COD_0 = 398 mg/L; Electrode material: aluminum)

• Iron/Aluminum Electrode

To evaluate the combined effect of iron and aluminum, electrode configuration was changed so that both iron and aluminum dissolution took place at the same time. The final COD's obtained during electrolysis are presented in Figures 4.3.

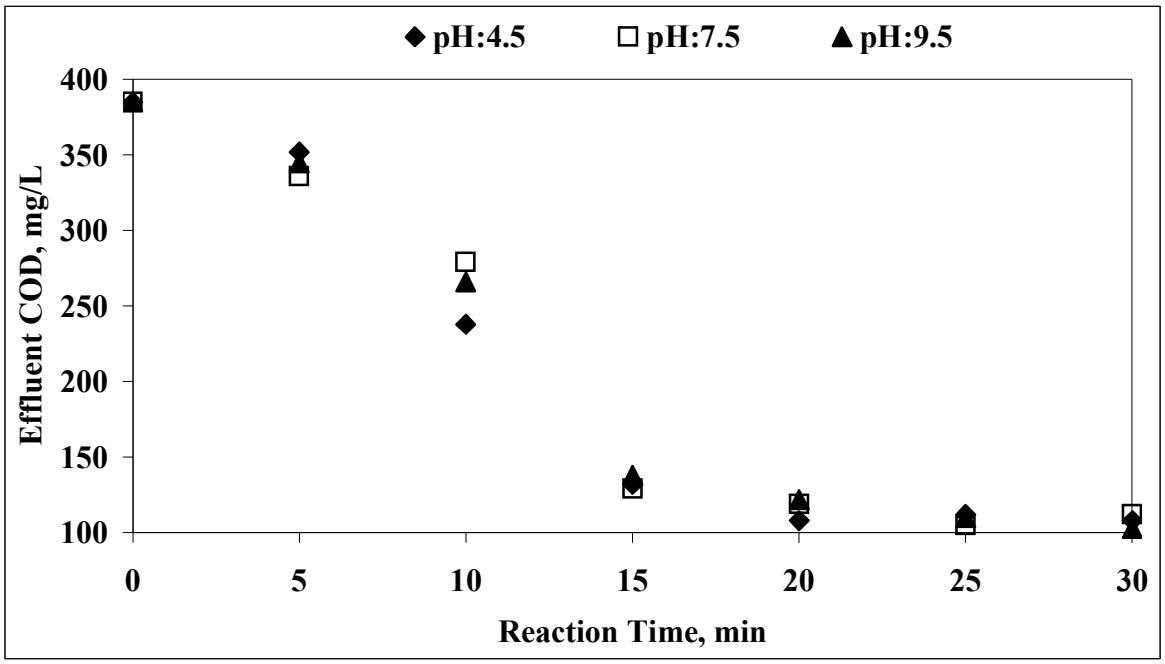

Figure 4.3. The effect of electrochemical reaction time on COD removal at varying pH (COD_0 = 385 mg/L; electrode material: iron/aluminum)

The use of combined iron/aluminum electrodes did not increase the COD removal efficiencies as compared with the use of iron electrodes separately. Although COD abatement continued over the time course of electrolysis, the major reduction in COD took place within the first 15 min. The removal efficiencies obtained after 15 min were 66%, 67%, and 64% for pH = 4.5, pH = 7.5, and pH = 9.5, respectively. Because of the effect of iron electrode, the pH sensitivity of electrolysis in terms of COD reduction was suppressed.

4.1.1.2. SS Reduction. The effluent leaving the biotreatment unit usually contains an SS concentration in the range of 80-200 mg/L under proper operation conditions. As a consequence of the significant SS concentration in the secondary treated dyehouse effluent, the optimization of electrolysis reaction time in terms of SS reduction must also be considered.

• iron electrode

Figure 4.4. shows effluent SS as a function of electrolysis time at different initial pH. At initial pH of 7.5 and 9.5, very similar SS reduction trends were obtained. After reaching minimum SS values in 15 min (15 mg/L and 27 mg/L for pH = 7.5 and 9.5, respectively), a slight increase in SS was observed at both pH values. At an initial pH of 4.5, the SS concentration of the effluent started to increase up to 15 min and achieved a maximum value of 195 mg/L. At the end of 30 min, the SS concentration was still higher than the initial SS concentration. The increase in the SS is mainly due to the fact that the iron anode dissolves very fast at acidic pH and this pH level is not sufficiently high for the development (aggregation) of the formed flocs. At the end of each experimental run the solutions were highly turbid even after 6 hours degassing and settling times. When using iron electrodes, the pH of the electrolyte steadily increased with the evolution of H_2 gas at the cathode. However, when the reaction started at low pH (pH = 4.5), the concentration of dissolved Fe^{+2} was so high that pH increase was not sufficient enough to get an acceptable level of aggregation. This may explain the fast increase of SS in the first 15 min of the experiments and the slow decrease after this point. Therefore, at low initial pH, longer reaction times must be allowed for more efficient SS removal.

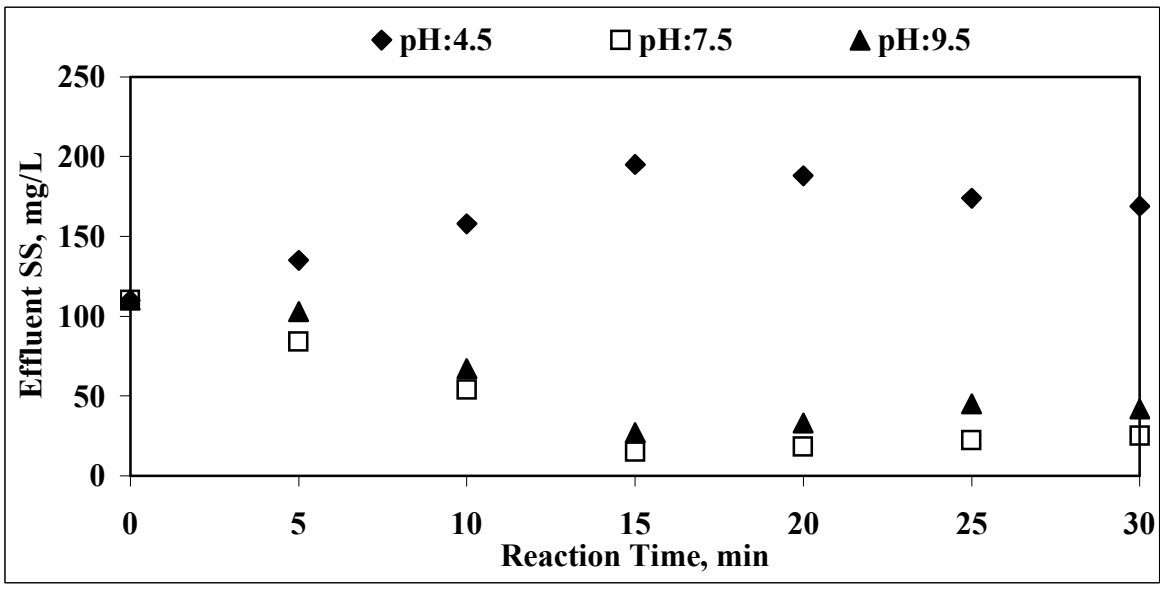

Figure 4.4. The effect of electrochemical reaction time on ss removal at varying pH (SS_0 = 110 mg/L; electrode material: iron)

• aluminum electrode

The final SS concentrations achieved with aluminum electrode (Figure 4.5.) are very similar to that of iron electrode except at low pH (4.5). In terms of SS removal, aluminum electrode shows less dependency on pH and allow a broader range of working pH. As it is obvious in Figure 4.5, SS removal is optimum in 15 min and increasing the reaction time has a negative influence on the removal efficiency. In fact, extending the treatment time increases the effluent SS content especially at pH 7.5 and 9.5. Aluminum is least soluble at pH 6.0 to 6.3 and coagulation at this pH converts most of the electrochemically added aluminum to solid floc particles and minimizes residual soluble Al, hence it is recommended that pH be controlled and maintained around these values (Reife and Freeman, 1996). When electrochemical treatment was started at pH 4.5, at the end of contact it reached that optimum range (6.0-6.5), whereas when started at neutral or basic pH, it rose beyond that optimum level (8.0-9.5). This is the major reason for higher COD and SS removal efficiencies at an initial pH of 4.5. The effect of the initial pH on the performance of COD and SS removal will be further discussed in section 4.2.2.

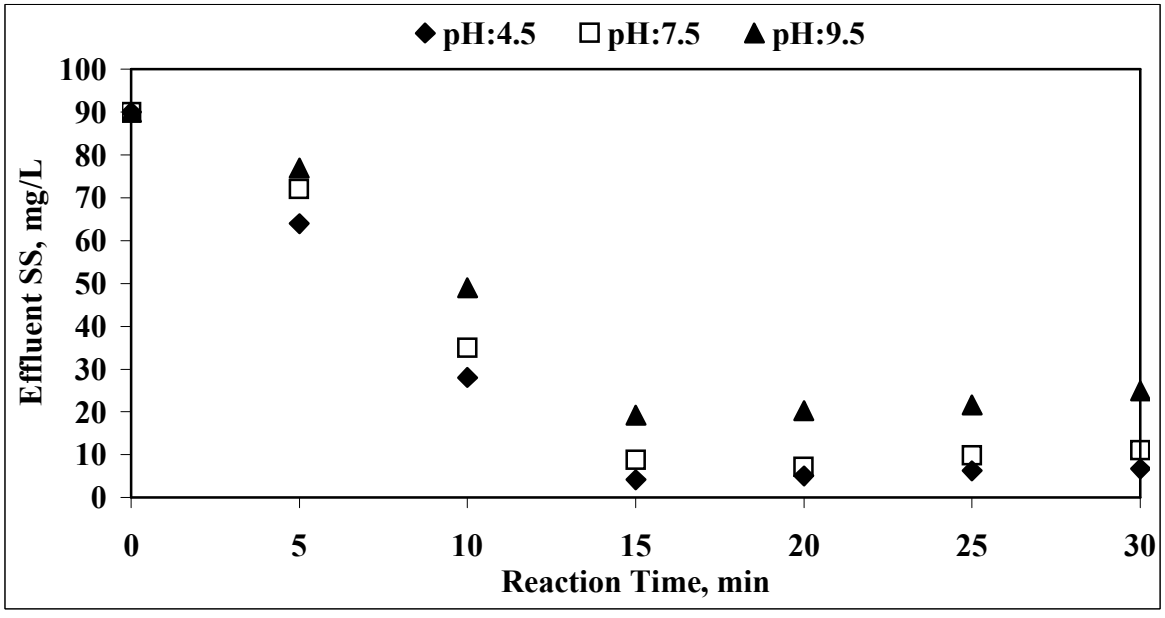

Figure 4.5. The effect of electrochemical reaction time on ss removal at varying pH (SS_0 = 90 mg/L; electrode material: aluminum)

• iron/aluminum electrode

The SS removal efficiency reached 95% at pH = 7.5 and 9.5 as presented in Figure 4.6. At pH 4.5, SS concentration was first increased from 96 to 118 mg/L and began to decrease only after 20 min of contact and at the end of 30 min a slight reduction was observed (28%). Although this trend seemed to be very similar to that obtained with the iron electrode alone, the increase in SS was lower with the iron/aluminum electrode. This is mainly because of the substitution of one of the iron sacrificial anodes by aluminum in iron/aluminum electrode matrix and hence reduction in the amount of ferrous iron transferred into the solution, which is the main reason for the increase in SS concentration.

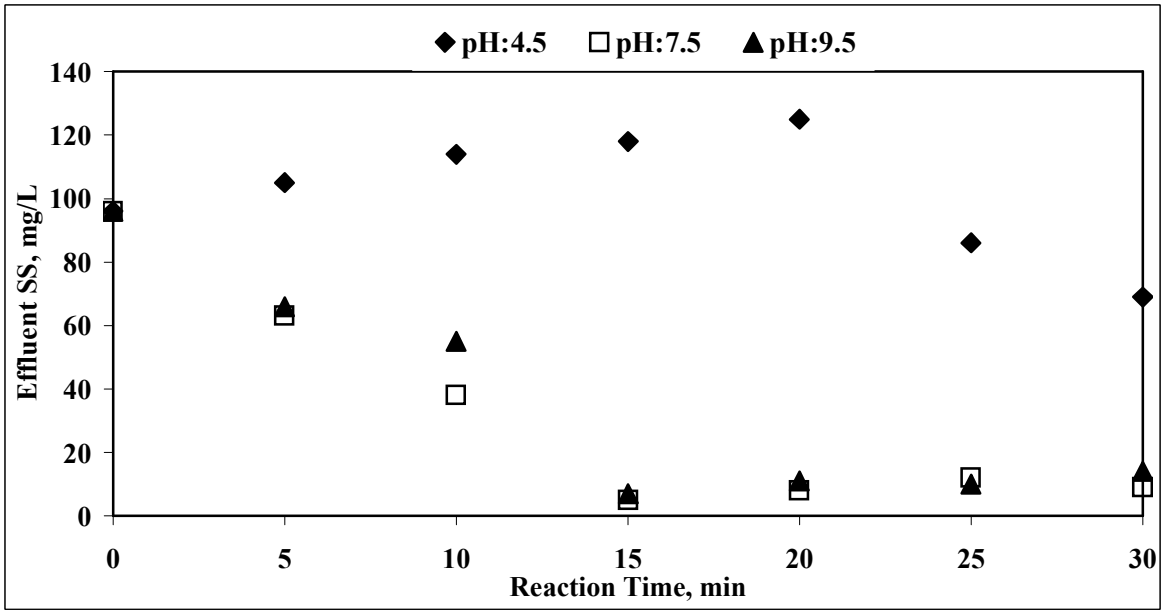

Figure 4.6. The effect of electrochemical reaction time on ss removal at varying pH (SS_0 = 96 mg/L; electrode material: iron/aluminum)

4.1.2. Effect of Contact Time and pH

Electrochemical tests with different electrode materials showed that for iron, aluminum and iron/aluminum electrodes fast COD removal occurs in 15 minutes and slight reduction obtained at extended retention times for all the tested initial pH. A very similar trend can be observed in SS removal except for the use of iron electrode at acidic pH. Therefore in the rest of the study optimum reaction time is selected as 15 min and the

effect of applied current at different initial pH is investigated for 15 min of electrolysis time.

The impact of initial pH on total COD and SS removal after 15 min contact with Fe, Al, and Fe/Al electrodes is listed in Table 4.1. It is obvious that iron is the most effective electrode at all pH levels for COD removal, followed by the Fe/Al combination. On the other hand, iron proved to be less effective for removing SS, and removal efficiencies became higher when iron is coupled with aluminum at pH = 7.5 and 9.5. At low pH (4.5) aluminum was the most effective electrode in terms of SS removal.

Table 4.1. COD and SS removal efficiencies for different type of electrode materials at varying initial pH (reaction time = 15 min, applied current = 20 A)

Electrode Material	Iron			Aluminum			Iron/Aluminum		
pH	4.5	7.5	9.5	4.5	7.5	9.5	4.5	7.5	9.5
COD Removal, %	66.6	68.2	71.3	57.8	49.2	43.5	65.7	66.5	64.2
SS Removal, %	-	86.4	75.5	95.3	90.2	78.7	-	94.8	92.7

4.1.3. Optimization of Applied Current

To evaluate the effect of the applied current, the same electrode materials were tested at varying initial pH and varying applied currents (5-10-20-30 A). The performance of the electrodes were examined in terms of COD, color, SS, TDS, and SO_4 removal. For better understanding of the electrochemical mechanism occurring during electrolysis, reduction potential was also monitored.

4.1.3.1. COD Removal.

• iron electrode

Figure 4.7. shows the effect of applied current on COD removal at different initial pH. The figure reveals that a steady increase in COD removal occurred with increasing current at pH 7.5, reaching a maximum of 72%. A similar trend and same maximum was observed at pH 4.5. On the other hand, at alkaline pH (9.5), maximum COD removal (76%) was achieved at 10 A, and no improvement was observed with further increases of current. Hence, it can be concluded that regardless of the initial pH quite similar overall COD removals can be achieved provided that a sufficiently high electrical current is supplied.

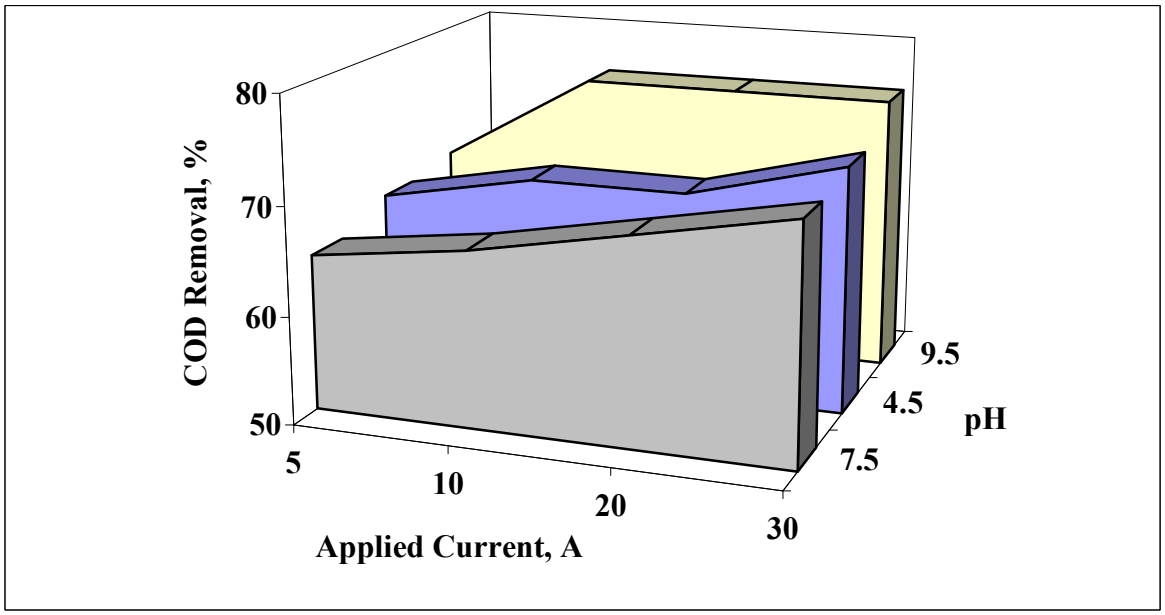

Figure 4.7. The fraction of COD removal at varying current and initial pH with the Fe electrode in 15 minutes

• aluminum electrode

Figure 4.8. shows the effect of applied current on COD removal for varying initial pH. As it is clear from the figure, a similar trend in COD removal efficiencies was observed at pH 7.5 and 9.5. COD removal efficiencies increased with increasing applied current reaching maximum values at 30 A. The COD removal efficiencies were found as 57% and 54% after 15 min electrolysis at 30 A current at initial pH of 7.5 and 9.5, respectively. However, similar COD removal efficiencies were obtained even at lower current inputs (52% at 5 A, and 59% at 10 A) at an initial pH of 4.5.

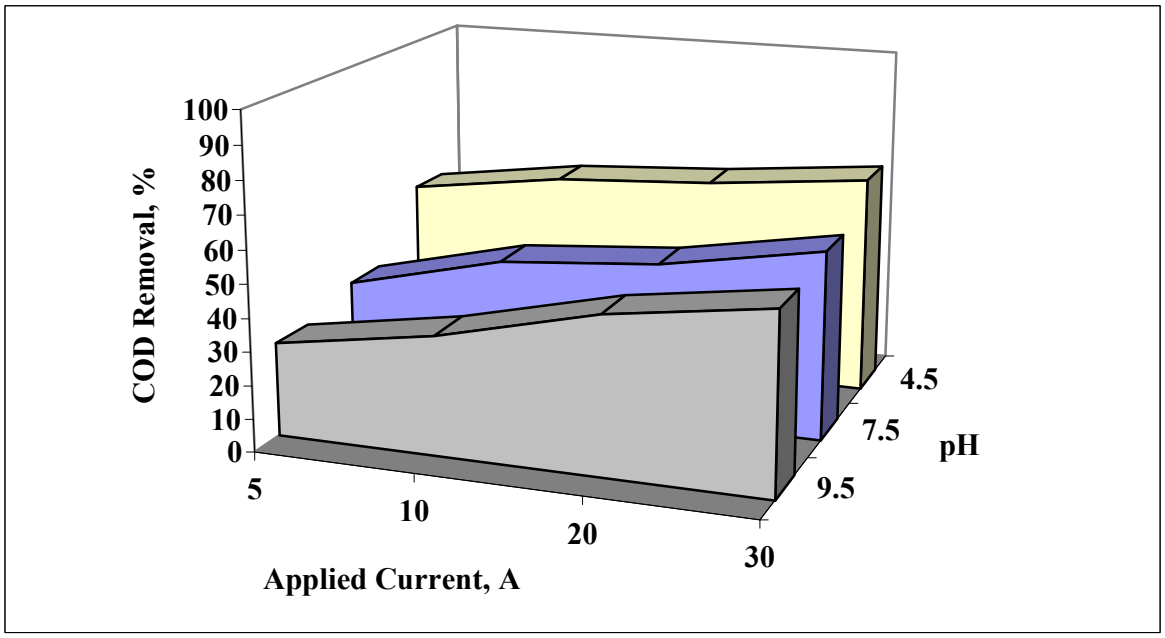

Figure 4.8. The fraction of cod removal at varying current and initial pH with the Al electrode in 15 minutes

The different effects of initial pH on COD removal can be attributed to the differences in aluminum solubilities at varying pH. Aluminum reaches its minimum solubility at a pH range of 6.0 - 6.5 (Edzwald, 1993), at which polymeric species (such as $Al_{13}O_4(OH)_{24}^{7+}$ and the precipitate $Al(OH)_3$ are formed. The removal of contaminants at this condition occurs by the following mechanisms:

i. coagulation with polymeric species,
ii. adsorption and charge neutralization (Do and Chen, 1994).

When pH is increased to 10.0, the amount of solid $Al(OH)_3$ decreases and the concentration of the monomeric anion, $Al(OH)_4^-$, becomes dominant, hence reducing the efficiency of charge neutralization, adsorption and precipitation.

Figure 4.9. portrays the changes in effluent pH for different current inputs (5 – 30 A). As shown in the Figure, when the reaction is started at pH 4.5, the final pH of the effluent is between 5.7 and 7.5, which is the most desired range for efficient contaminant removal using aluminum. The rate of pH increase in the effluent slowed down at the higher initial pH values (i.e. pH = 7.5 and 9.5) and the final pH of the effluents was still less than 10.0. However, as the Figure 4.8. supports, in order to obtain higher efficiencies in COD removal, it is necessary to initiate the reaction at a pH range within 4.5-7.5. In that case less Al and less power consumption is required to achieve sufficient contaminants removal.

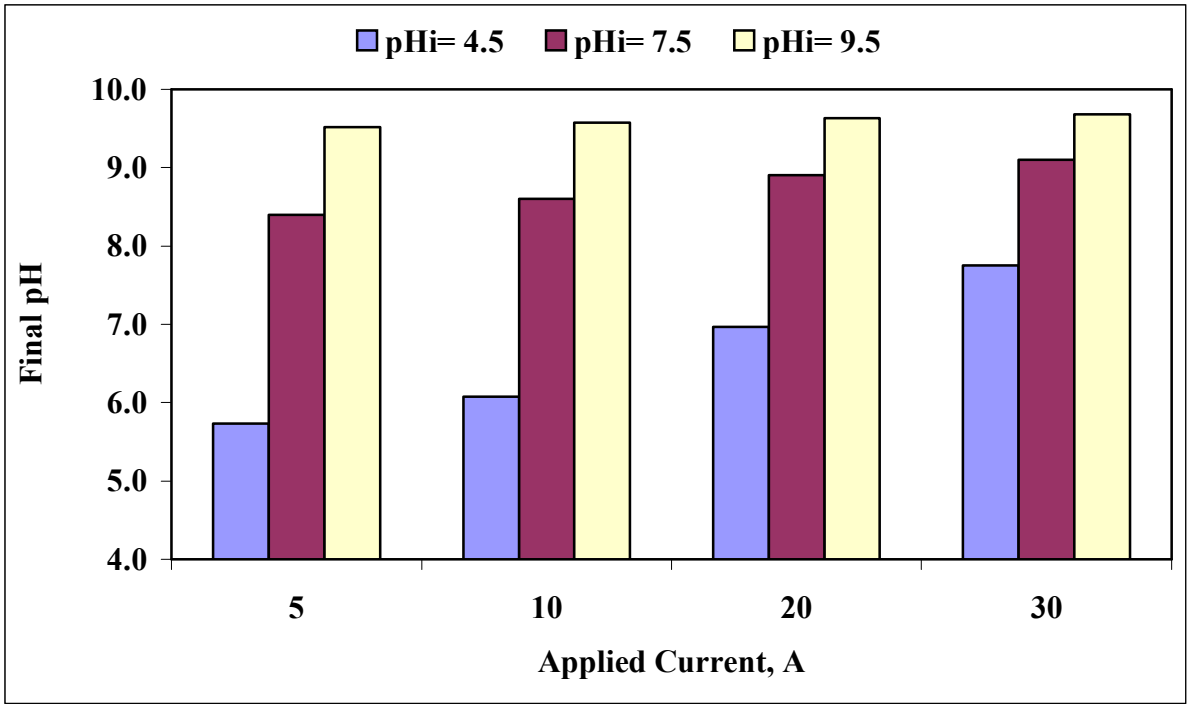

Figure 4.9. Changes in effluent pH after 15 min of electrochemical treatment at varying applied currents using aluminum electrodes

• iron/aluminum electrode

Experimental studies have shown that contaminant removal mechanisms are different in the case of iron and aluminum electrodes. Iron electrodes seem to be more effective than aluminum in terms of COD removal. In the present section, the impact of the applied current on COD removal was investigated using Al/Fe electrode.

Figure 4.10. displays the COD removed at different initial pH using 10, 20, and 30 A. The figure reveals that COD removal efficiencies were very close to each other for all initial pH and applied currents. The results indicated that by combining iron and aluminum electrodes, the pH sensitivity of aluminum could be eliminated. The lowest degree of COD removal was obtained at pH = 7.5 as 65%, whereas the highest COD removal was achieved at pH = 9.5 as 71%.

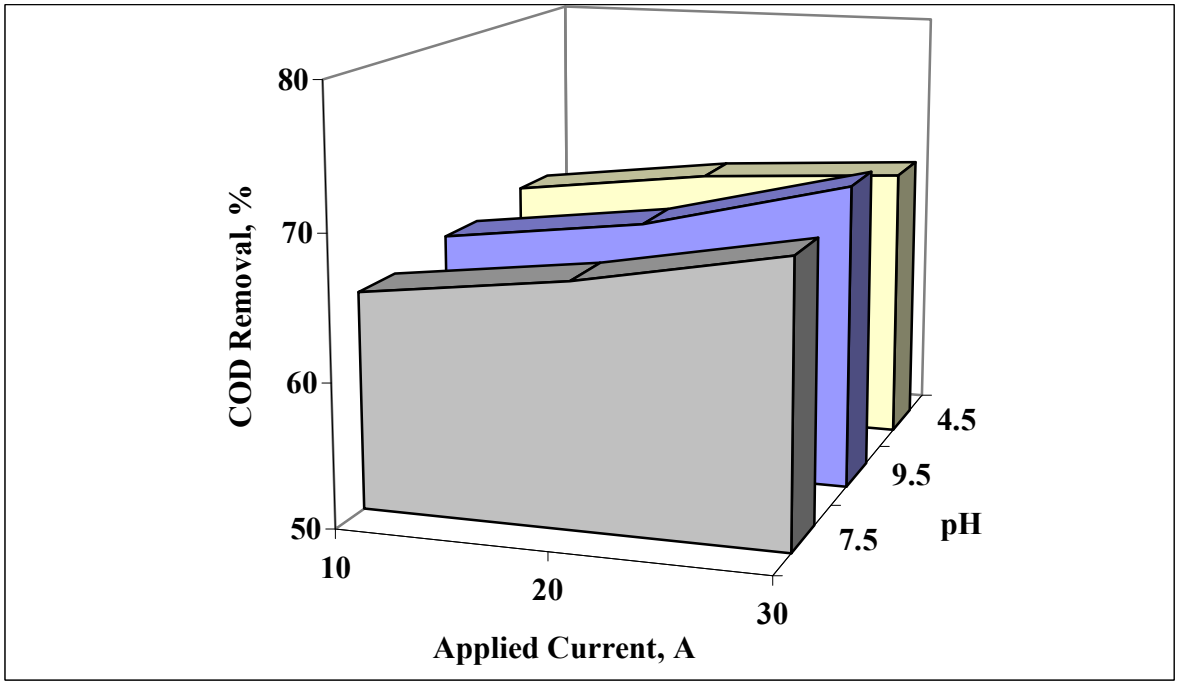

Figure 4.10. The fraction of COD removal at varying current and initial pH with the Fe/Al electrode in 15 minutes

4.1.3.2. Color Removal.

• iron electrodes

In general, color reduction occurred at all tested currents and pH levels. Figures 4.11, 4.12, and 4.13. present the changes in UV visible absorption spectra for different electrical currents (5, 10, 20, and 30 A) at initial pH = 4.5, 7.5 and 9.5, respectively. In all cases a control was used as reference, defined as biotreated effluent without any current application

As can be concluded from Figures 4.11. to 4.13, increasing the current input increased the reduction in absorption, and 20 A resulted in the highest reduction in absorption at all initial pH. Increasing the current over 20 A did not cause further reduction in absorption. When electrolysis was started at acidic pH (4.5) color abatement occurred in a similar manner to that of SS. At lower current inputs such as 5 A and 10 A, the final effluent pH increased to 5.5 and 6.2, respectively. Only at 20 A, the appropriate increase in pH provided sufficient floc formation and aggregation.

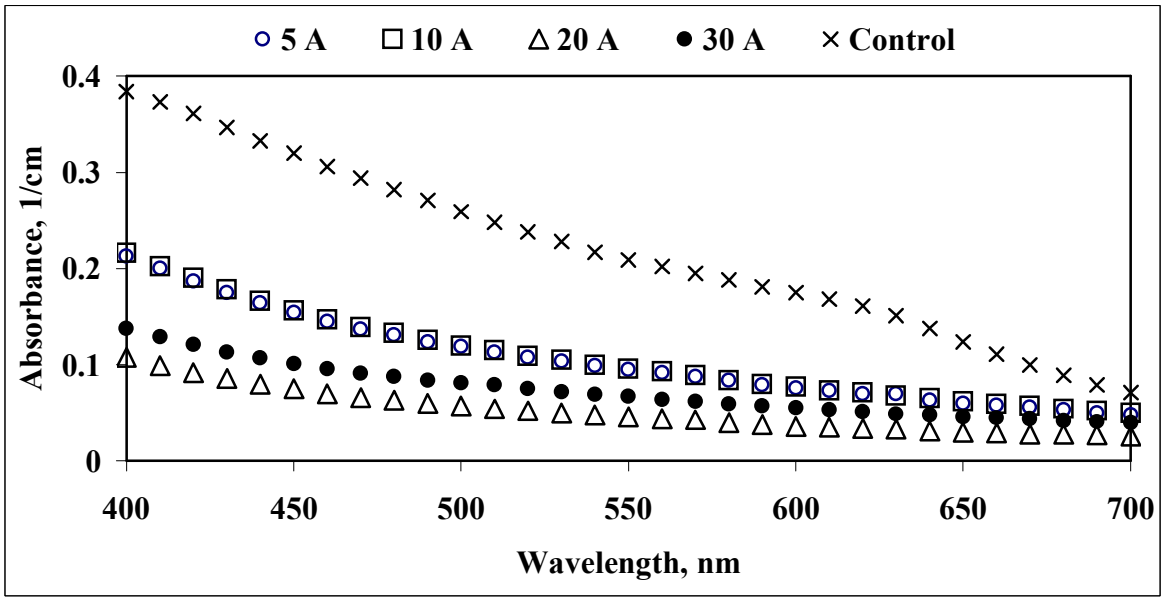

Figure 4.11. Changes in the absorption spectra of biotreated effluent with current (initial pH = 4.5; reaction time= 15 min; iron electrode)

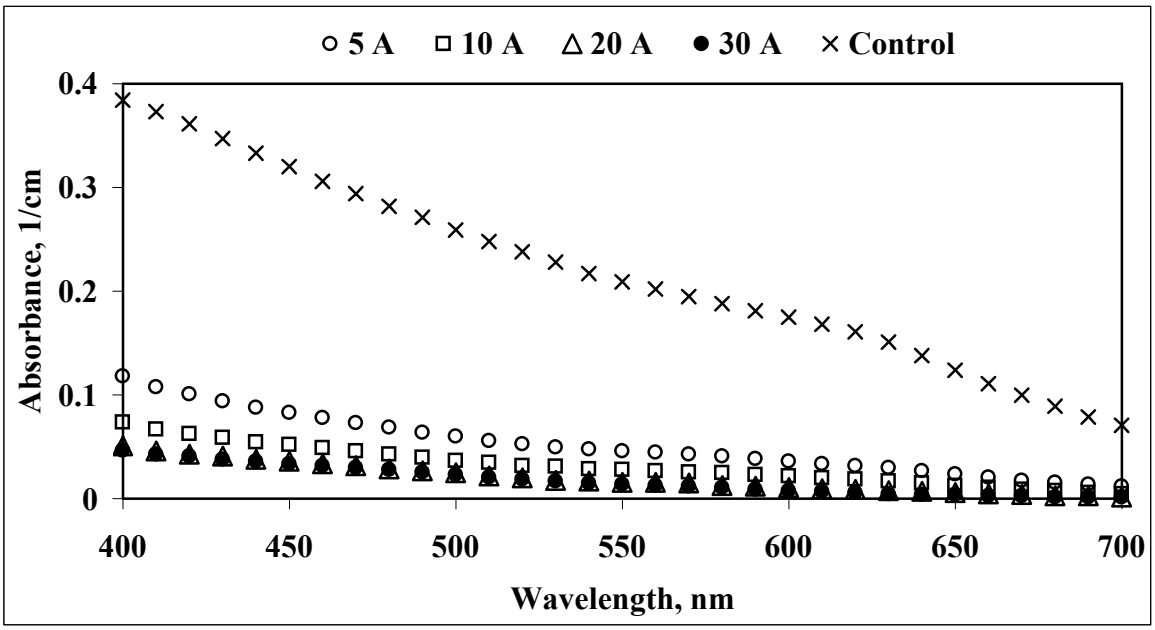

Figure 4.12. Changes in the absorption spectra of biotreated effluent with current (initial pH = 7.5; reaction time= 15 min; iron electrode)

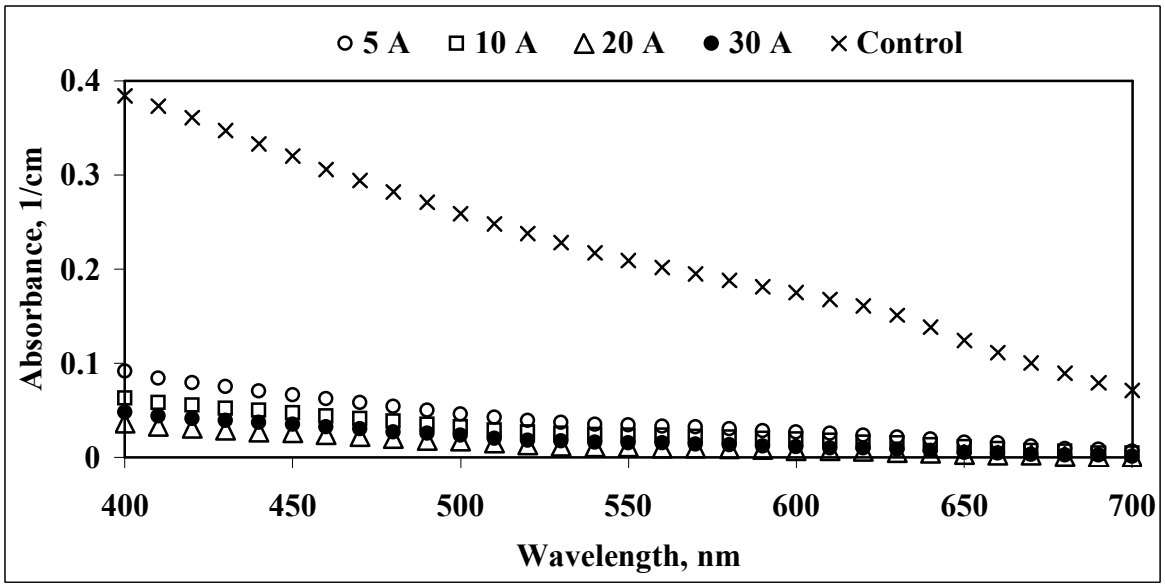

Figure 4.13. changes in the absorption spectra of the biotreated effluent with current (initial pH = 9.5; reaction time = 15 min; iron electrode)

Figures 4.14, 4.15, 4.16, and 4.17. present the effect of initial pH at different current inputs in terms of reduction in absorption. At all tested current inputs pH 7.5 and

pH 9.5 give similar and slightly higher reduction in absorption color when compared to that obtained at initial pH 4.5.

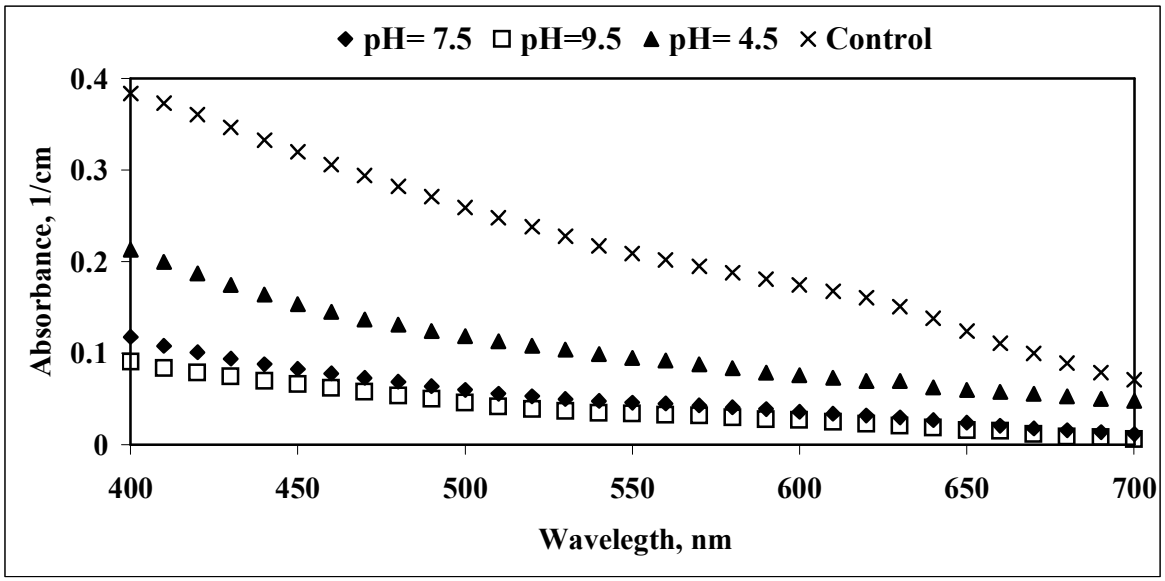

Figure 4.14. changes in the absorption spectra of the biotreated effluent with pH variations (applied current = 5 A; reaction time = 15 min; iron electrode)

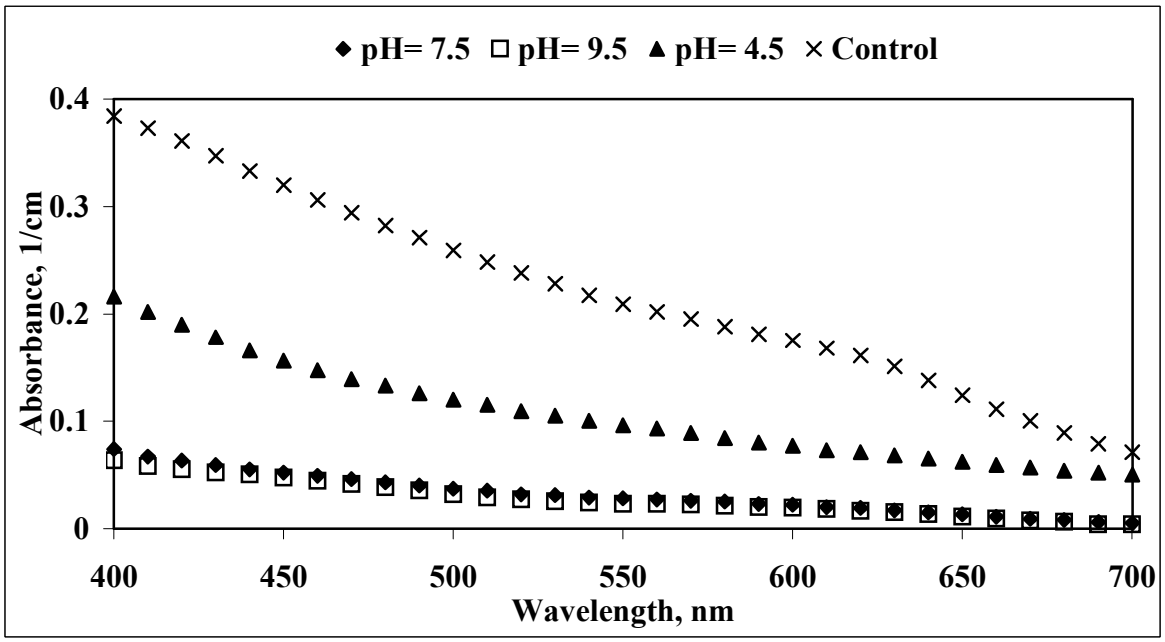

Figure 4.15. changes in absorption spectra of the biotreated effluent with pH variations (applied current= 10 A; reaction time= 15 min; iron electrode)

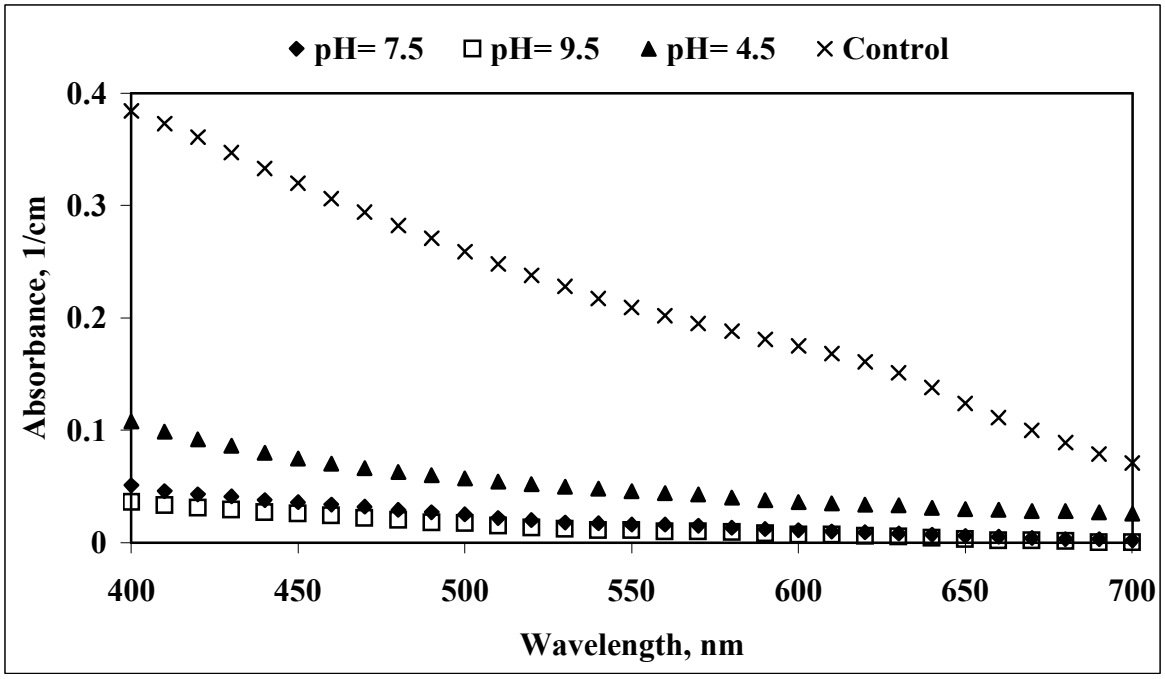

Figure 4.16. Changes in the absorption spectra of the biotreated effluent with pH variations (applied current = 20 A; reaction time = 15 min; iron electrode)

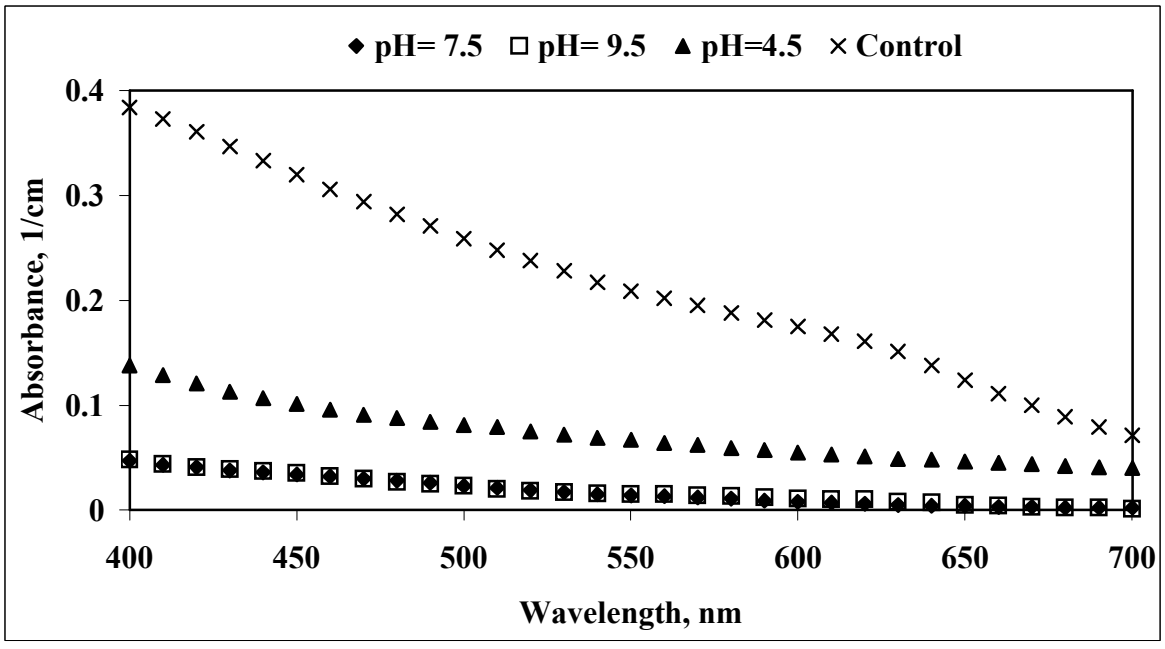

Figure 4.17. changes in the absorption spectra of the biotreated effluent with pH variations (applied current = 30 A; reaction time = 15 min; iron electrode)

• aluminum electrode

Color reduction occurred in a very similar manner to that of COD reduction when aluminum electrodes were used. Figures 4.18 to 4.20. present the changes in absorption for varying electrical currents (5, 10, 20 and 30 A) and varying initial pH (4.5, 7.5, 9.5), respectively. No significant improvement in color abatement could be observed with increasing current when electrolysis started at pH = 4.5 (Figure 4.18.). However, at pH 7.5 and pH 9.5, increasing the current input increased the reduction in absorption which again indicates the higher aluminum (and power) requirement for sufficient color removal as happened in the case of COD removal.

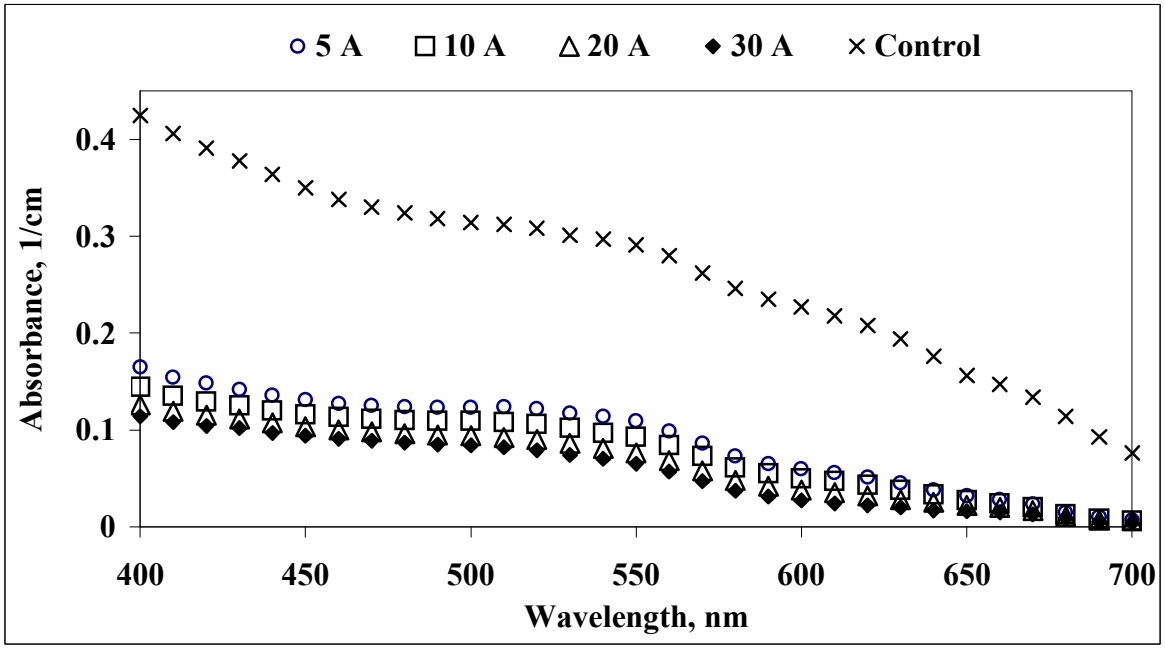

Figure 4.18. Changes in the absorption spectra of the biotreated effluent with current (initial pH = 4.5; reaction time = 15 min; aluminum electrode)

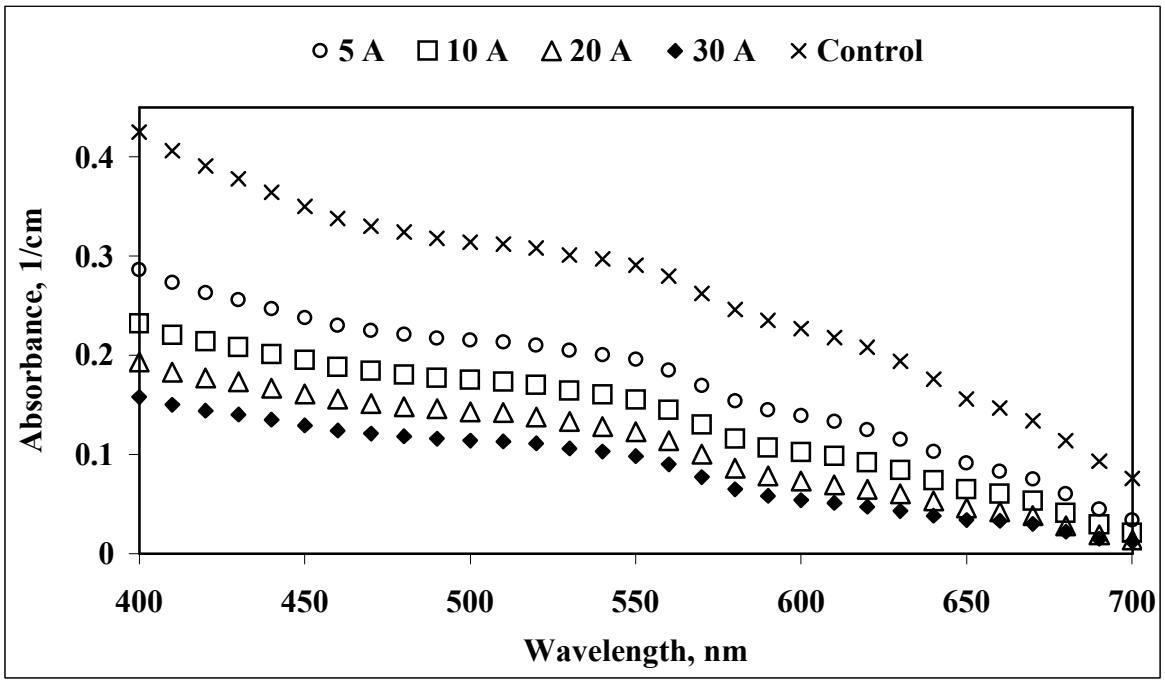

Figure 4.19. Changes in the absorption spectra of the biotreated effluent with current (initial pH = 7.5; reaction time = 15 min; aluminum electrode)

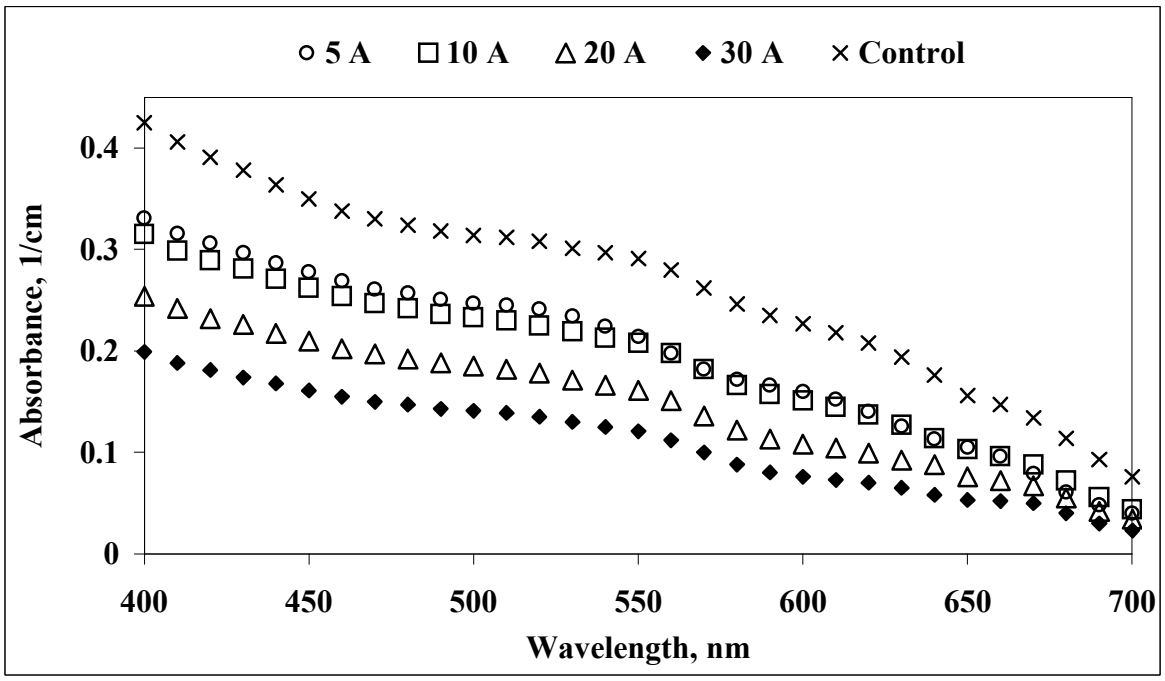

Figure 4.20. Changes in the absorption spectra of the biotreated effluent with current (initial pH = 9.5; reaction time = 15 min; aluminum electrode)

Figures 4.21, 4.22, 4.23, and 4.24. present the effect of initial pH at different current inputs in terms of reduction in absorption. At all tested currents initial pH = 4.5 resulted in higher reduction in absorption as compared to that obtained at pH 7.5 or pH 9.5. The reason for the narrow spectra at 20 A and 30 A is due to the excess anodic supply of aluminum at high current inputs and therefore, compensation of the deficiency of cationic monomers such as $Al(OH)_2^+$, polymeric species and $Al(OH)_3$.

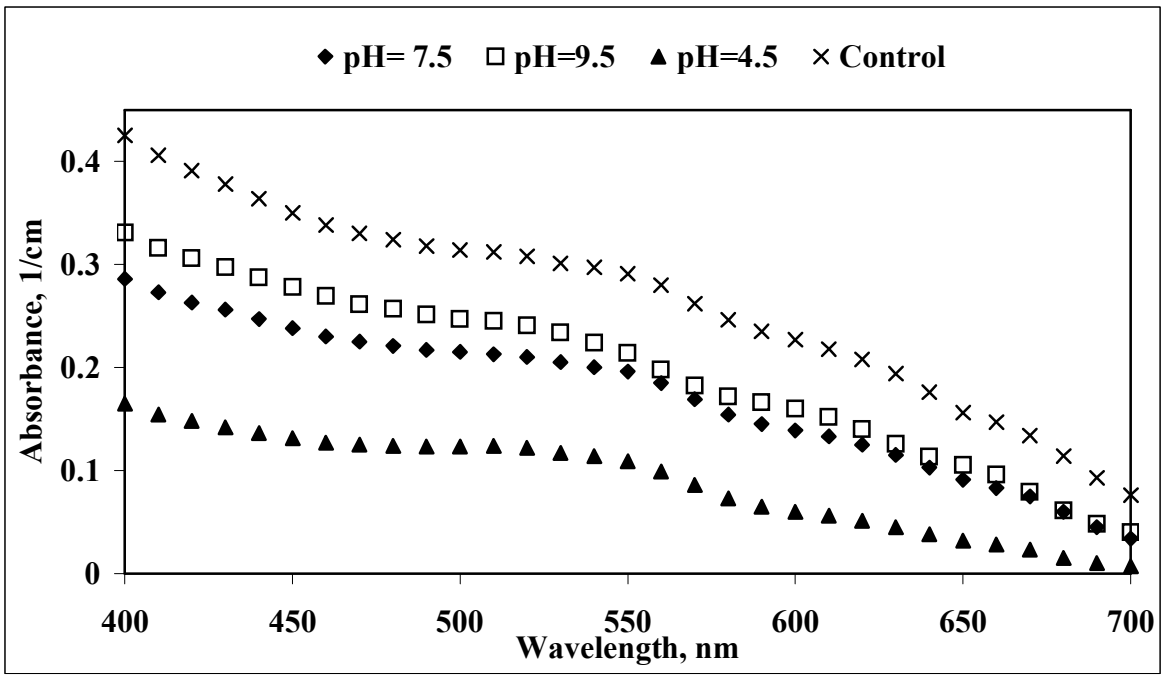

Figure 4.21. Changes in the absorption spectra of the biotreated effluent with pH variations (applied current = 5 A; reaction time = 15 min; aluminum electrode)

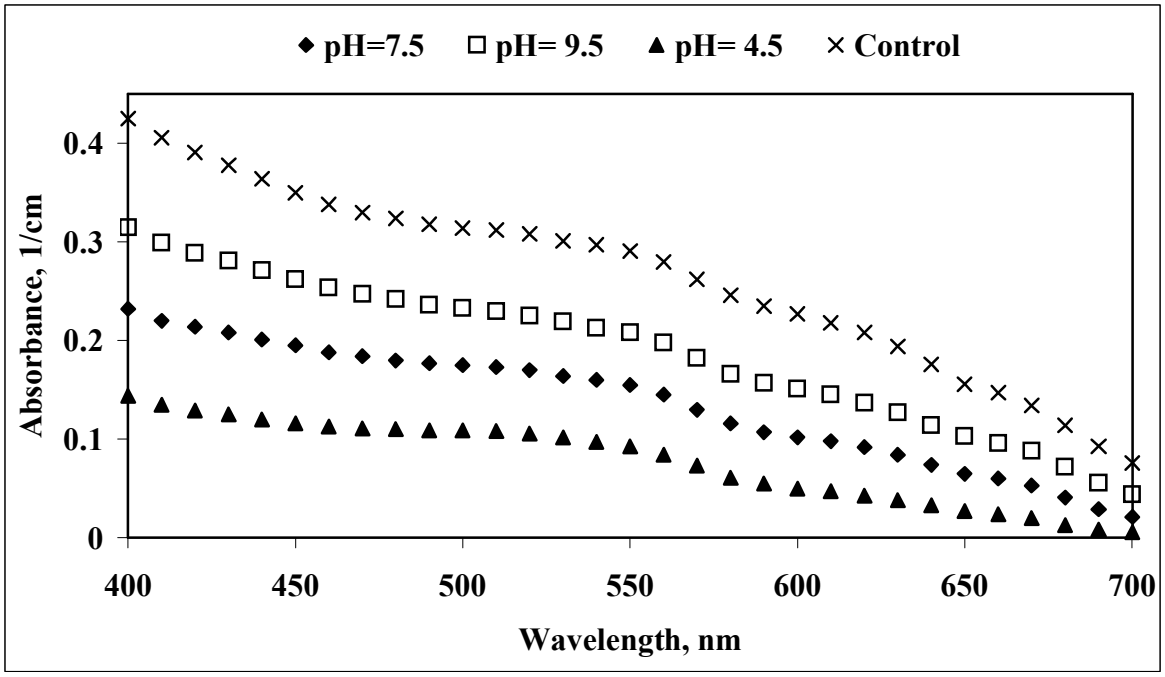

Figure 4.22. Changes in the absorption spectra of the biotreated effluent with pH variations (applied current = 10 A; reaction time = 15 min; aluminum electrode)

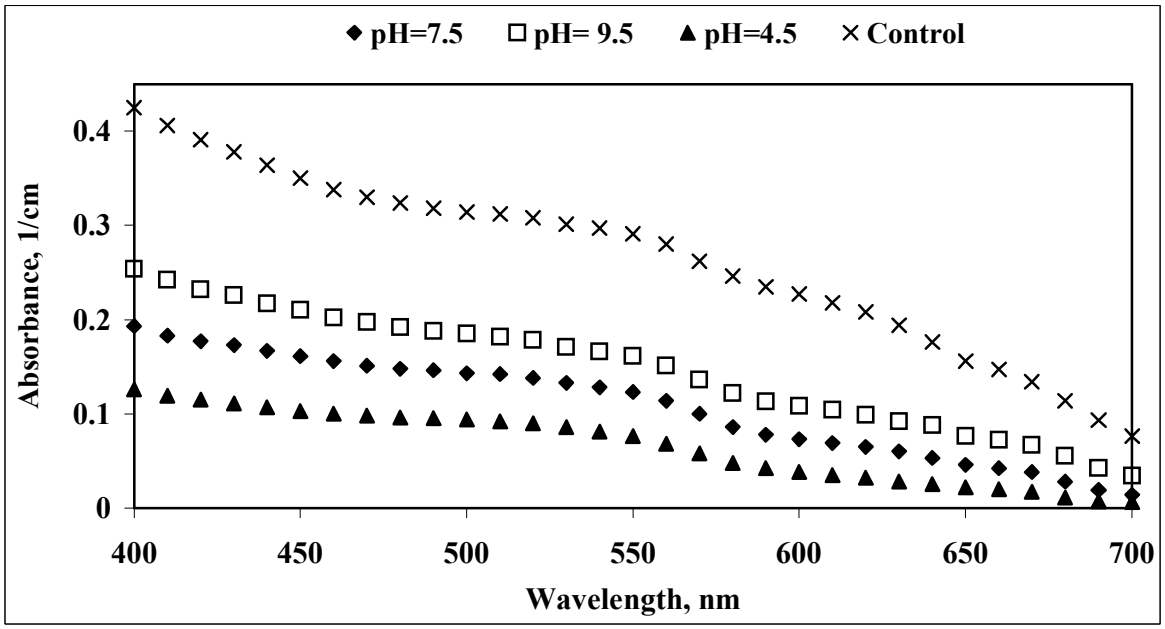

Figure 4.23. Changes in the absorption spectra of the biotreated effluent with pH variations (applied current = 20 A; reaction time = 15 min; aluminum electrode)

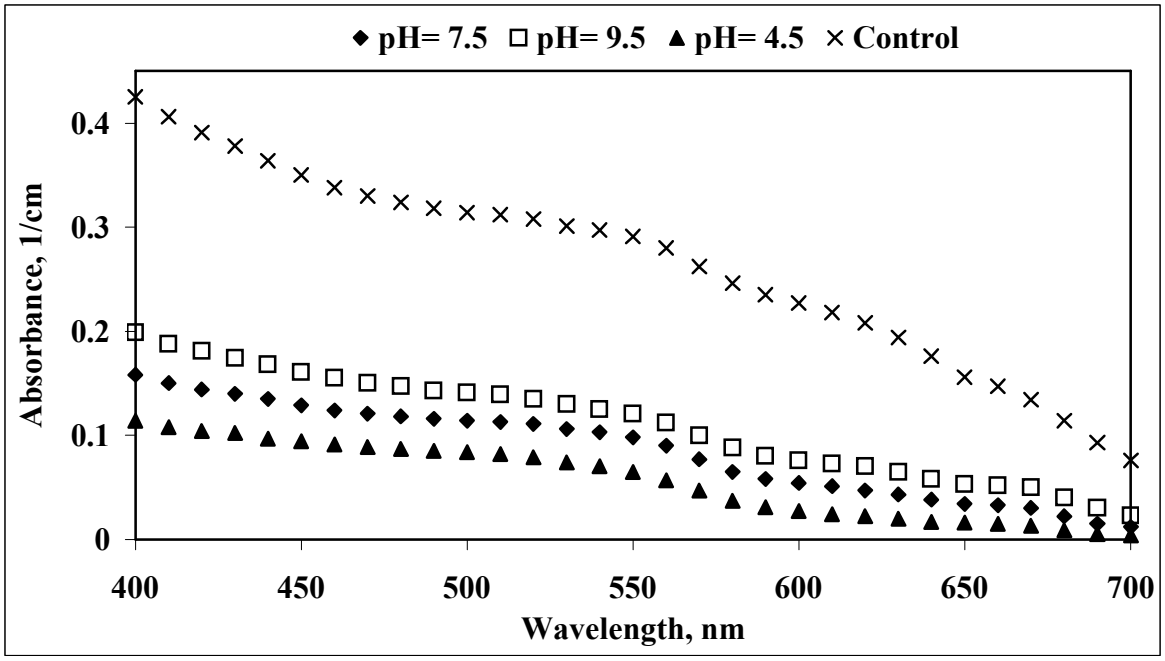

Figure 4.24. Changes in the absorption spectra of the biotreated effluent with pH variations (applied current = 30 A; reaction time = 15 min; aluminum electrode)

• iron/aluminum electrode

Color reduction with iron/aluminum electrodes occurred in a very similar manner to that of iron electrodes alone. Figures 4.25, 4.26, and 4.27. present the changes in absorption for different electrical currents (10, 20, and 30 A) at initial pH levels of 4.5, 7.5, and 9.5, respectively. At pH = 7.5 and 9.5 color reduction occurred in a same manner to that of COD removal. When the reaction initiated at pH = 4.5, satisfactory color removal performance obtained at only high current inputs (20 A and 30 A).

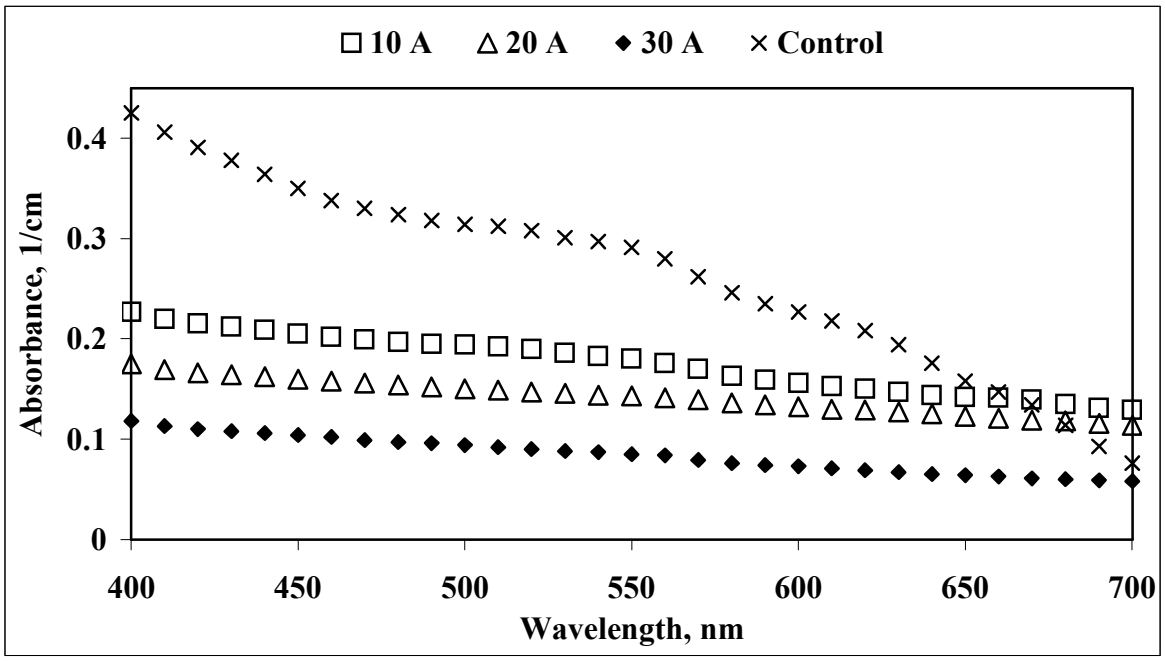

Figure 4.25. Changes in the absorption spectra of the biotreated effluent with current (initial pH = 4.5; reaction time = 15 min; iron/aluminum electrode)

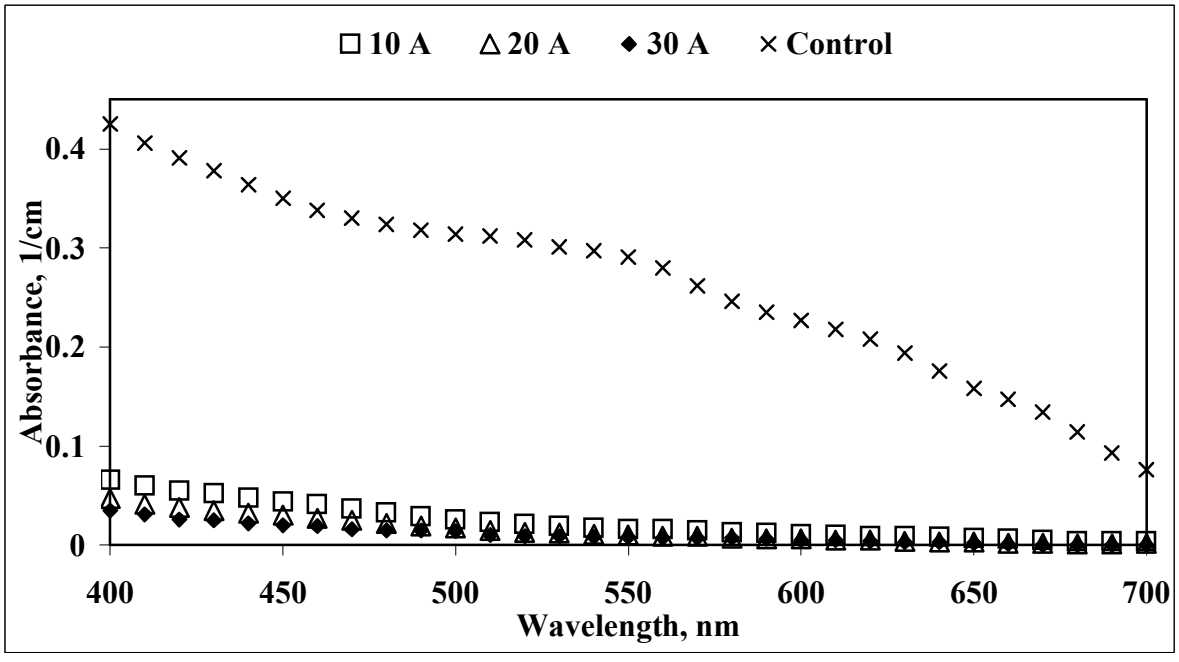

Figure 4.26. changes in the absorption spectra of the biotreated effluent with current (initial pH = 4.5; reaction time = 15 min; iron/aluminum electrode)

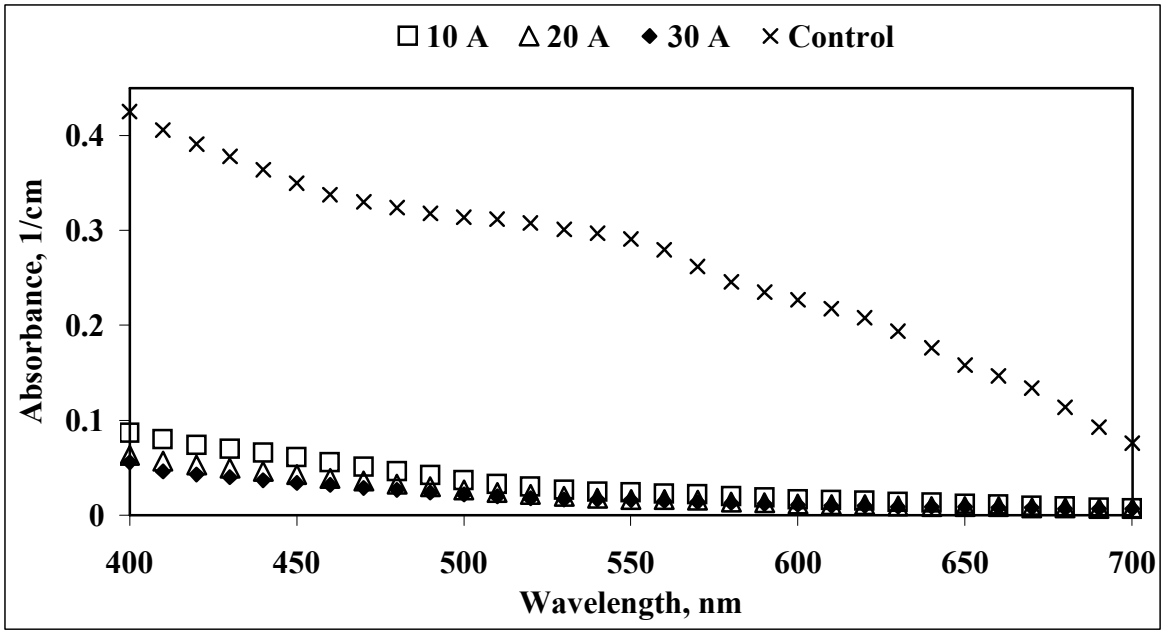

Figure 4.27. Changes in the absorption spectra of the biotreated effluent with current (initial pH = 7.5; reaction time = 15 min; iron/aluminum electrode)

Figures 4.28, 4.29, and 4.30, present the effect of initial pH at varying current inputs in terms of reduction in absorption. It is obvious that when iron/aluminum electrode couples were used together, even at low current inputs considerable color reduction could be obtained at pH 7.5 and 9.5. In case of pH = 4.5, the electrical energy requirement increased to obtain similar color abatement to that of pH = 7.5 and 9.5.

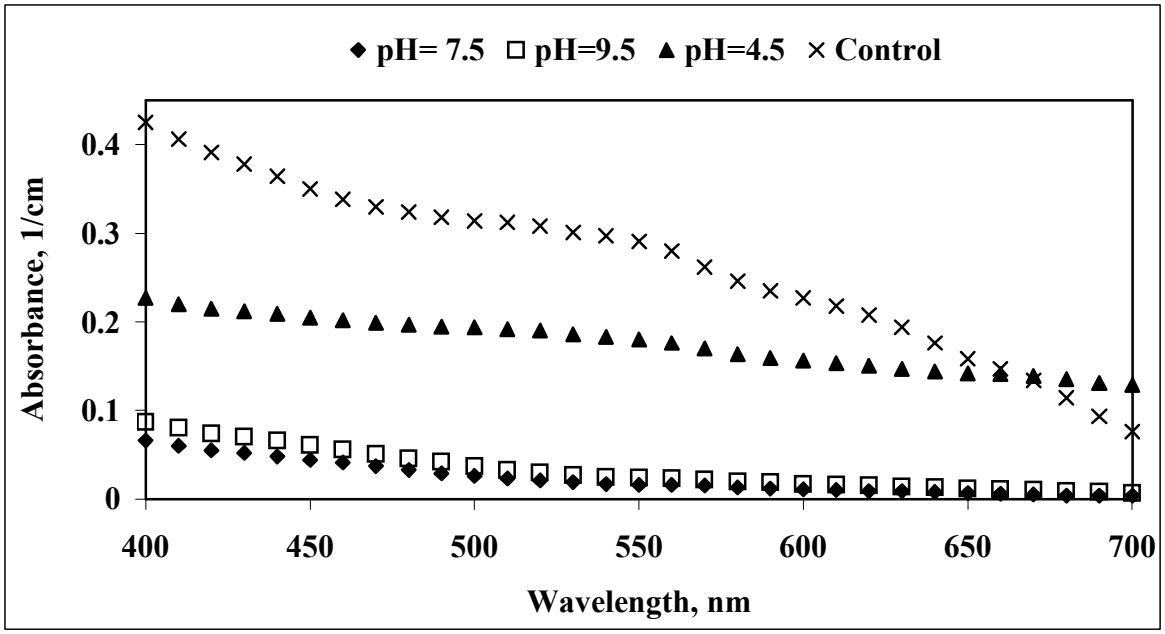

Figure 4.28. Changes in the absorption spectra of the biotreated effluent with pH variations (applied current = 10 A; reaction time = 15 min; iron/aluminum electrode)

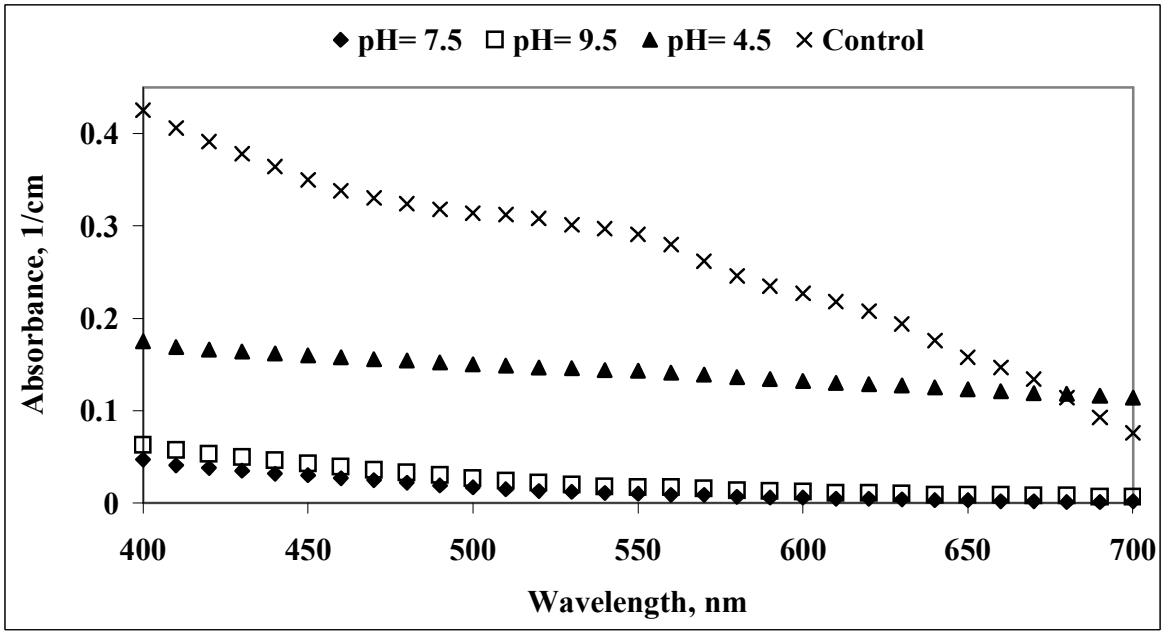

Figure 4.29. Changes in the absorption spectra of the biotreated effluent with pH variations (applied current = 20 A; reaction time = 15 min; iron/aluminum electrode)

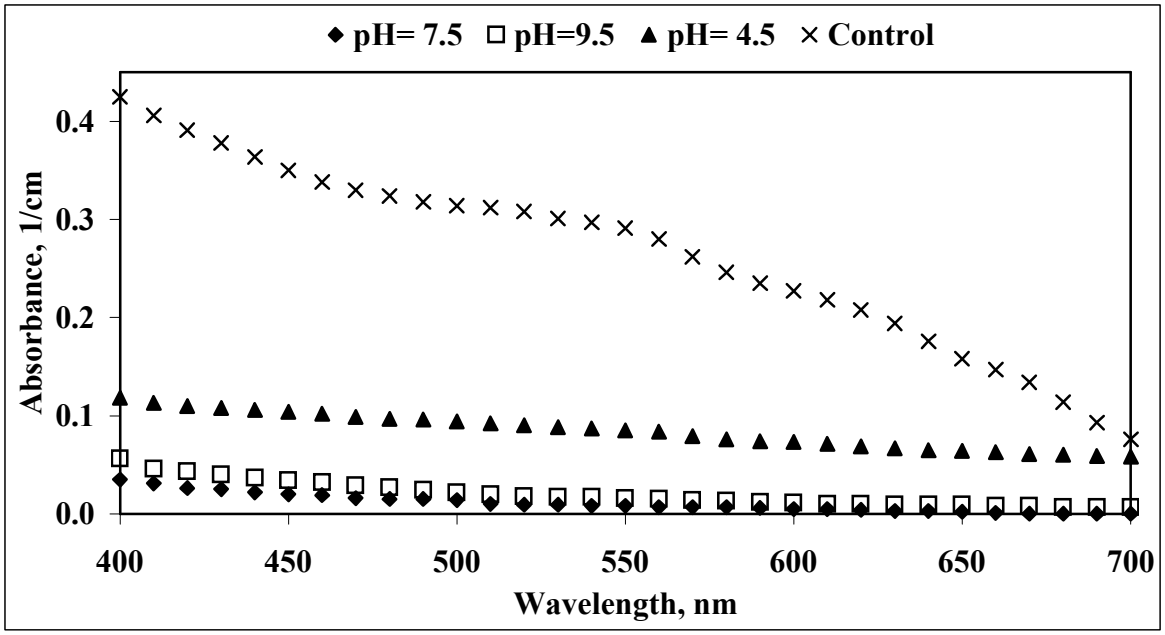

Figure 4.30. Changes in the absorption spectra of the biotreated effluent with pH variations (applied current = 30 A; reaction time = 15 min; iron/aluminum electrode)

• mechanism of electrochemical color removal in biotreated textile effluent

In the literature there are numerous reports on the electrolysis of textile effluents using sacrificial electrodes. In most of the cases, considerable COD and color reduction was reported. However, there is no or little information about the mechanism of contaminant removal. Although many of the researchers explain the removal of contaminants by a combination of oxidation, reduction, adsorption and coagulation processes, none of them suggest the governing mechanism.

In the previous sections, it was shown that electrolysis is highly effective for color removal in biotreated textile effluent. It is well known from dyestuff chemistry that most of the commercial textile dyes are more sensitive to reduction than oxidation (Okuhara et al., 1996). Especially the resistance of direct and disperse dyes to oxidation is so high that polyester/viscose fabrics can even be dyed simultaneously with bleaching where high concentrations of hydrogen peroxide are used at 130^{o}C in order to save time. In addition, when a poor (uneven) reactive dyeing occurs in production, the method of correcting is to

strip off the color completely using reductive chemicals (hydrosulphite) at alkaline conditions and then redye the fabric instead of using bleaching (oxidative) processes.

To assess if color abatement was a function of the reduction potential, changes in the reduction potential of the electrolyte solution was continuously monitored throughout electrochemical treatment of biotreated textile effluent as a function of varying pH at varying current inputs. During optimization of reaction time it was observed that color removal occurred in a different manner when iron electrodes were used from that of aluminum. Gradual reduction in color was observed with the aluminum electrodes, whereas in the case of iron electrodes color removal was initially very slow and a sharp abatement was observed, indicating that decolorization mechanism is different with different electrode materials.

- color removal during electrolysis with the iron electrode

Figures 4.31, 4.32, 4.33, and 4.34. display the changes in reduction potentials and percent color removal during electrolysis with the iron electrode at current inputs of 5, 10, 20 and 30 A, respectively. As it is clear from Figures 4.1.31. to 4.1.34, a significant degree of decolorization was accomplished over a specific range of reduction potential. The rate of color removal was slow up to a reduction potential of 600 to 650 mV, increased appreciably at this point and levelled off thereafter, reaching a value of 54 % at pH = 4.5 and 80 % at pH = 7.5 for an applied current of 5 A. The same trend was evident for higher current inputs. However, the time of significant decolorization was achieved at a faster rate at elevated currents. This is mainly due the faster achievement of the required above mentioned critical reduction potential.

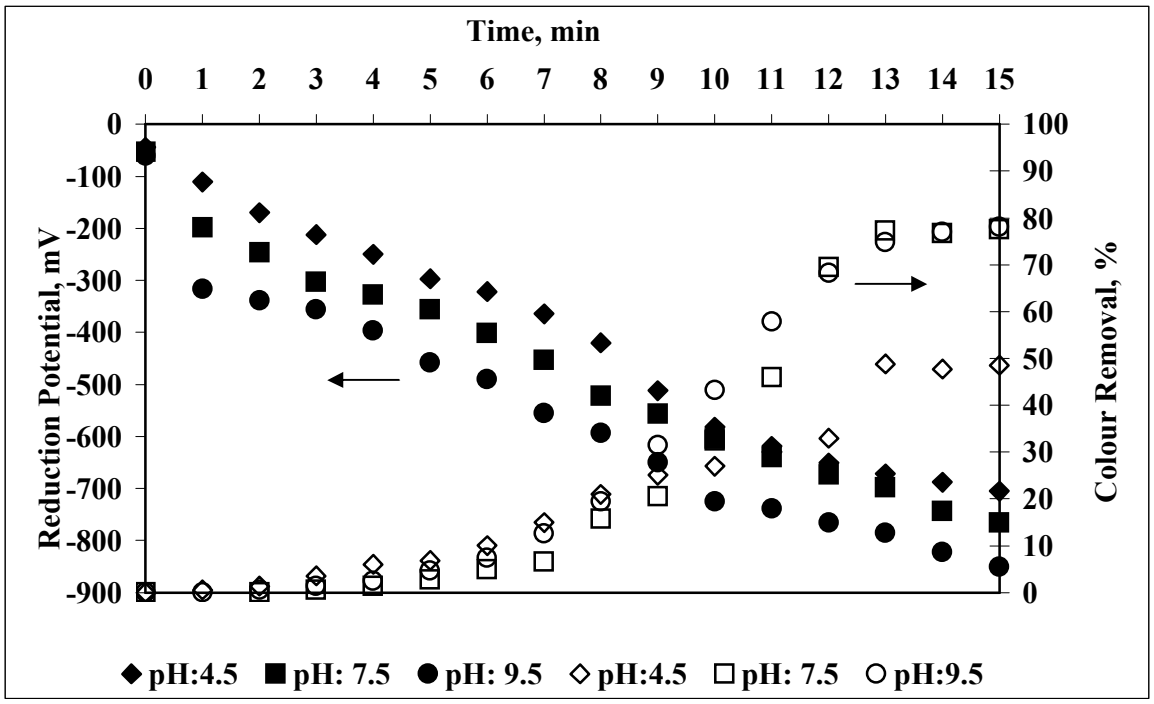

Figure 4.31. Changes in the reduction potential and percent color removal during treatment with the iron electrode at 5 A (initial absorbance at 436 nm = 0.365 cm^{-1})

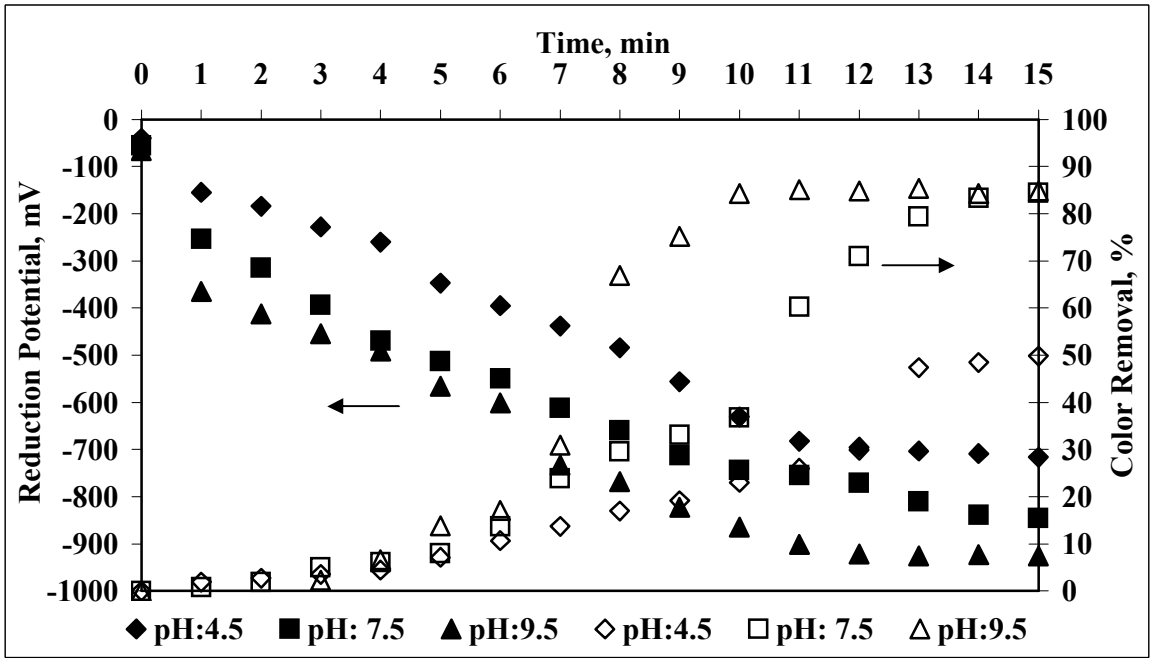

Figure 4.32. Changes in the reduction potential and percent color removal during treatment with the iron electrode at 10 A (initial absorbance at 436 nm = 0.365 cm^{-1})

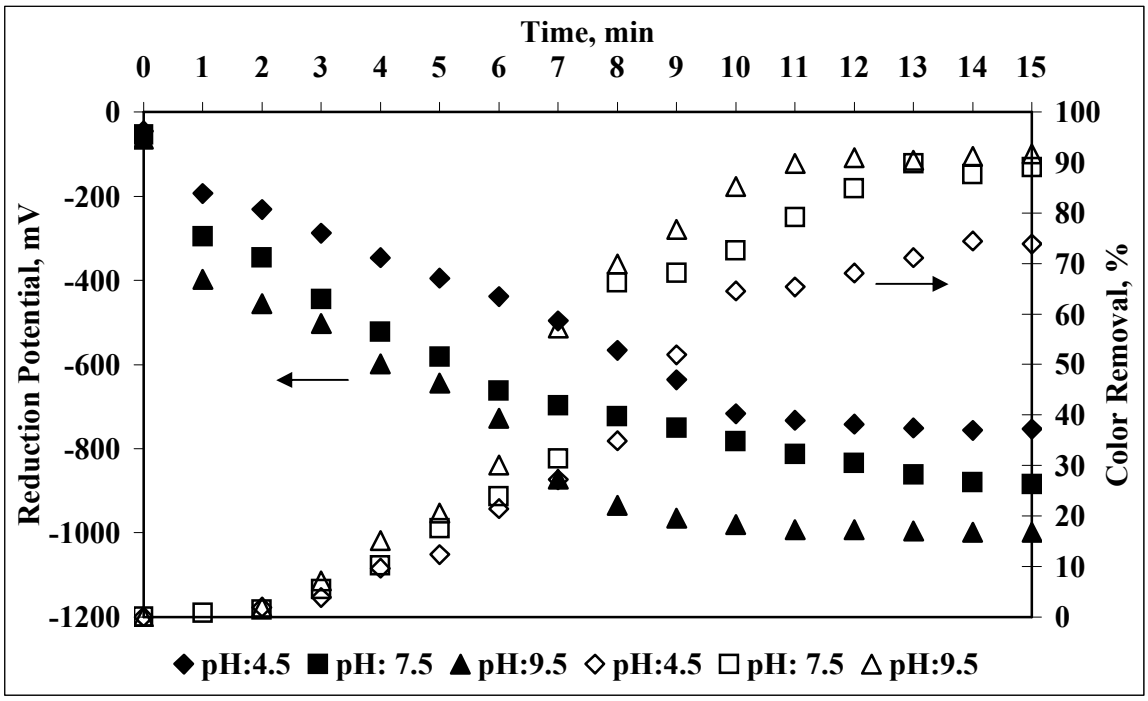

Figure 4.33. Changes in the reduction potential and percent color removal during treatment with the iron electrode at 20 A (initial absorbance at 436 nm = 0.365 cm^{-1})

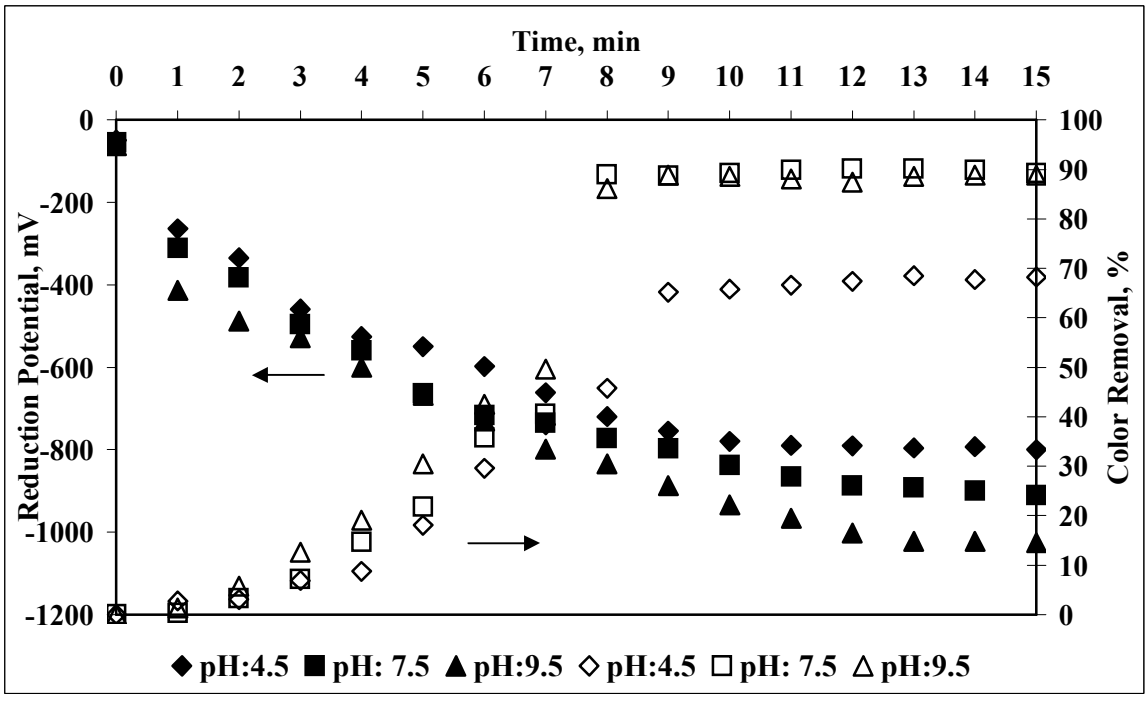

Figure 4.34. Changes in the reduction potential and percent color removal during treatment with iron electrode at 30 A (initial absorbance at 436 nm = 0.365 cm^{-1})

• Color Removal During Electrolysis with the Aluminum Electrode

As described previously, color reduction occurred gradually with the use of aluminum electrodes (Fig. 4.35.). The observed reduction potentials using aluminum were appreciably lower than those obtained for iron electrodes indicating that the mechanism of decolorization was different for the studied electrode materials. It appears that indirect reduction occurs during simultaneous oxidation of Fe^{+2} and Fe^{+3} for iron electrodes and adsorption on aluminum hydroxide in the case of aluminum electrodes. Figure 4.35. exemplifies the change in reduction potential during color removal with aluminum electrodes.

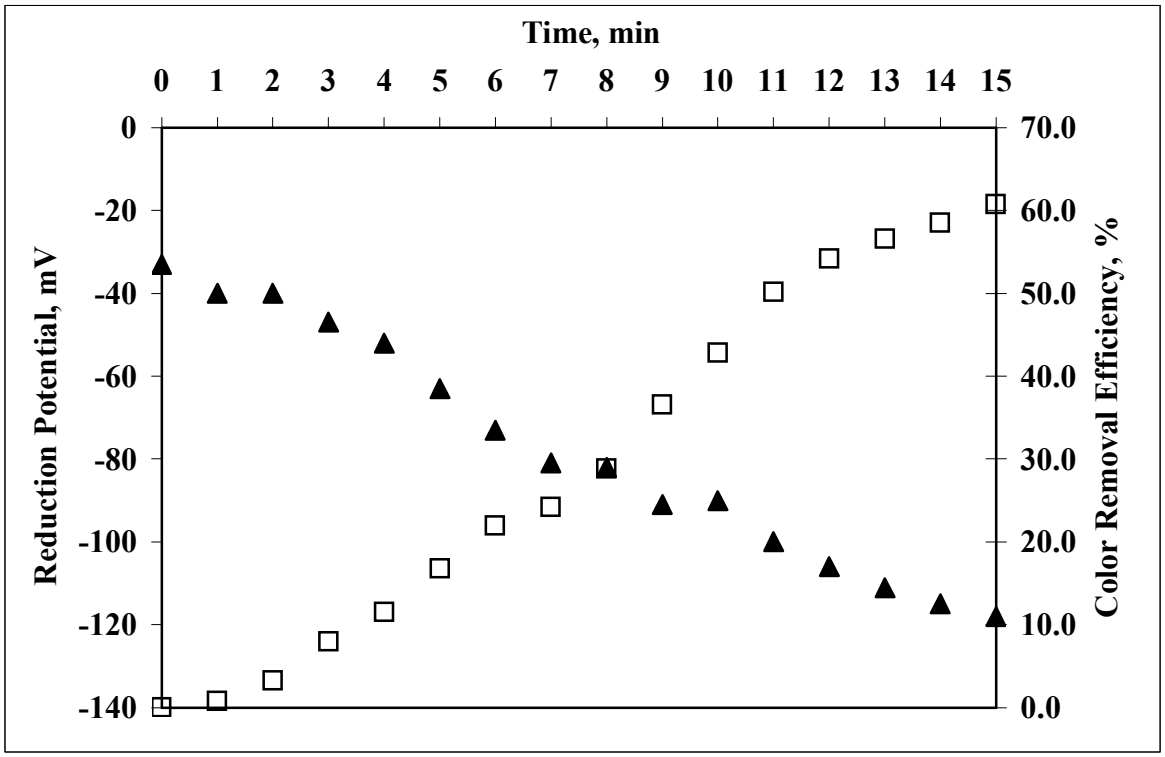

Figure 4.35. Changes in the reduction potential and percent color removal during treatment with Al electrodes at 5 A (initial absorbance at 436 nm = 0.364 cm^{-1}; treatment time = 15 min)

Wilcocks (1992) treated disperse dye effluent with aluminum electrodes instead of the more common iron electrodes and reported that the mechanism by which decolorization occurred involved physical adsorption rather than dye degradation.

Aluminum electrodes cannot act as reducing agents since aluminum enters the solution in a single valence state. In contrast, the iron electrodes used by McClung and Lemley (1992) cause the release of ferrous iron, which in turn is capable of acting as reducing agents for dye degradation.

4.1.3.3. SS and DS Removal. When iron and/or aluminum are produced electrochemically, there is no simultaneous addition of anions such as sulfate or chloride. This is in contrast to conventional chemical precipitation method that may introduce either chloride or sulfate anions, both of which interfere with contaminant removal and increase the DS in the effluent stream. This factor makes DS concentration significant if water reuse is considered. Therefore, besides SS, DS concentration and conductivity was also monitored after electrolysis.

- iron electrode

Figures 4.36, 4.37, and 4.38. present the changes in effluent SS, DS and conductivity as a function of applied current at pH = 4.5, 7.5, and 9.5, respectively. As observed previously when electrocoagulation initiated at pH = 4.5, the SS concentration of the effluent exceeded its initial value. Only at elevated current inputs ($\geq$ 20 A), the SS concentration of the effluent was reduced below the initial level. The increase in DS concentration is mainly because of the addition of sulfuric acid for the adjustment of the initial pH to the level of 4.5 (Figure 4.36.).

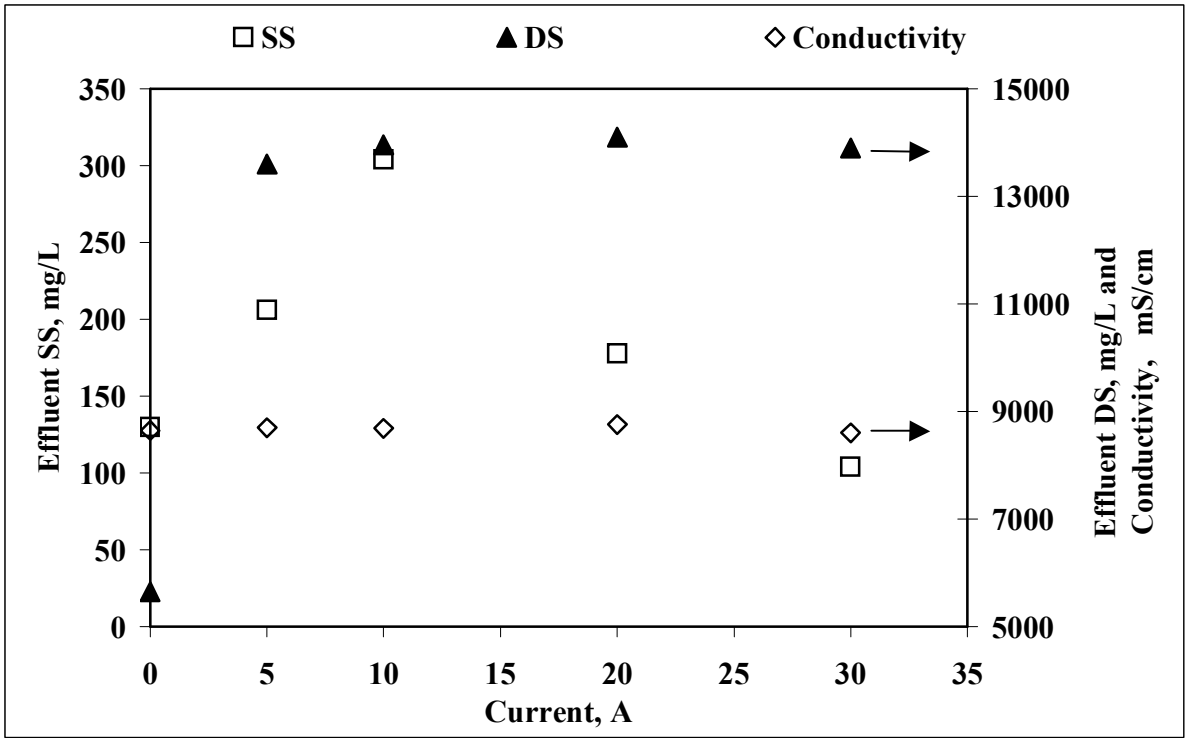

Figure 4.36. Variations in the environmental parameters as a function of the applied current (reaction time = 15 min; initial pH = 4.5; iron electrode)

When electrolysis was initiated at pH = 7.5, SS could effectively be removed even at low current inputs (5 A) and the effect of current input was insignificant in terms of SS removal over 10 A (Figure 4.37.). The maximum SS removal (94 %) achieved at 20 A. As the pH of biotreated effluent was around 7.5, when the electrolysis was started at pH = 7.5 no additional acid or base were added to the biotreated effluent at the beginning. Therefore, DS concentration and conductivity of wastewater was not affected via electrolysis at initial pH of 7.5 at all currents applied (Figure 4.37.).

A similar increase was observed in DS concentration at initial pH = 9.5, to that of pH 4.5 because of the pH adjustment of the wastewater. Nearly complete SS removal was achieved at 20 A and 30 A (Figure 4.38.).

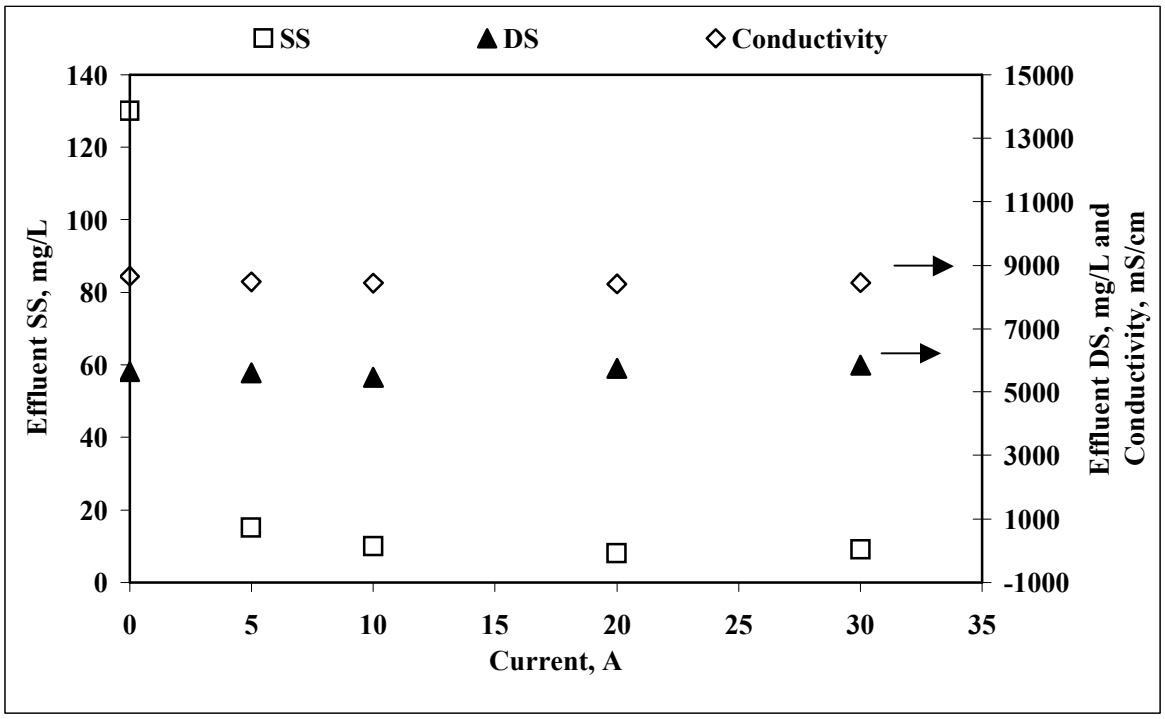

Figure 4.37. Variations in the environmental parameters as a function of the applied current (reaction time = 15 min; initial pH = 7.5; iron electrode)

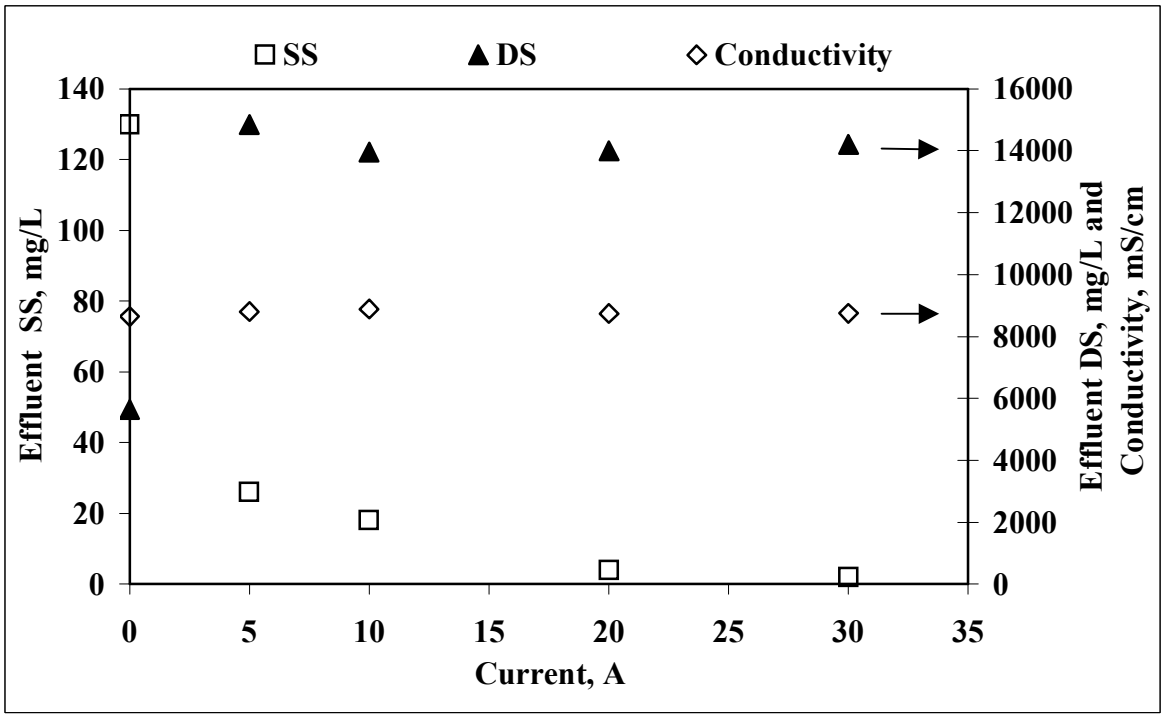

Figure 4.38. Variations in the environmental parameters as a function of the applied current (reaction time = 15 min; initial pH = 9.5; iron electrode)

• aluminum electrode

Figures 4.39, 4.40, and 4.41. present the changes in effluent SS, DS and conductivity as a function of applied current at pH = 4.5, 7.5, and 9.5, respectively. SS was removed very efficiently at all studied initial pH levels. Effluent SS concentrations decreased with increasing current from 130 mg/L to less than 10 mg/L at an applied current of 20 A. Effluent DS concentrations were also reduced at all initial pH from 12000 mg/L to about 8000-9000 mg/L. Due to the fact that no pH adjustment was required for pH 7.5, the lowest final DS value was obtained at this pH. The same trend was also observed for the effluent conductivity.

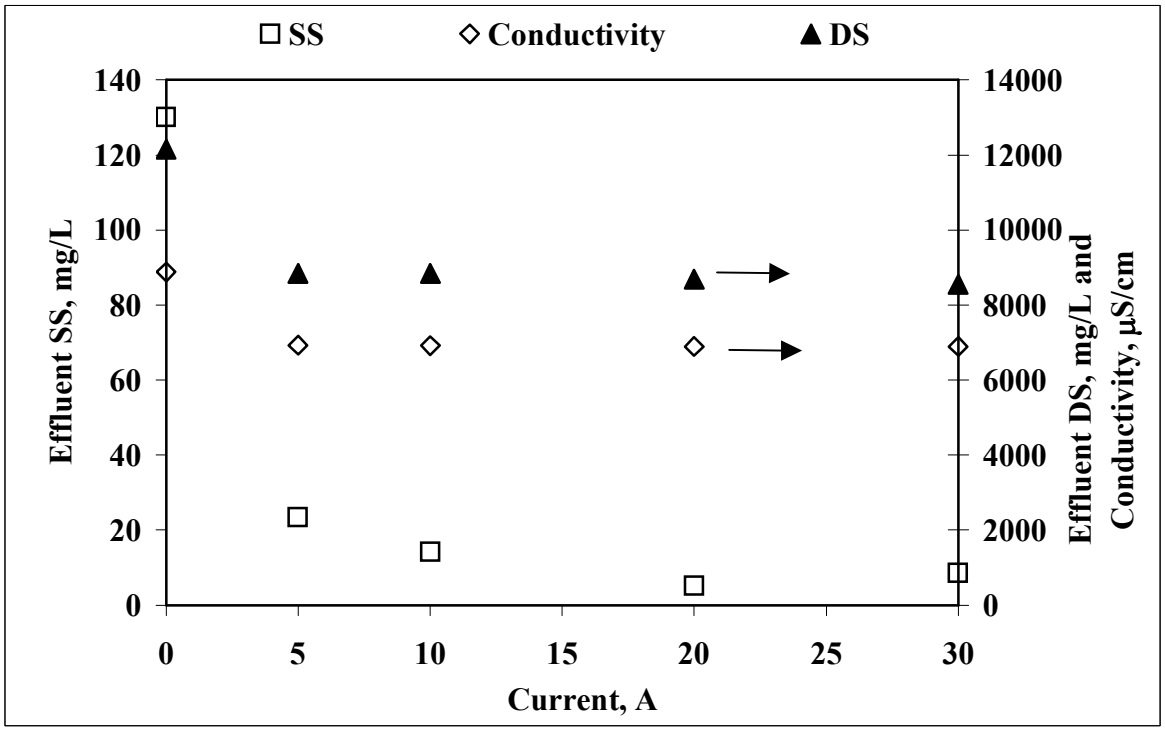

Figure 4.39. Variations in the environmental parameters as a function of the applied current (reaction time = 15 min; initial pH = 4.5; aluminum electrode)

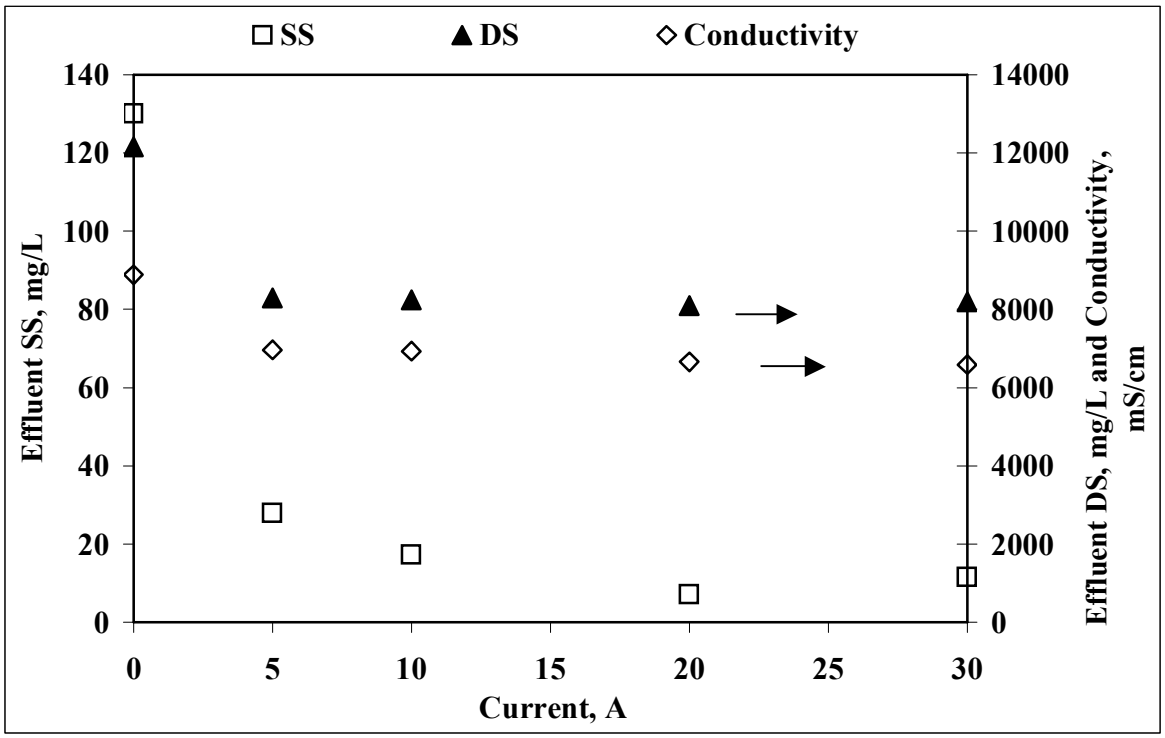

Figure 4.40. Variations in the environmental parameters as a function of the applied current (reaction time = 15 min; initial pH = 7.5; aluminum electrode)

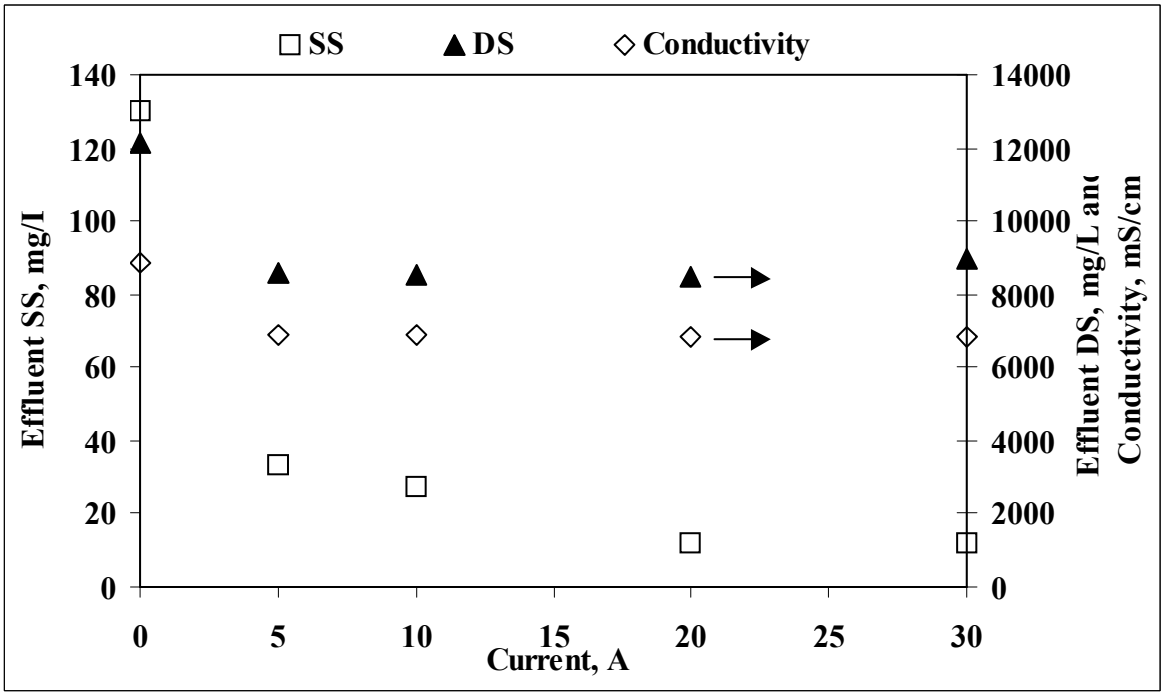

Figure 4.41. Variations in the environmental parameters as a function of the applied current (reaction time = 15 min; initial pH = 9.5; aluminum electrode)

• iron/aluminum electrodes

Figures 4.42, 4.43, and 4.44. present the changes in effluent SS, DS and conductivity as a function of applied current at pH = 4.5, 7.5, and 9.5, respectively. SS was removed very efficiently at all studied initial pH values. Effluent SS concentrations decreased with increasing current from 142 mg/L to a level of 10 mg/L at 20 A independent from the initial pH of the electrolysis. The highest DS reduction was obtained at an initial pH of 7.5 as 33%. The same trend was observed in the effluent conductivity levels. In general the initial conductivity of the biotreated effluent was reduced from 8870 mS/cm to 6590 mS/cm after 15 min of electrolysis using iron/aluminum electrodes.

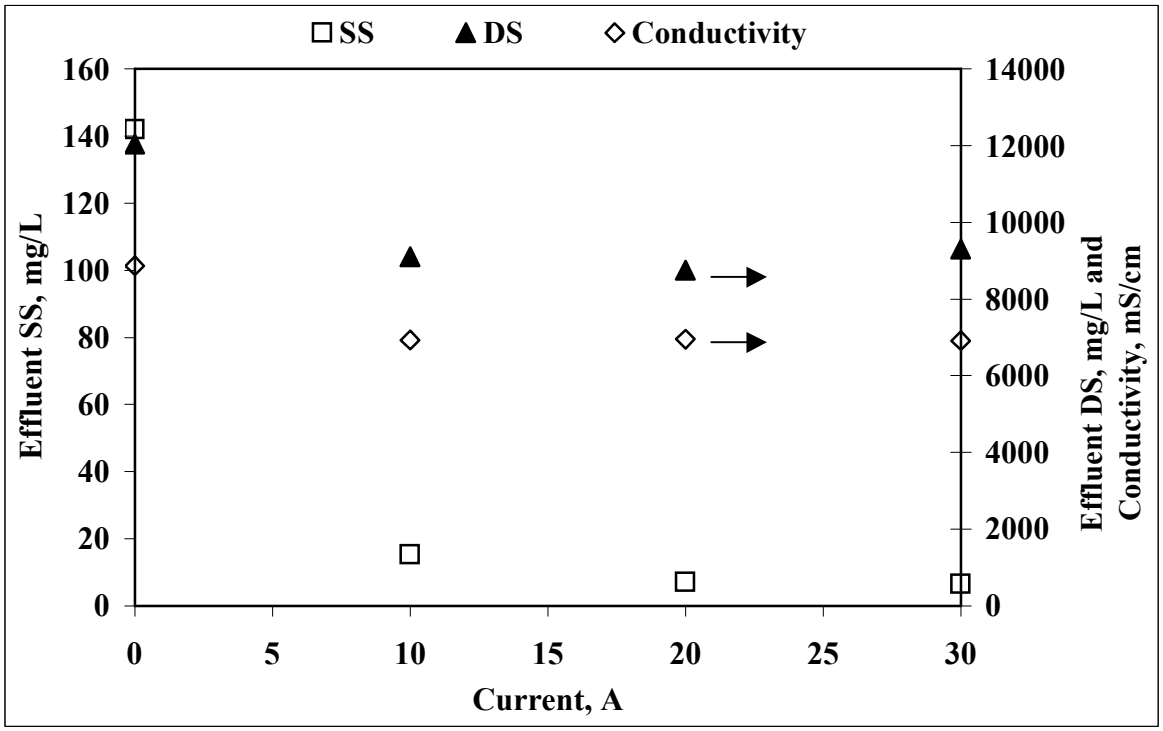

Figure 4.42. Variations in the environmental parameters as a function of the applied current (reaction time = 15 min; initial pH = 4.5; iron/aluminum electrode)

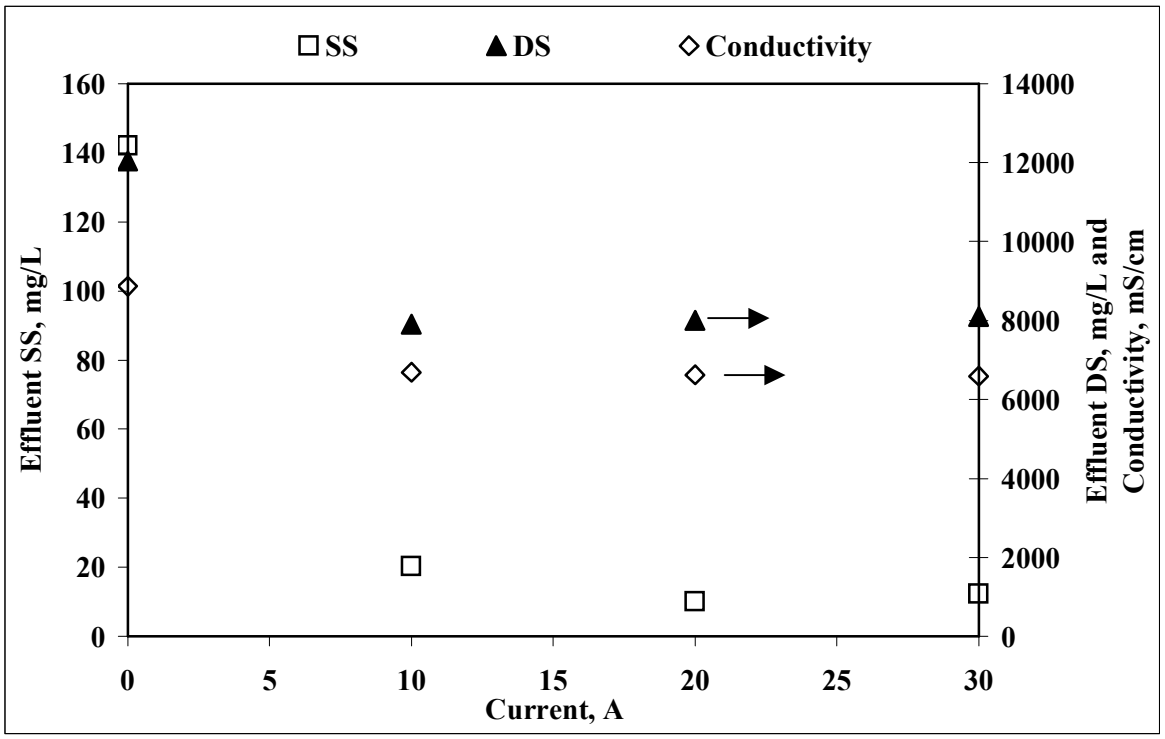

Figure 4.43. Variations in the environmental parameters as a function of the applied current (reaction time = 15 min; initial pH = 7.5; iron/aluminum electrode)

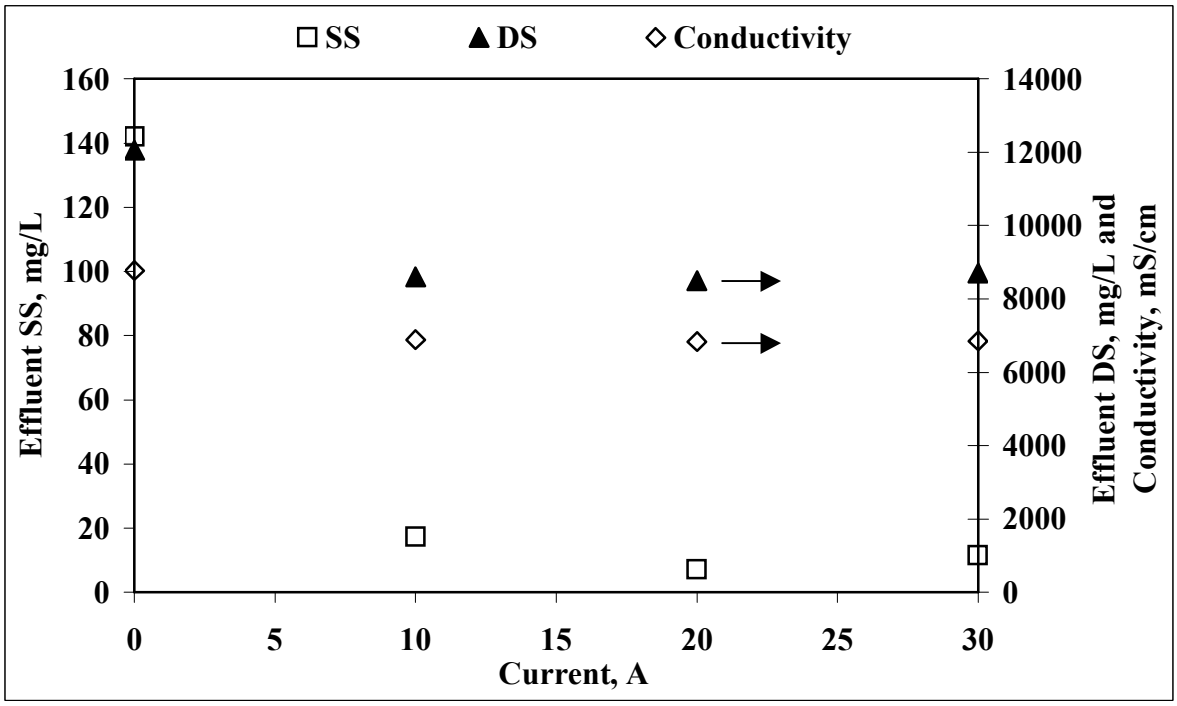

Figure 4.44. Variations in environmental parameters as a function of the applied current (reaction time = 15 min; initial pH = 9.5; iron/aluminum electrode)

4.1.3.4. Sulphate Removal. High sulphate concentration is one of the major problems encountered in effluents originating from textile dyeing and finishing processes that still needs to be solved. There are two sources of sulphate in textile wastewater, namely the dyeing process and the neutralization of the highly alkaline wastewaters. During the dyeing of cellulosic fabrics sodium sulfate or sodium chloride are commonly used to enhance the reactive dye exhaustion at concentrations up to 100 g/L. However, sodium sulfate is preferred to sodium chloride firstly because sodium chloride decreases the dye solubility and may cause dye spots on the fabric. Secondly, the use of sodium chloride may result in uncontrolled dye exhaustion and hence uneven appearance of finished fabric. Another source of sulfate in textile dyeing effluents originates from the use of sulphuric acid for the neutralization of wastewaters prior to biological treatment or before draining to the sewer system. Since sulfate is highly corrosive for the concrete, its concentration in the effluent is directed by discharge limits. Therefore during the experiments sulfate concentration was also monitored.

- iron electrodes

Although Ciardelli and Ranieri (2000) reported significant reduction in effluent sulfate ion concentrations of biotreated waste streams with electrocoagulation, in our study no significant reduction in sulphate concentration could be observed when iron was used as the electrode. Figure 4.45. presents the changes in effluent sulfate concentrations with the electrolysis of biotreated textile effluent at varying initial pH as a function of current. As it can be followed from the Figure 4.45, even a slight increase in effluent sulfate concentration occurred at pH = 4.5 because of the addition of more sulfuric acid for the adjustment of initial pH. On the other hand at pH 7.5 and 9.5 no significant change in effluent sulphate concentration was observed.

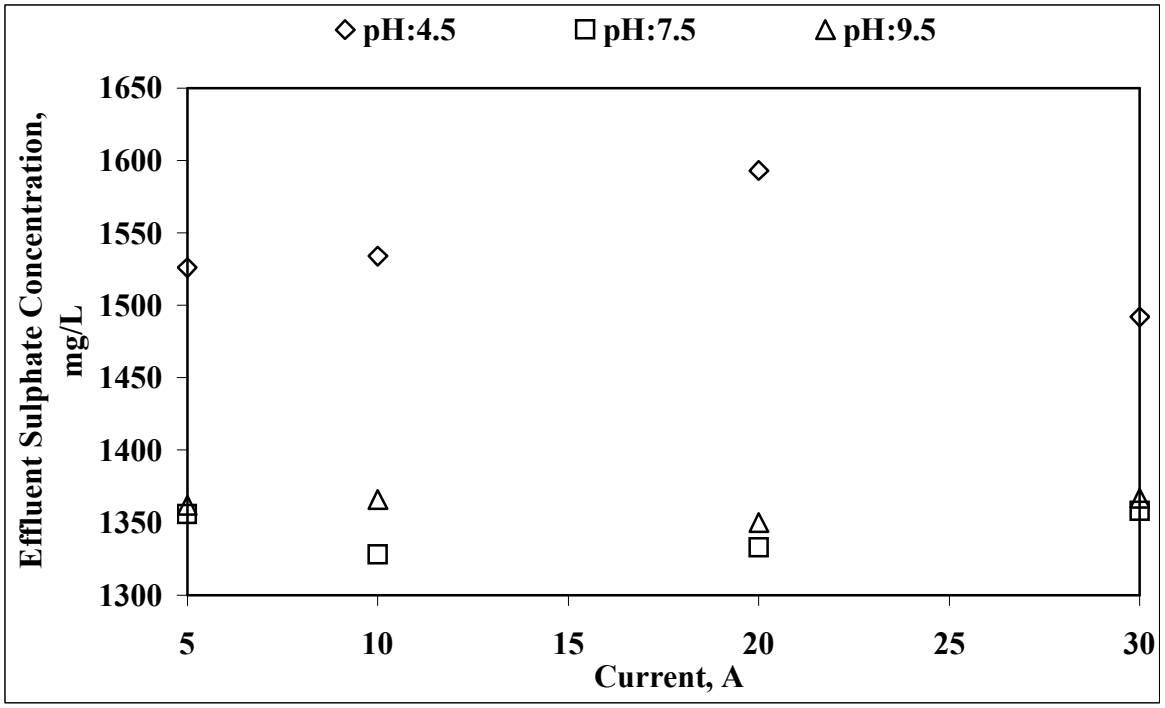

Figure 4.45. Effluent sulphate concentrations at varying initial pH as a function of the applied current; electrolysis time = 15 min; iron electrode

- aluminum electrodes

According to our experimental findings, sulphate could not be removed when iron was used as electrode material. However, during electrolysis with aluminum electrodes, significant sulphate reduction was observed. Similar results were obtained by Giardelli et al. (2001) who used iron/aluminum electrodes for the treatment of different streams from the textile industry. The effluent sulfate concentrations after electrolysis of biotreated textile effluent at varying initial pH and current using aluminum electrodes are given in Figure 4.46.

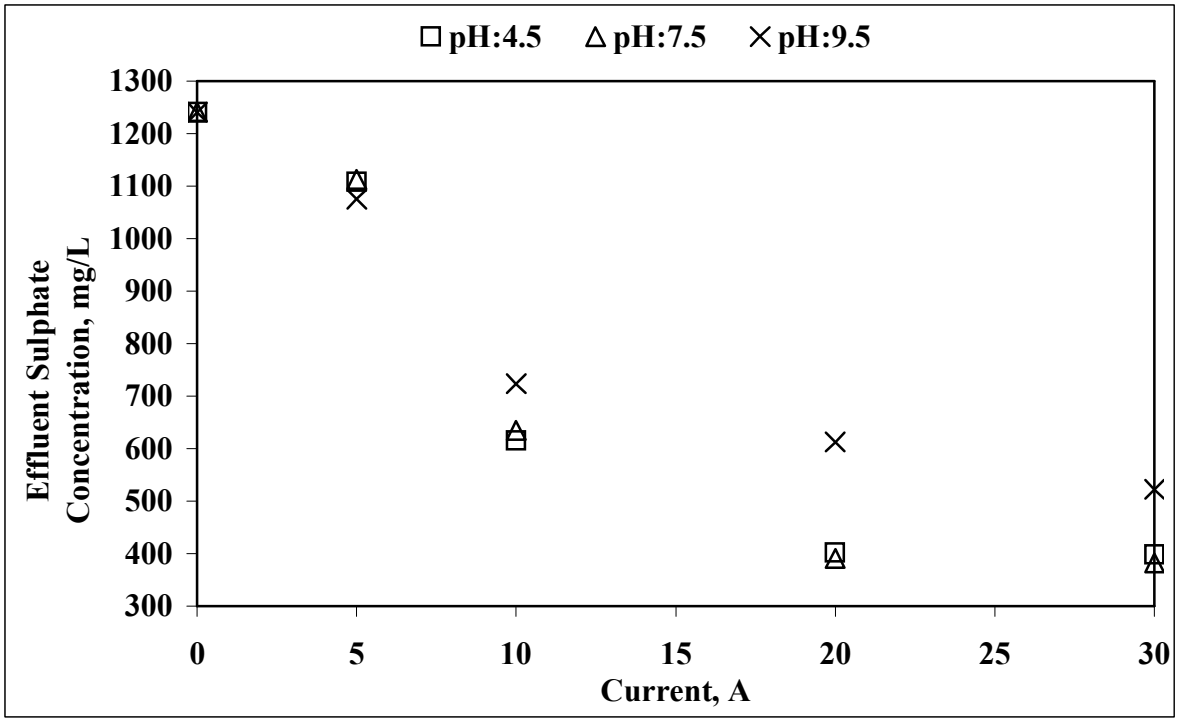

Figure 4.46. The profile of sulphate removal as a function of the applied current; electrolysis time = 15 min; aluminum electrode

As is evident from Figure 4.46, significant amounts of sulfate could be removed using aluminum electrodes at various pH. The mechanism of sulphate removal is thought to be charge neutralization and adsorption on positively charged monomeric and polymeric aluminum species. It should be noted that sulphate abatement rates were hence higher at 4.5 and 7.5 initial pH. Sulfate removal was reduced at pH = 9.5 speculatively due to the electrostatic repulsion between negatively charged aluminum hydroxide complexes and sulfate ion. The highest sulfate reduction was achieved at an initial pH of 7.5 (from 1240 mg/L to 380 mg/L) at 30 A current.

• iron/aluminum electrodes

When iron/aluminum electrodes were used simultaneously 65% sulfate removal was observed, emphasizing the positive effect of aluminum in sulfate removal from textile wastewater. No significant changes in effluent sulfate concentrations were observed when the current was increased above 20 A (Figure 4.47.). Highest sulfate reduction occurred at

an initial pH of 7.5 due to the effect of pH on the distribution of aluminum species as described in the previous section.

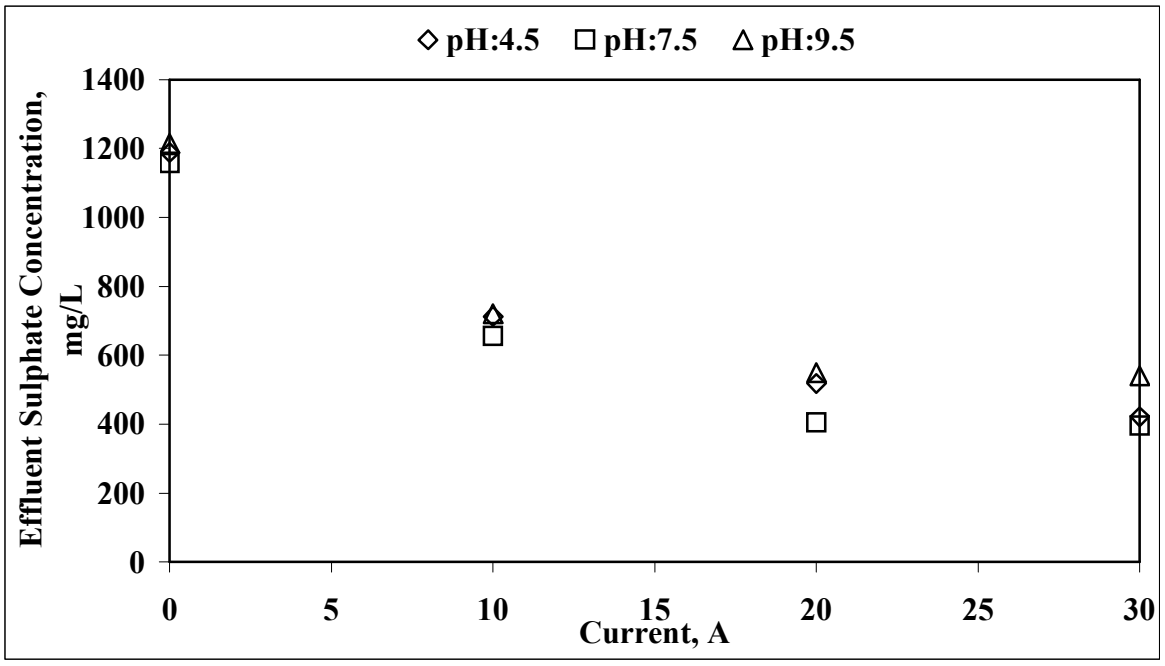

Figure 4.47. The profile of sulphate removal as a function of the applied current; electrolysis time = 15 min; iron/aluminum electrode

4.1.3.5. The Fate of Iron During Electrolysis. The effluent from biological treatment contains total iron concentration of about 2 mg/L of which 1.6 mg/L as ferrous iron and 0,4 mg/L as ferric iron. The effluent iron concentrations were measured in order to assess if the electrochemical system adds more iron to the wastewater.

- iron electrodes

Table 4.2, 4.3, and 4.4. summarize the effluent Fe^{+2}, Fe^{+3}, and total iron concentrations at varying initial pH and varying currents after 15 min electrolysis of biotreated textile effluent.

Table 4.2. Effluent total iron concentration after electrolysis with iron for 15 minutes

Current, A	Total Iron, mg/L		
	pH:4.5	pH:7.5	pH:9.5
5	14.83	3.17	0.84
10	14.60	1.36	0.60
20	6.56	0.90	0.53
30	3.48	0.62	1.14

Table 4.3. Effluent Fe^{+2} concentration after electrolysis with iron for 15 minutes

Current, A	Fe^{+2}		
	pH:4.5	pH:7.5	pH:9.5
5	9.03	0.70	0.49
10	8.93	0.45	0.38
20	3.52	0.52	0.39
30	2.29	0.48	0.83

Table 4.4. Effluent Fe^{+3} concentration after electrolysis with iron for 15 minutes

Current, A	Fe^{+3}		
	pH:4.5	pH:7.5	pH:9.5
5	5.80	2.47	0.35
10	5.67	0.91	0.22
20	3.04	0.38	0.19
30	1.19	0.14	0.32

Tables 4.2. to 4.4. explain the low performance of electrolysis at pH 4.5 where iron itself is responsible for the residual color. Even at high current input (30 A) the effluent iron concentrations were higher than the initial because of the low final pH of the effluent. For pH = 7.5 and 9.5, total iron was removed 69% at 30 A and 74% at 20 A, respectively. Differences in the removal pattern of iron (total and ionic) is due to the differences in the

initial and final pH. Figure 4.48. shows that, when the reaction is started at pH = 4.5, the final pH after 15 min is only 6.5, which is not sufficiently high for the formation of $Fe(OH)_3$ precipitate.

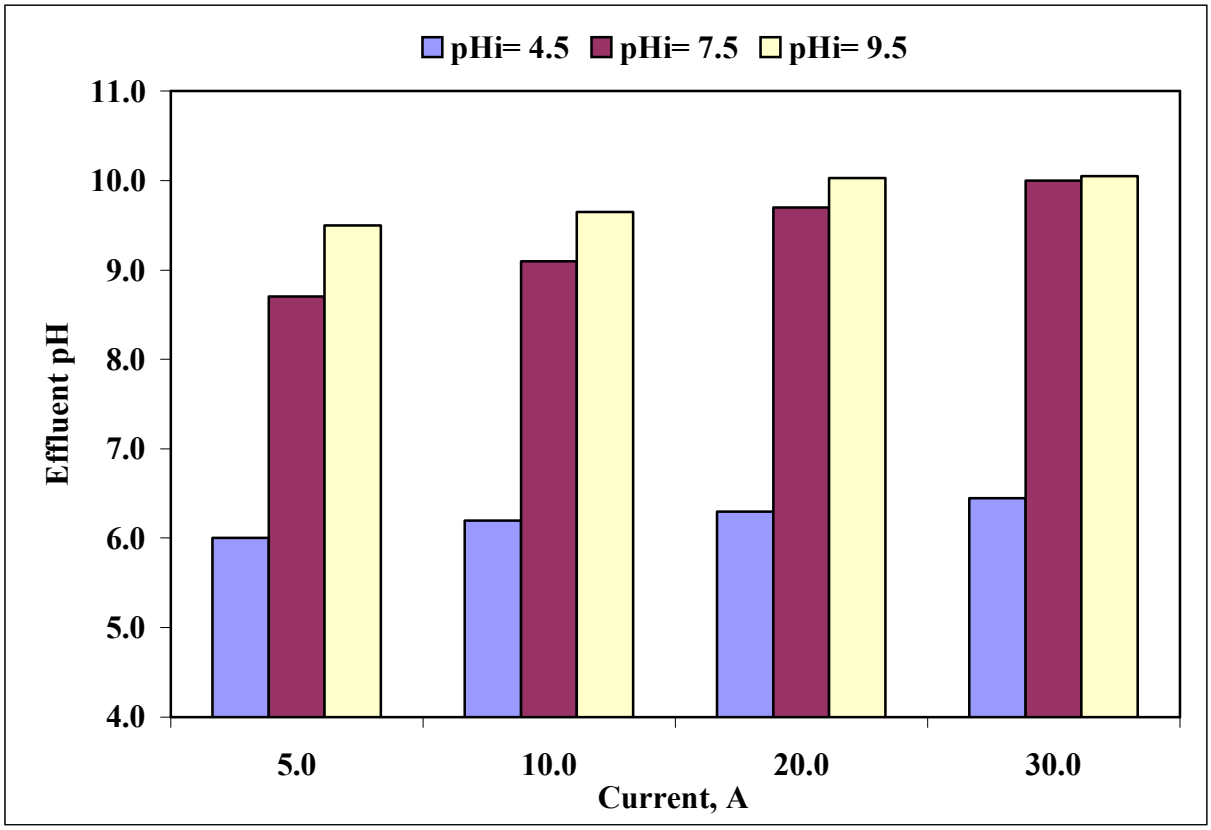

Figure 4.48. The change in effluent pH with electrolysis using the iron electrode; electrolysis time=15 min

• aluminum electrode

Effluent iron concentration was also monitored when electrolysis was conducted using Al electrodes in order to evaluate the performance of Al electrodes in terms of iron removal. Biotreated effluent initially contained 2.14 mg/L total iron. After 15 min of electrolysis using aluminum electrodes total iron removal was in the range of 70-80 % (Table 4.5.). No ferric ion could be detected so that all total iron was in the form of ferrous iron indicating that no oxidation of iron occurred in the electrolysis solution.

Table 4.5. Effluent iron concentration after electrolysis with aluminum for 15 minutes

Current, A	Fe^{+2}, mg/L		
	pH:4.5	pH:7.5	pH:9.5
5	1.40	1.56	1.68
10	0.85	1.25	1.37
20	0.65	0.86	0.91
30	0.63	0.82	0.85

- iron/aluminum electrode

The resulting iron concentrations are summarized in Table 4.6. After electrochemical treatment using iron/aluminum electrodes, the concentration of iron was reduced from 2.25 mg/L to 0.206 (91%) at pH = 7.5 and 20 A current input. In addition, no ferric ion could be detected, as was the case with the aluminum electrode alone, so that all of the total iron was in the form of ferrous iron indicating that iron was not oxidized.

Table 4.6. Effluent iron concentration after electrolysis with iron/aluminum for 15 minutes

Current, A	Fe^{+2}, mg/L		
	pH:4.5	pH:7.5	pH:9.5
10	1.14	0.35	0,46
20	0.88	0.21	0.22
30	0.77	0.21	0.24

4.1.4. Summary of Electrode Performances

Tables 4.7, 4.8, and 4.9, summarize the performance of the three electrode materials at 20 A and initial pH of 4.5, 7.5, and 9.5 for color, COD, SS, SO_4^{2-} and DS.

Table 4.7. Performance of the electrodes at pH = 4.5 and current = 20 A

Electrode Material	Removal Efficiency, %				
	Color	COD	SS	SO_4^{2-}	DS
Iron	76	69	-	-	-
Aluminum	71	62	96	68	28
Iron/Aluminum	55	68	95	56	27

Table 4.8. Performance of the electrodes at pH = 7.5 and current = 20 A

Electrode Material	Removal Efficiency, %				
	Color	COD	SS	SO_4^{2-}	DS
Iron	88	68	94	-	-
Aluminum	54	48	94	68	33
Iron/Aluminum	91	67	93	65	34

Table 4.9. Performance of the electrodes at pH = 9.5 and current = 20 A

Electrode Material	Removal Efficiency, %				
	Color	COD	SS	SO_4^{2-}	DS
Iron	92	76	97	-	-
Aluminum	40	47	90	67	30
Iron/Aluminum	87	68	95	55	29

Tables 4.7, 4.8, and 4.9. show that the performance of iron and iron/aluminum electrodes were significantly better at pH 7.5, whereas for the aluminum electrode the best performance was observed at pH 4.5. It should also be mentioned here that SS could be successfully removed at all conditions with the exception of electrolysis with iron electrodes at pH = 4.5, where the iron anode dissolves very fast and the pH of the solution is not sufficiently high to help the aggregation of the formed flocs. In addition, electrolysis using iron as the electrode was incapable of SO_4^{2-} removal, which was possible in the case of aluminum and iron/aluminum electrodes (up to 68% at pH 7.5 and 9.5). Note that the highest overall COD removal was obtained with the iron electrode at pH = 9.5.

For a successful reuse operation the increase in DS should be avoided, or controlled. However, when metal salts are added for coagulation, the salinity of treated effluent increases tremendously. This underlines the inherent advantage of electrochemical application, where no salt addition is present. In fact, even a significant decrease in DS content could be achieved after electrolysis with aluminum or iron/aluminum electrodes. Another advantage of electrolysis is that no pH adjustment is required to achieve high treatment efficiencies when the pH of effluent falls between 4.5-9.5.

4.2. Continuous Operation of Electrochemical Treatment (CET)

For full-scale implementation of an electrochemical process to treat dyehouse effluent, its continuous mode operation was evaluated under the light of previously conducted batch experiments (Apikyan and Ince, 2004). Additionally, in order to question the possibility of eliminating a preceding biological treatment step, continuous mode electrochemical treatment has also been applied to raw (untreated) textile wastewater.

4.2.1. Continuous Mode Electrochemical Treatment of Biotreated Wastewater

Continuous mode electrochemical treatment (CET) was conducted with iron, aluminum and iron/aluminum electrodes under conditions preliminary optimized during the batch electrolysis experiments. The experimental setup for CET enabled satisfactory floc formation, coagulation, flotation and sludge separation in one single reactor when iron electrodes were used. However, when aluminum was used as the electrode material, the

reactor suffered from serious phase separation problems probably due to the poor settling characteristics of the small sized flocs formed during electrolysis. In former studies using aluminum electrodes for electrochemical treatment, either separate settling tanks or batch mode systems were employed. In the present study coagulation and sludge separation stages also failed when aluminum electrodes were employed. For the same reason, CET using iron/aluminum combined electrodes did not work properly.

The performance of CET using iron electrode was evaluated in terms of COD, SS and color removal.

4.2.1.1. CET using Iron Electrode. Preliminary experiments indicated that flowthrough electrolysis resulted in sludge washout and poor color removal efficiencies. In order to improve the color and SS removal the reactor was first operated in batch mode until – 650 mV reduction potential was reached where decolorization and proper flotation of the aggregates were achieved. After this point, the reactor was continuously fed with fresh biotreated effluent. The flow of the biotreated effluent entering to the reactor was adjusted so that a minimum critical reduction potential of – 650 mV could be maintained throughout the experiments.

• COD and SS removal

At this stage of the investigation, electrochemical treatment was initiated at varying pH between 7.0 and 11.0 with iron electrodes at 20 A with a hydraulic retention time of 10 min (flowrate = 150 L/h). Figure 4.49. depicts COD and SS removal efficiencies after electrochemical treatment of biotreated effluent. The results showed that with CET, contaminant removal efficiencies in terms of both COD and SS were not as high as that obtained during batch tests. As can be seen in Figure 4.49, only 48% and 44% COD removal was observed at pH 7.5 and 9.5, respectively, whereas in batch tests 68% and 71% COD removal was achievable. In case of SS, the reduction in removal efficiency was not as high as which observed in COD removal.

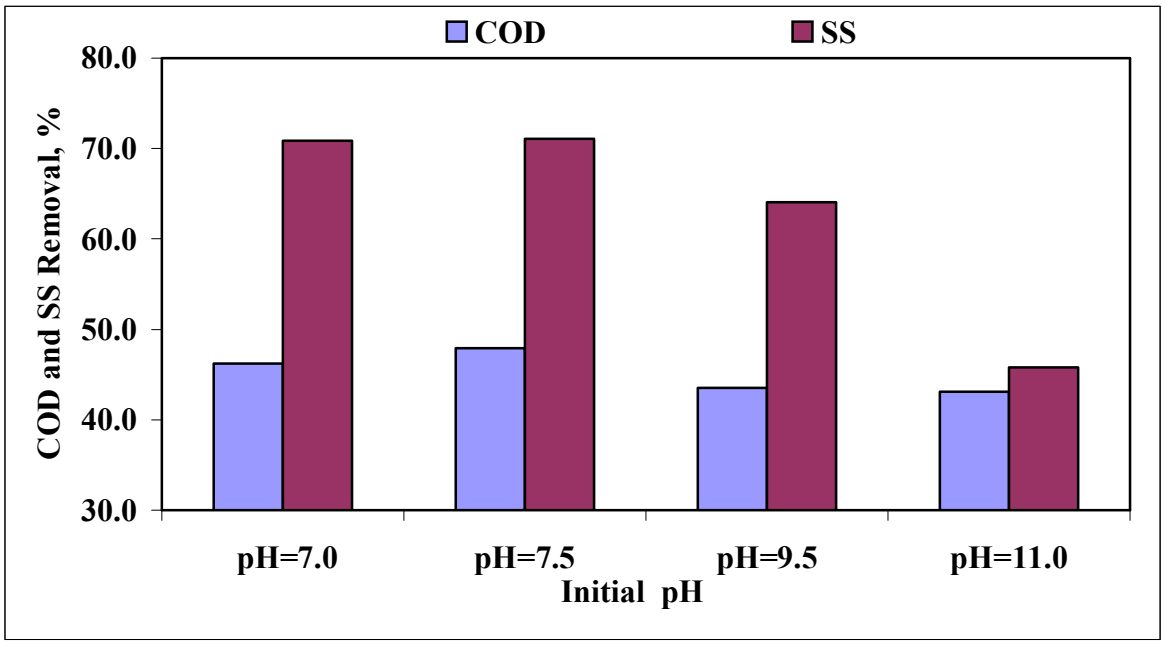

Figure 4.49. COD and SS of the biotreated and biologically + electrochemically treated textile effluent (current = 20 A; effluent flow = 150 L/h)

Tale 4.10. summarizes the COD and SS removal efficiencies for both batch and continuous electrolysis, and the reduction in system performance when continuous mode was applied. It is interesting to note that, although continuous electrolysis was still effective in terms of SS removal, a significant decrease in COD removal efficiency was observed.

Table. 4.10. Comparison of COD and SS removal efficiencies in batch and continuous electrolysis of biotreated textile effluent

	SS Removal, %		COD Removal, %		Reduction in Removal Efficiency, %	
Initial pH	Batch	Continuous	Batch	Continuous	SS	COD
7.5	86	71	68	48	17	30
9.5	75	64	71	44	15	38

In order to improve the COD removal efficiency, the hydraulic retention time was increased from 10 min to 12 min at pH 7.5 and 9.5. Figure 4.50. and 4.51. present SS and COD removal efficiencies during continuous electrolysis of biotreated effluent at varying flow rates at pH = 7.5 and pH = 9.5, respectively. Although the improvement in SS removal efficiency was not that much significant (7% at pH = 7.5, and 16% at pH = 9.5), a considerable increase in COD removal efficiency was observed (37% at pH = 7.5 and 55% at pH = 9.5) at reduced flow rates. The increase in COD removal efficiency can be explained by the higher reduction potentials achieved when the effluent flow was decreased. In addition, the increase in reduction potential was higher at pH = 9.5 (660 mV at 150 L/h and 980 mV at 125 L/h) than that of pH = 7.5 (650 mV at 150 L/h and 880 mV at 125 L/h) which also explains the more pronounced effect of effluent flow rate on COD removal efficiency at higher pH. As a conclusion the results confirmed that reduction in COD and SS were attributable to different removal mechanisms.

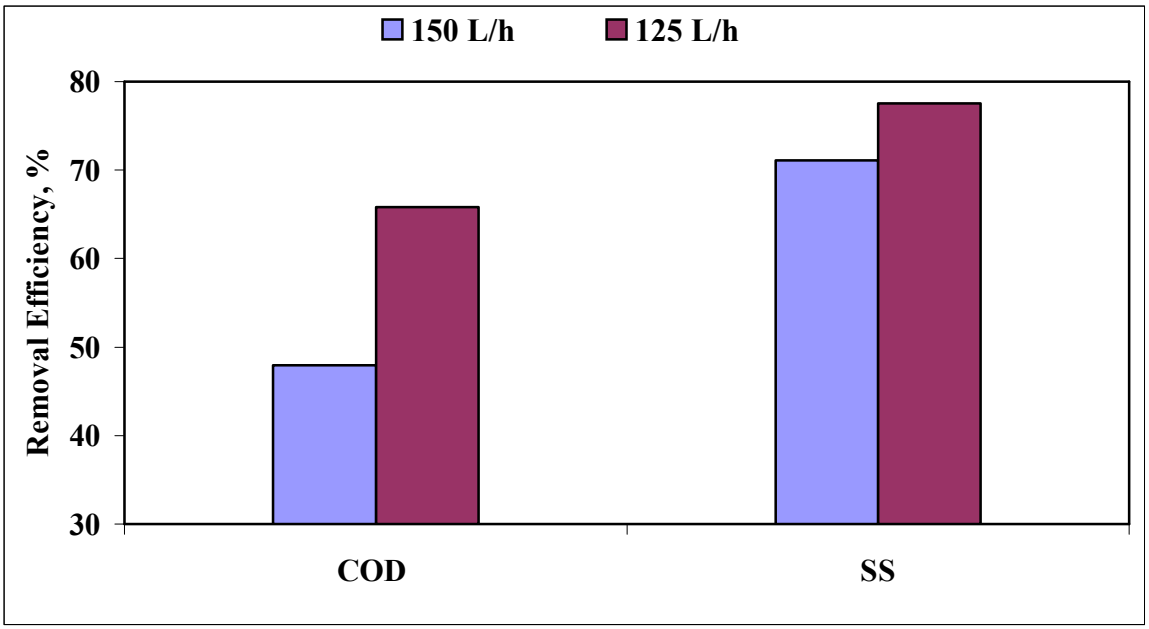

Figure 4.50. COD and SS removal efficiencies via continuous electrolysis of biotreated effluent under varying flow conditions (pH = 7.5; current = 20 A)

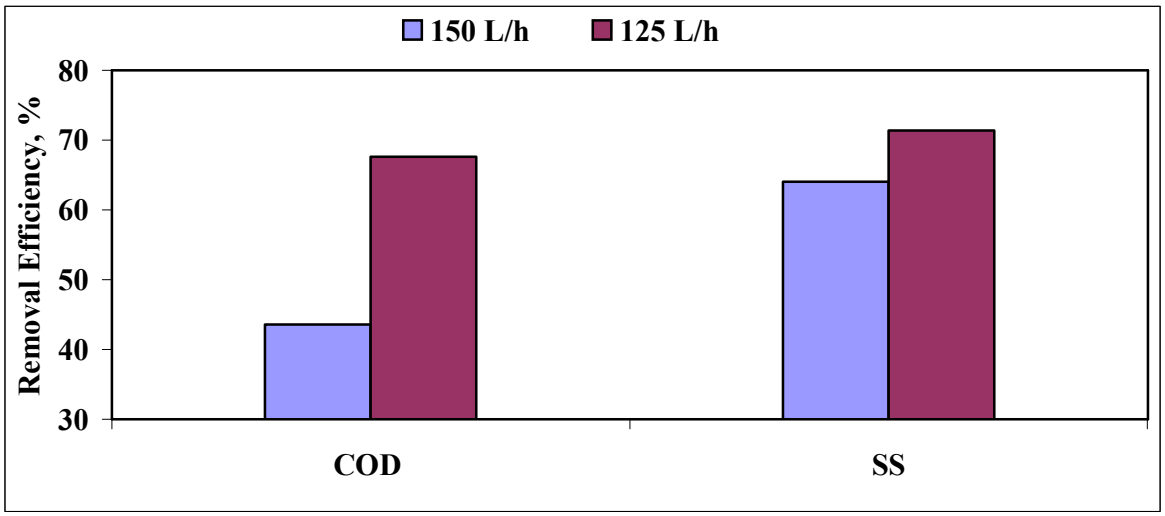

Figure 4.51. COD and SS removal efficiencies via continuous electrolysis of biotreated effluent under varying flow conditions (pH = 9.5; current = 20 A)

- color removal

During batch electrolysis of biotreated textile effluent, at 20 A current, color was effectively removed independent from the initial pH. However, with 150 L/h effluent flow, color could not be removed effectively when compared with batch electrolysis. Color removal efficiency did not change with varying initial pH (Figure 4.52.).

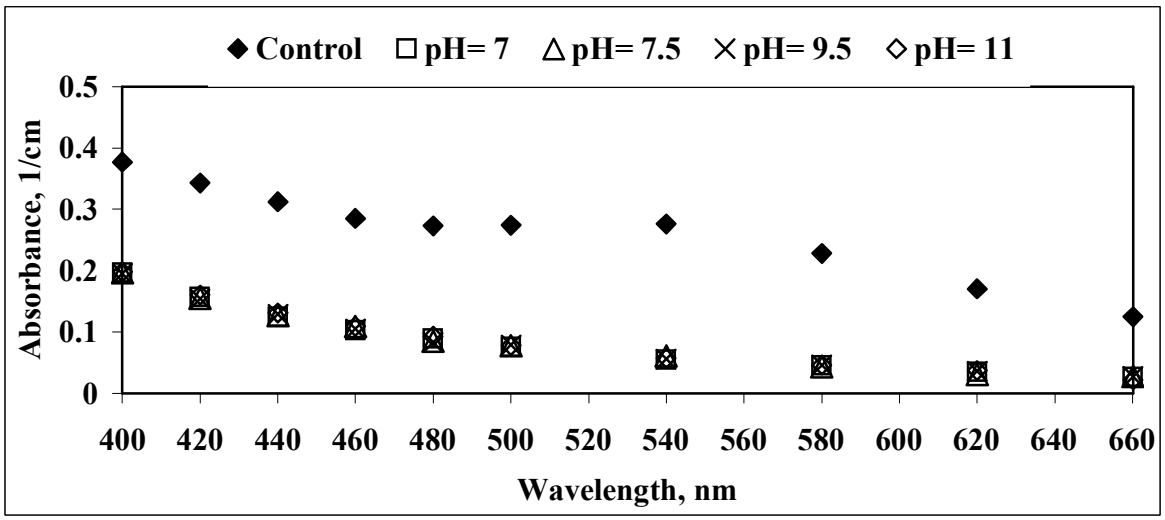

Figure 4.52. Variations in the absorption with pH during continuous electrochemical treatment of biotreated effluent at 20 A

When the reduction potential of the electrolysis solution was increased to a range of 850 - 950 mV by reducing the effluent flow to 125 L/h, decolorization was achieved more effectively at both pH = 7.5 and pH = 9.5 at the same current. Figure 4.53. exhibits the increase in color abatement with reducing effluent flow during continuous electrolysis of biotreated effluent.

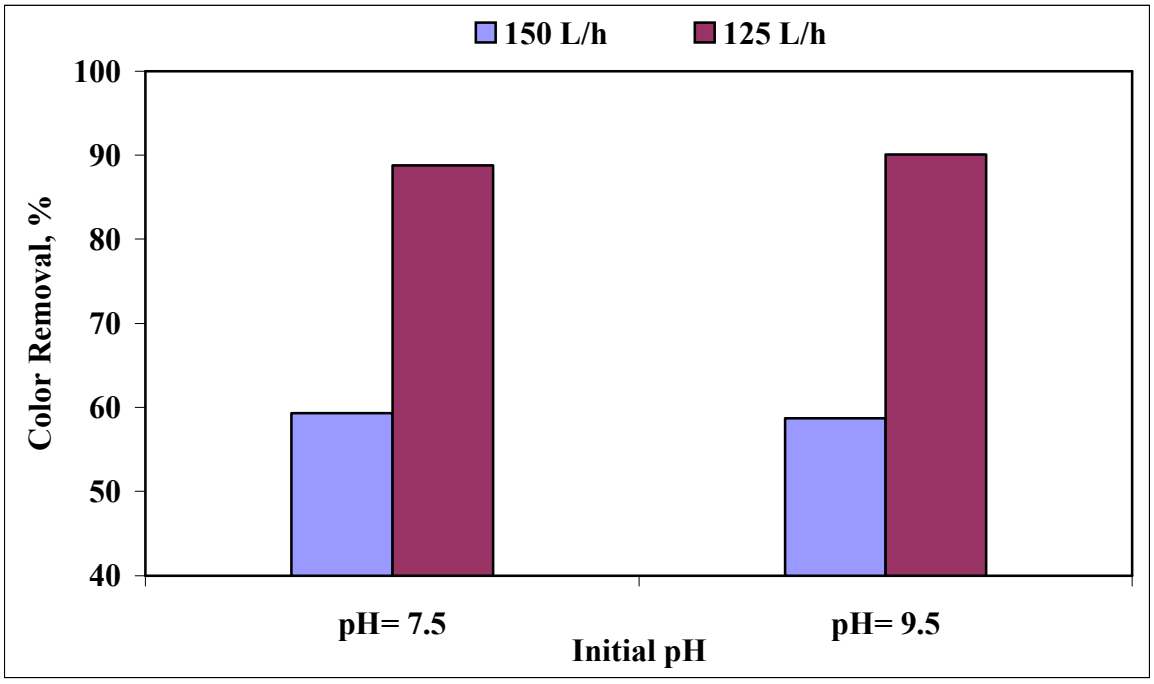

Figure 4.53. Color removal efficiencies via continuous electrolysis of biotreated effluent under varying flow conditions (current = 20 A; iron electrode)

4.2.2. Continuous Mode Electrochemical Treatment of Raw Wastewater

At this stage of the investigation, CET was applied to raw (untreated) textile wastewater in order to question the possibility of eliminating a preceding biological treatment step using iron electrodes. The performance of this system was evaluated in terms of COD, SS and color removal at varying initial pH under 20 A current.

4.2.2.1. COD and SS Removal. COD and SS concentrations before and after CET of raw wastewater are shown in Figure 4.54. The experimental results showed that COD removal using CET was effective at all studied initial pH, whereas poor SS removal was obtained at acidic pH. Final SS achieved with the treatment of raw wastewater were very similar to that of biotreated effluent. The maximum COD and SS removal was achieved at the pH of raw wastewater (9.5) as 57% and 83%, respectively.

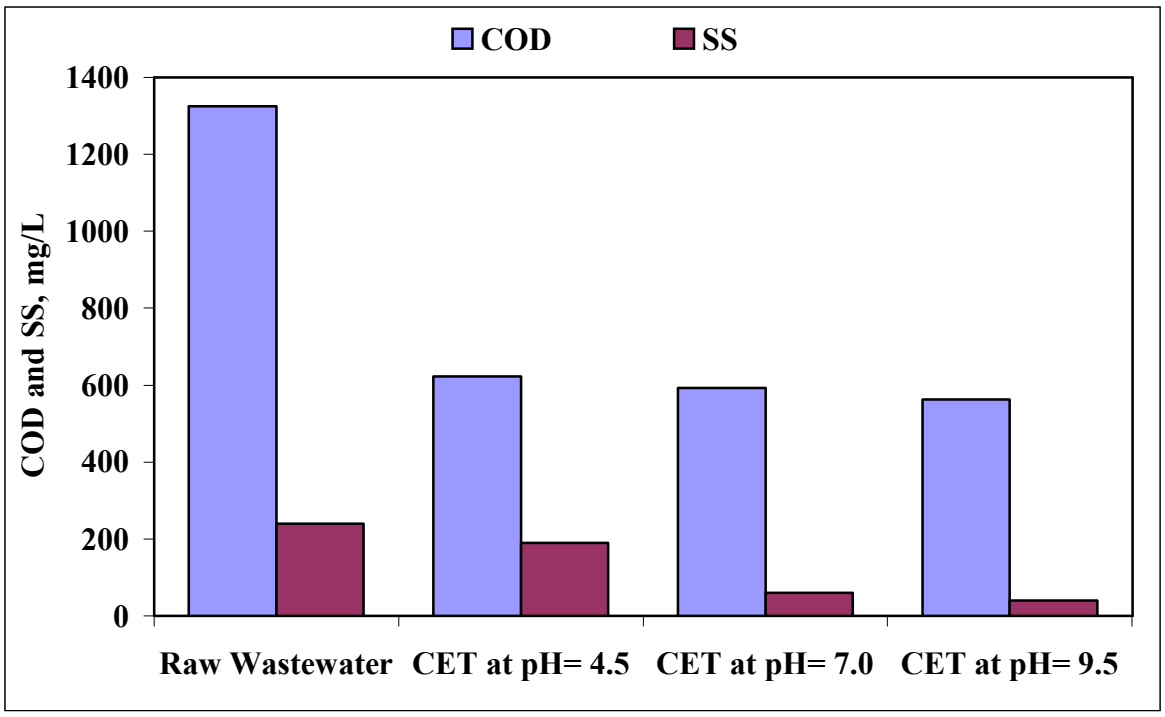

Figure 4.54. COD and SS concentrations before and after cet of raw wastewater (current = 20 A; effluent flow = 150 L/h)

From the above results, it can be concluded that considering the final SS (40 mg/L at pH = 9.5), CET can replace biological treatment. However, after direct CET of the raw wastewater effluent COD remained too high (563 mg/L at pH = 9.5) to omit biological pretreatment. In addition, further attempts to improve the efficiency of COD removal by reducing wastewater flow to 125 L/h at pH = 9.5 ended up with only 5% improvement whereas no difference could be observed in SS. It should also be pointed out here that, CET of the raw textile effluent was sufficient to meet the requirements of the local sewage treatment works for pretreatment.

4.2.2.2. Color Removal. As shown in Figure 4.55. the color of raw wastewater is stronger than biotreated effluent. It is well known that most of the dyes in dyehouse effluents are eliminated by adsorption, chemical destruction, rather than biological degradation. During the treatment of commercial dyes in the effluent stream at sewage works, both aerobic and anaerobic metabolic pathways are followed. In anaerobic conditions several types of microorganisms can reduce azo compounds to the corresponding amines, but usually the process is incomplete. Despite the presence of oxygen, the first step of aerobic decomposition is assumed to be reduction to amines, as in anaerobic systems. In most cases degradation does not occur in aerobic conditions. Long adaptation periods are usually necessary to obtain cultures capable of degrading azo dyes effectively. Therefore, in our case the reason for color abatement during SBR may be most probably due to the adsorption of less soluble (especially disperse, acid/metal complex dyes) dyes on bacteria.

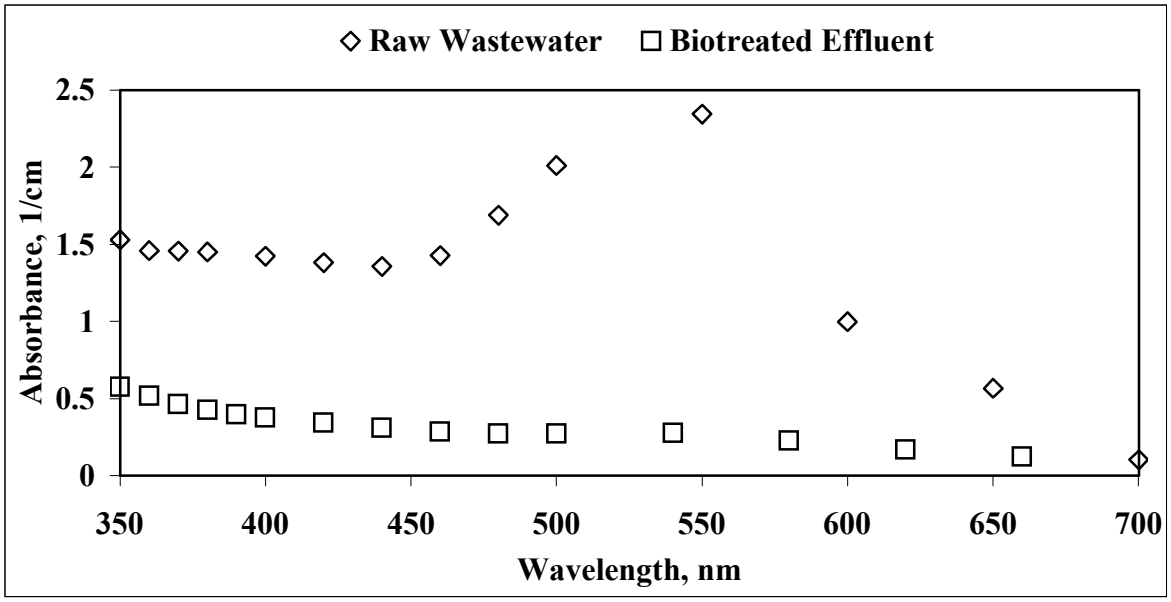

Figure 4.55. Absorption spectra of raw and biotreated dyehouse effluent

Although the raw wastewater was stronger in color than biotreated effluent CET of raw dyehouse wastewater ended up with comparably high color abatement especially at pH 7.0 and pH 9.5 (Figure 4.56.).

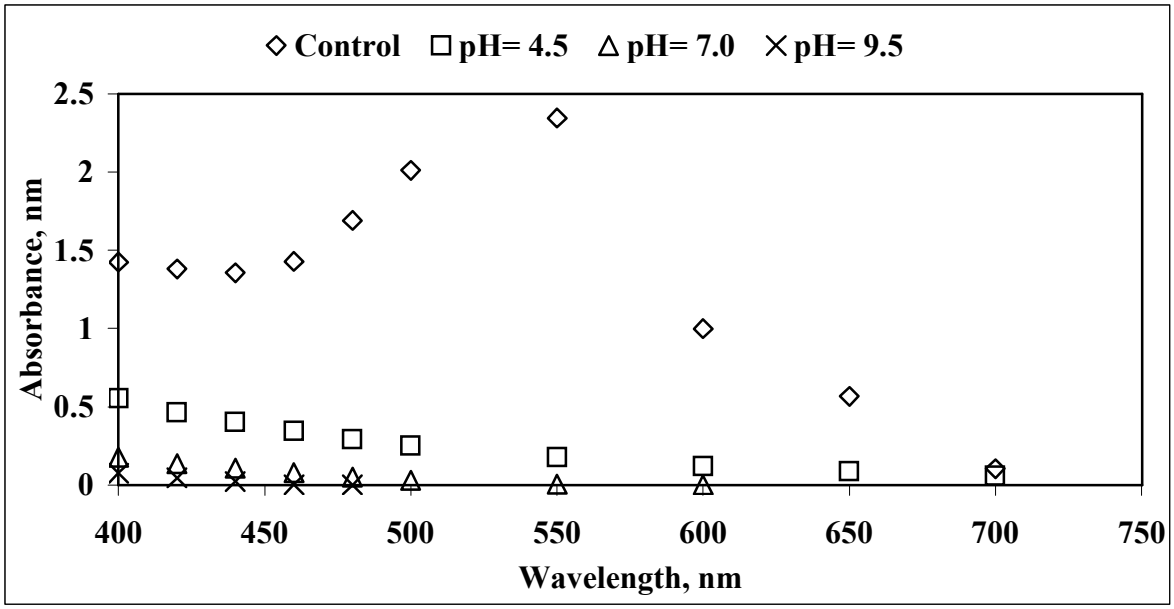

Figure 4.56. The change in absorption spectra with CET of raw textile dyehouse effluent at varying initial pH (current= 20 A; Effluent flow = 150 L/h)

For both raw and biotreated effluents highest color removal after CET was obtained at pH = 9.5. As shown in Figure 4.57, CET of biotreated effluent resulted in 60% color removal (final absorbance at 436 nm=0.129 1/cm), whereas in the case of raw wastewater CET accounted for 98% reduction in color (final absorbance at 436 nm= 0.022 1/cm). This observation may be attributable to the different characteristics and degradation products of the investigated effluents. More specifically, biotreatment may have resulted in intermediate degradation products that are more amenable to reduction and consequently, more substrates may undergo reduction during CET making decolorization process under the same operating conditions less efficient.

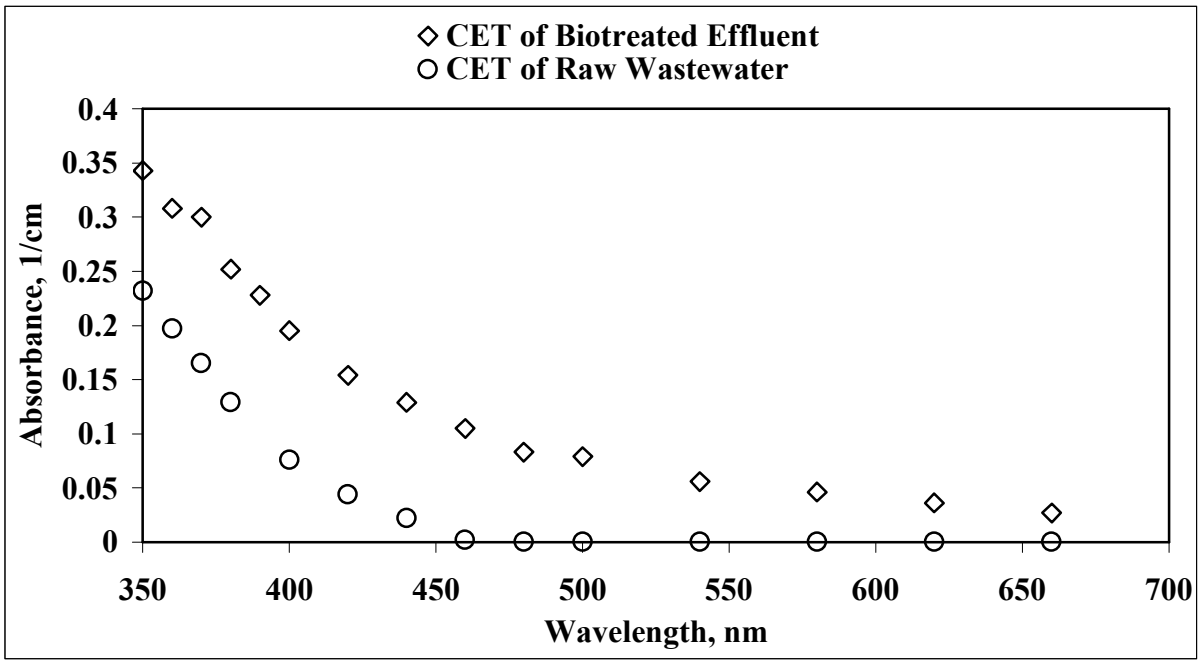

Figure 4.57. Final absorption spectra of raw wastewater and biotreated effluent after CET (current = 20 A; Effluent flow = 150 L/h; initial pH = 9.5)

4.3. Effect of Biological Treatment Efficiency on Electrolysis Performance

The efficiency of biological treatment systems may vary due the fluctuations in the quality and quantity of textile wastewater. Most of the time these variations end up with low COD removal and high SS content in the biotreated effluent. In case of poor settling, or low COD removal, there is no chance to extend the settling time or aeration time because of the high volumetric loading being typical at textile dyehouses. Therefore if reuse is considered at the plant using advanced filtration systems like membranes following biological treatments, precautions should be taken in the form of a treatment stage between biological and membrane processes.

The performances of batch and continuous electrochemical systems were tested for the worst operating conditions of the sequential batch reactor (SBR), which is operated for secondary treatment in the dyehouse under investigation. The operating parameters of the SBR were intentionally deteriorated to simulate the worst conditions that may be encountered during biological treatment. Table 4.11. presents the standard and worsened operating conditions for the SBR.

Table 4.11. Standard and worsened operating conditions for biological treatment system

Treatment Stage	Standard Operating Time, min	Stressed Operating Time, min
Filling and aeration	270	270
Aeration	60	30
Settling	60	30
Draining	90	90

As shown in Table 4.11. the simulation of the operational failures encountered in biological treatment has been accomplished in the following manner:

- Case I: Reduced Aeration
- Case II: Reduced Settling
- Case III: Reduced Aeration and Reduced Settling.

Table 4.12. presents the final COD and SS contents of the effluents collected under standard and three worst case scenarios for the SBR. When aeration time is reduced as in Case I, effluent COD increased since contact time was not sufficient for efficient treatment. In Case II, poor (reduced) settling ended up with high SS and accompanying COD as the unsettled bacteria constitutes a significant part of the effluent COD. Case III, (a combination of Case I and Case II) represented the worst case of the SBR, because both aeration and settling times were inappropriate. Therefore, effluent COD and SS even exceeded that of the untreated wastewater.

Table 4.12. SBR effluent COD and SS under standard and worst conditions

Parameter	Standard Operating Conditions	Case I	Case II	Case III
COD, mg/L	368	725	1125	1780
SS, mg/L	124	148	540	623

4.3.1. Effect of Biological Treatment Efficiency on Batch Electrolysis Performance

Tables 4.13. to 4.15. summarize the performance of electrochemical operation using different electrode materials at 20 A current input and 15 min of electrolysis time, for Case I, Case II and Case III, respectively.

Table 4.13. Impact of Case I conditions on the performance of electrolysis for COD and SS removal from biotreated effluent

	COD, mg/L	SS, mg/L
Control	725	148
Electrode Material		
Iron	233	12
Aluminum	322	10
Iron/Aluminum	224	11

Table 4.14. Impact of Case II conditions on the performance of electrolysis for COD and SS removal from biotreated effluent

	COD, mg/L	SS, mg/L
Control	1125	540
Electrode Material		
Iron	118	21
Aluminum	154	16
Iron/Aluminum	121	15

Table 4.15. Impact of Case I conditions on the performance of electrolysis for COD and SS removal from biotreated effluent

	COD, mg/L	SS, mg/L
Control	1780	623
Electrode Material		
Iron	247	24
Aluminum	358	15
Iron/Aluminum	239	20

When the biological treatment system was run as in Case I, the electrochemical cell received high COD. In this situation, electrochemical operation gave COD removal efficiencies between 55-70%, which at the end compensate the poor treatment performance of the SBR unit (Table 4.13.). In Case II, all tested electrode materials gave outstanding efficiencies in terms of both COD and SS removal (Table 4.14.). The reason is thought to be the fact that the major portion of the COD present in the Case II effluent was in the form of SS, which could be easily removed via electrolysis. Finally, the effluent COD and SS contents after electrolysis of Case III effluent were obtained (Table 4.15.) very close to those of Case I, as expected. When SS was removed via electrolysis, the remaining COD approached the initial COD of Case I.

4.3.2. Effect of Biological Treatment Efficiency on Continuous Electrochemical Treatment Performance

The effect of biological treatment efficiency on CET was evaluated for the worst operating condition that involved reduced aeration and reduced settling (Case III) at the same time. As iron was found to be the only applicable electrode material for CET in the previous part of the present study, the response of CET to Case III effluent was only investigated for iron electrodes. Tables 4.16. presents the performance of CET using iron electrode at 20 A current input and 150 L/h flow of Case III effluent.

Table 4.16. Impact of Case III conditions on the performance of CET for COD and SS removal from biotreated effluent (current = 20 A; Effluent Flow = 150 L/h)

Effluent	COD, mg/L		SS, mg/L	
	Control	After CET	Control	After CET
Standard Effluent of SBR	388	202	114	33
Effluent of Case III	1604	498	630	45

As is evident in Table 4.16, CET could even handle the high SS load of Case III (i.e. 630 mg/L). The final SS concentrations achieved after CET of both Standard Effluent of SBR and Case III effluent were close to each other (33 mg/L and 45 mg/L, respectively).

In conclusion, the proposed electrochemical treatment system is capable of compensating the operational failures of the SBR system resulting in high COD and SS effluent. Electrochemical process acted as a compensating/intermediate treatment stage located between the SBR and the membrane filtration units.

4.4. Ozonation

4.4.1. Ozonation of Biotreated Textile Wastewater

Previous research has demonstrated that ozonation is an effective treatment technology for the decolorization and partial oxidation of dyehouse effluent. In the present work, biotreated textile effluent was first subjected to ozonation for 1 h at a dose of 1440 mg/(L×h) and at varying initial pH (pH = 4.5, 7.5, 9.5, and 11.5) in unbuffered reaction solutions (without pH control), and, changes in color (measured as absorbance at 436 nm) and COD were monitored as a function of ozonation time. The amount of absorbed ozone (O_{3A}) after 1 h treatment was also monitored as a measure of ozone transfer and consumption efficiency.

4.4.1.1. Color Removal. Figure 4.58.presents color abatement during ozonation at varying initial pH. The pH did not change significantly throughout the experiments mainly because the biotreated effluent had a high alkalinity acting as an effective pH buffer.

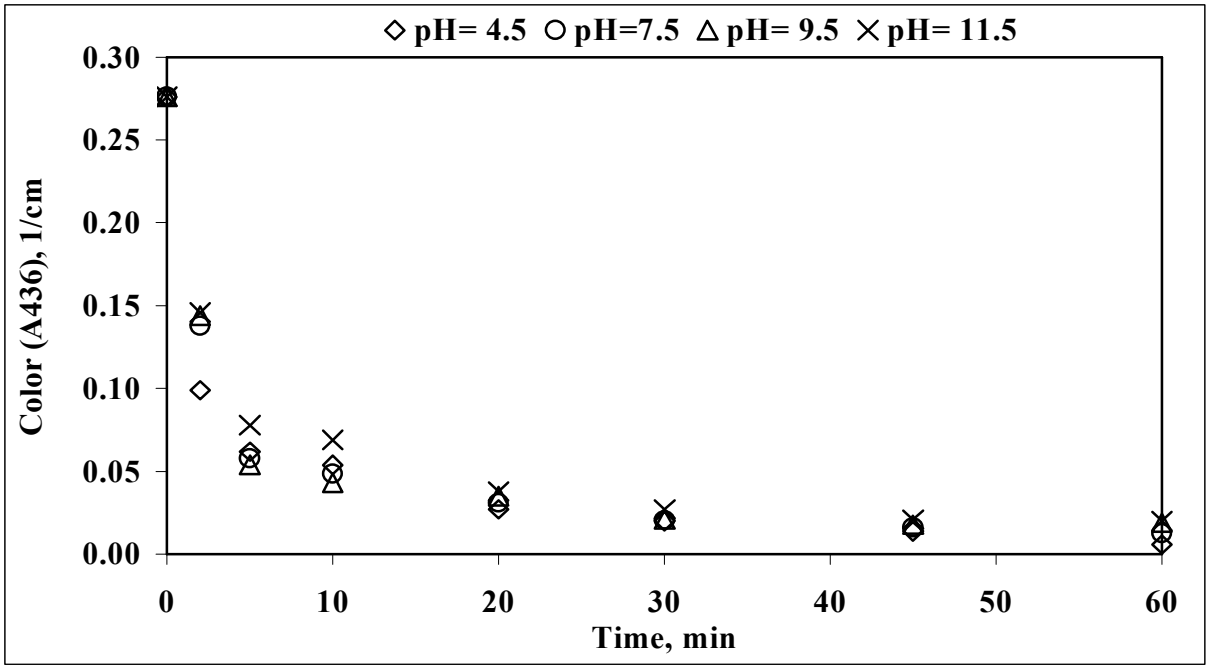

Figure 4.58. Color abatement during ozonation at varying pH

As can be seen in Figure 4.58, color removal was fast and almost complete after 10 min ozonation. In other words, only 240 mg/L ozone was required to achieve acceptable color removal. From the figure it is also evident that color removal was almost equally fast at all studied pH. This is not surprising due to the fact that ozone readily reacts with color causing aromatic compounds even via direct, molecular ozone at diffusion controlled rates (Beltran, 2004). Conclusively, pH - independent color removal profiles were obtained in the present study. The above findings were in complete agreement with former investigations where ozone decolorized water-soluble textile dyes and textile wastewater at a rate being almost equal at different pH provided that the bicarbonate alkalinity of the wastewater is high (Arslan - Alaton et al., 2002; Arslan-Alaton and Seremet, 2004).

4.4.1.2. COD Removal. Figure 4.59. displays the reduction in COD for biotreated wastewater at varying initial pH as a function of ozonation time. As can be seen from the Figure, an average of 57% COD was removed in the first 5 min of ozonation, and another

30% reduction was obtained in COD at the end of 60 min. A similar trend was observed in color removal, revealing that COD and color removal proceeded in two phases. In the first phase of ozonation, a considerable part of COD was removed via destruction of color causing and other fast reacting compounds present in the effluent. In the second phase, the organic compounds were converted into more difficult to oxidize intermediates. The transition from fast-reaction activity to a slower one implied a decrease about one order of magnitude in the COD abatement rate as can be seen in Figure 4.60. The degradation of COD followed first order kinetics in accordance with:

$$\ln\left(\frac{C}{C_0}\right) = -k.t \qquad (4.1)$$

where,

C_o is the initial COD of effluent

C is the COD of effluent at time t, and

k is the first order rate coefficient (1/min)

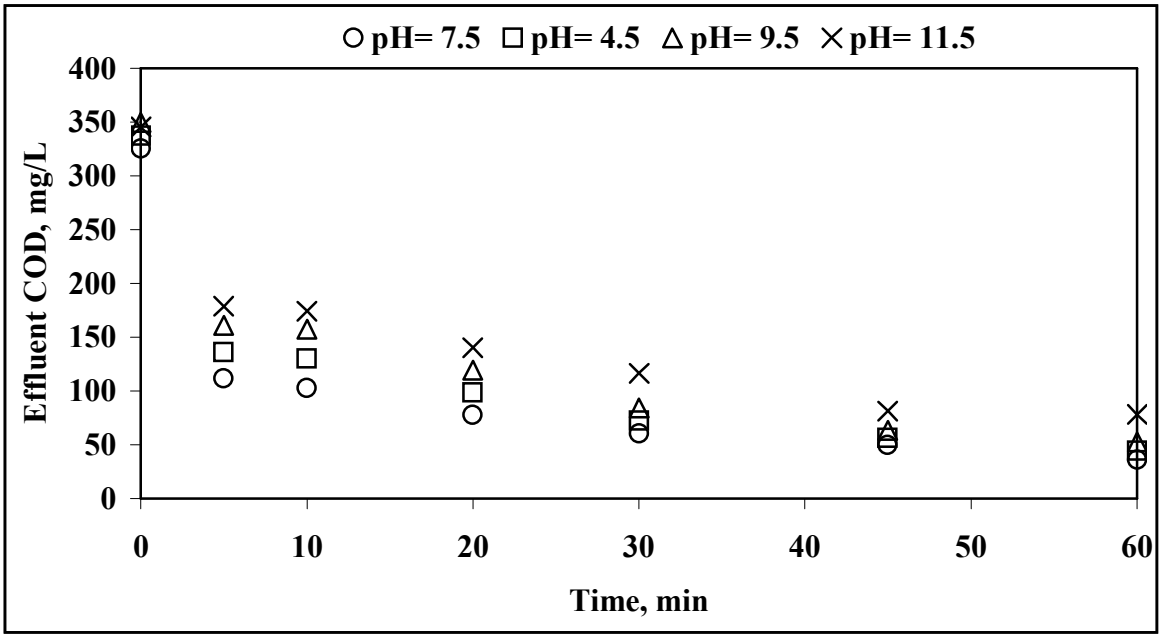

Figure 4.59. Changes in COD during ozonation (applied dose = 1440 mg/h) of biotreated textile effluent at varying initial pH

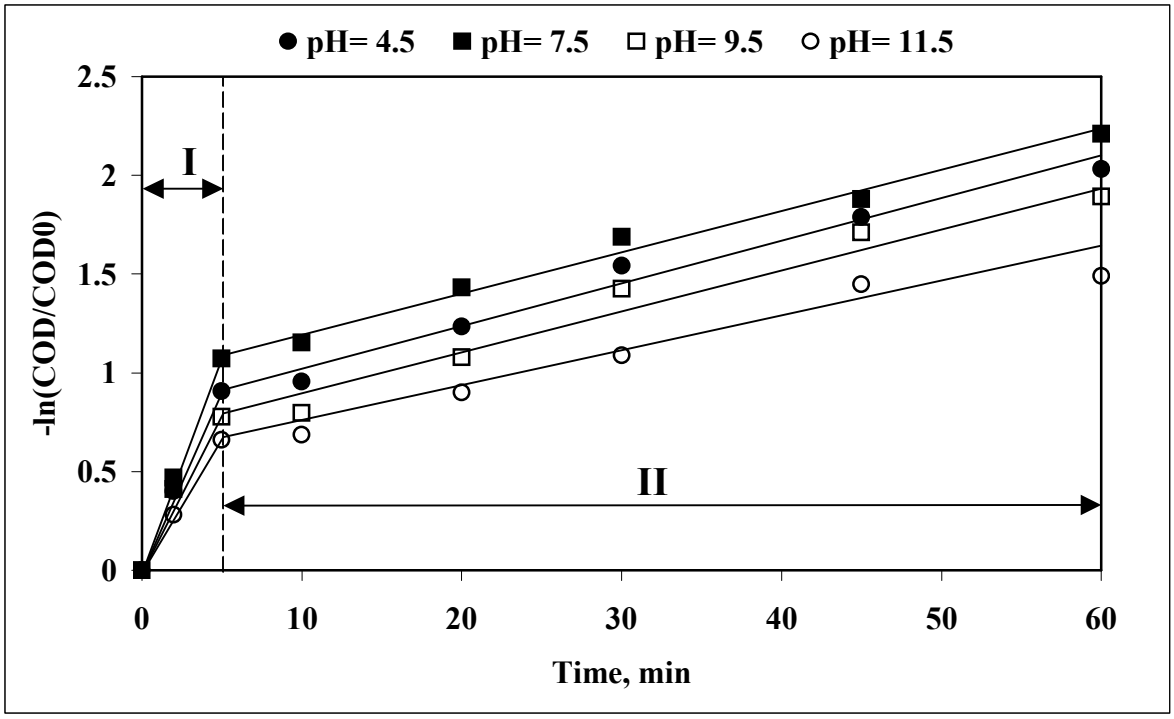

Figure 4.60. First order kinetic model fit of the COD removal data for the ozonation of biotreated textile effluent at varying pH; I: first phase oxidation, II: second phase oxidation

Table 4.17. presents the rate coefficients for the COD removal during ozonation of biotreated textile effluent at varying pH.

Table 4.17. First order COD removal rate coefficients for the ozonation of biotreated textile effluent

	k_{COD}, min^{-1}	
pH	Phase I	Phase II
4.5	0.18	0.0214
7.5	0.21	0.0202
9.5	0.15	0.0222
11.5	0.13	0.0170

From the COD removal rates presented in Table 4.4.1, it is apparent that an optimum pH of 7.5 for which the fastest COD removal was obtained. COD removal rates

decreased with increasing ozonation pH. This observation can be simply explained on the basis of ozone chemistry in water. There was again strong evidence that oxidation of textile wastewater relies on two cross-mechanisms of ozone chemistry in water; namely that ozone decomposition to free radicals and hence high pH is required for efficient COD removal, but, on the other hand, a strongly alkaline pH in turn amplifies the inhibiting effect of bicarbonate/carbonate ions that are known as one of the strongest inorganic $OH^{\bullet}$ scavengers;

$$HCO_3^- + HO^{\bullet} \longrightarrow HCO_3^{\bullet} + OH^- \qquad k = 1.5 \times 10^7\ 1/M.s \qquad (4.2)$$

$$CO_3^{2-} + OH^{\bullet} \longrightarrow CO_3^{\bullet -} + OH^- \qquad k = 4.2 \times 10^8\ 1/M.s \qquad (4.3)$$

4.4.1.3. Ozone Absorption Efficiency. The ozone absorption efficiency ($O_{3A,}$ in percent) is an important parameter to estimate the ozone requirements of a certain pollutant COD. Figure 4.61. presents the relationship between O_{3A}, k_d (first order color abatement rate coefficient) and COD removal efficiencies obtained after 1 h ozonation of biotreated textile effluent at varying pH. The figure reveals that percent O_{3A} values slightly increased with increasing pH, however they remained rather low for all studied pH values indicating that ozone was either not utilized effectively or the ozone demand of the effluent was rather low. In other words, the ozone demand was satisfied at low ozone doses, i.e. within the first min of ozonation during color removal, and further extension of the treatment time was not necessary. The increase in O_{3A} is attributable to the enhanced ozone decomposition at elevated pH, that at the same time enhances ozone transfer from gas to liquid phase, thus accelerating ozone absorption rates. From the figure it is also evident that parallel to ozone absorption k_d values increased slightly with increasing pH up to 7.5, beyond which pH k_d decreased drastically, that once again can be explained by the coinciding positive effect of accelerated ozone decomposition into free radicals at elevated pH, and the inhibitory effect of carbonate alkalinity becoming dominant at pH > 7.5-8.0, thereby acting as free radical scavengers. COD removal efficiencies at varying pH were appreciably high and again close to each other. However, still an optimum value was observed; 89%, 86 %, 85 % and 77 % removals in COD were achieved after 1 h ozonation at pH = 4.5, 7.5, 9.5, and 11.5, respectively (Figure 4.61.).

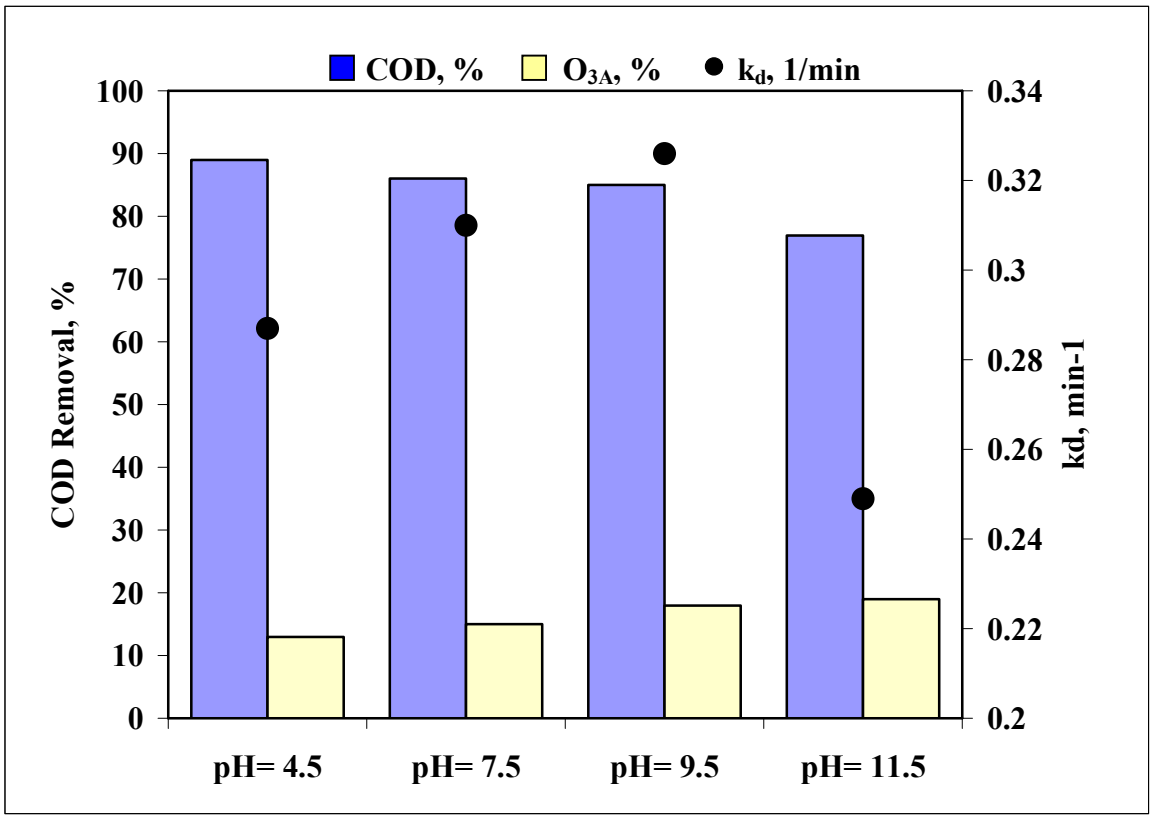

Figure 4.61. The impact of pH on the rate of ozone decomposition, ozone absorption efficiency and fractions of COD removal (ozone dose = 1440 mg/h)

As can be deduced from studies conducted by Staehelin and Hoigné (1985), ozone decomposition is significantly accelerated at elevated pH values and seriously retarded in the presence of bicarbonate/carbonate alkalinity. Accordingly, it is not surprising that under the present reaction conditions an optimum pH above which the inhibitory effect of high carbonate alkalinity of the wastewater became more pronounced (i.e. at pH = 9.5). After 1 h ozonation 216 mg/L O_3 was absorbed and 290 mg/L COD was removed. Consequently, the optimum ozonation pH was selected as 7.5 in order to eliminate pH adjustment and hence salinity increase of the effluent.

4.4.2. Ozonation of Biologically and Electrochemically Pretreated Effluent

In the forthcoming sections, the effects of ozonation on biologically and electrochemically pre-treated effluent will be discussed. In this way, the use of ozone as the final stage in advanced post-treatment of secondary treated textile effluents will be examined. Batch electrolysis were conducted at 20 A involved iron, aluminum, and iron/aluminum electrodes. Performance will be presented in terms of absorbance spectra and COD abatement rates as a function of ozonation time. Electrolysis of biotreated effluents was performed at the optimum pH determined in previous sections and the effluents of electrolysis were ozonated without pH adjustment to avoid further increase in salinity.

4.4.2.1. Color Removal.

- iron electrode

The initial pH of ozonation was 9.5 for the wastewater being electrochemically pre-treated at pH = 7.5, and 10.10 for the wastewater being electrochemically pre-treated at pH = 9.5. Figure 4.62. presents changes in absorption during ozonation of simply biotreated textile wastewater at pH = 7.5, whereas Figures 4.63. and 4.64. show changes in absorption during ozonation of biotreated + electrochemically treated (applied current = 20 A) wastewater using iron electrodes at pH = 7.5 and 9.5, respectively.

Upon inspection of Figures 4.63. and 4.64. it can be concluded that color removal during ozonation of effluent being electrochemically pre-treated at pH = 9.5 proceeded faster than at pH = 7.5. This is mainly due to the enhanced ozone decomposition to free radicals at elevated pH. When biotreated effluent was directly ozonated color removal appeared to be independent from effluent pH because of the high alkalinity in the effluent. However, the alkalinity of biotreated effluent was reduced from 450 mg/L to below 50 mg/L via electrolysis and free radical reactions became more pronounced during ozonation. Figure 4.4.6. also shows that in the first 20 min of ozonation, a slight increase in absorbance occurred possibly due to the formation of colored oxidation intermediated

formed with iron. After extended ozonation, the color of the reaction solution disappeared indicating the destructive removal of colored intermediates.

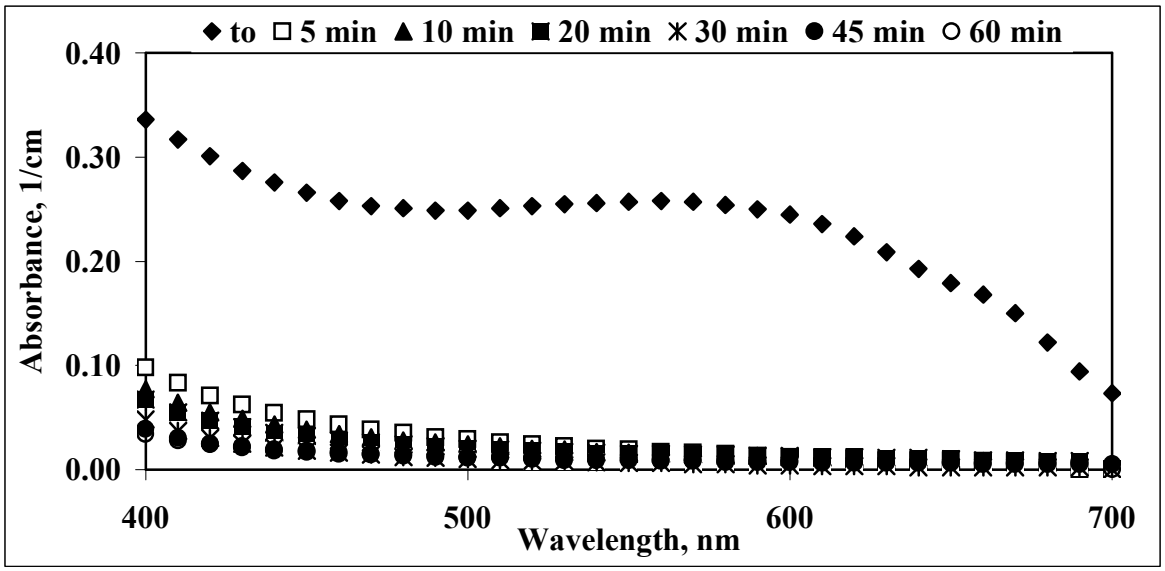

Figure 4.62. Variations in the UV-Visible absorption of biotreated effluent during 1 h ozonation at pH = 7.5

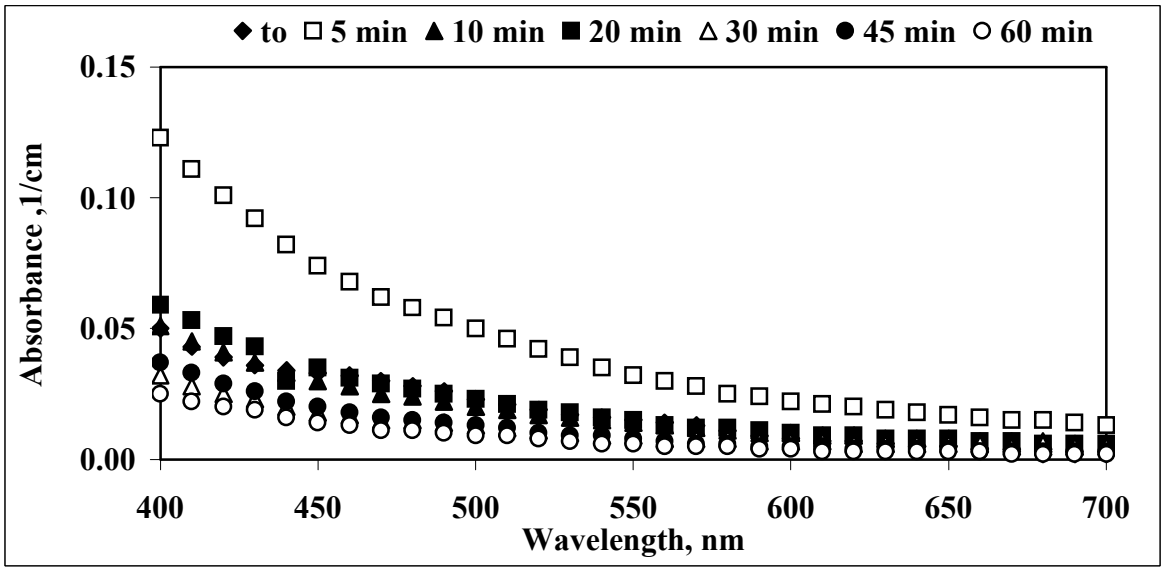

Figure 4.63. Variations in the UV-visible absorption of biotreated + electrotreated ffluent during 1 h ozonation (electrolysis: pH = 7.5; electrode: iron; current = 20 A; reaction time = 15 min, ozonation: pH = 9.5)

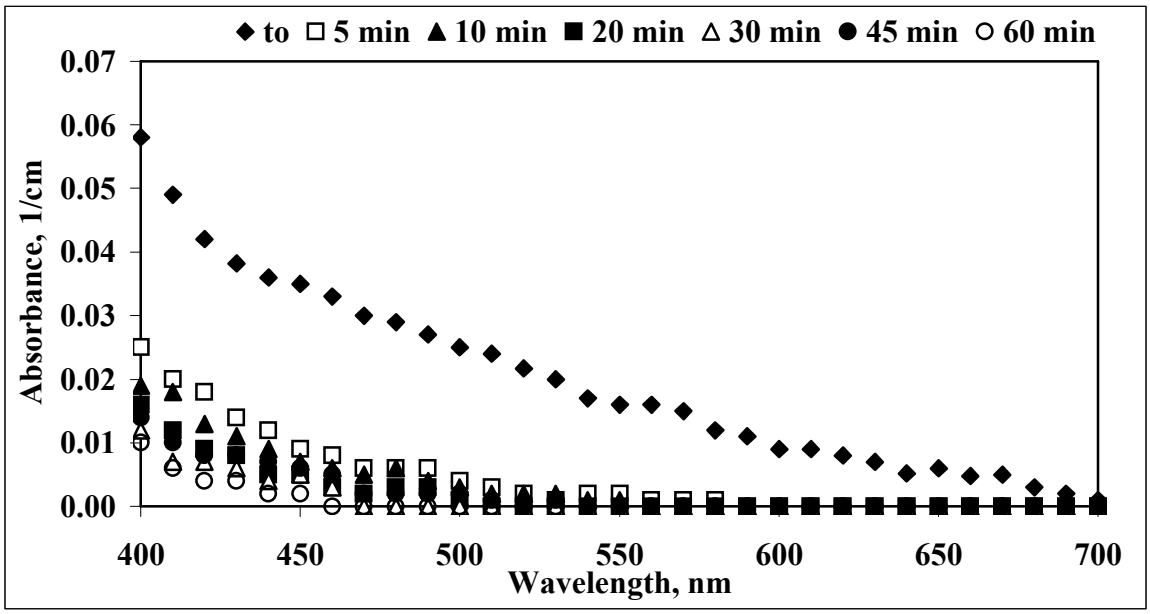

Figure 4.64. Variations in the UV-visible absorption of biotreated + electrotreated effluent during 1 h ozonation (electrolysis: pH = 9.5; electrode: iron; current = 20 A; reaction time = 15 min, ozonation: pH = 10.10)

- aluminum electrode

Figures 4.65. and 4.66. display the results obtained for ozonation of biotreated textile effluent being electrochemically treated at pH = 4.5 and pH = 7.5, respectively. The pH of the effluents after electrochemical treatment at pH 4.5 and 7.5 were 7.0 and 9.0, respectively, i.e. the initial pH of the proceeding ozonation experiments.

A different behavior was observed when the biotreated textile effluent was exposed to ozonation after elecrochemical treatment at pH = 4.5 and 7.5 using aluminum electrode at 20 A. Unlike iron electrode, higher initial pH did not have a positive effect on absorbance abatement during ozonation. During batch electrolysis tests conducted with biotreated effluent, it was determined that COD removal efficiency was lower at pH = 7.5 (48%) than that of pH = 4.5 (62%) when aluminum electrode was used. Therefore, higher organic content of the effluent (other than color causing compounds), reduced the efficiency of color removal during ozonation when electrolysis was conducted at pH = 7.5 with aluminum electrode.

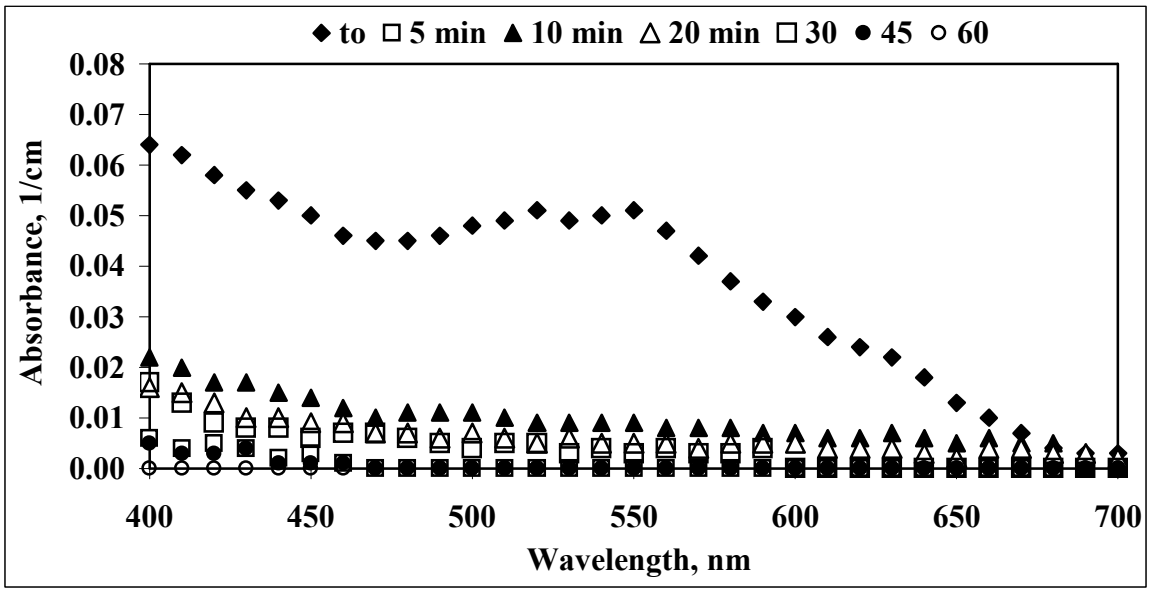

Figure 4.65. Variations in the UV-visible absorption of biotreated + electrotreated effluent during 1 h ozonation (electrolysis: pH = 4.5; electrode: aluminum; current = 20 A; reaction time = 15 min, ozonation: pH = 7.0)

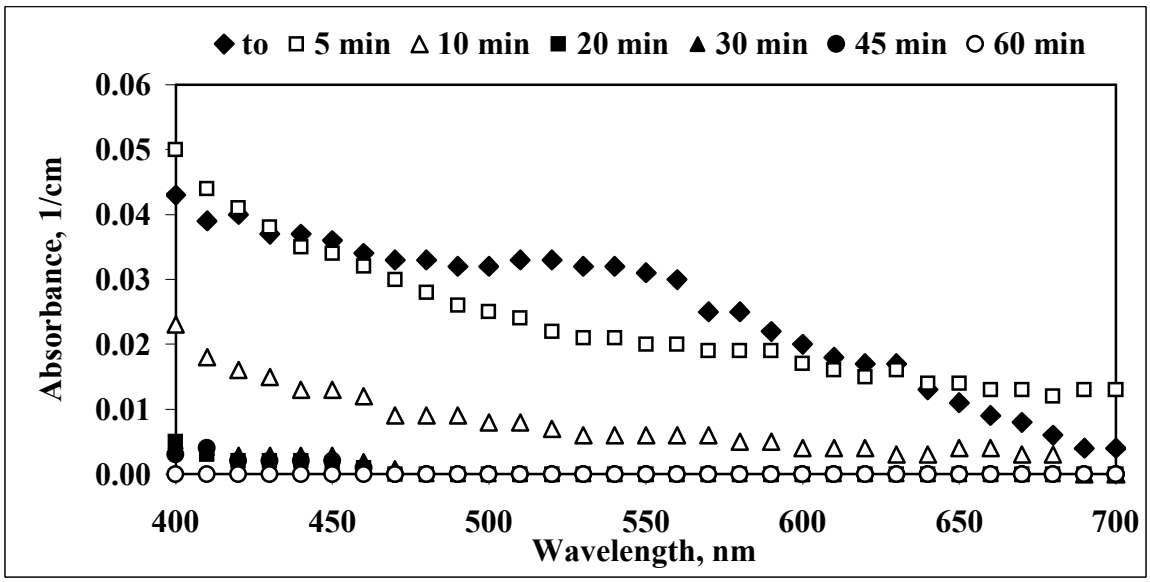

Figure 4.66. Variations in the UV-visible absorption of biotreated + electrotreated effluent during 1 h ozonation (electrolysis: pH = 7.5; electrode: aluminum; current = 20 A; reaction time = 15 min, ozonation: pH = 9.0)

• iron/aluminum electrode

In the final step of the present study, biotreated textile effluent being electrochemically pre-treated at 20 A using an iron – aluminum electrode combination, was subjected to 1 h ozonation at initial pH = 9.0 (i.e. the final pH of Fe-Al electrolysis at pH = 7.5) and pH = 9.5 (the final pH of Fe-Al electrolysis at pH = 9.5). Figures 4.67. and 4.68. present changes in the absorption during ozonation of biotreated textile effluent at the final pH of electrochemical treatment using Fe-Al electrode at 20 A for 15 min. As can be seen from the Figures, a slight increase observed in absorbance at the beginning of ozonation as happened previously, however, complete decolorization occurred in both cases.

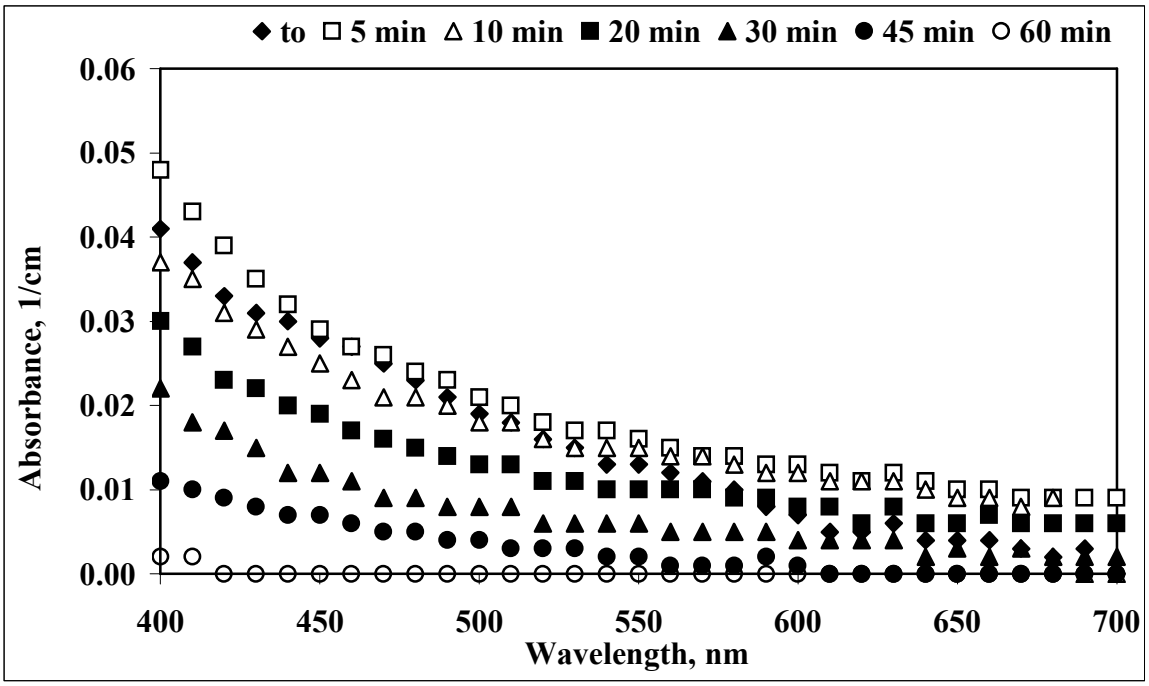

Figure 4.67. Variations in the UV-visible absorption of biotreated + electrotreated effluent during 1 h ozonation (electrolysis: pH = 7.5; electrode: iron/aluminum; current = 20 A; reaction time = 15 min, ozonation: pH = 9.0)

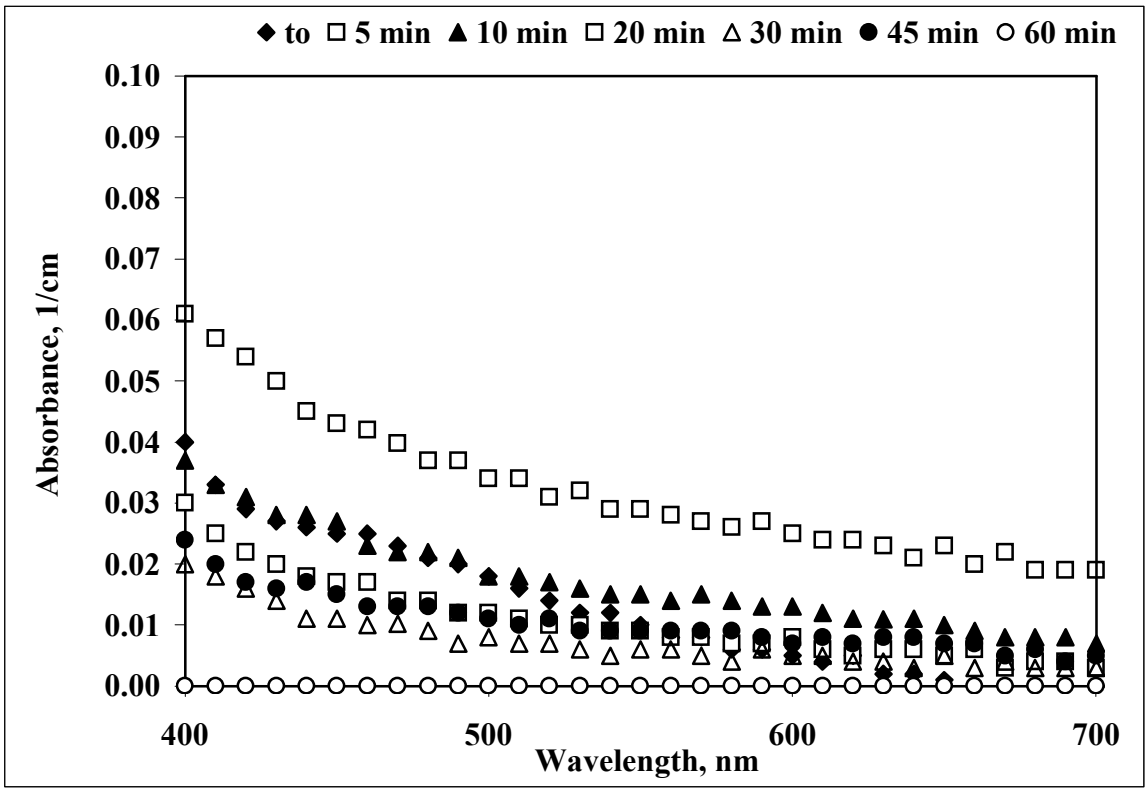

Figure 4.68. Variations in the UV-visible absorption of biotreated + electrotreated effluent during 1 h ozonation (electrolysis: pH = 9.5; electrode: iron/aluminum; current = 20 A; reaction time = 15 min, ozonation: pH = 9.5)

- comparison of color removal rates

In order to evaluate the effect of electrolysis performance using different electrode materials on color removal via ozonation, the absorbance at 20 min (the time at which reduction in absorbance occurred in all cases) for each ozonation experiments were plotted in Figure 4.69. As can be concluded in Figure 4.69, an apparent improvement in color removal via ozonation occurred when biotreated effluent was first subjected to electrolysis using aluminum electrodes. Almost complete decolorization was achieved all electrolysis + ozonation experiments, and final color in the effluents were mostly suitable for reuse in dyeing processes except ozonation alone.

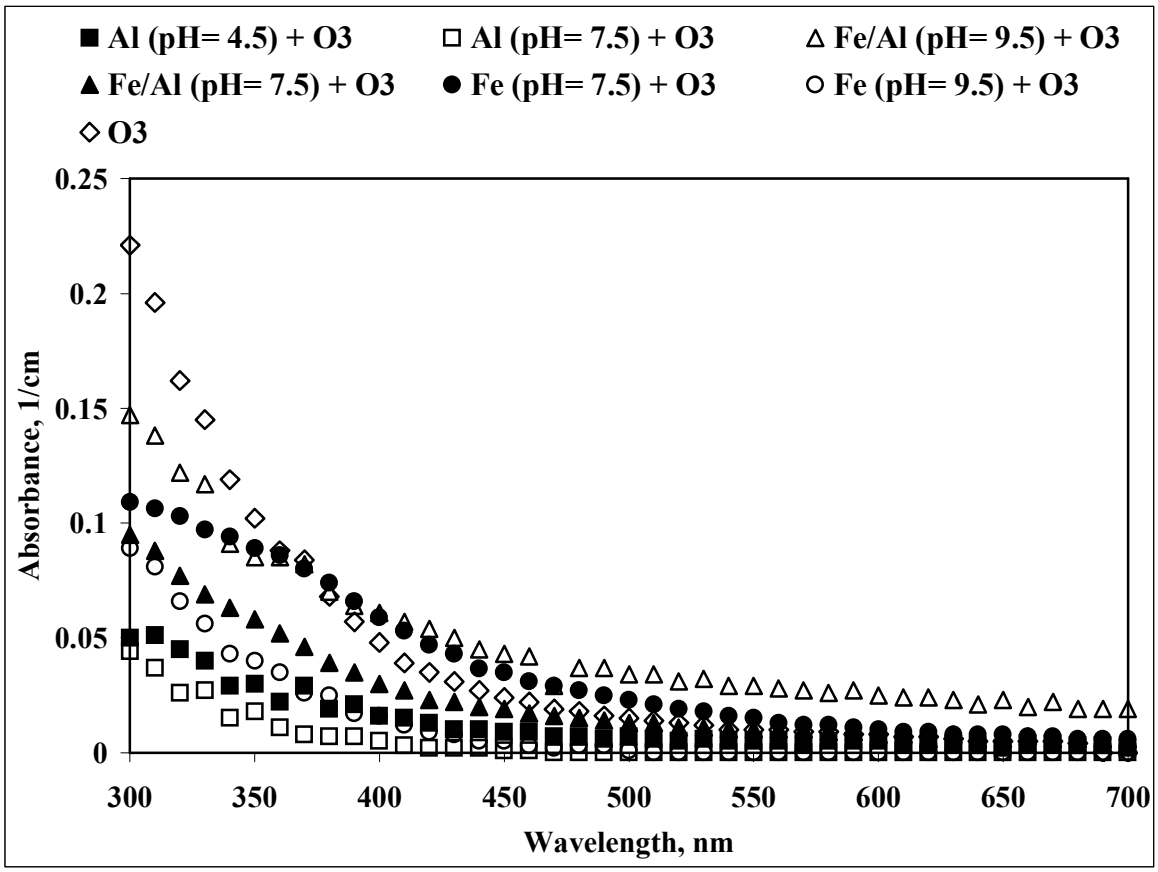

Figure 4.69. Impact of electrolysis conditions on color removal by ozone

4.4.2.2. Comparison of COD Removal Efficiencies. In the present experimental section, COD removal rates are compared for 1 h ozonation of biotreated textile wastewater with that being previously subjected to electrochemical treatment at different pH using varying electrode materials. In all cases, the applied current and duration of electrolysis were fixed as 20 A and 15 min, respectively. Figure 4.70. elucidates changes in COD abatement rates during ozonation of textile effluent being electrochemically pre-treated with different elecotrodes and at varying pH.

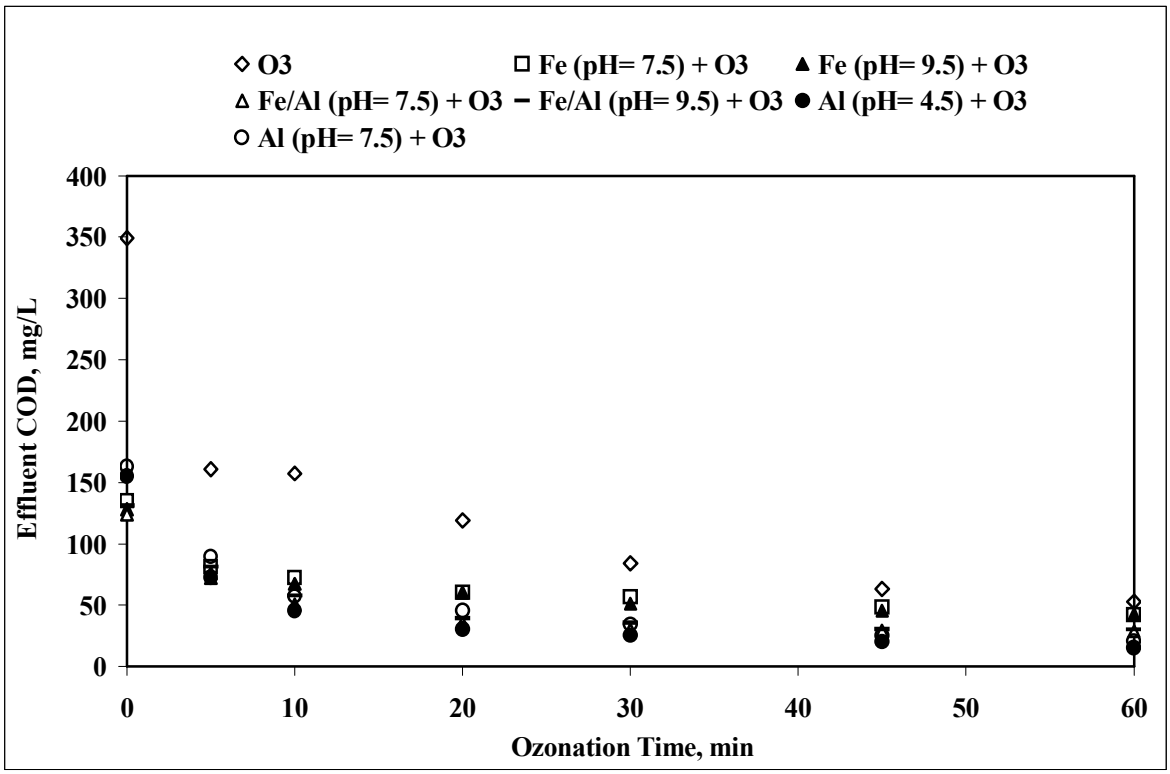

Figure 4.70. Impacts of electrochemical pretreatment conditions (electrode material and pH) on the rate of COD removal during 1 h ozonation of the pretreated textile effluent

From Figure 4.70, it is clear that electrochemical pre-treatment further improved COD removal rates during ozonation considerably. Highest improvement in COD removal efficiency was achieved via electrolysis using aluminum electrode. Figure 4.71. summarizes COD removal efficiencies achieved after ozonation for 20 min, i.e. the time at which complete decolorization took place. As clear from Figure 4.71, 66% COD removal was obtained via ozonation of biotreated textile effluent at pH = 7.5, whereas the COD removal increased to 80% and 72% when biotreated effluent was first subjected to electrolysis with aluminum at pH = 4.5 and 7.5, respectively. In addition, the final COD of the biotreated + ozonated effluent was 119 mg/L, while the final COD was reduced to 30 mg/L via electrolysis with aluminum + ozonation.

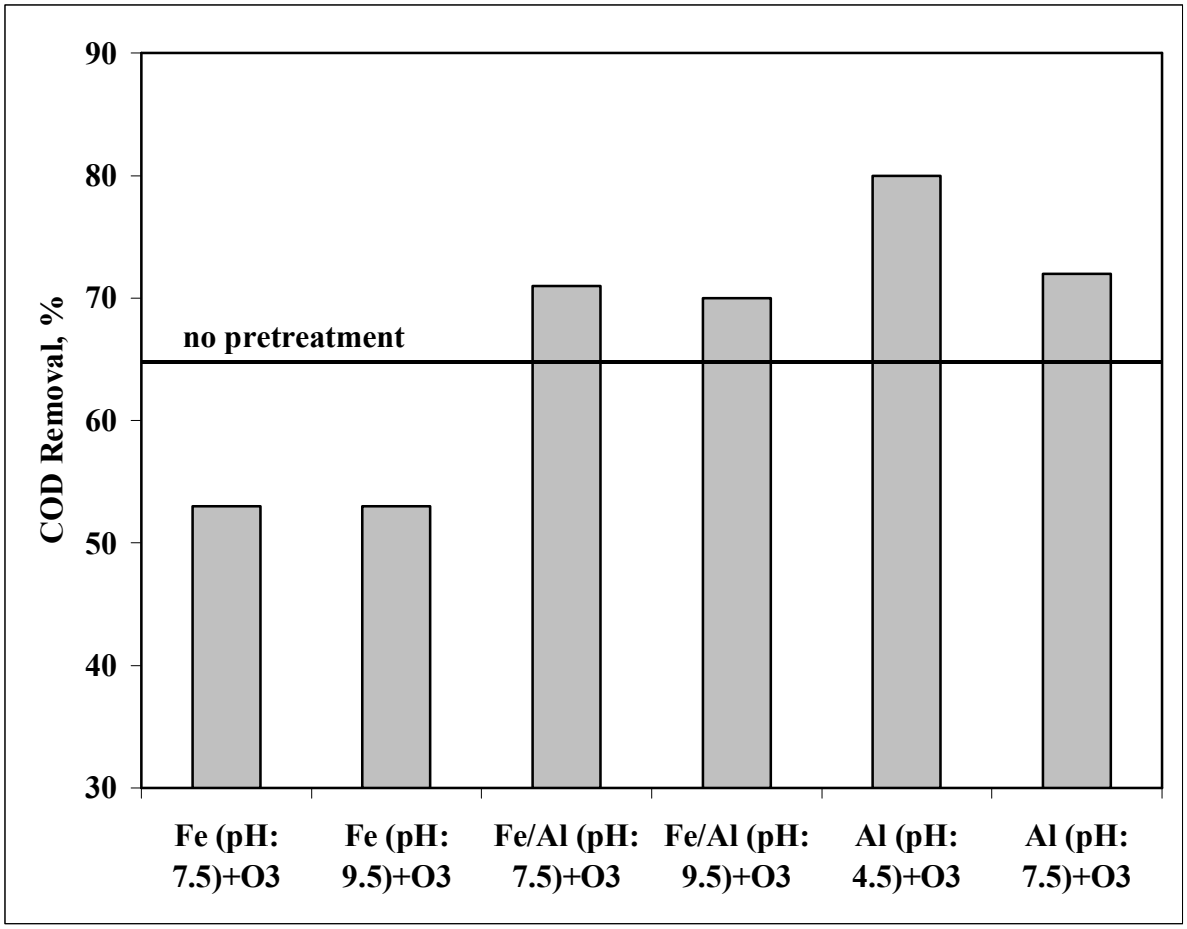

Figure 4.71. Comparison of COD removal in ozonated (20 min) effluents exposed to biotreatment and electrochemical pretreatment at various pH and electrode materials

4.5. Sonolysis Experiments

4.5.1. Rate of Color Decay

Decolorization profiles during 1 h sonication of the tested dyebaths is presented in Figure 4.72. It was found that after 1 h irradiation, the rate and degree of absorption abatement (decoloration) was highest for DB1 (68%), followed by DB2 (54%) and DB3 (49%). The analysis of the obtained absorbance - time plots via non-linear regression showed that color decay followed first-order kinetics for all tested dyebaths. The first-order color decay rate constants were found as 0.062 1/min, 0.038 1/min and 0.028 1/min for DB1, DB2 and DB3, respectively. It should be noted here that color removal was not

complete after 1 h sonication and the absorbance values ultimately decayed to a non-zero plateau ($A_{final} > 0.0$).

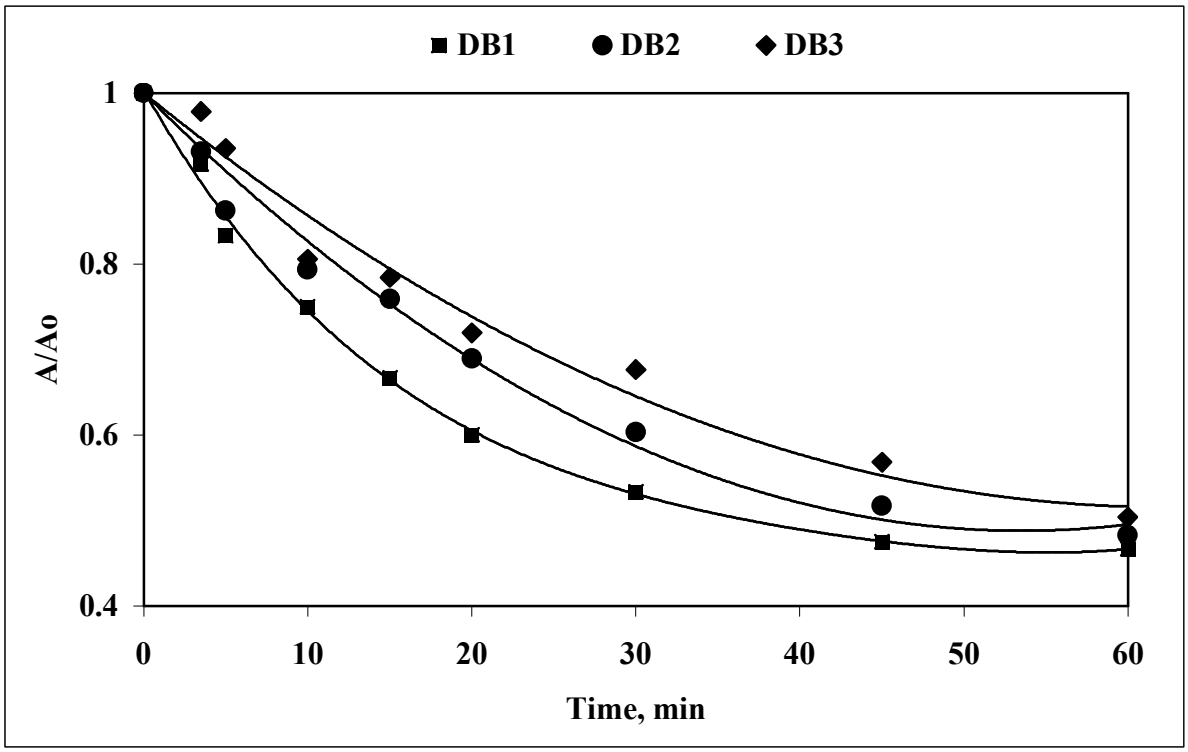

Figure 4.72. Comparative profiles of dyebath decolorization as a function of irradiation time (sonication at 300 kHz; pH = 4.5)

The difference in color abatement rates observed for DB2 and DB3, despite the fact that both dyebaths contained the same type and amount of dye assisting chemicals, was attributable to the differences in structure and molar concentrations of their dye content. For instance, the hydroxyl group in the α-position of the azo dye in DB2 makes the structure of this dye more susceptible towards the attack of secondary radicals such as $HO_2^{\bullet}/O_2^{\bullet-}$. In addition, the initial dye concentration in DB3 (0.065 mM) was higher than in DB2 (0.059 mM). Despite the facts that DB1 contains:

- A dyestuff bearing a benzoquinone type dye chromophore, for which $^{\bullet}OH$ has a lower reactivity than for azo chromophores ($k_{OH,azo} = 2.0 \cdot 10^{10}$ 1/M.s; $k_{OH,benzoq} = 1.2 \cdot 10^{9}$ 1/M.s),

- Larger quantities of carbonates and chlorides (both of which are strong $^{\bullet}OH$ scavengers),

color abatement in DB1 proceeded significantly faster than in the other two dyebaths, speculatively due to its lower dyestuff and different auxiliary chemical content.

4.5.2. Effect of H_2O_2 Addition

The rate of color removal was appreciably enhanced in the presence of 7 mM H_2O_2 due to formation of the free radicals $HO_2^{\bullet}$ according to equation 4.4, respectively. The accelerating effect of H_2O_2 on color abatement rates is presented in Figure 4.73, 4.74. and 4.75. for DB1, DB2 and DB3, respectively.

$$^{\bullet}OH + H_2O_2 \longrightarrow H_2O + HO_2^{\bullet} \qquad (4.4.)$$

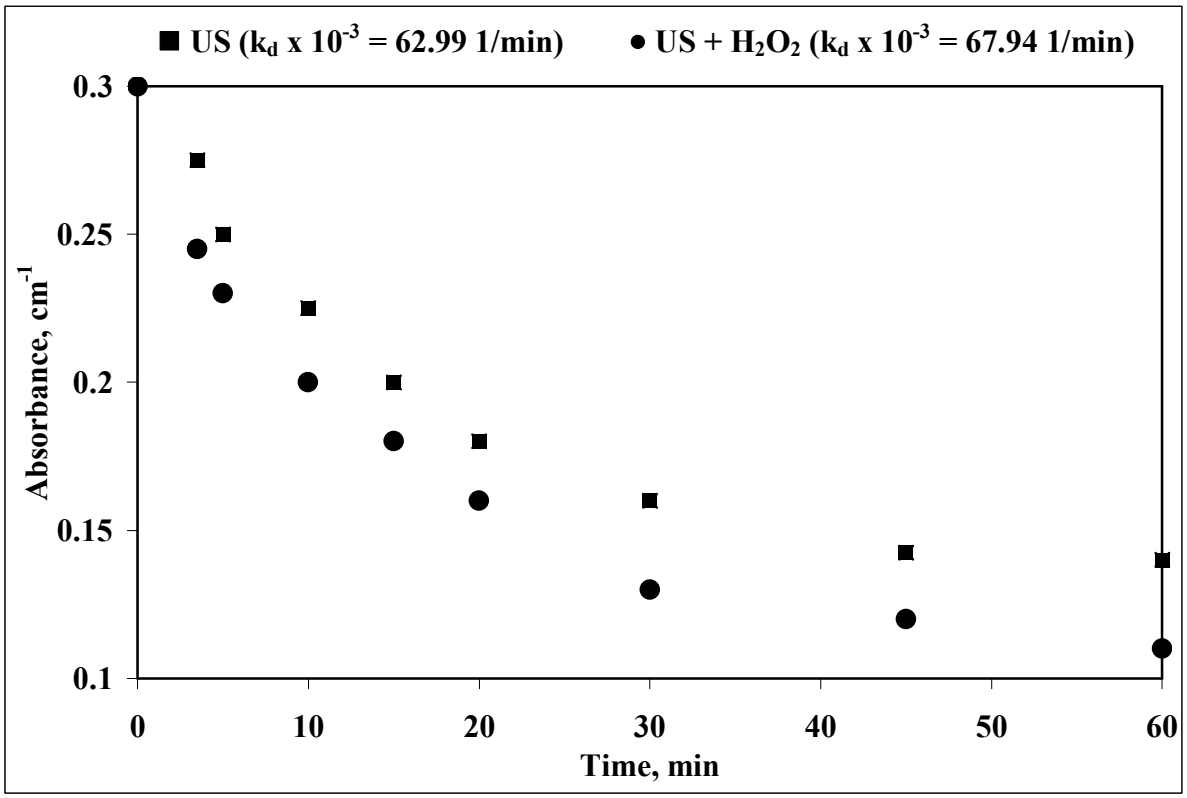

Figure 4.73. Color decay for sonication of DB1 at pH = 4.5 with and without H_2O_2 (7.0 mM)

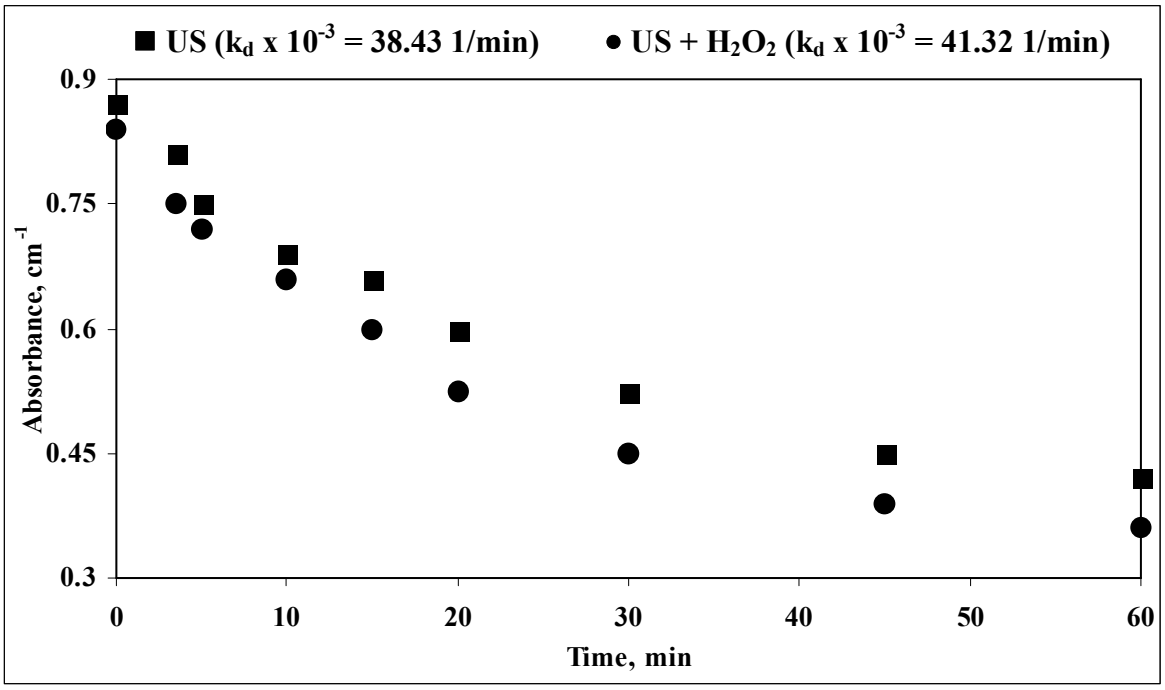

Figure 4.74. Color decay for sonication of DB2 at pH = 4.5 with and without H_2O_2 (7.0 mM)

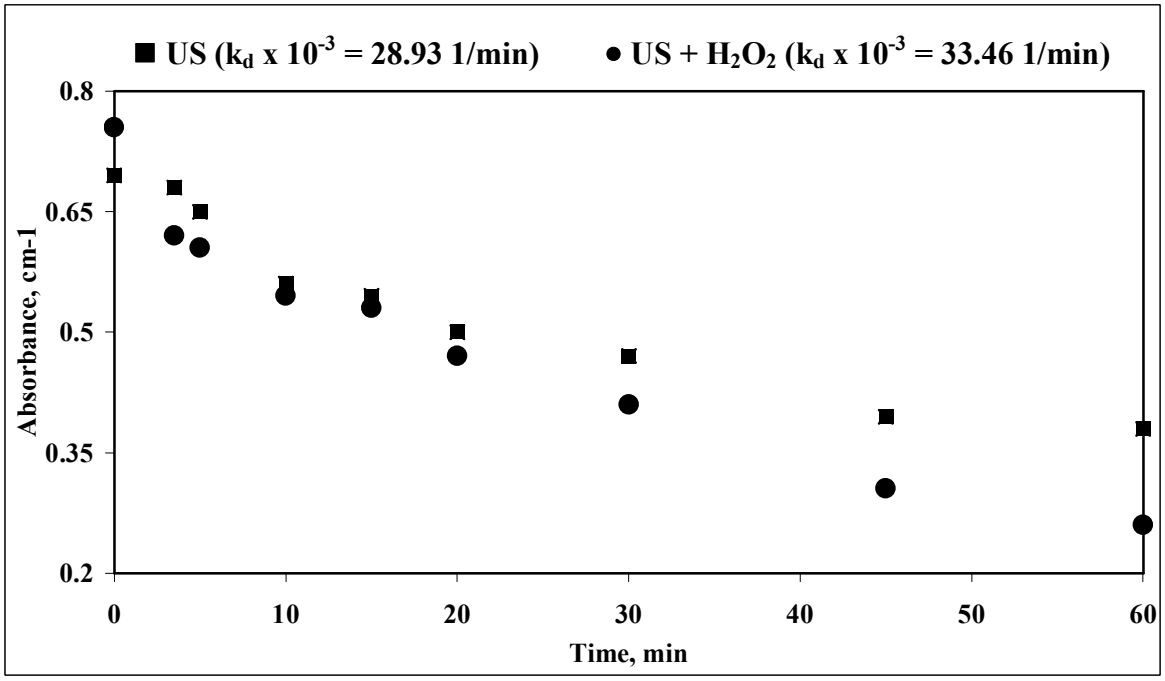

Figure 4.75. Color decay for sonication of DB3 at pH = 4.5 with and without H_2O_2 (7.0 mM)

Figure 4.76. and 4.77. illustrate overall percent color and COD removal efficiencies, respectively, obtained for the three dyebaths after 1 h sonication with and without H_2O_2 addition. From the figure it is apparent that COD removal is much more positively affected than color abatement upon H_2O_2 addition. This may be attributable to the

- higher reactivity of free radicals with the dye intermediates and/or dye auxiliaries,
- possibility of direct oxidation of some dye intermediates and auxiliaries with H_2O_2, and
- diffusion of some oxidation intermediates into the gaseous bubble phase undergoing thermolytic decomposition (pyrolysis).

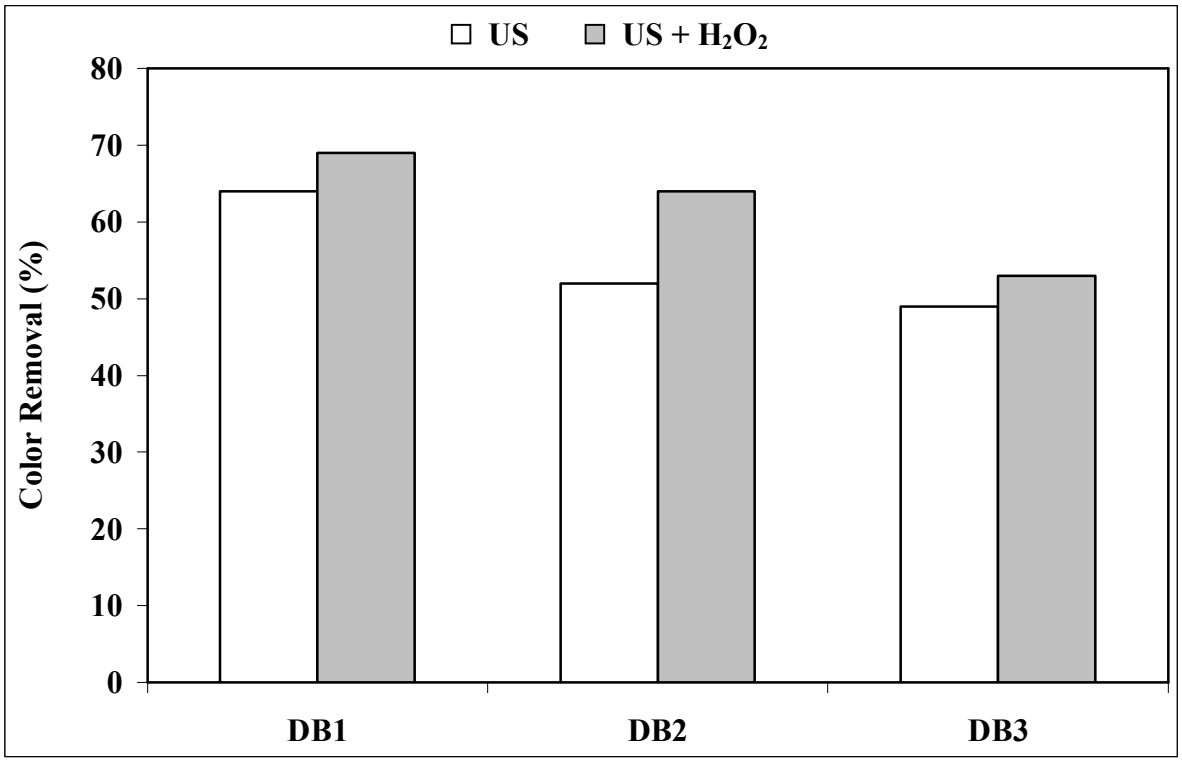

Figure 4.76. Percent color removal obtained after treatment of DB1, DB2 and DB3 with US and US + H_2O_2 (irradiation at 300 kHz; initial H_2O_2 dose = 7 mM; irradiation time = 1 h at pH = 4.5)

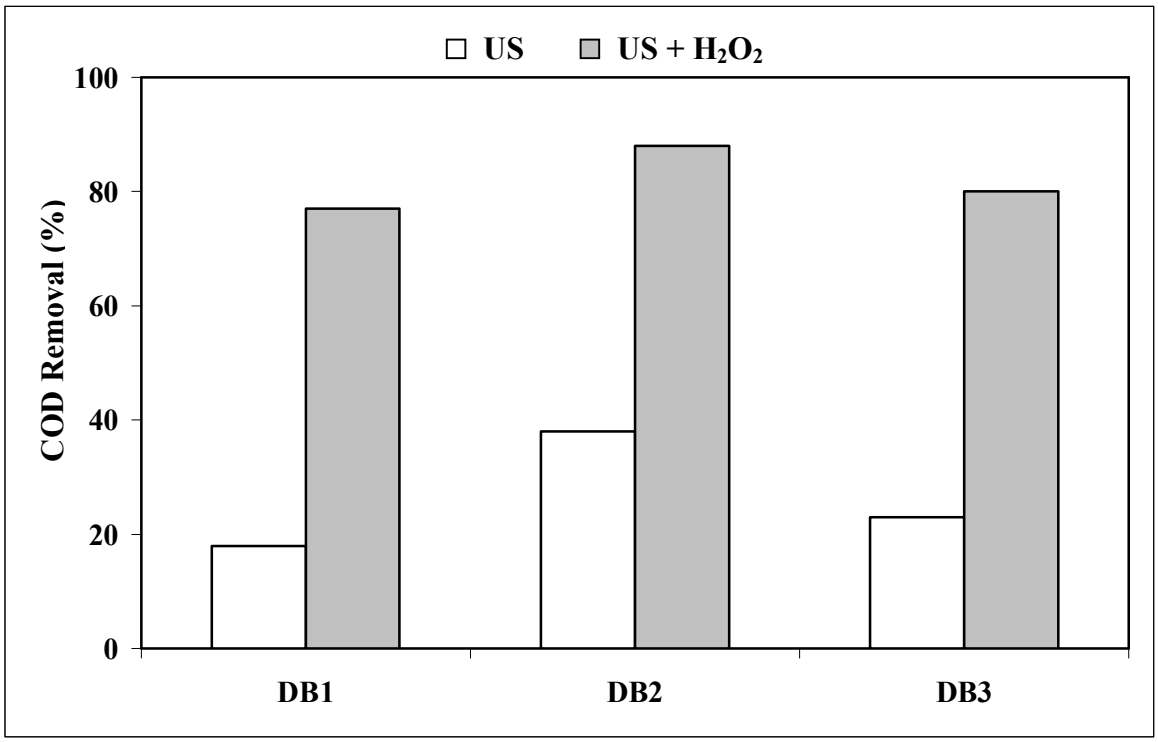

Figure 4.77. Percent COD removal obtained after treatment of DB1, DB2 and DB3 with US and US + H_2O_2 (irradiation at 300 kHz; initial H_2O_2 dose = 7 mM; irradiation time = 1 h at pH = 4.5)

Table 4.18. summarizes the color decay coefficients (k_d, in 1/min) determined for the sonication of the dyebaths in the absence and presence of H_2O_2. The table reveals that color removal was not appreciably affected when H_2O_2 was added to the system.

Table 4.18. Color decay coefficients for sonication (US) and sonication in the presence of H_2O_2 (US + H_2O_2) for DB1, DB2 and DB3 at an initial pH = 4.5

Dyebath Nr.	$k \cdot 10^{-3}$ (1/min)	R^2	P* (1/cm)
DB1			
US	63	0.99	0.46
US + H_2O_2	68	1.00	0.11
DB2			
US	38	0.99	0.44
US + H_2O_2	41	0.99	0.38
DB3			
US	29	1.00	0.41
US + H_2O_2	34	0.99	0.32

* P, indicates the ultimate plateau values reached after 1 h sonication.

4.6. Cost Analysis

4.6.1. Cost of Electrolysis

The operating costs for electrolysis of biotreated dyehouse effluent were evaluated for two systems:

a. Batch electrolysis: The cost of batch electrolysis was calculated for varying conditions such as applied current and electrode material to present the effect of operating conditions on the cost of electrochemical treatment.

b. Continuous Electrochemical Treatment (CET): The cost of CET was calculated for iron electrode at 20 A current.

The operating cost arises mainly from the electrical energy requirement and the electrode material consumption. Unit costs for electrode materials and electrical energy were obtained from manufacturing companies and listed below (Pisa Tekstil, 2005):

Electrical Energy: 0.088 USD/kWh (4.5)
Iron Electrode: 0.32 USD/kg (4.6)
Aluminum Electrode: 1.95 USD/kg (4.7)

4.6.1.1. Electrical Energy Consumption.

- batch electrolysis

The electricity consumption for 5 liters of wastewater was calculated at varying currents applied and for different electrode materials for fixed reaction time of 15 minutes. Table 4.19. shows the electricity consumption per unit volume of treated effluent at varying currents and electrode materials. In Table 4.19, the electrical energy consumption is calculated as follows (Özgövde, 1998):

(Energy Consumed/Wastewater Treated)= (Applied Current, A x Voltage, V x 1h)
/(Volume of wastewater treated, L/h) (4.8)

Ex. Electrical energy consumed on iron electrode for 10 A and 5 V is:

(10 A x 5 V x 1h)/(20 L/h x 1h) = 2.5 Wh/L, and 2.5 kWh/m^3 (4.9)

The cost of electrical energy consumption is:

2.5 kWh/m^3 x 0.088 USD/kWh = 0.22 USD/m^3 (4.10)

Table 4.19. Electricity consumption per unit volume of treated effluent

	Iron Electrode			Aluminum Electrode		
Current Applied, A	10	20	30	10	20	30
Voltage, V	5	7	13	4	6	11
Electrical Energy Consumption, Wh/L	2.5	7	19.5	2	6	16.5
Electrical Energy Consumption, USD/m^3	0.22	0.62	1.73	0.18	0.53	1.46

- CET

The cost of CET of biotreated effluent was calculated for iron electrode at 20 A for 125 L/h effluent flowrate. Electrical energy consumed on iron electrode for 20 A and 11 V is:

(20 A x 11 V x 1h)/(125 L/h x 1h) = 1.76 Wh/L, and 1.76 kWh/m^3 (4.11)

The cost of electrical energy consumption is:

$$1.76\ kWh/m^3 \times 0.088\ USD/kWh = 0.15\ USD/m^3 \quad (4.12)$$

4.6.1.2. Electrode Material Consumption.

- batch electrolysis

Iron and/or Aluminum electrodes were used as sacrificial anodes, therefore they continuously dissolved during electrolysis. Table 4.20. summarizes the amount of electrode material consumed for the treatment of 1 m^3 of wastewater treated at varying current. In Table 4.20, the quantity of charge passes to 1 liter of wastewater can be calculated as:

$$(10\ A \times 1h \times 3600sec/h)/(20L/h \times 1h) = 1800\ Q/l \quad (4.13)$$

Therefore, weight of iron dissolved as 1800 Q passes is calculated as:

$$W = (E \times Q)/F = (56/3\ g/eq \times 1800\ Q)/96500\ Faraday \quad (4.14)$$

$$\text{Iron consumption} = 0.35\ g\ Fe/l = 350\ g\ Fe/m^3\ ww \quad (4.15)$$

Table 4.20. Electrode material consumption during electrochemical treatment

	Iron Electrode			Aluminum Electrode		
Current Applied, A	10	20	30	10	20	30
Electrode Consumption, g/m^3	350	696	1044	168	336	504
Electrode Consumption, USD/m^3	0.11	0.22	0.33	0.33	0.65	0.98

• CET

The consumption of iron electrode for continuous electrochemical treatment of 125 L/h of effluent at 20 A current can be calculated as:

(20 A x 1h x 3600 sec/h)/(125L/h x 1h) = 576 Q/L (4.16)

Therefore, weight of iron dissolved as 575 Q passes is calculated as:

W = (E x Q)/F = (56/3 g/eq x 576 Q)/96500 Faraday (4.17)

Iron consumption = 0.11 g Fe/L = 111 g Fe/m^3 ww (4.18)

The cost of electrode consumption:

(111 g Fe/m^3 ww x 0,32 USD/kg)/1000 g/kg= 0,112 USD/m^3 (4.19)

4.6.1.3. Total Cost of Electrolysis.

• batch electrolysis

Table 4.21. shows electrical energy, electrode material consumption and total cost for electrochemical treatment at varying currents and electrode materials for batch electrolysis of biotreated dyehouse effluent.

Table 4.21. Total cost of electrochemical treatment of biotreated wastewater

	Iron Electrode			Aluminum Electrode		
Current Applied, A	10	20	30	10	20	30
Electrical Energy Consumption, USD/m^3	0.22	0.62	1.73	0.18	0.53	1.46
Electrode Consumption, USD/m^3	0.11	0.22	0.33	0.33	0.65	0.98
Total Cost, USD/m^3	0.33	0.84	2.06	0.51	1.18	2.44

- CET

The cost of CET for biotreated textile effluent consists of electrical energy and electrode material consumption and calculated as:

(0.15 USD/m^3+0.112 USD/m^3)= 0.262 USD/m^3 (4.20)

4.6.2. Cost of Ozonation

For calculation of operation costs of ozonation it was assumed that for 1 kg ozone production 15 kWh electrical energy is necessary (CCOT, 1995). Based on this information, operation costs were calculated for the following cases:

CASE I: Ozonation of biotreated wastewater at pH = 7.5 for 5 min where major removal of the organic content occurred (65% COD removal, COD after 5 min ozonation = 110 mg/L; accompanied with practically complete decolorization).

CASE II: Ozonation of biotreated wastewater at pH = 7.5 for 60 min to reduce the COD of the effluent below the recommended textile process water reuse standards (COD after 60 min ozonation = 50 mg/L; accompanied with practically complete decolorization)

CASE III: Ozonation (pH = 7.5, 5 min, applied ozone = 120 mg) of biologically + electrochemically treated (aluminum electrode, pH = 4.5, 15 min, 20 A) effluent to achieve a final COD of 73 mg/L, SS of 4 mg/L and complete decolorization.

CASE IV: Ozonation (pH = 9.5, 5 min, applied ozone = 120 mg) of biologically + electrochemically treated (iron electrode, pH = 7.5, CET at 20 A, 125 L/h) effluent to achieve a final COD of 76 mg/L, SS of 28 mg/L and complete decolorization.

As the applied ozone dose was 1440 mg/Lh, the ozone requirement for each cases can be calculated as:

CASE I, III, IV: (1440 mg/Lh x 5 min x 1h)/60 min = 240 mg/L = 0.12 kg/m^3 (4.21)

CASE II: (1440 mg/Lh x 60 min x 1h)/60 min = 1440 mg/L = 1.44 kg/m^3 (4.22)

Since 15 kWh electrical energy is required for 1 kg of ozone production and the cost of electricity is 0.088 USD/kWh, the cost of ozonation can be calculated as follows:

CASE I, III, IV: (0.12 kg/m^3 x 15 kWh/kg x 0.088 USD/kWh) = 0.16 USD/m^3 (4.23)
CASE II: (1.44 kg/m^3 x 15 kWh/kg x 0.088 USD/kWh) = 1.9 USD/m^3 (4.24)

When the cost of electrolysis is added to the cost of ozonation for Case III and IV, the total cost of treatment becomes:

Case III: 1.18 USD/m^3 + 0.16 USD/m^3= 1.34 USD/m^3 (4.25)

Case IV: 0.26 USD/m^3 + 0.16 USD/m^3= 0.42 USD/m^3 (4.26)

4.6.3. Cost of Sonolysis

The cost of sonolysis for the treatment of simulated dyebath effluents was calculated for 60 min sonolysis (in the presence of H_2O_2) DB1 and DB2. After 60 min

irradiation of 100 ml wastewater samples, COD and color removed at a range of 80 % and 65 %, respectively. As the electrical energy contributes the main portion of the cost, the calculation was made considering electricity cost alone. Since the power requirement of the transducer was 25 W, the electrical energy consumption of the system can be calculated as:

$$(25\ W \times 60\ min \times 1h)/(100\ ml \times 60\ min) = 250\ kWh/m^3 \quad (4.27)$$

the cost of electrical energy consumption is,

$$250\ kWh/m^3 \times 0{,}088\ USD/kWh = 22\ kWh/m^3 \quad (4.28)$$

5. SUMMARY, CONCLUSIONS AND RECOMMENDATIONS

5.1. Summary and Conclusions

As a summary of the research carried out within the scope of this dissertation, the following issues must be pointed out:

1. Sonolysis, electrolysis and ozonation processes were tested and evaluated to assess the use of single or a combination of these for preparing textile dyehouse effluents to reuse.

2. All systems were compared for effluent parameters and cost efficiency.

3. Possible alteration in the existing biological treatment system were investigated (reduced aeration and/or settling) to test the robustness of the systems and to improve cost effectiveness.

The conclusions of the study are:

- batch electrolysis

(i) The optimum electrolysis time was found as 15 min in terms of both COD and SS removal efficiencies during batch electrolysis tests at 20 A current.

(ii) The performance of different electrode systems were considered in terms of color, COD and SS removal efficiencies at different pH. In our case, batch electrolysis tests for biotreated textile effluents showed that highest efficiencies were obtained with iron electrodes at pH= 9.5 (color= 92%, COD= 76%, SS= 97%). However, pH= 7.5 can be proposed as the optimum initial pH instead of 9.5, since it is very important not to increase the dissolved constituents of the highly salin dyehouse effluents for pH adjustment. It should also be pointed out that the removal efficiencies obtained at pH= 7.5 (color= 88%, COD= 68%, SS= 94%) and pH= 9.5 were quite similar to each other.

(iii) Batch electrolysis tests also showed that aluminum electrodes were effective at pH= 4.5, and an increase in pH resulted in dramatic reduction both in terms color and COD removal. For instance, color removal was reduced from 71% to 54% and COD from 62% to 48% upon an increase in pH to 7.5. In general, iron electrodes seemed to be a better alternative for both color and COD removal.

The optimum initial pH for the electrolysis of biotreated effluent using iron/aluminum electrodes was obtained as 7.5, and when compared with iron electrodes the efficiencies for color, COD and SS removal were quite similar to each other.

(iv) Sulfate could only be reduced using aluminum (68% at pH=7.5) and iron/aluminum (65% at pH=7.5) electrodes. The highest sulfate reduction was achieved at an initial pH of 7.5 (from 1240 mg/L to 380 mg/L) at 30 A current. No sulfate removal could be achieved using iron electrode alone.

- continuous electrochemical treatment (CET)

(i) The experimental setup for CET suffered from serious settling and sludge separation problems when aluminum electrodes were used mainly due to the small sized floc formation during electrolysis using aluminum as the electrode material. In case of iron electrodes, the system enabled satisfactory floc formation, coagulation, flotation and sludge separation in one single reactor.

(ii) The performance of CET using iron electrodes was evaluated in terms of COD, SS and color removal. Color and COD removal were achieved as 89% and 66%, respectively. At higher effluent flowrates (150 L/h), the system failed to remove COD such that only 48% reduction was observed at pH 7.5.

(iii) CET was also evaluated for the treatment of raw dyehouse effluent as a stand alone option. The system could achieve the requirements of the local sewage treatment works set for pretreatment. Unlike biological treatment CET was able to successfully decolorize the dyehouse effluent, hence outperforming the existing biological treatment system. Overall

removal efficiencies were obtained as 57%, 83%, and 98% for COD, SS and color, respectively at pH 9.5, 20 A current.

- effect of SBR performance on batch and continuous electrolysis

(i) A worst – case scenario was simulated, in which less time for aeration and/or wastewater settling was allowed. No deteroriation of the electrochemical treatment efficiency was observed for both batch and continuous electrolysis, emphasizing the robustness of electrochemical treatment acting as a "buffer" stage between secondary and tertiary treatment.

- ozonation

(i) During the ozonation of biotreated textile effluents, pH-Independent color removal profiles were obtained due to the high alkalinity of effluent (450 mg/L).

(ii) COD and color removal proceeded in two phases. In the first phase of ozonation (5 min), 57% COD was removed via destruction of color causing and other fast reacting compounds present in the effluent. In the second phase, the organic compounds were converted into more difficult to oxidize intermediates and only 30% COD reduction was observed in 55 min of ozonation. The transition from fast-reaction activity (k_{COD}= 0,21 min^{-1} for Phase I) to a slower one (k_{COD}= 0,02 min^{-1} for Phase II) implied a decrease about one order of magnitude in the COD abatement rate.

(iii) Ozone absorption was increased with increasing pH, mainly due to the enhanced ozone decomposition at elevated pH, enhancing ozone transfer from gas to liquid phase.However, ozone absorption remained rather low for all studied pH values indicating that ozone was either not utilized effectively or the ozone demand of the effluent was rather low.

(iv) The rate of color removal increased parallel to ozone absorption with increasing pH up to 7.5. Beyond this pH, k_d decreased drastically, which can be explained by the coinciding positive effect of accelerated ozone decomposition into free radicals at elevated pH, and

the inhibitory effect of carbonate alkalinity becoming dominant at pH > 7.5-8.0, thereby acting as free radical scavengers. COD removal efficiencies at varying pH were appreciably high and again close to each other. However, still an optimum was observed; 89%, 86 %, 85 % and 77 % removals in COD were achieved after 1 h ozonation at pH= 4.5, 7.5, 9.5, and 11.5, respectively.

- electrolysis + ozonation

(i) The highest improvement in color removal via ozonation occurred when biotreated effluent was first subjected to electrolysis using aluminum electrodes. Almost complete decolorization was achieved during all electrolysis + ozonation experiments, and final color in the effluents was mostly suitable for reuse in dyeing processes except the effluent ozonated alone.

(ii) Highest improvement in COD removal efficiency was achieved via electrolysis using aluminum electrode. 66% COD removal was obtained via 20 min ozonation of biotreated textile effluent at pH= 7.5, whereas the COD removal increased to 80% and 72% when biotreated effluent was first subjected to electrolysis with aluminum at pH= 4.5 and 7.5, respectively. In addition, the final COD of the biotreated + ozonated effluent was 119 mg/L, while the final COD was reduced to 30 mg/L via electrolysis with aluminum + ozonation.

(iii) In conclusion, the following advanced treatment scheme was recommended for secondary treated textile wastewater; 15 min electrochemical treatment using Al electrodes at pH 4.5 and 20 A, followed by ozonation at an optimum dose of 1440 mg/h at pH 7.5. Final removal efficiencies were obtained as follows: COD = 96 %; Color = 99 %; SS = 92 %; DS = 32 % ; and SO_4^{2-} = 70 %.

- sonolysis

(i) Two reactive (DB1 and DB2) and one basic type (DB3) dyebath effluents were irradiated at 300 kHz. The first-order color decay rate constants were found as 0.062 min^{-1}, 0.038 min^{-1} and 0.028 min^{-1} for DB1, DB2 and DB3, respectively.

(ii) The effect of H_2O_2 addition (7 mM) on color and COD removal efficiencies was also examined. The obtained results revealed that color removal rates were not appreciably affected in the presence of H_2O_2, whereas overall COD removal efficiencies increased from and 18, 38 and 23 % to 77, 88 and 80 % upon H_2O_2 addition for DB1, DB2 and DB3, respectively.

5.2. Recommendations

The following issues should be pointed out for the future work:

(i) Despite the robustness and high removal efficiencies in terms of COD, SS, color and DS, the sequential use of electrolysis + ozonation processes failed due to the high operating cost for the preparation of dyehouse effluent to be reused by membranes. Therefore, more attention should be paid to reduce operating costs by concentrating on electrochemical reactor, ozone contactor and electrode design.

(ii) The performance of the existing biological treatment plant can be improved by modifying it to a membrane bioreactor (MBR) so that the effluent of the MBR system can be directly sent to the Reverse Osmosis (RO) unit.

REFERENCES

APHA-AWWA-WPCF, 1998. Standard Methods for the Examination of Water and Wastewater, 20th Ed. American Public Health Association, Washington DC.

Apikyan, G.I. and Ince, N.H., 2004. The Application of Electrochemical Treatment for Effluent Reuse in the Textile Industry.

Arslan, I. and Balcioglu, I.A., 2000. Effect of Common Reactive Dye Auxiliaries on the Ozonation of Dyehouse Effluents containing Vinylsulphone and Aminochlorotriazine Dyes, Desalination, 130, 1, 61-71.

Arslan-Alaton, I., Kornmueller, A. and Jekel, M. R., 2002. Ozonation of Spent Reactive Dye-baths: Effect of HCO_3^-/CO_3^{2-} Alkalinity, ASCE Journal of Environmental Engineering, 128, 8, 689-69.

Arslan-Alaton, I. and Seremet, O., 2004. Advanced Treatment of Biotreated Textile Industry Wastewater with Ozone, Virgin/Ozonated Carbon Granular Activated Carbon and their Combination, Journal of Environmental Science and Health Part A, A39, 1681-1694.

Aurich, C. W., 1975. PVA Recovery by Ultrafiltration, AATCC Symposium Series, Textile Technology/Ecology Interface, Charlotte, NC.

Balcioglu, I.A. and Arslan, I., 2001. Partial Oxidation of Reactive Dyestuffs and Synthetic Textile Dye-Bath by the O_3 and O_3/H_2O_2 Processes, Water Science and Technology, 43, 2, 221-228.

Bandara, J., Herrera, F. G., Kiwi, J. T. and Pulgarin, C. O., 1998. Degradation of Concentrated Solutions of Non-biodegradable Orange II by Photocatalytic and Electrochemical Methods, Journal of Chemistry Research, 45, 5, 234-235.

Beltran, J. F., 2004. Kinetics of the Ozonation of Wastewaters, in: Ozone Reaction Kinetics for Waters and Wastewaters, Chapter 6, CRC Press LLC, Boca Raton, Florida, 113-150.

Bes-Pia, A., Mendoza-Roca, J.A., Alcaina-Miranda, M.I., Iborra-Clar, A., Iborra-Clar, M.I., 2003. Combination of Physico-Chemical Treatment and Nanofiltration to Reuse Wastewater of a Printing, Dyeing and Finishing Textile Industry, Desalination, 157, 1-3, 73-80.

Bes-Pia, A., Mendoza-Roca, J.A., Roig-Alcover, L., Iborra-Clar, A., Iborra-Clar, M.I. and Alcaina-Miranda, M.I., 2003. Comparison between Nanofiltration and Ozonation of Biologically Treated Textile Wastewater for its Reuse in the Industry, Desalination, 157, 1-3, 81-86.

Biswas, N. and Lazarescu, G., 1991. Removal of Oil from Emulsions using Electrocoagulation, International Journal of Environmental Studies, 38, 65-68.

Brandon, C. A., 1980. Closed Cycle Textile Dyeing: Full-scale Hyperfiltration Demonstration, Demonstration Design, U.S. Environmental Protection Agency, EPA-600/2-80-005.

CCOT, 1995. The AOP Handbook, Calgon Carbon Oxidation Technologies, Markham, Ontario.

Chen, X., Chen, G. and Lock Yue, P., 2003. Anodic Oxidation of Dyes at Novel Ti/B-Diamond Electrodes, Chemical Engineering Science, 58, 995-1001.

Ciardelli, G. and Ranieri, N., 2001. The Treatment and Reuse of Wastewater in the Textile Industry by Means of Ozonation and Electroflocculation, Water Research, 35, 2, 567-572.

Ciardelli, G., Capannelli, G. and Bottino, A., 2001. Ozone Treatment of Textile Wastewaters for Reuse, Water Science and Technology, 44, 5, 61-67.

Chua, H., Fung, J. P. C. and Chan, J. S. M., 1998. Decolorization of Textile Dyeing and Finishing Wastewater using Electrocoagulation and Sequence – Pipe Reactors, Water Science and Technology, 38, 6, 261-268.

Correia, V. M., Stephenson, T. and Judd, S. J., 1994. Characterization of Textile Wastewaters – A Review, Environmental Technology, 15, 917-929.

Davila-Jimenez, M. M., Elizalde-Gonzalez, M. P., Guiterez-Gonzalez, A. and Pelaez-Cid, A. A, 2000. Electrochemical Treatment of Textile Dyes and their Analysis by High–Performance Liquid Chromatography with Diode Array Detection, Journal of Chromatography A, 889, 253-259.

Do, J. S. and Chen, M. L., 1994. Decolorization of Dye-containing Solutions by Electrocoagulation, Journal of Applied Electrochemistry, 24, 785-790.

Easton, J. R., 1995. The Dye Maker's View, in Cooper, P. (Ed.), Color in Dyehouse Effluent, 6-21, The Society of Dyers and Colorists, Alden Press, Oxford.

Edwards, J. D., 1995. Industrial Wastewater Treatment: A Guidebook, CRC Press, New York.

Edzwald, J.K., 1993. Coagulation in Drinking Water Treatment: Particles, Organics, and Coagulants, Water Science and Technology, 27, 11, 21-35.

EPA, 1991. Handbook of Photochemical Oxidation Technologies, Environmental Protection Agency, Athens, Georgia.

Fischer, C.H., Hart, E.J. and Henglein, A., 1997. Ultrasonic Irradiation of Water in the Presence of $^{18,18}O_2$: Isotope Exchange and Isotopic Distribution of H_2O_2, Journal of Physical Chemistry, 90, 1954-1956.

Gaddis, J. L., Spencer, H. G. and Jernigan, P. A., 1988, Caustic Recovery and Recycling in at a Textile Dyeing and Finishing Plant, Advances in RO and UF, Proceedings of the American Chemical Society Meeting, Toronto, Canada.

Gaehr, F., Hermanutz, F. and Oppermann, W., 1994. Ozonation – An Important Technique to Comply with New German Laws for Textile Wastewater Treatment, Water Science and Technology, 30, 3, 255-263.

Glaze, W. H., Kang, J. W. and Chapin, D. H., 1987. The Chemistry of Water Treatment Processes involving Ozone, Hydrogen Peroxide and Ultraviolet Irradiation, Ozone Science and Engineering, 9, 335-352.

Gottschalk, C., Libra, J. A. and Saupe, A, 2000. Ozonation of Water and Waste Water: A Practical Guide to Understanding Ozone and its Application, Wiley-VCH, Weinheim.

Hassan, M.M. and Hawkyard, C.J., 2002. Decolorization of Aqueous Dyes by Sequential Oxidation Treatment with Ozone and Fenton's Reagent, Journal of Chemical Technology and Biotechnology, 77, 7, 834-841.

Henglein, A., 1987. Sonochemistry-Historical Developments and Modern Aspects, Ultrasonics, 25, 6-16.

Hepel, M. and Luo, J., 2001. Photoelectrochemical Mineralization of Textile Diazo Dye Pollutants using Nanocrystalline WO_3 Electrodes, Electrochimical Acta, 47, 729-740.

Hassan, M.M. and Hawkyard, C.J., 2002. Effect of Dyebath Additives on Decolorization Efficiency in the Ozonation of Dyehouse Effluent, Ozone Science and Engineering, 24, 4, 261-270.

Hua, I. and Hoffmann, M.R., 1997. Optimization of Ultrasonic Irradiation as an Advanced Oxidation Technology, Environmental Science and Technology, 31, 2237-2243.

Hung, H.M. and Hoffmann, M.R., 1998. Kinetics and Mechanism of the Enhanced Reductive Degradation of CCl_4 by Elemental Iron in the Presence of Ultrasound, Environmental Science and Technology, 32, 19, 3011-3016.

Ince, M. A., 2004. OSB'de Çevre Sorunları ve Çözüm Yaklaşımları, The Ninth Industrial Pollution Control Symposium, EKK'2004, Istanbul Technical University, June 2-4, 85-94.

Ince, N.H. and Tezcanli, G., 2001. Reactive Dyestuff Degradation by Combined Sonolysis and Ozonation, Dyes and Pigments, 49, 145-153.

Ince, N.H. and Tezcanli, G., Belen, R.K., Apikyan, I.G., 2001.Ultrasound as a Catalyzer of Aqueous Reaction Systems: the state of the art Environmental Applications, 29, 167-176.

Jerome, O., Nriagu, M. and Simmons, M. S., 1994. Environmental Oxidants, Wiley Interscience, New York.

Johnston, L. and Wett, T. W., 1989. Caustic Recovery by an UF system: System Sizing and Cost Savings, Chemical Proceedings, 36.

Kang, J.W. and Hoffmann, M.R., 1998. Kinetics and Mechanism of the Sonolytic Destruction of Methyl Tert-Butyl Ether by Ultrasonic Irradiation in the Presence of Ozone, Istanbul Technical University, 32, 3194-3199.

Karahan, O., Dulkadiroglu, H., Kabdasli, I., Sozen, S., Germirli-Babuna, F.G. and Orhon, D., 2002, Effect of Ozonation on the Biological Treatability of a Textile Mill Effluent, Environmental Technology, 23, 12, 1325-1336.

Khraisheh, M.A.M., 2003. Effect of Key Process Parameters in the Decolorization of Reactive Dyes by Ozone, Coloration Technology, 119, 1, 24-30.

Kos, L. and Perkowski, J., 2003. Decoloration of Real Textile Wastewater with Advanced Oxidation Processes, Fibers and Textile in Eastern Europe, 11, 4, 81-85.

Langlais, B., 1991. Ozone in Water Treatment: Application and Engineering, Cooperative Research Report, Lewis Publishers, Chelsea, Michigan.

Leonard, F., 1981. The Design of an Indigo Dye Recovery System, Seminar on Membrane Separation Technology, Continuing Engineering Education, Clemson University.

Lin, S. H. and Peng, C. F., 1994. Treatment of Textile Wastewater by Electrochemical Method, Water Research, 28, 2, 277-282.

Lopez, A., Benbelkacem, H., Pic J.S. and Debellefontaine, H., 2004. Oxidation Pathways for Ozonation of Azo Dyes in a Semi-Batch Reactor: A Kinetic Parameters Approach, Environmental Technology, 25, 3, 311-321.

Lorimer, J.P., Mason, T.J., Plattes, M. and Phull, S.S., 2000. Dye Effluent Decolorization Using Ultrasonically Assisted Electro-oxidation, Ultrasonics Sonochemistry, 7, 237-242.

Lu, S.G., Imai, T., An, D.N. and Ukita, M., 2001. A Pilot-Scale Study of Tertiary Treatment of Jizhuangzi Wastewater Treatment Plant by Continuous Preozonation-Microflocculation-Filtration Process, Environmental Technology, 22, 3, 331-337.

Makino, K., Mossoba, M. and Reisz, P., 1982. Chemical Effects of Ultrasound on Aqueous Solutions. Evidence for –OH and –H by Spin Trapping, Journal of the American Chemical Society, 104, 3537-3539.

Marcucci, M., Ciardelli, G., Matteucci, A., Ranieri, L. and Russo, M., 2002. Experimental Campaigns on Textile Wastewater for Reuse by Means of Different Membrane Processes, Desalination, 149, 1-3, 137-143.

Marechal, M. L., Slokar, Y. M. and Taufer, T., 1997. Decoloration of Chlorotriazine Reactive Azo Dyes with H_2O_2/UV, Dyes and Pigments, 33, 181-298.

Mason, T. J. and Lorimer, J. P., 1989. Sonochemistry, Theory, Applications and Uses of Ultrasound in Chemistry, Ellis Horwood Publications, Chichester, 56-67.

Mason, T. J. and Cordemans, E.M., 1998. Synthetic Organic Sonochemistry, Wiley, New York, 301.

Mason, T.J., 1999. Sonochemistry, Oxford University, Primer Series, Oxford University Press, UK, 70.

Mason, T.J., 1990. Chemistry with Ultrasound: Critical Reports on Applied Chemistry, Society for Chemical Industry, Elsevier, London, 28.

Mason, T.J. and Lorimer, C.P., 1988. Sonochemistry, in: T.L. Kem (Ed.), Wiley, New York.

Minero C. Maurino V. and Pelizzetti, E., 1997. Photocatalytic Transformations of Hydrocarbons at the Sea Water Air Interface under Solar Radiation, Marine Chemistry, 58, 3-4, 361-372.

Mrowetz, M., Pirola, C. and Celli, E., 2003. Degradation of Organic Pollutants through Sonophotocatalysis in the Presence of TiO_2, Ultrasonics, 10, 247-254.

Muthukumar, M., Sargunamani, D., Selvakumar, N. and Rao, J.V., 2004. Optimization of Ozone Treatment for Color and COD Removal of Acid Dye Effluent using Central. Composite Design Experiment, Dyes and Pigments, 63, 2, 127-134.

Neppiras, E. A., 1984. Acoustic Cavitation Series 1. Acoustic Cavitation-an Introduction, Ultrasonics, 22, 25-28.

Noltingk, B. E. and Neppiras, E. A., 1950. Cavitation Produced by Ultrasonics, Proceedings of the Physical Society, B63, 674-685.

Ogutveren, U.B., Toru, E., Koparal, S., and Poyraz, Z., 1993. Removal of Cyanide by Anodic Oxidation for Wastewater Treatment, The 44th Meeting of the International Society of Electrochemistry, Berlin.

Ozgovde, B.A., 1998. Design and Construction of an Electrofloatation Treatment Plant for the Cleaning Waters of Wax-Coated Vehicles, M.S. Thesis, Boğaziçi University.

Pétrier, C., Lamy, M.F., Francony, A., Benahcene, A., David, B., Renaudin, V. and Gondrexon, N., 1994. Sonochemical Degradation of Phenol in Dilute Aqueous-Solutions-Comparison of the Reaction Rates at 20-kHz and 487-kHz, Journal of Physical Chemistry, 98, 41, 10514-10520.

Petriér, C., Jiang, Y. and Lamy, M.F., 1998. Ultrasound and Environment: Sonochemical Destruction of Chloroaromatic Derivatives, Environmental Science Technology, 32, 9, 1316-1318.

Pisa Tekstil Boya Fab., 2005. Monthly Performance Evaluation Report, 3, 2-3.

Poon, C.S., Huang, Q. and Fung, P.C., 1999. Degradation Kinetics of Cuprophenyl Yellow RL by UV/H_2O_2/US in Aqueous Solution, Chemosphere, 38, 5, 1005-1014.

Pouet, M., Persin, F. and Rumeau, M., 1992. Intensive Treatment by Electrocoagulation-flotation-tangential Flow Microfiltration in Areas of High Seasonal Population, Water Science and Technology, 25, 247.

Radetski, C.M., Rosa, S.M.C., Rosa, E.V.C., Sierra, M.M.D. and Simionatto, E.L., 2002. Ozonation of Textile Wastewater: Physicochemical and Phytotoxic Aspects, Environmental Technology, 23, 5, 537-545.

Rajeshwar, K. and Ibanez, J. G., 1993. Environmental Electrochemistry, Fundamentals and Applications in Pollution Abatement, Academic Press, San Diego, California, 776.

Reife, A., 1997. Dyes: Environmental Chemistry, in: Kirk Othmer Encyclopedia of Chemical Technology, John Wiley & Sons, Inc, New York, 753-784.

Reife, A. and Freeman, H. S., 1996. Environmental Chemistry of Dyes and Pigments, John Wiley and Sons, Canada, 329-345.

Reisz, P., Kondo, T. and Krishna, C.M., 1990. Sonochemistry of Volatile and Nonvolatile Solutes in Aqueous-Solutions-EPR and Spin Trapping Studies, Ultrasonics, 28, 5, 295-303.

Riveria-Ceron, M., Davila-Jimenez, M. M. and Elizalde-Gonzalez, M. P., 2004. Degradation of the Textile Dyes Basic Yellow 28 and Reactive Black 5 using Diamond and Metal Alloys Electrodes, Chemosphere, 55, 1-10.

Scott, K., 1995. Electrochemical Processes for Clean Technology, The Royal Society of Chemistry, Cambridge, UK, 306.

Seghal, C., Sutherland, R.G. and Verrall, R.E., 1991. Optical Spectra of Sonoluminescence from Transient and Stable Cavitation in Water Saturated with various Gases, Journal of Physical Chemistry, 84, 388-395.

Shen, Z, Wang, W., Jia, J., Feng, X., Hu, W. and Peng, A., 2002. Catalytically Assisted Electrochemical Oxidation of Dye Acid Red B., Water Environment Research, 74, 2, 117-121.

Slokar, Y. M. and Marechal, A. M., 1998. Methods of Decoloration of Textile Wastewaters, Dyes and Pigments, 33, 4, 335-356.

Sotelo, J.L., Beltran, F.J. and Benitez, F.J., 1989. Henry's Law Constant for the Ozone Water-System, Water Research, 23, 1239-1246.

Staehelin, S. and Hoigné, J., 1982. Decomposition of Ozone in Water: Rate of Initiation by Hydroxide Ions and Hydrogen Peroxide, Environmental Science and Technology, 16, 10, 676-681.

Staehelin, S. and Hoigné, J., 1985. Decomposition of Ozone in Water in the Presence of Organic Solutes acting as Promoters and Inhibitors of Radical Chain Reactions, Environmental Science and Technology, 19, 1206-1212.

Sundstrom, D. W. and Klei, H. E., 1979. Wastewater Treatment, Prentice-Hall, Englewood Cliffs, New Jersey, 155.

Suslick, K.S., 1986. Organometallic Sonochemistry, Advances in Organometals Chemistry, 25, 73-119.

Suslick, K.S., 1989. Ultrasound; its Chemical, Physical, and Biological effects, VCH Publishers, New York.

Szpyrkowicz, L., Juzzolino, C. and Kaul, S. N., 2001. A comparative Study on Oxidation of Disperse Dyes by Electrochemical Process, Ozone, Hypochlorite and Fenton Reagent, Water Research, 35, 9, 2129-2136.

Tezcanli-Guyer, G. and Ince, N.H., 2003. Degradation and Toxicity Reduction of Textile Dyestuff by Ultrasound, Ultrasonics Sonochemistry, 10, 235-240.

Tezcanli-Guyer, G., Alaton, I. and Ince, N.H., 2003. Sonochemical Destruction of Textile Dyestuff in Wasted Dyebaths, 119, 292-296.

Tezcanli-Guyer, G. and Ince, N.H., 2004. Individual and Combined Effects of Ultrasound, Ozone and UV Irradiation: A Case Study with Textile Dyes, Ultrasonics, 42, 1-9, 603-609.

The General Secretariat of Istanbul Textile and Apparel Exporters' Association (ITKIB), 1998. 1997 Figures, Istanbul.

United Nations Environment Programme (UNEP) Industry and Environment, 1993. The Textile Industry and the Environment, Technical Report Nr. 16, United Nations Publication, Cedex, France.

Vandevivere, P. C., Bianchi, R. and Verstraete, W., 1998. Treatment and Reuse of Wastewater from the Textile Wet-Processing Industry: Review and Emerging Technologies, Journal of Chemical Technology and Biotechnology, 72, 289-302.

Vinodgopal, K. and Peller, J., 2003. Hydroxyl Radical-mediated Advanced Oxidation Processes for Textile Dyes: A Comparison for Sonolytic and Radiolytic Degradation of the Monoazo Dye Acid Orange 7, Research Chemistry Intermediates, 29, 3, 307-316.

Wang, C.X., Yediler, A., Lienert, D., Wang, Z.J. and Kettrup, A., 2003. Ozonation of an Azo Dye CI Remazol Black 5 and Toxicological Assessment of its Oxidation Products, Chemosphere, E 52, 7, 1225-1232.

Weavers, L.K., Ling, F.H. and Hoffmann, M.R., 1998. Aromatic Compound Degradation in Water Using a Combination of Sonolysis and Ozonolysis, Environmental Science Technology, 32, 18, 2727-2733.

Wedley, S. and Waite, T. D., 2004. Fenton Processes, in Parsons, S. (Ed.), Advanced Oxidation Processes for Water and Wastewater Treatment, IWA Publishing, Cornwall, UK, 111-136.

Weintraub, M. H., Gealer, R. L., Golovoy, A., Dzieciuch, M. A., and Durham, H., 1983. Development of Electrolytic Treatment of Oily Wastewater, Environmental Progress, 2,32-46.

Wendt, H. and Kreysa, G., 1999. Electrochemical Engineering, Science and Technology in Chemical and other Industries, Springer Verlag, Heidelberg, Germany, 404.

Wilcock, A., Tebbens, J. Fuss, F., Wagner, J. and Brewster, M., 1992. Textile Chemistry and Coloration, 24, 11, 111-117.

Wilcock, A., Brewster, M. and Tincher, W., 1992. Using Electrochemical Technology to treat Textile Wastewater: Three Case Studies, American Dyestuff Reporter, 15, 81-86.

ÖZET

Bu çalışmada, literatürden yararlanarak, RS CVn çift yıldızlarının genel özellikleri incelenmiştir. Giriş Bölümünde, daha güvenilir teorilerin ortaya konması bakımından RS CVn türü sistemlerin gözlemlerinin ve açıklamaların önemi vurgulanmaya çalışılmıştır. Bölüm 2'de RS CVn çift yıldızlarının sınıflamasından ve genel özelliklerinden söz edilmiştir. Bölüm 3'te, RS CVn türü sistemlerin fotometrik etkinlikleri, moröte, X-ışını ve radyo gözlemleri ve bunların açıklamaları cinsinden manyetik aktiviteleri tartışıldı.

RS Canum Venaticorum (RS CVn) çift sistemleri aktif çift sistemlerin özel bir sınıfı olup ilk kez Hall (1976) tarafından sınıflandırılmışlardır. Bu sınıfın üyesi olmak gereken özellikler; 1-14 gün yörünge dönemli çift yıldız olmak, en az bir bileşenin tayf türünün F-G ve ışıtma sınıfının V-IV olması ve tutulmalar dışında CaII H ve K salma çizgileri göstermesidir (Gunn, 1996). Soğuk bileşen genellikle bir K türü alt-dev yada dev yıldız olup daha küçük kütlelidir. RS CVn sistemlerinde her iki yıldız, her nekadar aralarında kütle alışverişleri yaptıklarına ilişkin gözlemsel kanıt bulunmasına rağmen, Roche loblarını doldurmayan yani ayrık olan çift yıldızlardır (Huenemoerder ve ark., 1989). Fotometrik gözlemler, ışık eğrilerinde tutulmalar dışında küçük genlikli yarı çevrimsel yapılı değişimler gösterir. Bu değişimler, çoğu zaman soğuk yüzey yıldız lekeleri olarak açıklanır. Uzun zamanlar boyunca elde edilen gözlemlerde, bu fotometrik bozunma dalgasının yörünge evresine bağlı olarak değiştiği gözlenmiş ve yıldız lekelerinin boylamsal yer değiştirme (göç) hareketi olarak açıklanmıştır (örneğin AB Dor, Jarvinen ve ark. 2005). Bunun yanısıra diğer genel özellikleri, güçlü bir koronal X-ışını ve radyo salması, değişen Hα salması ve kromosfer ve geçiş bölgesinde güçlü bir UV salması göstermeleri (örneğin MgII h & k ve CIV çizgilerinde), parlama (flaring) göstermeleri ve aktivite çevriminden ve/yada kütle kaybından dolayı yörünge döneminde değişimler Kalimeris ve ark., 1995; Doyle ve ark., 1994) göstermeleridir.

RS CVn grubu, genelde üç alt gruba ayrılır: Yörünge dönemleri 1 günden kısa olan RS CVn'ler, yörünge dönemleri 1-14 gün arasında olan klasik RS CVn'ler ve yörünge dönemleri 14 günden büyük olan uzun dönemli RS CVn'ler. Kısa dönemli RS CVn'ler, yörünge-dönme kilitlenmesinden dolayı eşdönme gösterirler ve hızla dönerler (De Campli & Baliunas, 1979 ve Scharlemann, 1981). Linsky (1983), eşdönme kriteri

için RS CVn çift sistemlerinde yörünge döneminin 20 günden daha kısa olması gerektiğini önermektedir.

Literatürde, RS CVn yıldızlarının optik ve morötesi bölgelerdeki karaktererini araştıran çok sayıda çalışma vardır. Işık eğrilerinde tutulmalar ve yakınlık etkileri dışında görülen bozunmalar, soğuk yıldız lekelerine atfedilmektedir. Böylesi çalışmalarda modellenen yıldız lekeleri, çevrelerinden 500-1000 K kadar soğuk olup yıldız yüzeyinin yaklaşık % 40ına kadar alanı kaplarlar (Eaton & Hall 1979; Doyle ve ark. 1988) ve hatta uçlak bölgelerinde bile oluşabilirler (Schüssler & Solanki, 1992). Öte yandan Ramsey (1990), çoğu RS CVn çiftlerinin tayflarından görülen aşırı TiO soğurmasının yıldız lekelerinin varlığına işaret olabileceğini açıklamıştır. Aktiviteyi temsil eden optik ve moröte bölgedeki çizgilerin yıldızın eksenel dönmesinden dolayı çevrimsel değişimleri (modülasyonları) plaj benzeri materyallerin bulunduğuna bir kanıt sayılır. Örneğin Rodono ve ark. (1987), II Peg sistemi üzerinde parlak aktif bölgelerin soğuk fotosferik lekelerin hemen hemen yakınlarında ortaya çıktığını göstermişlerdir. Bundan başka Neff ve Neff (1987), AR Lac sisteminde kromosferik salma çizgileri gözlemişlerdir. Huenomerder ve ark. (1990), IUE uydusunun IM Peg sisteminin optik ve morötesi bölgesindeki ölçümlerini kullanarak sistemin bir yıllık zaman ölçeğinde güçlü modülasyonlar sergilediğini ortaya koymuşlardır. Ayrıca, Nations ve Ramsey (1980) ve Barden (1984) tarafından RS CVn sistemlerinde plaj bölgelerinin Hα ve CaII H ve K çizgi yeğinlik modülasyonları çalışılmıştır. RS CVn yıldızlarının atmosferlerinin güneş benzeri yapısı koronal bölgerin içine kadar uzanır. Bu bölgeler koronada kapalı manyetik loplar içine kuşatılmış olup yaklaşık 10^7 K sıcaklığında plazmalar içerir (Gunn, 1996). RS CVn'lerde X-ışını salması güneş için geliştirilen modellemeler kullanılarak koronal lop yapılarına atfedilmiştir (Doyle ve ark., 1992; Rosner ve ark., 1978). Mutel ve ark. (1985) RS CVn yıldızlarının X-ışını ve radyo gözlemlerini kullanarak "çekirdek-halo" modelini önermişlerdir. Uchida ve Sakurai (1983)'e göre; yıldızların radyal yöndeki diferansiyel dönmeleri, bileşenlerin manyetik akı tüplerinin birleşmesine ve koronal bölgenin genişlemesine neden olur. İki bileşen yıldızın X şeklinde bileşen manyetik lopların kesişim (çekirdek) yerinde sıkışan plazma yüksek sıcaklıklara ulaşarak X-ışını yayar. Daha sonra yıldızların dönme hareketi bu kesişen lopları ortak korona bölgesinin (Halonun) içine yaymasına neden olur. Böylece uzayan ve genişleyen lop içindeki plazma soğur ve azalan manyetik kuvvetten dolayı ivmelenerek radyo bölgesinde salma yapar.

RS CVn çiftlerinde parlama benzeri olayları optik bölgede fark etmek çok zordur. Çünkü sıcak bileşen, sistemin ışıtmasına bu dalga boylarında tamamen hakimdir. Ancak parlama gözlemleri X-ışını, morötesi ve radyo dalga boylarında kolayca gözlenebilir (Walter ve ark., 1987; Trigilio ve ark., 1983). Bu olayların genel açıklamasında güneş parlama modeli kullanılır: parlama olayının manyetik lopların yıldızın yüzeyine bağlandığı/kenetlendiği iki yerde lop boyunca yüksek enerjiyle fışkıran/ivmelenen yüklü parçacıklar tarafından oluştuğu vurgulanır (Doyle ve ark., 1989; Byrne, 1989).

Tezin 4. Bölümünde, tez çalışmasının uygulama kısmı için seçilen RS CVn türü V1430 Aql çift yıldızının fotometrik çalışması sunulmaktadır. V1430 Aql sistemi Çanakkale Onsekiz Mart Universitesi Gözlemevinde, 2004 gözlem sezonunda, fotoelektrik olarak *BVR* renklerinde gözlenmiştir. Gözlemler, HEC22 programı (Harmanec ve Horn, 1998) kullanılarak standart parlaklığa çevrilmiştir. Standart *B-V* renk ölçeği, sistemin tayf türünü KO olarak vermektedir. Yeni gözlemler ile literatürde yayınlanan tüm minimum zamanları toplanarak sistemin yörünge dönemi incelenmiş ve sistem için yeni fotometrik ışık öğeleri bulunmuştur. V1430 Aql sisteminin *BVR* ışık eğrilerinin analizi için iki farklı fotometrik çözüm yöntemi (PHOEBE ve ILOT) kullanılmıştır. Ayrıca, PHOEBE yöntemi ile *BVR* ışık eğrilerinin ve dikine hız eğrilerinin eşzamanlı çözümü yapılmıştır. Sonuç olarak, gözlemler ile uydurulan kuramsal eğrilerin uyuşumu uygun olup bu farklı iki yöntemin sonuçları arasında genel bir uyuşum vardır. Fotometrik sonuçlar, V1430 Aql sisteminin bileşenlerinin kendi Roche loplarını %75 oranında doldurduğu bir ayrık sistem olarak tanımlar. Bu çalışmada bulunan genel fiziksel belirteçler (özellikle sistemin uzay hızının küçük çıkması), sistemin bileşenlerinin muhtemelen anakol öncesi yıldızlar olduğunu ortaya koyar. Yine de bu olasılığın kesin bir yargı olabilmesi için sistemin bileşenlerinin yüzey metal bolluğunu (özellikle lityum bolluğunu) veren taysal gözlemlere gerek duyulmaktadır. Fotometrik çözümler, ayrıca, sistemin baş bileşen yıldızının zıt yarı kürelerde uzun ömürlü soğuk iki lekeye sahip olduğunu göstermektedir. Bu konfigürasyon, göreli olarak pek karşılaşılmayan ancak güneş leke yada manyetik alan modeline uygun olan bir "eksenel-simetrik (poloidal alanlı) yıldız leke modelini" önerir. Bu yüzden bu çalışma, yıldızların manyetik ativitesine ilişkin teoriler için verimli bir test olanağını vermektedir.

Sunulan bu tezin 5. bölümünde RS CVn Çift Yıldızlar Kataloğu başlıklı bir katalog sunulmaktadır. Aslında genel olarak kromosferik aktif çift yıldızlar için bir katalog ilk kez Strassmeier ve ark. (1988) tarafından yapılmış ve sonrasında Strassmeier ve ark. (1993) tarafından güncellenmiştir. Strassmeier ve ark. (1993)'nın kataloğunda yaklaşık 130 RS CVn çift yıldızı ile birlikte BY Dra yıldızları ve bazı aktif algol çift yıldızları bulunmaktadır. Bu çalışmada yalnızca RS CVn çift yıldızlarının özelliklerine değinmek bunların istatistiksel analizlerini olası kılmak, yeni keşfedilen RS CVn çift yıldızlarını katmak ve 1993 yılından bu yana biriken yeni bilgilerle veriyi güncelemek için ayrı bir katalog sunulmaktadır. Katalog 6 ayrı çizelge halinde yaklaşık 182 RS CVn çift yıldızına ait bilgiyi içerir. Bu çizelgelerde genel bilgi, fotometrik özellikler, ışık eğrisi öğeleri, tayfsal özellikler ve dikine hız eğrisi öğeleri, salt öğeler ve aktivite belirteçleri ele alınmıştır.